OLIGOPEPTIDE TRANSPORT ACROSS THE BASOLATERAL MEMBRANE OF RAT SMALL INTESTINE

Emma Jayne Shepherd

Submitted for the degree of Doctor of Philosophy

Biology Department
University of York
York
UK

January 2001

List of Contents

Acknowledgements

Abbreviations

Declaration

Collaborations

List of figures

List of tables

Abstract

CHAPTER 1: INTRODUCTION

1.1 Anatomy of the small intestine **1**

1.1.1 Basic structure and functions 1

1.1.2 Anatomy of the intestinal wall 2

1.1.3 Villi 4

1.1.4 Compartmentalisation of the epithelia 4

1.1.5 The intestinal vascular system 5

1.1.6 Absorptive cells 7

1.1.6.1 The apical membrane 9

1.1.6.2 The unstirred water layer 10

1.1.6.3 The basolateral membrane 10

1.1.6.4 Junctional complexes 10

1.2 Peptide transport **11**

1.2.1 History of protein absorption 11

1.2.2 Peptide transport 15

1.2.2.1 Advancement in the study of peptide transport 15

1.2.2.2 Sites of oligopeptide transport 15

1.2.2.3 Importance of peptide transporters 16

1.2.2.3.1 *Nutritional implications* 16

1.2.2.3.2 *Clinical implications* 17

1.2.2.3.3 *Pharmacological implications* 17

1.2.3 Mechanism of peptide transport 18

1.2.3.1 Driving force for active transport 18

1.2.3.2 Role of the acidic microclimate 21

1.2.3.3 pH-dependence of transport 23
1.2.3.4 Mechanism of H^+/peptide cotransport 24
1.2.4 Membrane preparations used to study peptide transport 25
1.3 Molecular physiology of the peptide transporters 26
1.3.1 Cloning of the intestinal peptide transporter, PepT1 26
1.3.2 Cloning of the renal peptide transporter, PepT2 28
1.3.3 Sequence similarity of mammalian peptide transporters with other proteins 29
1.3.4 Cloning of other H^+/peptide co-transporters 31
1.3.5 Tissue distribution of peptide transporters 32
1.3.6 One or two intestinal peptide transporters? 34
1.4 Structure and function of the peptide transporters 35
1.4.1 Membrane model of the peptide transporters 35
1.4.1.1 Species differences in PepT1 structure 37
1.4.1.2 Species differences in PepT2 structure 37
1.4.1.3 Additional structural features 40
1.4.2 Essential amino acid residues of the peptide transporter(s) 40
1.4.2.1 Histidine residues 41
1.4.2.2 Thiol residues 42
1.4.2.3 Tyrosine residues 43
1.4.3 Substrate transport 43
1.4.3.1 Maximum size of oligopeptides 44
1.4.3.2 Stereospecificity of substrates 44
1.4.3.3 Charged substrates 48
1.4.3.3.1 *Distinct pH-dependence in the transport of charged peptides* 48
1.4.3.3.2 *Distinct H^+ flux coupling ratios of charged substrates* 49
1.4.4 Substrate binding site 50
1.4.4.1 Localisation of the substrate binding site 50
1.4.4.2 Template for the substrate binding site 51
1.4.5 Exploitation of PepT1 for efficient drug delivery 53
1.5 Peptide transport at the basolateral membrane 57
1.5.1 Mechanism of peptide transport 58

1.5.2 Transport kinetics 58
1.5.3 Essential residues of the transporter 61
1.5.4 Is basolateral peptide transport the rate-limiting step in absorption? 61
1.6 Regulation of intestinal peptide transport 62
1.6.1 Long-term regulation of peptide transport 63
1.6.1.1 Adaptation to changes in luminal nutrient levels 63
1.6.1.2 Adaptation to fasting and/or starvation 67
1.6.2 Short-term regulation of peptide transport 68
1.6.2.1 Amino acid regulation 69
1.6.2.2 Hormonal regulation 69
1.6.2.3 Additional regulatory mechanisms 70
1.7 Aims of this thesis 71

CHAPTER 2: MATERIALS AND METHODS

2.1 Procedure for the study of peptide transport in the isolated luminally and vascularly perfused rat jejunum *in situ* 73
2.1.1 Animals 73
2.1.2 Chemicals and materials 73
2.1.3 Solutions 75
2.1.4 Perfusion apparatus 76
2.1.5 Operative procedure 78
2.1.6 Sample treatment 81
2.1.7 Tissue sample treatment 82
2.1.8 Sample Analysis 82
2.1.8.1 Glucose Analysis 82
2.1.8.2 HPLC Analysis 83
2.1.9 Expression of results 84
2.1.9.1 Viability of perfusions determined by glucose utilisation, by the isolated jejunum, from the vascular perfusate 84
2.1.9.2 Intestinal transport of a dipeptide as determined by its appearance in the vascular effluent 85
2.1.9.3 Tissue accumulation of peptide and corresponding exit ratio 85

2.1.9.4 Statistical analysis 86

2.2 Dual preparation of brush-border and basolateral membrane vesicles from rat jejunal mucosa 86

2.2.1 Animals 86

2.2.2 Chemicals and materials 87

2.2.3 Solutions 87

2.2.4 Membrane vesicle preparation 87

2.2.4.1 Basolateral membrane purification 88

2.2.4.2 Brush-border membrane purification 89

2.2.5 Assays to establish vesicle purity 89

2.2.5.1 Protein assay 90

2.2.5.2 Alkaline phosphatase assay 90

2.2.5.3 Sucrase assay 91

2.2.5.4 Ouabain-sensitive Na^+/K^+-ATPase assay 92

2.2.5.5 Enrichment factors of marker enzymes 94

2.3 Identification of peptide transporters by photoaffinity labelling of intestinal membrane proteins using [4-azido-3,5-^{3}H-D-Phe]-L-Ala 95

2.3.1 Photoaffinity labelling of membrane vesicles 95

2.3.1.1 Chemicals and materials 95

2.3.1.2 Solutions 95

2.3.1.3 Labelling protocol 96

2.3.2 SDS-polyacrylamide gel electrophoresis of photoaffinity labelled membrane vesicles 97

2.3.2.1 Chemicals and materials 97

2.3.2.2 Solutions 98

2.3.2.3 Casting of the gels 99

2.3.2.4 Sample preparation and electrophoresis 100

2.3.2.5 Detection of a labelled protein 100

2.3.2.6 Expression of results 101

2.3.3 Isoelectric focusing (IEF) of photoaffinity labelled membrane proteins 103

2.3.3.1 Chemicals and materials 103

2.3.3.2 Solutions 103
2.3.3.3 Casting of the IEF gels 104
2.3.3.4 Sample preparation and electrophoresis 105
2.3.3.5 Detection of a labelled protein 107
2.3.3.6 Expression of results 107
2.3.4 Papain digestion of membrane vesicles prior to photoaffinity labelling 107
2.3.4.1 Chemicals and materials 108
2.3.4.2 Solutions 108
2.3.4.3 Papain digestion protocol 108
2.4 Isolation and purification of an individual membrane protein 109
2.4.1 Identification of a protein by photoaffinity labelling 110
2.4.2 Isolation of a specific protein using SDS-PAGE slab gels 110
2.4.3 Silver staining 111
2.4.4 Protein isolation and concentration 112
2.4.5 Determination of protein content in the pure sample 112
2.5 Two-dimensional electrophoresis of membrane proteins using an immobilised pH gradient 113
2.5.1 Chemicals and materials 113
2.5.2 Solutions 114
2.5.3 First dimension: Isoelectric focusing 115
2.5.3.1 Sample loading 115
2.5.3.2 Rehydration and isoelectric focusing 116
2.5.4 Equilibration of the focused IPG strip 117
2.5.5 Second dimension: SDS-PAGE 117
2.5.6 Staining of the 2-D gel with brilliant blue G-colloidal 118
2.6 In gel tryptic digest of an individual membrane protein isolated by 2-D electrophoresis 119
2.6.1 Chemicals and materials 119
2.6.2 Solutions 120
2.6.3 Digest protocol 120
2.7 MALDI-TOF mass spectrometric analysis of peptide fragments produced from tryptic digest of a protein 122

2.7.1 Chemicals and materials 122
2.7.2 Concentration and desalting procedure using C_{18} ZipTips 122
2.7.2.1 Solutions 123
2.7.2.2 Procedure 123
2.7.3 MALDI-TOF analysis of peptide fragments 124
2.7.3.1 Solutions 124
2.7.3.2 Sample plate preparation 124
2.7.3.3 Matrix and sample preparation 124
2.7.3.4 Sample analysis 125
2.8 Q-TOF mass spectrometric analysis of peptide fragments produced from tryptic digest of a protein 127
2.9 Protein identification using on-line database searches 129
2.9.1 Data input and search parameters 129
2.9.2 Elimination of false peptides 131

CHAPTER 3: INTERACTION OF A POTENTIAL PHOTOAFFINITY LABEL WITH PEPTIDE TRANSPORTERS IN RAT JEJUNUM
3.1 Development and synthesis of the photoaffinity label 132
3.2 Aims of the experiments 133
3.3 Viability of the vascular perfusions 133
3.4 Transmural transport of [4-azido-D-Phe]-L-Ala across the jejunum 137
3.5 Direct interaction of [4-azido-D-Phe]-L-Ala with peptide transporters 141
3.6 Comparison of the transport properties of D-Phe-L-Ala and [4-azido-D-Phe]-L-Ala 146
3.7 Discussion 152
3.7.1 Peptide transport was studied with an inwardly-directed proton gradient 152
3.7.2 Interaction of the photoaffinity label with PepT1 and the basolateral transporter 153
3.7.3 Asymmetrical binding of [4-azido-D-Phe]-L-Ala to the basolateral peptide transporter 154

3.7.4 Modifications to the D-Phe-L-Ala structure confers an increased affinity for the peptide transporters 156
3.7.5 Stimulation of substrate transport by D-Phe-L-Ala 157
3.8 Conclusions 161

CHAPTER 4: PHOTOAFFINITY LABELLING OF PEPT1 IN RAT JEJUNAL BRUSH-BORDER MEMBRANE VESICLES USING [4-AZIDO-3,5-^{3}H-D-PHE]-L-ALA

4.1 Tritiation of [4-azido-D-Phe]-L-Ala to allow its detection 163
4.2 Purity of BBMV prepared from rat jejunum 163
4.3 Feasibility of using [4-azido-3,5-^{3}H-D-Phe]-L-Ala to identify PepT1 in membrane vesicles 163
4.4 Labelling procedure and expression of results 166
4.5 Photoaffinity labelling of BBMV to identify PepT1 167
4.6 Effect of bestatin on singular identification of PepT1 170
4.7 Papain treatment of BBMV to digest peptide hydrolases 171
4.8 Discussion 174
4.8.1 PAL of BBMV: labelling of peptide hydrolases 174
4.8.2 Distinct molecular weight of PepT1 178
4.8.3 Inhibition of label interaction with peptidases by bestatin 179
4.8.4 Papain digestion of peptidases 180
4.8.5 pH-dependence of label interaction with PepT1 181
4.9 Conclusions 182

CHAPTER 5: IDENTIFICATION OF A CANDIDATE PEPTIDE TRANSPORTER IN THE BASOLATERAL MEMBRANE BY PHOTOAFFINITY LABELLING USING [4-AZIDO-3,5-^{3}H-D-PHE]-L-ALA

5.1 Purity of BLMV prepared from rat jejunum 183
5.2 Viability of using [4-azido-3,5-^{3}H-D-Phe]-L-Ala to identify the basolateral peptide transporter in membrane vesicles 183
5.3 Labelling procedure and expression of results 185
5.4 Photoaffinity labelling of BLMV 186
5.5 Effect of medium osmolarity on label incorporation 189

5.6 Two-dimensional electrophoresis of the photoaffinity labelled basolateral membrane protein 193
5.7 Identification of the candidate basolateral peptide transporter 198
5.7.1 Isolation and purification of the 112 kDa protein from membrane vesicles 198
5.7.2 2-DE of the 112 kDa protein using an immobilised pH gradient 200
5.8 Mass spectrometric sequence analysis 205
5.8.1 MALDI-TOF MS analysis 205
5.8.2 Database searches with the peptide fingerprint 209
5.8.3 Elimination of peptides generated by autolysis of trypsin 211
5.8.4 Is the photoaffinity labelled 112 kDa protein PepT1? 212
5.8.5 Q-TOF MS analysis 212
5.9 Discussion 220
5.9.1 Photoaffinity labelling of BLMV to identify the peptide transporter 220
5.9.2 Isolation of the candidate peptide transporter by 2-DE in rod gels 223
5.9.3 Preparation of the candidate basolateral peptide transporter for sequence analysis 224
5.9.4 Identification of the candidate basolateral peptide transporter 227
5.9.4.1 MALDI-TOF mass spectrometric analysis 227
5.9.4.2 Peptide fingerprint of the candidate basolateral peptide transporter 229
5.9.4.3 Proteolysis of the candidate basolateral peptide transporter 230
5.9.4.4 Database searches 231
5.9.5 Is PepT1 responsible for the basolateral transport of peptides? 233
5.10 Conclusions 234

CHAPTER 6: SHORT-TERM REGULATION OF PEPTIDE TRANSPORT IN RAT JEJUNAL MUCOSA

6.1 Aims of the experiments 236
6.2 Viability of the vascular perfusions 236
6.3 Regulation of peptide transport by leucine 237
6.4 Effect of rapamycin in the vasculature 240
6.5 Effect of rapamycin in the lumen 243

6.6 Effect of wortmannin in the vasculature 246
6.7 Effect of wortmannin in the lumen 249
6.8 Discussion 252
6.8.1 Regulation of basolateral peptide transport by leucine 252
6.8.2 Role of mTOR in leucine/$p70^{S6k}$-stimulated basolateral peptide transport 255
6.8.3 Role of mTOR in the regulation of apical membrane peptide transport 257
6.8.4 Role of PI 3-kinase in leucine/p70S6k-stimulated basolateral peptide transport 259
6.8.5 Role of PI 3-kinase in the regulation of apical membrane peptide transport 260
6.9 Future work 261
6.10 Conclusions 261

CHAPTER 7: DISCUSSION

7.1 Interaction of a potential photoaffinity label with intestinal peptide transporters 263
7.2 Modifications to the D-Phe-L-Ala structure confers an enhanced affinity for the peptide transporters 265
7.3 Identification of PepT1 in the apical membrane 266
7.4 Identification of a candidate basolateral peptide transporter 268
7.5 Sequence analysis of the candidate basolateral peptide transporter 269
7.6 Short-term regulation of intestinal peptide transport 273
7.6.1 Substrate regulation of its own transport 273
7.6.2 Protein kinase cascades involved in regulation of intestinal peptide transport 274

Appendix I: HPLC elution profiles of dipeptide substrates 279
Appendix II: Proteomics search tools 280
Appendix III: Molecular masses of amino acid residues 281
References 282

ACKNOWLEDGEMENTS

I would like to thank Dr. George Kellett for his supervision and constant enthusiasm for the work contained within this thesis. Without the invaluable help and guidance given, it would have been an impossible task.

I would also like to thank other members of my lab, in particular Mrs. Julie Affleck and Mrs. Norma Lister, for not only their technical help in obtaining very important results, but also for their friendship and support throughout my time at York (so far!!). Thank you also to Professor Bronk for advice on the vascular perfusion data. In addition, I owe thanks to are our collaborators in Oxford and Edinburgh, especially to Prof. Pat Bailey and Dr. Ian Collier for the synthesis of the photoaffinity label and other dipeptides used - without which there wouldn't be a thesis. Other people have been indispensible in the acquisition and interpretation of mass spectrometry data; Dr. Dave Ashford for MALDI-TOF analysis, and Alison Ashcroft for Q-TOF analysis.

I must also thank the Wellcome Trust for funding my studies.

Very importantly, I want to give a huge thanks to all of my friends who have supported me, and provided entertainment - mostly in the form of nights out clubbing when the stress became too much; these include Debbie, Vicky, Debs, Amanda, Sam, Collette, Nicola, Sarah, Jo and everyone else, past and present, who I've not mentioned but know who they are.

My parents and family deserve my greatest thanks, for providing emotional and financial support (mum and dad) throughout my time at university, and also for the first 20 or so years of my life. Without them I wouldn't have achieved anything, but with them I can finally get a job!

And finally, to Max - thanks for everything!

ABBREVIATIONS

2-DE:	two-dimensional electrophoresis
[4-azido-D-Phe]-L-Ala:	4-azido-D-Phenylalanyl]-L-Alanine
4-HCCA:	α-cyano-4-hydroxy cinnamic acid
ACE inhibitors:	angiotensin-converting enzyme inhibitors
AmBic:	ammonium bicarbonate
APS:	ammonium persulphate
ATP:	adenosine 5'-triphosphate
BBM(V):	brush-border membrane (vesicles)
BLM(V):	basolateral membrane (vesicles)
Bq:	Becquerels
BSA:	bovine serum albumin
CCCP:	carbonyl cyanide *p*-trichloromethoxyphenylhydrazone
cDNA:	complementary DNA
CHO cells:	Chinese hamster ovary cells
DAG:	diacylglycerol
DEPC:	diethylpyrocarbonate
D-Phe:	D-Phenylalanine
D-Phe-L-Ala:	D-Phenylalanyl-L-Alanine
D-Phe-L-Gln:	D-Phenylalanyl-L-Glutamine
Dpm:	disintegrations per minute
EDTA:	diaminoethanetetra-acetic acid disodium salt
EST:	expressed sequence tag
FCCP:	carbonyl cyanide *p*-trifluoromethoxyphenylhydrazone
FRAP:	FK506-binding protein rapamycin-associated protein
Gly:	glycine
Gly-Gln:	glycylglutamine
Gly-Phe:	glycylphenylalanine
Gly-Pro:	glycylproline
Gly-Sar:	glycylsarcosine
hPepT1:	human PepT1
HPLC:	high performance liquid chromatography

IEF:	isoelectric focusing
IPG:	immobilised pH gradient
kBq:	kiloBecquerels
L-Gln:	L-Glutamine
L-Leu:	L-Leucine
MALDI-TOF MS:	matrix assisted laser desorption/ionisation time of flight mass spectrometry
MAPK:	mitogen-activated protein kinase
MDCK cells:	Madin-Darby canine kidney cells
MES:	2-[N-Morpholino]ethanesulphonic acid
mTOR:	the mammalian target of rapamycin
NBD-Cl:	7-chloro-4-nitrobenz-2-oxa-1,3-diazole
NEM:	*N*-ethylmaleimide
NHE-3:	Na^+/H^+ exchanger 3
NMR:	nuclear magnetic resonance
$p70^{S6k}$:	p70 S6 kinase
PAL:	photoaffinity labelling
PCA:	perchloric acid
PCMBS:	*p*-chloromercuri-benzenesulfonic acid
pI:	isoelectric point
PI 3-kinase:	phosphatidylinositol 3-kinase
PKA/B/C:	protein kinase A/B/C
PMSF:	phenylmethylsulphonylfluoride
POT/PTR family:	proton-dependent oligopeptide transport family
PtdIns-3,4,5-P_3:	phosphatidylinositol-3,4,5-triphosphate
Q-TOF MS:	quadrupole time of flight mass spectrometry
SDS-PAGE:	sodium dodecyl sulphate polyacrylamide gel electrophoresis
SGLT1:	sodium glucose cotransporter
TCA:	trichloroacetic acid
TFA:	trifluoroacetic acid
TGN:	trans-Golgi network
TM domains:	transmembrane domains
TTFB:	tetrachlorotrifluoromethylbenzimidazole

DECLARATION

Some of the data which was used in the preparation of this thesis has been presented in the form of oral and poster communications at the following scientific meetings:

The Physiological Society Meeting, Cambridge, July 2000.
The Physiological Society Meeting, London, December 2000.
The Rank Prize Fund Meeting, Grasmere, Cumbria 2001.

The following refereed abstracts have been published:

Shepherd, E.J., Affleck, J.A., Lister, N., Bronk, J.R., Kellett, G.L., Boyd, C.A.R., Collier, I.D. & Bailey, P.D. (2000). Identification of a candidate peptide transporter in the basolateral membrane of rat intestinal mucosa. *J. Physiol.* **527.P** 35P.

Shepherd, E.J., Lister, N., Bronk, J.R., Kellett, G.L., Boyd, C.A.R., Collier, I.D., and Bailey, P.D. Regulation of peptide transport across the intestinal basolateral membrane by leucine. *In press.*

COLLABORATIONS

Initial experiments using the photoaffinity labelling technique were performed by Mrs. Julie Affleck, who has also provided technical help with other subsequent experiments in this field, in particular the final 2-D gel.

Initial experiments on the short-term regulation of transport using the vascular perfusion technique were performed by Mrs. Norma Lister, who also performed a number of additional experiments, therefore enabling a greater variation of regulatory conditions to be researched.

Despite this, I solely designed and performed the vast majority of experiments myself and carried out all of the data analysis.

LIST OF FIGURES

Figure 1.1	Structure of the lining of the small intestine	3
Figure 1.2	The vascular system of the small intestine	6
Figure 1.3	Structural polarity of an absorptive cell of the small intestine	8
Figure 1.4	Uptake of peptides into BBMV indicating active transport	20
Figure 1.5	Transport systems involved in intestinal peptide absorption	22
Figure 1.6	Membrane model of the intestinal peptide transporter, PepT1	36
Figure 1.7	Effect of substrates on the membrane potential of the small intestine	45
Figure 1.8	Template for the substrate binding site of PepT1	52
Figure 1.9	Structure of cephalosporins	55
Figure 1.10	Long-term regulation of peptide transport; PepT1 abundance in the apical membrane	65
Figure 1.11	Long-term regulation of peptide transport; mRNA abundance and half life	66
Figure 2.1	Vascular perfusion apparatus	77
Figure 2.2	Schematic diagram of the operative procedure for vascular perfusions	79
Figure 3.1	Structure of the photoaffinity label ([4-azido-D-Phe]-L-Ala)	134
Figure 3.2	Glucose utilisation by the isolated jejunum during vascular perfusion	136
Figure 3.3(I)	Transport of D-Phe-L-Gln and [4-azido-D-Phe]-L-Ala	139
Figure 3.3(II)	Tissue accumulations and exit ratios of D-Phe-L-Gln and [4-azido-D-Phe]-L-Ala	140
Figure 3.4(I)	Effect of [4-azido-D-Phe]-L-Ala on transport of D-Phe-L-Gln	143
Figure 3.4(II)	Effect of [4-azido-D-Phe]-L-Ala on tissue accumulation and exit ratios of D-Phe-L-Gln	144
Figure 3.5	Perturbation method of vascular perfusions with D-Phe-L-Gln	145

Figure 3.6(I)	Transport of D-Phe-L-Gln, [4-azido-D-Phe]-L-Ala and D-Phe-L-Ala	147
Figure 3.6(II)	Tissue accumulations and exit ratios of D-Phe-L-Gln, [4-azido-D-Phe]-L-Ala and D-Phe-L-Ala	148
Figure 3.7(I)	Effect of D-Phe-L-Ala on transport of D-Phe-L-Gln	150
Figure 3.7(II)	Effect of D-Phe-L-Ala on tissue accumulation and exit ratios of D-Phe-L-Gln	151
Figure 3.8	Relationship between luminal concentration and transport of D-Phe-L-Gln	159
Figure 4.1	Structure of the radioactive photoaffinity label ([4-azido-3,5-^{3}H-D-Phe]-L-Ala)	164
Figure 4.2	Enzyme assays of BBMVs	165
Figure 4.3	Photoaffinity labelling of BBMV	168
Figure 4.4	Substrate inhibition of labelling of BBMV	169
Figure 4.5	Effect of bestatin on labelling of BBMV	172
Figure 4.6	Extent of inhibition on labelling of BBMV by bestatin	173
Figure 4.7	Effect of papain digestion on labelling of BBMV	175
Figure 4.8	Extent of inhibition on labelling of BBMV by papain digestion	176
Figure 5.1	Enzyme assays of BLMVs	184
Figure 5.2	Photoaffinity labelling of BLMV	187
Figure 5.3	Substrate inhibition of labelling of BLMV	188
Figure 5.4	SDS-PAGE analysis of the photoaffinity labelled BLM protein	190
Figure 5.5	Effect of osmolarity on photoaffinity labelling of BLMV	191
Figure 5.6	Inhibition of labelling by medium osmolarity	192
Figure 5.7	Multiple, identical photoaffinity labelling of unprotected BLMV	195
Figure 5.8	IEF of the labelled 112 kDa protein from BLM	196
Figure 5.9	SDS-PAGE analysis of the 112 kDa protein following IEF	197
Figure 5.10	IEF of free [4-azido-3,5-^{3}H-D-Phe]-L-Ala	199
Figure 5.11	Calibration curve gel to determine protein content of sample	201

Figure 5.12	2-DE of the isolated 112 kDa protein	203
Figure 5.13	2-DE of the isolated 112 kDa protein plus protease-inhibitors	204
Figure 5.14	MALDI-TOF spectra showing monoisotopic peaks of a peptide	206
Figure 5.15	MALDI-TOF spectra of tryptic digest fragments if spot A	207
Figure 5.16	MALDI-TOF spectra of tryptic digest fragments if spot B	208
Figure 5.17	Primary amino acid sequence of rat PepT1	213
Figure 5.18	Q-TOF spectra showing peptide peaks of spot A	216
Figure 5.19	Q-TOF fragmentation sites within a peptide backbone	217
Figure 5.20	Q-TOF fragmentation of a tryptic peptide fragment from spot A	218
Figure 6.1(I)	Regulation of peptide transport by leucine	238
Figure 6.1(II)	Localisation of the regulation of peptide transport by leucine	239
Figure 6.2(I)	Effect of vascular rapamycin on the leucine-stimulation of peptide transport	241
Figure 6.2(II)	Localisation of the effect of vascular rapamycin on the leucine-stimulation of peptide transport	242
Figure 6.3(I)	Effect of luminal rapamycin on the leucine-stimulation of peptide transport	244
Figure 6.3(II)	Regulation of peptide transport by vascular leucine and luminal rapamycin	245
Figure 6.4(I)	Effect of vascular wortmannin on the leucine-stimulation of peptide transport	247
Figure 6.4(II)	Regulation of peptide transport by vascular leucine and wortmannin	248
Figure 6.5(I)	Effect of luminal wortmannin on the leucine-stimulation, and control levels, of peptide transport	250
Figure 6.5(II)	Regulation of peptide transport by vascular leucine and luminal wortmannin	251
Figure 6.6	$p70^{S6k}$-dependent pathway which regulates basolateral membrane peptide transport	256

LIST OF TABLES

Table 1.1	History of peptide absorption	12
Table 1.2	Predominant reasons for the fall of the 'Classical hypothesis'	14
Table 1.3	Proteins with sequence similarity to peptide transporters	30
Table 1.4	Species comparison of PepT1 structural features	38
Table 1.5	Comparison of PepT1 and PepT2 structure and function from rat	39
Table 1.6	Stereospecificity study using dipeptides	47
Table 1.7	Kinetic comparison of PepT1 and the basolateral transporter	60
Table 3.1	Explanation of tissue exit ratios	138
Table 4.1	Photoaffinity labelling of BBMV	169
Table 4.2	Effect of bestatin on labelling of BBMV	173
Table 4.3	Effect of papain digestion on labelling of BBMV	176
Table 5.1	Photoaffinity labelling of BBMV	188
Table 5.2	Effect of medium osmolarity of labelling of BLMV	192
Table 5.3	MALDI-TOF peptide fingerprint of spots A & B	210
Table 5.4	Tryptic peptide fragments of spots A & B which match to rat PepT1	214
Table 5.5	Sequence tag of a tryptic peptide from spot A	219
Table 5.6	Partial amino acid sequence comparison to known proteins from databases	221

ABSTRACT

Oligopeptide transport in rat small intestine has been studied in intact tissue, using the luminally and vascularly perfused isolated jejunum *in situ* technique, and a hydrolysis-resistant dipeptide (D-Phe-L-Gln). The data in this thesis can be divided into two main sections: (1) identification of the transporter proteins, and (2) short-term regulation of transport.

The basolateral peptide transporter protein has not, to date, been identified. A candidate protein was identified from membrane vesicles by a photoaffinity labelling technique using a dipeptide derivative ([4-azido-3,5-^{3}H-D-Phe]-L-Ala), previously shown to be an efficient substrate for the basolateral transporter. The labelled candidate protein was successfully isolated by 2-DE, which revealed an apparent M_r of 112 ± 2 kDa and a pI of approximately 6.5. Initial sequence analysis, tryptic digestion followed by MALDI-TOF analysis and Q-TOF fragmentation of a tryptic peptide, produced a peptide fingerprint and a sequence tag of 9 amino acids, respectively, which, together, did not completely and conclusively match to any known protein sequence contained within databases, therefore suggesting that the 112 kDa protein may be novel.

Short-term regulation of peptide transport was also investigated using the vascular perfusion method. An amino acid-sensing pathway was discovered, using L-Leucine as the regulator, involving protein kinase cacades leading to $p70^{S6k}$ activation and subsequent stimulation of basolateral membrane peptide transport.

A major conclusion arising from the data was the distinction between PepT1 and the basolateral transporter, i.e. the sequence data obtained from the candidate protein did not match to the PepT1 sequence; in addition there appeared to be distinct mechanisms of regulatory control at the two membranes.

Efficient delivery of peptidomimetic drugs when adminsitered by the oral route requires knowledge of short-term regulation of intestinal peptide transport, in addition to the sequence and structure of the basolateral transporter. This thesis provides essential information, which may eventually contribute to the unequivocal identification and sequencing of the intestinal basolateral peptide transporter, ultimately leading to the future development of compounds with high bioavailability.

CHAPTER 1: INTRODUCTION

1.1 ANATOMY OF THE SMALL INTESTINE

1.1.1 Basic structure and functions

The small intestinal epithelium, as with many other epithelia, has the immense task of separating the general internal milieu of the organism from a harsh external environment. The main duties of the epithelium are to act as a major barrier to potentially threatening luminal agents, for example ingested bacteria or antigens in food, in addition to participating in the digestion and selective absorption of major nutrients whilst actively absorbing and/or secreting electrolytes and water. Due to the vast extent of its roles, the epithelium is structurally complex and its precise architectural design enhances its functional capabilities.

The small intestine is part of the alimentary canal, beginning at the pyloric valve of the stomach and terminating at the caecum. Three consecutive sections; the duodenum, jejunum and ileum, constitute its total length (approximately 6 m in humans).

The duodenum is the most proximal region and also the smallest of the three, forming only one twelfth of its total length. It originates at the pyloric valve of the stomach and descends to the ligament of Treitz. It is secured to the rear wall of the abdominal cavity by attachment to the mesentery (membranous tissue), in contrast to the remainder of the small intestine, which is able to move freely (Moog, 1981).

The jejunum commences at the ligament of Treitz, and is anatomically located in the upper left side of the abdominal cavity. The jejunum comprises one third of the total length of the small intestine and is the predominant site for the absorption of luminal nutrients.

The small intestine terminates after the ileum, the most distal region. The ileum is the longest section and extends to the large intestine via the ileocaecal valve. It occupies the lower abdomen and is not primarily involved in the absorption of nutrients. Both the ileum and jejunum are tightly coiled so as to enable their containment within the peritoneal cavity.

1.1.2 Anatomy of the intestinal wall

All three longitudinal sections of the small intestine possess an identical structural organisation. The walls are composed of four concentric layers; the serosa, muscularis, submucosa (the three outer strata) and the mucosa itself (figure 1.1a) (Moog, 1981). The serosa is the layer most distant from the lumen and is formed by visceral peritoneum combining with connective tissue. It is in direct contact with the vascular system of capillaries. The muscularis lies close to its inner surface. This layer consists of two discrete types of muscle, longitudinal and circular; the two types collectively function to maintain the overall shape of the small intestinal wall. Adjacent to the muscle layer is the submucosa, containing the blood and lymph vessels. The submucosa is a deep, connective tissue layer that physically supports the mucosa.

The mucosa is the most physiologically significant tissue region in terms of nutrient absorption. It is an aggregate of three separate layers; the muscularis mucosa, lamina propria and the epithelial layer, each having distinct roles due to their highly specific structures. The muscularis mucosa is the outermost sheath of this tissue and forms a muscle sheet, three to ten cells deep. Contraction of these muscle cells causes movement of the villi and secretion of mucous from goblet cells. The lamina propria is adjacent to the muscularis and underlies the epithelium. It consists of glycosaminoglycan chains, entangled and cross-linked to produce a gel-like structure, forming a continuous connective tissue that acts as a mechanical support for the epithelium. It contains many different cells which confer its immunological importance, e.g. plasma cells, lymphocytes and macrophages. An additional role is that it permits the transfer of nutrients away from the intestine via its blood vessels. Small nerve fibres are sparsely scattered throughout the lamina propria and by releasing substances, such as biologically active peptides or neurotransmitters, these nerves may potentially regulate epithelial function. The epithelial layer is the only tissue of the small intestine in direct contact with the luminal contents. It cellular constituents are described in section 1.1.4.

The surface area of the intestine is greatly enhanced by three specialised structural features that extend into the lumen (in commonly used laboratory animals only the latter two are found) (Moog, 1981).. These structures, in order of diminishing size and increasing physiological importance, are designated the circular

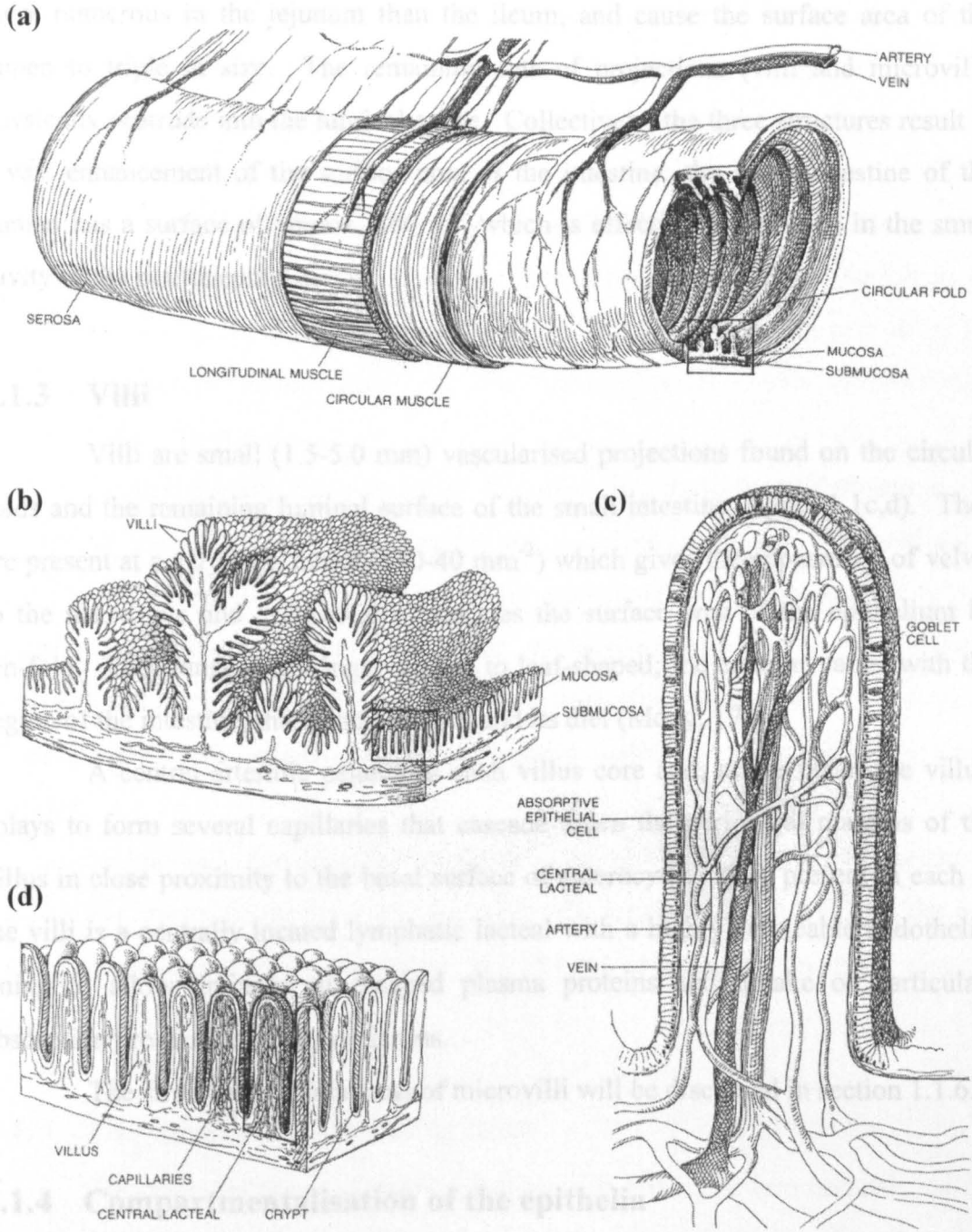

Figure 1.1

Structure of the lining of the small intestine, in particular; the organisation of the intestinal wall (a), and the circular folds (plicae circulares) (b) and villi (c,d) which function to increase the absorptive area of the luminal surface. Source: Moog (1981).

folds, villi and microvilli. The circular folds (plicae circulares) are ridges of approximately 8-10 mm that are orientated circumferentially around the lumen (figure 1.1b). They are periodically found in one-half to two-thirds of the lumen, more numerous in the jejunum than the ileum, and cause the surface area of the lumen to triple in size. The remaining sets of projections (villi and microvilli) physically protrude into the luminal space. Collectively, the three structures result in a vast enhancement of the surface area of the intestine; the small intestine of the human has a surface of approx. 300 m^2, which is effectively contained in the small cavity of the peritoneum.

1.1.3 Villi

Villi are small (1.5-5.0 mm) vascularised projections found on the circular folds and the remaining luminal surface of the small intestine (figure 1.1c,d). They are present at a very high density (10-40 mm^{-2}) which gives the appearance of velvet to the naked eye and dramatically increases the surface area of the epithelium by ten-fold. They range from finger-shaped to leaf-shaped; the contour varies with the region of the intestine, the animal species and its diet (Moog, 1981).

A central arteriole penetrates each villus core and, at the tip of the villus, splays to form several capillaries that cascade down the peripheral margins of the villus in close proximity to the basal surface of enterocytes. Also present in each of the villi is a centrally located lymphatic lacteal with a highly permeable endothelial lining to allow drainage of escaped plasma proteins and uptake of particulate absorption products, e.g. chylomicrons.

The structure and functions of microvilli will be discussed in section 1.1.6.1.

1.1.4 Compartmentalisation of the epithelia

The small intestinal epithelium can be segregated into three individual compartments; crypts, villi and Peyer's patches, each possessing a distinct cellular composition.

The chief cellular component in the crypts of Lieberkuhn are undifferentiated cells, but also present are enteroendocrine cells, Paneth cells, goblet cells and occasional cuplike cells. The undifferentiated crypt cell acts as a progenitor from which all types of cell originate. The cells migrate towards the villus surface,

with the exception of Paneth cells, and many of the undifferentiated cells begin to acquire structural and functional characteristics of absorptive cells.

The villus base contains nascent absorptive cells originated from the crypt. They migrate up the villus axis (the transient layer of cells on the surface of the villus is only one cell thick), where they reside for a few days at the tip, before being sloughed off from an exclusion zone. The whole process only takes 3-4 days, so a near complete turnover of the epithelium occurs on a weekly basis; approx. 17 billion cells are discarded along the length of human small intestine per day. This cycle of cellular proliferation and migration occurs in roughly the same time period in all mammals. During the migratory period, the cells mature by distinct processes, for example, enterocytes express enzymes involved in digestion while differentiating into their final structure.

Peyer's patches are clusters of follicular domes scattered throughout the intestine at irregular sites, which overlay dense accumulations of lymphoid cells. Larger patches are visible by eye as pale oval plaques on the surface of the epithelium. Although cells present in other compartments are also found in Peyer's patches, a minor population of a functionally important class of cells is also present; M cells provide an effective immune response within the small intestine when required.

In summary, the specific functions of the individual compartments are as follows: the crypts are the sites for electrolyte and water secretion, villi are the loci for electrolyte and nutrient absorption and Peyer's patches are the major sites of antigen sampling from the lumen.

1.1.5 The intestinal vascular system

The aorta supplies the small intestine with blood via two branches of the mesenteric circulation; the superior and inferior mesenteric arteries. Blood exiting the small intestine drains into a tributary of the hepatic portal vein.

Aside from this systemic circulation, there is an additional extensive microcirculation within the small intestinal tissue. The muscularis externa and the mucosa itself have distinct microvasculatures, which are connected in parallel at the level of the submucosa (figure 1.2). The microvasculature of the muscularis externa initially originates from a small artery in the mesentery, which extends into a large

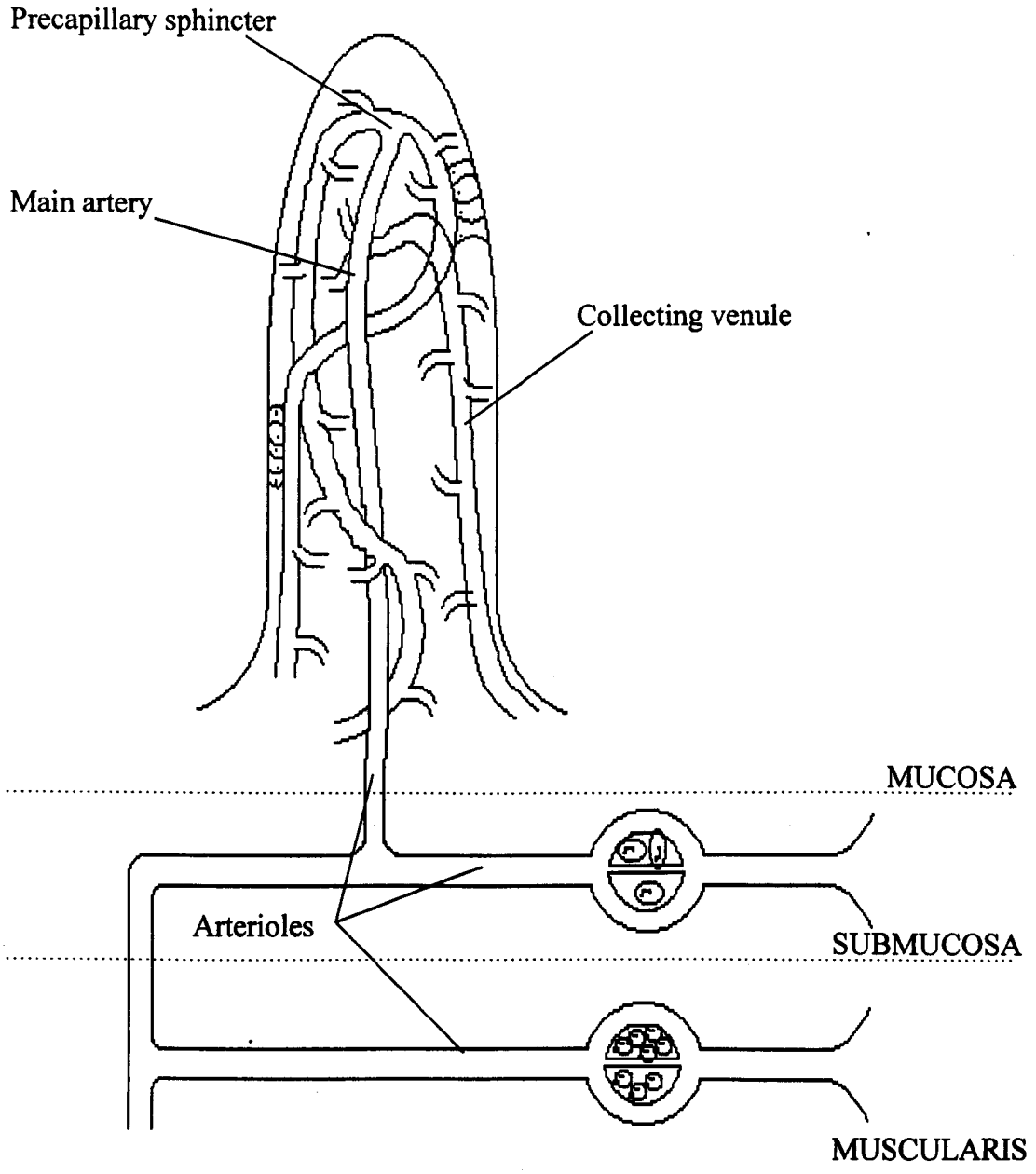

Figure 1.2

Schematic diagram of the vascular system of the small intestine (adapted from Cooke, 1987).

arteriole leading eventually to the microvasculature. The large arteriole penetrates both the longitudinal and circular muscle layers and runs to the outer surface of the submucosa. It then gives rise to smaller second and third order arterioles, which eventually branch to form a complex series of vessels. These vessels lie perpendicular to the muscle fibres and supply the longitudinal and circular muscle capillaries which, in turn, run parallel to the muscle fibres in each layer. These capillaries then join a network of vessels, which return the blood from the muscle, and connect with the small veins in the mesentery.

The vasculature of the mucosa is composed of distinct independent units; each villus has a miniature vascular bed with separate arterial and venous vasculatures. As mentioned previously in section 1.1.3, a single main arteriole supplies the villus; this is usually a terminal extension of a third order arteriole descending from the muscularis mucosa. Blood is drained from the villi by capillaries within the mucosa joining venules, which then lead to collecting venules in the muscularis mucosa. All blood leaving the small intestine does so via the hepatic portal vein.

1.1.6 Absorptive cells

Absorptive cells (enterocytes) are tall columnar cells with a highly polar nature that allows the vectorial transport of ions and nutrients from the lumen of the small intestine eventually to the systemic circulation. The structural polarity of enterocytes can be easily examined using a light microscope, where two distinct plasma membranes at opposing ends of the cell can be observed (figure 1.3a). The two membranes differ both morphologically and biochemically, and meet at the intercellular junctional complex. The cellular location of cytoplasmic organelles also forms the basis for cellular polarity. The nucleus is situated in the basal portion of the cell with the Golgi apparatus directly above. Other organelles are scattered throughout the cytoplasm (including the rough endoplasmic reticulum) whereas the smooth endoplasmic reticulum is most abundant in the apical half of the cell, beneath the terminal web.

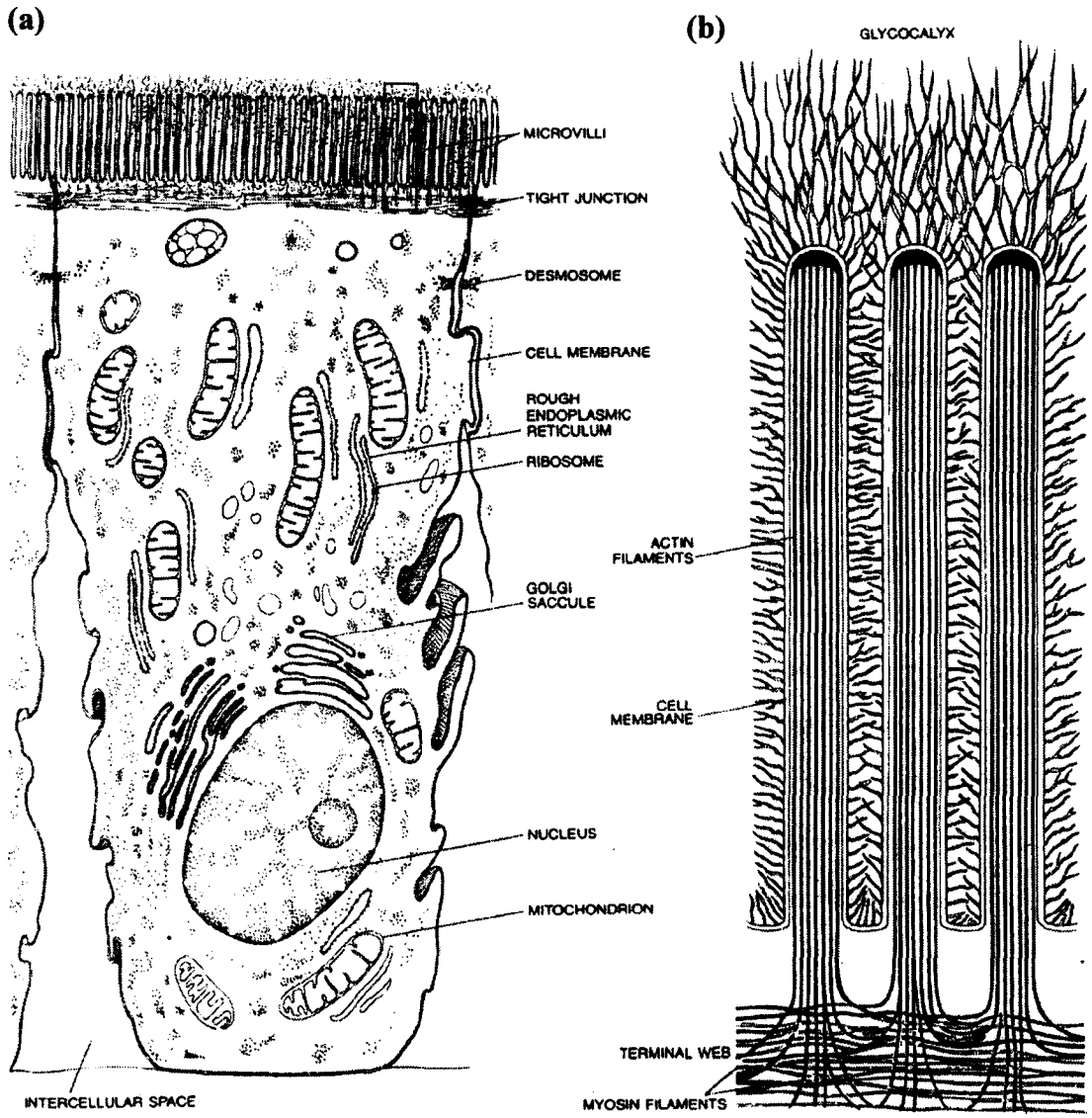

Figure 1.3

Structural polarity of an absorptive cell of the small intestine (a) and an enhanced view of the microvilli at the apical membrane (b), showing the underlying terminal web and surrounding glycocalyx. Source: Moog (1981).

1.1.6.1 The apical membrane

Under the light microscope it can be seen that the apical membrane, facing directly into the lumen of the intestine, has a striated border composed of microvilli, at a density of approx. 2×10^5 mm^{-2}. Microvilli have a relatively uniform height (1 μm); their presence expands the surface area of the epithelium by a factor of 20, thereby significantly increasing the efficiency of the small intestine for nutrient absorption. The apical (or brush-border) membrane has an unusually high protein to lipid ratio (1.7:1) and this, in conjunction with a high cholesterol/glycolipid to phospholipid ratio, confers a relatively low fluidity of the membrane. The brush-border membrane (BBM) is also 20% thicker than plasma membranes in most other mammalian cells (approx. 10 nm), which is also due to the enhanced protein to lipid ratio.

Directly below the microvilli is the terminal web (figure 1.3b). This area is free from organelles but contains proteins such as α-actinin and filamin. It is also integrated with a cytoskeleton consisting of approx. 20-30 microfilaments lying in parallel, which consist of a protein similar to actin. The terminal web, in conjunction with the cytoskeleton, functions to stabilise the microvilli by extending upwards into each individual microvillus to form an internal network. This network provides rigidity and, as the cytoskeleton contracts, it causes brush-border motility which, in turn, causes circulation of the gut contents and maintains continuous contact of the microvilli with nutrients.

Projecting from the surface of the microvilli is a 'fuzzy coat' or glycocalyx (figure 1.3b). This network is composed of thin branching filaments, rich in polysaccharide that extend approx. 0.5-2.0 μm. Aside from forming a separate compartment through which substrates must cross to gain access to the cell, the exact function of the glycocalyx is not clear. Various roles have been speculated, including a barrier to molecular diffusion (Hamilton & McMicheal, 1968), a site for absorption of extracellular enzymes (Pritchard, 1969) and as a protective barrier. It is known to have a considerable influence on the transport properties of the intestine because it interacts with the unstirred water layer (Thompson & Dietschy, 1977).

1.1.6.2 The unstirred water layer

Adjacent to the surface of the apical membrane is an aqueous boundary layer; a proportion of this is trapped within the interstices of the glycocalyx filaments and the remainder forms a distinct region. The presence of the unstirred water layer increases the diffusion path for the movement of solutes which, in turn, influences the kinetics of membrane transport (Thompson & Dietschy, 1977). During investigations using intestinal perfusion techniques it is common to initiate stirring of the bulk medium adjacent to the unstirred water layer to reduce its effects on solute transport (Gardner, 1978).

1.1.6.3 The basolateral membrane

The basolateral (or basal) membrane is structurally, chemically and physically distinct to the apical membrane, i.e. it is of similar composition as the majority of mammalian plasma membranes. In contrast to the presence of microvilli on the BBM, the surface of the BLM forms smooth contours with broad folds that may interdigitate with similar folds of adjacent cells (figure 1.3a). Also in contrast to the brush-border membrane, it has a relatively high fluidity, due to a lower abundance of cholesterol. Its basal surface is closely associated with the basal lamina and an intercellular junctional complex separates it from the apical membrane.

1.1.6.4 Junctional complexes

Junctional complexes, or intercellular attachment zones, form the basis by which adjacent epithelial cells associate. The complex consists of three components that have distinct structural and functional characteristics.

The component situated closest to the lumen is the tight junction (or zona occludens) which binds neighbouring cells just below the microvilli surface. These junctions are known to play an important role in regulating epithelial permeability by influencing the paracellular flow of fluid and ions. The structure of tight junctions appears to correlate inversely with permeability, i.e. as the number of interlocking ridges forming the junction increases, permeability is reduced. In addition to this major permeability role, the tight junction also serves as a barrier to the movement of integral membrane proteins and thereby preserves membrane polarity within the enterocyte.

Directly below the tight junction is the intermediate junction (or zonulae adherens) forming a zone approx. 15-20 nm wide. It is made of a fibrous material that forms a mesh of microfilaments, which radiate into the terminal web. As with the tight junctions, the intermediate junctions bind adjacent enterocytes together to form a continuous sheet as the cells traverse the villi.

The third and final component of the junctional complex is the spot desmosome (or macula adherens). Unlike the tight and intermediate junctions, the spot desmosomes form a discontinuous belt around the cell. The lateral membranes of adjacent cells run parallel and, in the region of the spot desmosomes, the cytoplasm of the cells contains numerous tonofilaments embedded into a disc-like plaque (Kelly, 1966). These tonofilaments loop through the terminal web and attach onto other spot desmosomes. Finer filaments spread from the plaque and anchor onto the tonofilaments and the lateral membrane. The spot desmosomes predominantly function to complete the structure of the junctional complex, to act as attachment sites for stabilising the cytoskeleton and to serve as spot welds between adjacent epithelial cells.

1.2 PEPTIDE TRANSPORT

1.2.1 History of protein absorption

The early theories on protein absorption are covered in great depth by Matthews (1991); a brief description of the key ideas from the last two hundred years concerning the mechanism by which ingested protein is absorbed across the intestinal wall is given here and is summarised in table 1.1.

It was long assumed that digestion predominantly occurred in the lumen of the small intestine and the intestinal lining served only as a passive membrane for the movement of the digestion products into the bloodstream (Moog, 1981). However, investigations into intestinal tissue demonstrated this was not the case. By the early 20th century it was established that proteins comprised of chains of individual amino acids linked by peptide bonds. It had also been realised that the action of trypsin and 'erepsin' (peptidases) resulted in the breakdown of proteins to peptones (small peptides) and amino acids, respectively. Absorption of intact proteins was no longer thought probable; digestion of proteins to peptones occurred, and the peptones were

Haller (mid 18th century)	A substance that was an essential constituent of animal and plant tissue was discovered; this substance resembled modern protein.
Hallé (1792)	**Theory of animalisation of vegetable matter;** nitrogen was incorporated into plant material in the lumen of the gut by highly nitrogenous intestinal secretions. Other theories suggested incorporation of nitrogen from the air.
Dumas (1843)	**Solution theory;** protein was dissolved within the gut lumen into a form that could be absorbed.
Prout (1843)	The level of protein 'lowered' during digestion and formed Albuminose, which was later renamed as 'peptones' by Lehman in the 1950's.
Funk (1850's)	**Proteins were absorbed as peptones** by a combination of passive processes i.e. filtration, simple diffusion and osmosis. This theory was not widely accepted for a number of years because peptones could not be detected in the blood.
Cohnheim (1901)	**Erepsin** was discovered and shown to digest peptones to their constituent free amino acids.
1920-1950	**'Classical Theory of protein absorption':** proteins are digested completely to amino acids before passive absorption into the tissue.
Van Syke & Meyer (1921)	α-amino nitrogen detected in blood
Cathcart (1921)	Demonstration that the **intestinal tissue could accumulate intact peptides**. This theory was also overlooked at the time.
Wiseman (1951)	**Active transport of amino acids** was demonstrated; additional experiments confirming this theory soon followed.
Matthews (1968)	Formation of the **'Dual Hypothesis'** due to the transmural transport of intact peptides. This was the beginning of the end for the 'Classical Theory of protein absorption'.

Table 1.1

A summary of historically important ideas regarding the mechanism of intestinal protein absorption (Matthews, 1991).

readily, but passively, absorbed from the lumen by the gut tissue. However, scepticism with regard to this process flourished due to the fact that peptones could not be detected in the tissues or in blood (in retrospect this was due to the insensitivity of the assay methods used) and this theory, which is similar to the modern view, was completely overlooked for many years.

The 'Classical Hypothesis of Protein Absorption' was widely accepted by the 1920's; ingested protein was thoroughly digested to free amino acids within the gut lumen and the amino acids were absorbed across the intestine into the bloodstream via passive mechanisms. Confirmation of this theory came with the detection of α-amino nitrogen in the bloodstream. Despite the controversial recognition by Cathcart (1921; see Matthews, 1991) that small peptides could be absorbed intact by tissues, this 'Classical Theory' dominated the world of protein absorption for more than 30 years.

In the 1950's, Wiseman (1951; see Matthews, 1991) demonstrated that the transport of amino acids was an active process and, due to this revelation, the cellular mechanism of amino acid transport and protein absorption in general, received much attention. A great number of advances were made; transport was shown to be saturable, sodium-coupled and to obey Michaelis-Menten kinetics, mutual inhibition between some amino acids was observed and the idea was formed that different systems existed for the transport of distinct amino acids.

Some years later, between 1956 and 1964, Newey and Smyth demonstrated that small peptides could be absorbed intact into the intestinal wall and then underwent cytosolic degradation to their constituent amino acids, the form in which they were released into the serosa (Newey & Smyth, 1960). The 'Dual Hypothesis' was instigated by the demonstration of transmural peptide transport by Matthews (1968; see Matthews, 1991), who stated that protein could be absorbed across the intestine in two ways; peptide transport followed by intracellular hydrolysis or luminal hydrolysis followed by amino acid absorption. These revelations, coupled with ever-increasing evidence that the 'Classical Hypothesis' could not adequately explain many experimental observations (table 1.2), opened the way for studies into the importance and mechanism of peptide transport in protein absorption. Therefore, some 20 years after the controversial revelations by Cathcart, the process of intact peptide absorption was finally accepted.

Predominant reasons for the fall of the 'Classical Hypothesis of protein absorption'

(1) Complete intraluminal peptide hydrolysis to amino acids was never unequivocally demonstrated

(2) Long standing notion that intestinal peptidases did not function in the lumen

(3) Absorption of protein and free amino acids were equally as rapid

(4) During protein absorption, amino acid plasma levels peaked prior to intracellular levels of the enterocytes

(5) Inferiority of amino acid mixtures in simulating protein composition

(6) Emergence of numerous reports claiming large scale entry of peptides into the blood

(7) Absence of protein malnutrition in patients with amino acid absorption diseases e.g. Hartnup disease and cystinuria

(8) Initial experiments examining peptide transport showed that dipeptide hydrolysis occurred at an intracellular location and not in the lumen.

Table 1.2

A summary of the experimental observations that could not be fully explained by the 'Classical Theory' of protein absorption (Matthews, 1991).

1.2.2 Peptide transport

The transmembrane transport of peptides is a phenomenon widely distributed throughout nature; it is found in animals (including man), in bacteria, in yeast, in mould and also in germinating seeds of higher plants (Matthews, 1991). Peptide transport is not only conserved as a process throughout evolution, its operational mechanism has also been stringently preserved. In biological systems, the transport of organic solutes is an active step coupled primarily to transmembrane ion gradients. The principal inorganic coupling ion in microbes is H^+, and it is the proton-motive force that provides the primary energy source for solute transport. In contrast the principal coupling ion in the animal kingdom is Na^+, though peptide transport is an exception. The energetics of ion-coupled peptide transport are unique; the evolutionary shift in the coupling ion, i.e. from H^+ to Na^+, that occurred in the case of amino acids and sugars, did not occur in the case of peptides, and this alone distinguishes it from most other mammalian solute transport processes.

1.2.2.1 Advancement in the study of peptide transport

The cellular mechanism of peptide transport has only been seriously investigated for about the last 20 years and so our understanding of the precise nature of transmural peptide transfer across the membrane has fallen considerably behind that for amino acid and sugar transport. A major obstacle in the progression of our comprehension of peptide transport has been due to the reluctance of many different groups, who were interested in absorption, to accept its important nutritional role. Furthermore, a lack of suitable hydrolysis-resistant substrates with which to investigate the characteristics of transport only augmented this mainstream resistance. A couple of major advances rapidly paved the way for a great number of studies into peptide transport; the first was the development of the method for efficiently isolating membrane vesicles (Sigrist-Nelson, 1975) and the second was the realisation that Gly-containing di- and tripeptides were relatively resistant to hydrolysis.

1.2.2.2 Sites of oligopeptide transport

The small intestine is obviously an important site of protein absorption from a nutritional point of view and therefore much attention has focused on the

mechanisms of oligopeptide (di- and tripeptide) transport in this tissue. In addition to an intestinal location, other important sites of transmural peptide transfer have now been recognised in various epithelial tissues; these include the apical membrane of the kidney proximal tubule, the lung (Meredith & Boyd, 1995) and the placenta (Meredith & Laynes, 1996). Peptide transport in the kidney proximal tubule serves to reabsorb peptides from the tubule lumen, including those from the glomerular filtrate, and also oligopeptides formed from the action of brush-border membrane peptidases on large filtered endogenous peptides.

1.2.2.3 Importance of peptide transporters

The function of peptide transporters has three distinct implications; nutritional, pharmacological and clinical.

1.2.2.3.1 Nutritional implications

Peptide transporters in both the intestine and the kidney are involved in the nutritional status of the organism, in a direct and indirect manner, respectively. The absorption of protein digestion products occurs primarily as peptides, not amino acids; intact uptake of peptides provides an efficient and economic route for cells to absorb amino acids which are needed for growth and development. Early experiments have shown that 3 h after a protein meal, the intestinal lumen contains a higher proportion of peptides than amino acids (Adibi & Mercer, 1973; see Matthews, 1991); approx. 80% of jejunal contents were in the form of small peptides (2-4 amino acids) and the remainder in the form of free amino acids. It is also well known that peptides are absorbed more rapidly than free amino acids (Matthews, 1991). In addition, more than 50% of the plasma amino acid pool is in the form of peptides, one quarter to a half of this percentage are di- or tripeptides (Leibach & Ganapathy, 1996).

Peptide transporters in the kidney play a role in conserving the peptide-bound amino nitrogen, which would otherwise be lost in the urine; the excretion of peptide-bound amino acids in the urine is extremely low demonstrating the efficiency of the system.

1.2.2.3.2 Clinical implications

In current clinical practice, small peptides are seriously considered as viable substitutes for free amino acids to provide a nitrogen source in enteral and parenteral solutions. These peptide solutions may provide an absorptive advantage to patients that have a severely reduced intestinal absorptive area and also to patients who are acutely catabolic (trauma, sepsis or burns) (Leibach & Ganapathy, 1996). The use of peptides, rather than free amino acids, has several advantages, for example it is well known that all amino acids are absorbed more efficiently as part of a peptide than alone, with the exception of arginine (Adibi, 1997). In addition, the absorption of free amino acids is highly selective whereas the absorption of peptides is less so, possibly due to the carrier having a greater capacity for transport and a very broad substrate specificity. Certain free amino acids cannot be included in enteral solutions for various reasons, e.g. glutamine is very unstable and tyrosine is insoluble, and so current elemental diets are lacking in them. The use of peptides can be used to overcome this major problem. Elemental diets are also very hypertonic; this high pressure can be reduced with the replacement of amino acids for peptides. A reduced osmolarity is an advantage especially for patients with severe fluid restriction (Leibach & Ganapathy, 1996).

1.2.2.3.3 Pharmacological implications

A number of orally active peptide antibiotics possess structural features similar to physiologic substrates of the peptide transporters. They are accepted as substrates by the peptide carriers; the transporters in the lumen of the intestine act as vehicles for their efficient absorption when administered by the oral route. The relative efficacy of the peptidomimetic drugs is determined by their relative affinity for the peptide transporters; their pharmacological potency is not only determined by their rate of absorption from the small intestine, but also by their half-life in circulation. Peptide transporters in the kidney are responsible for the reabsorption of these drugs from the glomerular filtrate and function to prolong their time spent in the bloodstream (i.e. increase their bioavailability) in order to aid in their pharmacological action. Peptidomimetic drugs can be used to treat infection (β-lactam antibiotics), hypertension (angiotensin-converting enzyme (ACE) inhibitors and renin inhibitors) and cancer (bestatin). Intravenous administration of

drugs is often associated with a wide range of potential problems, which can be avoided with an oral delivery.

It has also been suggested that peptide transporters, in conjunction with the action of cytosolic peptidases, can be exploited for the systemic delivery of certain drugs in the form of peptide pro-drugs. For example, α-methyldopa is a poorly-absorbed antihypertensive agent and amino acid analogue. Dipeptide analogues of α-methyldopa, for example, L-α-methyldopa-Phe (Tsuji *et al.*, 1990) and L-α-methyldopa-Pro (Hu *et al.*, 1989), are found to be absorbed from the intestinal lumen significantly better than α-methyldopa because they can utilise the peptide transporters. Once inside the enterocyte the peptide analogues are hydrolysed by cytosolic peptidases to release L-α-methyldopa.

There are also possibilities of utilising oligopeptide transporters in the chemotherapeutic treatment of cancer. A dipeptide transport system, which is similar, but not identical to PepT1 and PepT2, has been discovered in fibroblast-derived tumour cells but which is not present in normal fibroblast cells (Nakanishi *et al.*, 1997). This novel finding could form the basis for a strategy in the delivery of peptidomimetic anticancer drugs specifically into the tumour cells. However, further work is required in order to elucidate whether there is selective expression of this transport system in various tumour cells, but not in normal cells.

1.2.3 Mechanism of peptide transport

1.2.3.1 Driving force for active transport

Peptide transport was demonstrated to be an active process by early studies using everted sacs of hamster jejunum (Addison *et al.*, 1972); Gly-Sar was shown to accumulate inside the jejunal sacs. However, unlike amino acid transport, peptide transport was not driven by a sodium gradient, demonstrated by sodium replacement experiments (Cheeseman & Parsons, 1974). Boyd & Ward (1982) revealed that peptide transport was electrogenic (i.e. influenced by changes in membrane potential) by investigations in which the application of neutral peptides (Leu-Leu, Val-Val) to the apical membrane of the mud puppy *Necturus maculosus* small intestine, even in the absence of sodium, caused depolarisation of the membrane. The use of peptides with no net charge signified that the membrane depolarisation was not due to the flux

of the peptide itself, but that the flow of another ionic species was associated with entry of the peptide into the epithelium.

The stimulation of peptide transport by an inwardly directed proton gradient (suggesting H^+-coupled transport) was initially detected using intestinal epithelial brush-border membrane vesicles (BBMV) by Ganapathy & Leibach (1983). They found that peptide uptake was optimal at an extravesicular pH of 5.5-6.0. It was thought that this optimisation in transport was not a result of a change in the abundance of transportable zwitterionic species of the peptides used (Gly-Pro, carnosine), because they have widely different pI values (5.8 and 8.7, respectively). Neither was it due to a change in external pH *per se*, but a result of generating an inwardly directed H^+ gradient, due to the acidity of the external medium relative to intracellular medium. An equivalent stimulation of peptide transport in renal BBMV was demonstrated virtually simultaneously by subsequent experiments performed by Ganapathy *et al.* (1984) and Takuwa *et al.* (1985). In particular, Takuwa and colleagues revealed that the uptake of Gly-Gly into BBMV exhibited the classical 'overshoot' phenomenon (figure 1.4), providing the first evidence for the transient uphill transport of the peptide against its concentration gradient.

Ganapathy & Leibach (1983) agreed with previous investigations by Boyd & Ward (1982) that the H^+ gradient-dependent transport of peptides was electrogenic. An inside-negative membrane potential (generated by valinomycin) enhanced the proton-dependent transport of Gly-Pro two-fold, whereas an inside-positive membrane potential (generated by FCCP) significantly reduced transport. This indicated that peptide transport across the brush-border membrane was associated with the net transfer of a positive charge. This proton-dependent and membrane potential-stimulated transport of zwitterionic peptides also occurred in the absence of Na^+, suggesting that peptides were cotransported with a cation other than Na^+. Further work by Ganapathy & Leibach (1985) demonstrated the specific inhibition of H^+ gradient-stimulated transport by the presence of a proton ionophore; this was the first real indication that H^+ may be cotransported with peptides and, therefore, that an electrochemical H^+ gradient might be the driving force for peptide transport.

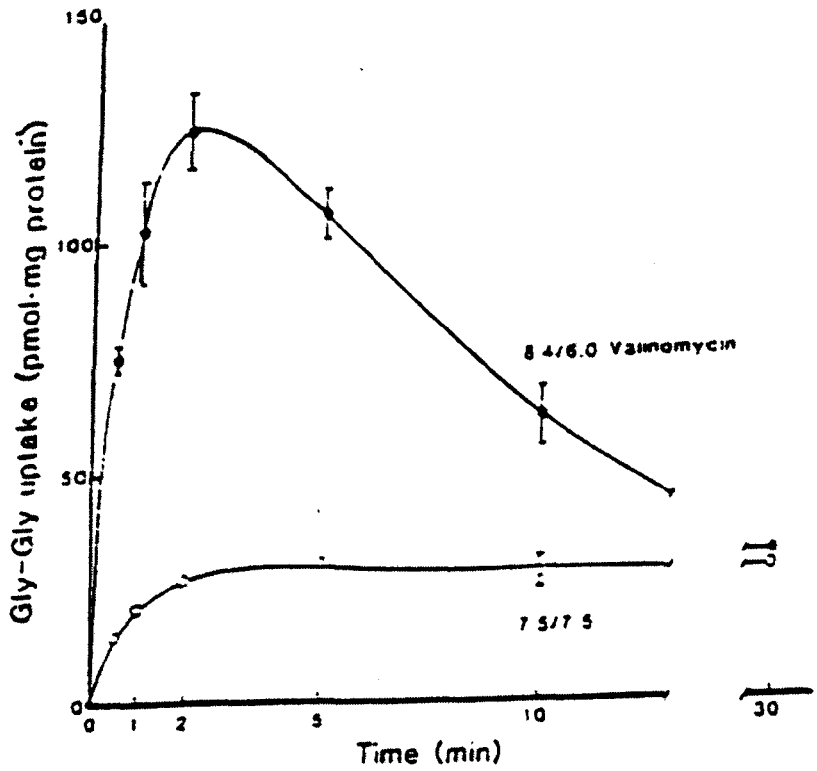

Figure 1.4

The time course for the uptake of the neutral dipeptide (Gly-Gly) into renal brush-border membrane vesicles in the absence (open symbol) and presence (filled symbol) of an inwardly directed proton gradient and an inside negative membrane potential. The transport of Gly-Gly exhibits the classical 'overshoot' phenomenon in the presence of an electrochemical H^+ gradient, demonstrating that the transport of the peptide is an active step and is performed against its concentration gradient. Source: Takuwa *et al.* (1985).

1.2.3.2 Role of the acidic microclimate

The presence of an acidic microclimate, an area of low pH immediately adjacent to the brush-border membrane, has been well documented. The first evidence of its existence *in vitro* was achieved using everted sacs of rat proximal jejunum by Lucas *et al.* (1975), using microelectrodes. It was then demonstrated *in vivo* (McEwan *et* al., 1988). A region of low pH (pH ~ 5.5) was found at the luminal surface of the apical membrane, although the pH of the bathing solution was pH 7.2. Additional studies using biopsy samples have demonstrated its presence in man (Lucas *et al.*, 1976; Lucas *et al.*, 1978, see Ganapathy & Leibach, 1985).

The precise mechanisms involved in the generation and maintenance of the acidic microclimate are not well understood, but the Na^+/H^+ exchanger located in the apical membrane (NHE-3) is at least partially responsible for the secretion of protons into the lumen *in vivo*. The action of this membrane protein indirectly provides the driving force for peptide transport and as such is described as a secondary transport system (figure 1.5). The luminal concentration of Na^+, *in vivo*, is greater than its intracellular concentration (originating from the diet and gastric, pancreatic and intestinal secretions). These high levels would drive the exchanger in the direction of proton secretion, thus generating an inwardly-directed proton gradient across the brush-border membrane. The co-transfer of protons with peptides into the cell causes the intracellular pH to drop and this increase in cytosolic H^+ concentration would stimulate the Na^+/H^+ exchanger to transport H^+ out, and Na^+ into the cell. The action of the exchanger means that both the intracellular pH and the transmembrane electrical potential would be restored to basal levels. Intracellular Na^+ concentration is maintained low by the action of a primary transport system, the Na^+/K^+-ATPase located in the basolateral membrane. This protein functions to re-establish the high extracellular Na^+ gradient, at the cost of ATP hydrolysis. Due to the actions of these two ion transporters in providing the driving force for peptide transport, the peptide transporter in the apical membrane is classified as a tertiary transport system.

In addition to the role of the apical Na^+/H^+ exchanger in restoring intracellular pH following peptide-induced acid load in the enterocytes, Thwaites *et al.* (1993) demonstrated that pH_i recovery also occurred in the absence of external Na^+. They suggested that an alternative transporter (H^+/K^+-ATPase) may also

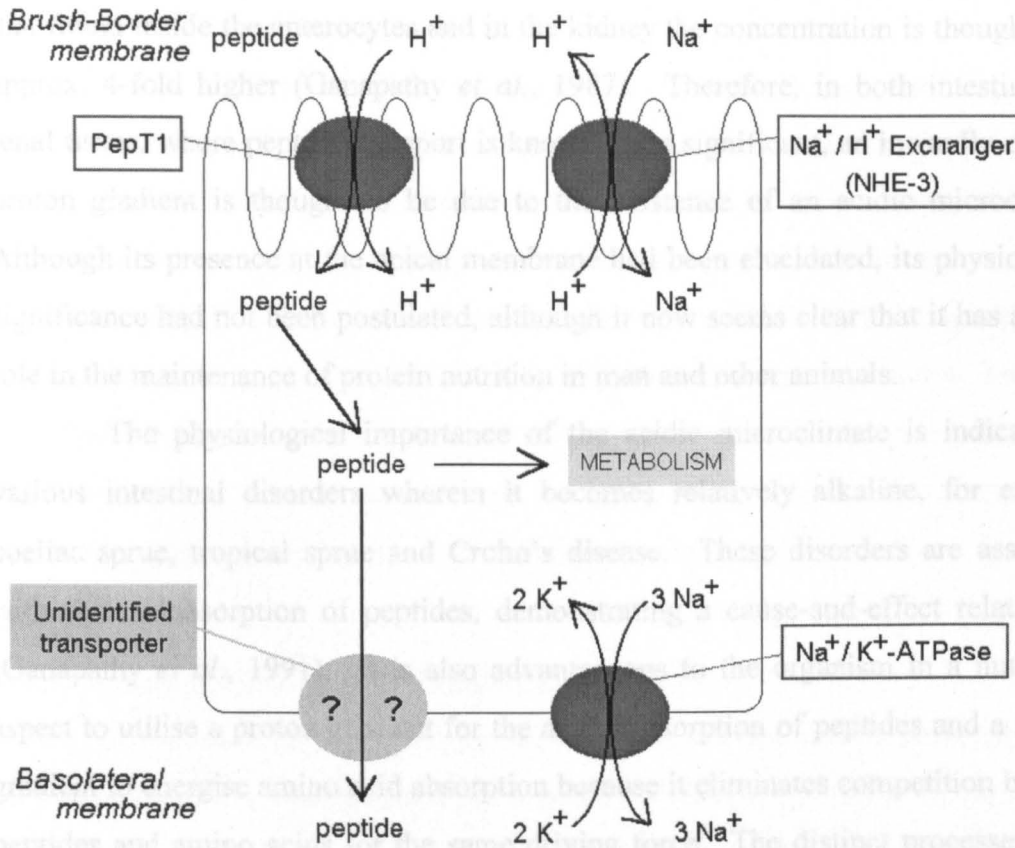

Figure 1.5

Schematic diagram showing the transport systems involved in intestinal peptide absorption, either directly or indirectly. The primary transport system is the Na^+/K^+-ATPase located in the basolateral membrane, which forms the sodium gradient across the apical membrane. The secondary system is the Na^+/H^+ exchanger in the apical membrane, which, in turn, creates the transmembrae H^+ gradient (the acidic microclimate) to drive peptide uptake into the cell by PepT1 (the tertiary system). The peptide transporter in the basolateral membrane has not yet been identified.

function in this capacity, albeit to a lower extent. The relative roles of the two transporters would depend on the nutritional status of the intestinal contents.

The acidic microclimate is present in the lumen of both the intestine and the kidney. In the intestine the H^+ concentration of the microclimate is at least ten times that found inside the enterocytes and in the kidney the concentration is thought to be approx. 4-fold higher (Ganapathy *et al.*, 1987). Therefore, in both intestinal and renal tissue, where peptide transport is known to be significant, an inwardly-directed proton gradient is thought to be due to the existence of an acidic microclimate. Although its presence at the apical membrane had been elucidated, its physiological significance had not been postulated, although it now seems clear that it has a major role in the maintenance of protein nutrition in man and other animals.

The physiological importance of the acidic microclimate is indicated by various intestinal disorders wherein it becomes relatively alkaline, for example coeliac sprue, tropical sprue and Crohn's disease. These disorders are associated with the malabsorption of peptides, demonstrating a cause-and-effect relationship (Ganapathy *et al.*, 1991). It is also advantageous to the organism in a nutritional aspect to utilise a proton gradient for the active absorption of peptides and a sodium gradient to energise amino acid absorption because it eliminates competition between peptides and amino acids for the same driving force. The distinct processes allow both systems to operate simultaneously and in parallel to increase the efficiency of the absorption of amino nitrogen by the small intestine.

1.2.3.3 pH-dependence of transport

As previously mentioned, it is thought that any effect of extracellular pH on peptide transport is indirect and is due specifically to changes in the inwardly-directed proton gradient. However, a protein has been identified from the Caco-2 cell line by Saito *et al.* (1997) which they suggest is a novel pH-sensing regulatory factor that modulates transport activity of the human peptide transporter (hPepT1). The 23 kDa protein, consisting of 208 amino acids, was identified from a human duodenum cDNA library during the course of homology screening using a partial cDNA fragment coding for hPepT1 in an attempt to obtain related proteins. The novel cDNA clone has been termed hPepT1-RF. Hydropathy analysis of its primary amino acid sequence indicates five transmembrane (TM) α-helices, but no

potential sites for either protein kinases C or A, or *N*-linked glycosylation sites have been speculated. Interestingly, the 18-195 amino acid sequence of hPepT1-RF is identical to the corresponding sequence (8-185) in hPepT1, whereas the N-terminal residues (1-17) and C-terminal residues (196-208) were unique and showed no homology with the corresponding regions of hPepT1.

hPepT1-RF does not have transport activity but co-injection of its cRNA into *Xenopus laevis* oocytes with hPepT1 cRNA causes a shift in the pH optimum for Gly-Sar transport from pH 5.4 to a more neutral pH 6.0, when compared to hPepT1 expression alone. However, hPepT1-RF did not appear to have any regulatory activity at pH 6.0-7.4, suggesting that it does not function by affecting membrane insertion/targeting or synthesis of hPepT1. A structural interaction has been hypothesised due to extensive homology between the two proteins, especially the entire amino acid identity around their predicted TM domains. However, further work is required to elucidate the role of this protein in peptide transport.

1.2.3.4 Mechanism of H^+/peptide cotransport

In contrast to the work by Saito *et al.* (1997) above, Nussberger and co-workers (1997) proposed that PepT1 is able to sense the pH of both the external and intracellular medium and it is this ability which regulates peptide transport, not an additional associated protein. They state that PepT1 has a single H^+-binding site which is accessible from both faces of the apical membrane, and that binding of a proton at either surface results in a conformational change of the protein. If the proton binds at the extracellular surface, the protein adopts an outwardly occluded conformation, and vice versa. However, the protonated states of the protein are not able to cycle between the two faces of the membrane without associated binding of a peptide. It is thought that it is the ratio of H^+ concentration on either side of the membrane which determines the direction of transport, i.e. if $pH_o < pH_i$ then H^+ will bind predominantly at the extracellular surface to induce transport of peptides into the cell, and vice versa. H^+ binding has been shown to be voltage dependent (Läuger & Jauch, 1986), however, the charge movements of transport are due to reorientation of the empty, charged carrier within the membrane field, in addition to H^+ binding/dissociation from the carrier (MacKenzie *et al.*, 1996).

The exact mechanism they propose is as follows; H^+ bind to PepT1 prior to substrate, in an orderly manner (MacKenzie *et al.*, 1996). At low pH_o the number of PepT1 protein molecules that exist in the outwardly-occluded state, due to bound H^+, increases and in this state the carrier has an increased affinity for substrates (MacKenzie *et al.*, 1996; Nussberger *et al.*, 1997). Binding of the substrate completes this process and translocation of both H^+ and substrate occurs simultaneously in the same reaction step (MacKenzie *et al.*, 1996). The process makes physiological sense, i.e. the acidic microclimate would promote the existence of the proton bound/outwardly-occluded conformation and therefore stimulate efficient peptide absorption.

1.2.4 Membrane preparations used to study peptide transport

A number of different preparations have been used to study peptide transport, including brush-border and basolateral membrane vesicles (Temple *et al.*, 1995; Dyer *et al.*, 1990, respectively), isolated cells (Cheeseman & Devlin, 1985), cell lines, e.g. Caco-2 (Thwaites *et al.*, 1993b), MDCK cells (Brandsch *et al.*, 1995), and intact epithelial tissue (Lister *et al.*, 1995). Each of these has distinct advantages and disadvantages with respect to the other preparations.

Intact tissue preparations provide information on transmural substrate transport. However, transmural transport involves a solute traversing two distinct membranes, apical and basolateral, and these can be difficult to distinguish in intact tissue (except when using the vascular perfusion, *in situ*, technique – for details see the relevant results chapters (3 & 6)). Vesicles produced from either apical or basolateral membranes can be used to separate the transport mechanisms at the distinct membranes. Isolated cells are useful for electrophysiological studies and for fluorescence studies, i.e. in the measurement of intracellular pH, but the polarity of epithelial cells begins to dissipate within a few hours of isolation. Cell lines (e.g. Caco-2) have the same polarity as intestinal epithelial cells and retain it for longer. Due to the advancement in recent years, many solute transporters have now been cloned (see section 1.3) and these proteins can be over-expressed in cells which have little or no endogenous transport activity for the protein under investigation to allow the study of a single protein in isolation. For example, *Xenopus laevis* oocytes are used to over-express PepT1 and study apical peptide transport. This is an

advantage if there are a number of different members of a transporter family present in a native membrane and only one is of interest, but if a number of different proteins interact with each other for substrate transport this will not be feasible.

However, what is observed *in vitro* might not actually be the same as what occurs *in vivo*, and so a range of different preparations should be used for the study of a transport process.

1.3 MOLECULAR PHYSIOLOGY OF THE PEPTIDE TRANSPORTERS

1.3.1 Cloning of the intestinal peptide transporter, PepT1

Although considerable progress has been made in the elucidation of transporter function and mechanism over the last decade, the precise structure and molecular properties of the proteins had not been determined until recent years.

An initial step towards cloning and characterisation of the mammalian peptide transporters was performed in 1991 by Miyamoto and co-workers. Microinjection of rabbit intestinal poly(A)$^+$ mRNA into *Xenopus laevis* oocytes led to the first functional expression of a peptide transport system with characteristics similar to those of the transporter in its native tissue. Transport inhibition studies using dipeptides and free amino acids demonstrated that the transporter retained its H^+-dependence and substrate specificity.

The year of 1994 saw the beginning of a new era of peptide transport studies, which progressed from this preliminary study. The rabbit intestinal peptide transport system was the first mammalian transporter to be cloned and sequenced (Fei *et al.*, 1994). Briefly, poly(A)$^+$ mRNA was isolated from rabbit small intestine and injected into *Xenopus laevis* oocytes. Transport activity of mRNA-injected oocytes was assessed against water-injected cells using radioactively labelled peptides as substrates. This was followed by size-fractionation of the mRNA, and an RNA-pool containing the required message was used to construct a cDNA library in a bacterial vector. Individual cDNA clones from the library were transcribed into the corresponding cRNAs, which were then individually injected into oocytes. The oocytes containing distinct cRNAs were assayed for the induced peptide transporter activity. This screening procedure was performed to isolate a single clone encoding

the transport activity of interest. The cDNA of the specific clone was analysed to determine the primary amino acid sequence of the transport protein. Hydropathy analysis of the protein's amino acid sequence permitted initial predictions of the topological arrangement of the transporter protein within the plane of the cell membrane.

Using this approach Fei *et al.* (1994), followed closely by Boll *et al.* (1994), identified a 2.7 bp and 2.9 bp cDNA, respectively, that, after injection of the corresponding cRNAs into oocytes, induced a transport activity resembling all aspects of peptide transporter characteristics observed in intestinal vesicles. The cDNAs were obtained from rabbit mucosa and, following *in vitro* transcription and expression in oocytes, the uptake of ^{14}C-Gly-Sar was more than 63-fold above control oocytes (Fei *et al.*, 1994) and ^{3}H-cefadroxil uptake was 50-fold higher (Boll *et al.*, 1994). To investigate the characteristics and rheogenicity of transport, the two-electrode voltage clamp technique was applied. Large inward currents, causing depolarisation of the membrane, were found when substrates such as dipeptides, tripeptides and β-lactam antibiotics were applied, but single amino acids or tetrapeptides did not evoke a similar current (Fei *et al.*, 1994; Boll *et al.*, 1994). H^+ cotransport was demonstrated by monitoring the intracellular pH of the oocytes by using a pH-sensitive microelectrode (Fei *et al.*, 1994) or a pH-sensitive fluorescent dye (carboxy-SNARF1) (Boll *et al.*, 1994). In these studies, application of Gly-Sar or cefadroxil, respectively, to the oocytes caused pH_i to decrease significantly, whereas single amino acids did not evoke the same effect.

The functionally expressed protein isolated by both groups was found to be the same; the intestinal peptide transporter, PepT1. The cDNA coding for the expressed protein revealed 707 amino acid residues (71 kDa) and hydropathy analysis of its primary sequence designated 12 transmembrane (TM) domains and an unusually large hydrophilic loop located between TM 9 and 10. A detailed description and diagram depicting the membrane model of the protein is given in a later section (section 1.4.1).

Although the protein isolated by the two groups was thought to be identical, differences in transport function became apparent, for example, pH-dependence and effect of membrane potential. Boll *et al.* (1994) detected a pH optimum of 6.5 for cephadroxil uptake, whereas Fei *et al.* (1994) found the optimum uptake for Gly-Sar

was pH 5.5. Fei *et al.* (1994) also discovered that transporter activity was independent of membrane potential, in opposition to the situation that Boll *et al.* (1994) reported. It is clear that the observed discrepancies of pH-dependence are potentially due to the different substrate employed, but the distinct views on membrane potential were not explained.

Subsequent to the cloning and expression of rabbit PepT1, other groups followed suit and the following few years saw the cloning of many other mammalian peptide transporters. Human PepT1 was the next transporter to be cloned and sequenced (Liang *et al.*, 1995). A human intestinal cDNA library was screened with a probe derived from the rabbit peptide transporter previously cloned by this group (Fei *et al.*, 1994). A cDNA was identified which when expressed in oocytes or HeLa cells induced a H^+-dependent peptide transport activity.

At the same time, Saito *et al.* (1995) reported the cloning and sequencing of the peptide transporter from rat small intestine.

A detailed discussion of the structure, plus sequence comparisons, of the aforementioned PepT1 protein(s) cloned from the different species is given in section 1.4.1.

1.3.2 Cloning of the renal peptide transporter, PepT2

Although it was known that peptide transport occurred in the kidney, characterisation of the protein responsible was not conducted until after the intestinal isoform had been cloned in many species. Cloning and characterisation of PepT2 will be discussed only briefly, with a more detailed account of its structure given in section 1.4.1.

The first renal isoform cloned was from human tissue (Liu *et al.*, 1995). Its cDNA was predicted to encode a protein of 729 amino acids, expected to have a molecular weight of 81,940 Da and a pI of 8.26. The following year both rat (Saito *et al.*, 1996) and rabbit (Boll *et al.*, 1996) PepT2 were cloned and sequenced.

PepT2 mRNA is predominantly expressed in the kidney (especially in the medulla compared to the cortex) but cannot be detected in the small intestine. It has also been shown to be present in brain, lung and spleen where it is thought that it may participate in unrecognised physiological function(s) related to active transport of

oligopeptides into these tissues (Saito *et al.*, 1996). Rabbit PepT2 is also expressed in these tissues, but has an additional location in the heart (Boll *et al.*, 1996).

1.3.3 Sequence similarity of mammalian peptide transporters with other known proteins

PepT1 and PepT2 belong to the POT (proton-dependent oligopeptide transport) family recently identified by Paulsen & Skurray (1994). Following cloning and expression of rabbit PepT1 by Fei and co-workers (1994), they reported that two other proteins share limited sequence similarity; ChL1 (a proton-dependent nitrate transporter identified from *Arabidopsis thaliana*) and Ptr2 (a peptide transporter identified from *Saccharomyces cerevisiae*). Paulsen & Skurray used the rabbit sequence to scan the SwissProt database in an attempt to identify similar proteins. Several proteins were found including DtpT (an oligopeptide transporter from *Lactococcus lactis*), partially sequenced open reading frames from rice, yhiP (a hypothetical protein) and a region downstream of the *cadA* and *cadB* genes on the *Escherichia coli* chromosome. All of the proteins identified have 12 TM domains and share two highly conserved regions; sequence 1 (located between TM 2 & 3), sequence 2 (located within TM 5) (table 1.3). All of the proteins show H^+-dependence in the transport of their substrates.

Subsequent to this study, additional protein sequences have been deposited into this database (table 1.3); these transporter proteins are isoforms of those already published by Paulsen & Skurray.

A few years later, Graul & Sadée (1997) performed their own investigations in which they compared the primary sequences of all PTR family members (equivalent to the POT family described by Paulsen & Skurray, 1994) to determined whether the order of the TM domains, including adjoining loops, had changed during evolution. In addition, conserved domains and/or residues were identified in an attempt to relate them to POT transporter function. The results revealed the presence of highly conserved regions/residues interspersed with less well conserved sequences. The two consensus motifs found by Paulsen & Skurray were identified in this study, in addition to other regions and residues, including;

- a glycine-rich domain (GLALIALGTGGI) in TM 4, 8, 10, 11 – may represent a region of functional significance

Name	Source and function	Accession no.	Sequence 1	Sequence 2
PepT1#	rabbit intestine	P36836	LGALIADAWLGKFKTIVWLSIVYTIG	FSIFYLAINAGSLLS
PepT1	human intestine	P46059	LGALIAD+WLGKFKTIV LSIVYTIG	FSIFYLAINAGSLLS
PepT1	rat intestine	P51574	LGALIAD+WLGKFKTIV LSIVYTIG	FSIFYLAINAGSLLS
PepT2	rabbit kidney	P46029	LGA IAD+WLGKFKTI++LS+V +G	FS FYLAINAGSLLS
PepT2	Hhuman kidney	*S78203	LGA IAD+WLGKFKTI++LS+VY +G	FS+FYL+INAGSL+S
PepT2	rat kidney	*D63149	LGA IADAWLGKFKTI++LS+V +G	FS+FYLAINAGSL+S
PTR2#	yeast peptide transporter	P32901	G +AD + GK+ TI + +Y G	F FY IN GSL
PTR2	yeast peptide transporter	P46030	+G + D LG +TIV ++V IG	F++FY++IN GSL++
PTR2A	yeast peptide transporter	P46031	ALIAD +LG++ TIV +++Y IG	+ IFY IN GSL
PTR2B	yeast peptide transporter	P46032	+GA++ADA+ G++ TI S +Y IG	F+ FY +IN G+L+S
DTPT#	di/tri peptide transporter	P36574	+G +AD LG +TI I+ TIG	F+IF + IN GSL++
TAT2	yeast tryptophan transporter	P38967	A+ W ++W++I Y +	
CHL1#	nitrate/chlorate transporter	Q05085	LG IAD +LG++ TI + + G	F+ F IN GSLL+
NIRC	potential nitrate transporter	P25926	A++ WLG V+++++Y+ G	
NIRC	potential nitrate transporter	P11097	A++ WLG V+++++Y+ G	
QAY	quinate transporter	P11636	L A +LG+ K+++ S+V+ IG	
ATKB	K/Cu transporting ATPase	P05425	+G FK WLS++ IG	
YHIP#	Hhypothetical protein	P36837	+G + D LG +TIV ++V IG	F++FY++IN GSL++

Table 1.3
Membrane proteins which have identity/similarity (+) to two sequences in rabbit PepT1 (taken from Paulsen & Skurray, 1994, #), which are both conserved in members of the POT family of transporter proteins; sequence 1 (located between TM 2 & 3), sequence 2 (located within TM 5). NB only members of the POT family have sequence identity/similarity to sequence 2. Accession no. is for the Swiss Protein database (*Genbank). Source: C. Temple thesis (1996).

- several conserved proline residues in TM 1, 2, 7, 8 – structurally important because of their ability to induce bends in α-helices
- a glutamine residue in TM 10 – the only charged residue fully conserved, therefore may have a possible role in H^+ translocation
- glycine residues in several TM's – suggest a common structure for portions of the transporters.

They concluded that the PTR transporters have a modular structure, each module consisting of one or more TM domains that were rearranged by a number of evolutionary mechanisms to affect their order in the primary structure of the protein.

1.3.4 Cloning of other H^+/peptide co-transporters

A 92 kDa protein (HPT-1) has been cloned from Caco-2 cells which, when expressed in Chinese Hamster ovary (CHO) cells, enhances the transport of dipeptides and other PepT substrates (bestatin, cephalexin) in a pH-dependent manner (Dantzig *et al.*, 1994). However, it has only one putative TM domain, in contrast to the previously described peptide transporters, and is therefore thought unlikely to function as a transporter, although it may self-aggregate or associate with another (unidentified) protein to form a multimeric protein that exhibits transport activity. HPT-1 does not show any sequence homology with the POT family of transporters but database searches revealed a certain similarity (20-30% identity) to members of the cadherin superfamily of calcium-dependent, cell-cell adhesion proteins. In the single TM domain there are no residues which implicate it is a functional transporter, i.e. there are no charged groups for substrate interaction. Therefore, it may possibly act as a modulator of peptide transport in Caco-2 cells (Hediger *et al.*, 1995) through another carrier, e.g. PepT1 (HPT-1 is only expressed in the intestine).

Other putative mammalian peptide transporters that have been identified include a peptide/histidine transporter (PHT1) from a rat brain cDNA library (Yamashita *et al.*, 1997). This is the first neurospecific PepT member to be reported, however, it not only transports small peptides, but histidine is also a substrate. The amino acid sequence of PHT1 has 17% identity (32% similarity) to known PepT1 proteins, and 12% identity (27% similarity) to known PepT2 proteins.

Potential peptide transporters have also been found in non-mammalian species. Fei *et al.* (1998a) revealed the existence of two carrier proteins in *Caenorhabditis elegans* by performing database searches. The proteins, designated OPT1 and OPT2, are homologous to mammalian counterparts, PepT1 and PepT2. A moderate sequence identity is observed between the two distinct groups, i.e. 36-47% amino acid identity, in addition to some similarity with PHT1 (approx. 25%). Transport characteristics are comparable to the mammalian proteins; transport exhibited electrogenicity plus dependence on membrane potential and substrate concentration (transport is saturable).

A later study by Fei and co-workers (2000) identified a third putative peptide transporter (OPT3) from *C. elegans*, which was expressed only in neurons. The primary sequence of OPT3 has 49% identity (38% similarity) with OPT1, and 48% identity (39% similarity) with OPT2. However, this protein was also found to function as a H^+ channel, suggesting an important role in H^+ homeostasis, in addition to its likely role in the clearance of peptides formed from the metabolism of neuropeptides.

1.3.5 Tissue distribution of peptide transporters

It is widely known that PepT1 is predominantly expressed in the small intestine, whereas PepT2 is localised to the kidney. The functional characteristics of peptide transporters have been only investigated thoroughly in these tissues, but, in addition to these two predominant sites of expression, the transporters are also found in other tissues, although the localised function may not be known. Northern blot analysis of cloned PepT1 and PepT2 reveal distinct species differences in tissue distribution. Although PepT1 mRNA is found ubiquitously in the small intestine of rabbit, rat and human, and at lower levels in the kidney, it can also be detected in the liver (rabbit and human), in addition to the brain (rabbit) and pancreas (human) (Fei *et al.*, 1994; Liang *et al.*, 1995; Saito *et al.*, 1995). Ogihara and co-workers (1996) used immunoblotting and immunofluorescence techniques to demonstrate that PepT1 was localised to the apical membrane of intestinal enterocytes, with the jejunum showing the strongest signal (Miyamoto *et al.*, 1996a). The intensity of PepT1 staining in the villi increased from the villus base to the villus tip, indicating that during the maturational process the absorptive cells acquire and express PepT1

mRNA (Ogihara *et al.*, 1996), also demonstrated by Freeman *et al.* (1995) in which the maximum level of PepT1 mRNA was detected at approx. 100-200 μm from the crypt-villus junction and then reached a plateau towards the tip.

In contrast, PepT2 mRNA is detected in great abundance in the kidney of rat, rabbit and human and to a lower extent in rat and rabbit lung (Lui *et al.*, 1995; Saito *et al.*, 1996; Boll *et al.*, 1996). It can also be found in rat brain and spleen, and in the heart tissue of rabbit, but it is not detected in the small intestine.

The findings that PepT1 and PepT2 mRNA are both expressed in kidney are consistent with results of vesicle studies indicating that at least two transporters exist in this tissue (Miyamoto *et al.*, 1988; Daniel *et al.*, 1991; Takahashi *et al.*, 1998); they may be differentially expressed along the length of the nephron (Leibach & Ganapathy, 1996). It is likely that PepT2 is expressed predominantly in the proximal region of the nephron and PepT1 located in more distal parts, corresponding to a potential increase in peptide concentration through the length of the nephron due to the action of highly active BBM peptidases. Differential expression might provide an absorptive advantage under physiological conditions.

A comparison of rabbit PepT1 and PepT2 has indicated certain similarities between the two isoforms, but also distinctly different features (Boll *et al.*, 1994; 1996), some of which are also found in other species. For example, distinct pH dependencies are detected under identical experimental conditions. In addition, PepT2 has been shown to have a substrate affinity that is 40-fold higher than PepT1, plus different substrate specificities (see section 1.4.5). As such, PepT1 is generally classified as a low affinity/high capacity transporter, whereas PepT2 is a high affinity/low capacity transporter. This is related directly to their individual roles in peptide absorption within the body.

Various functions of the peptide transporter(s) in other tissues have been proposed; these include a role in the liver, whereby PepT1 at the surface of hepatocytes may be involved in removal of degradation products of peptide hormones and peptide-derived drugs from circulation. In the brain tissue it may serve to clear degraded neuropeptides from the bloodstream (Fei *et al.*, 1994). In other tissues, the transporters participate in as yet undetermined physiological functions.

1.3.6 One or two intestinal peptide transporters?

In previous years it wasn't clear whether PepT1 was the only peptide transporter mediating the absorption of small peptides and peptide-like drugs from the intestinal lumen; for example Inui *et al.* (1988) suggested the existence of two different transporters. They named these distinct transport systems Type I (a neutral pH-preferring system) and Type II (an acidic pH-preferring system). Zwitterionic substrates were shown to be transported by both systems, whereas a double-negatively charged cephalosporin was only accepted by Type II. Kramer *et al.* (1993) also implied, from vesicle studies, that differently charged β-lactam antibiotics used different transporters. However, mutual inhibitions in transport between zwitterionic and dianionic cephalosporins were observed (Inui *et al.*, 1988). Therefore, the difference in transport of the various compounds may have been due to distinct pH-dependencies, i.e. convincing evidence for kinetic heterogeneity in the intestine was lacking.

Recent evidence provided by Hediger's group (Fei *et* al., 1994) during cloning and expression of rabbit PepT1 implied that there was only one intestinal peptide transporter, located on the brush-border membrane, that was involved in the transport of Gly-Sar. Hybrid depletion of rabbit small intestinal poly(A)$^+$ RNA, to block PepT1 expression before injection into oocytes, resulted in a loss of induced peptide transport activity, i.e. levels were comparable to water-injected oocytes. Although a clear conclusion was reached with Gly-Sar as a substrate, the existence of additional peptide transporters for other substrates cannot be completely disregarded.

They further suggested that peptide transporter activity in the basolateral membrane is also due to expression of PepT1. However, it is possible that the anti-sense to PepT1 mRNA might bind to the mRNA for the basolateral transporter, therefore simultaneously blocking its expression with PepT1. In addition, work by a number of groups have provided convincing evidence of a distinct transporter protein at this membrane (see section 1.5).

1.4 STRUCTURE AND FUNCTION OF THE PEPTIDE TRANSPORTERS

1.4.1 Membrane model of the peptide transporters

Cloning and expression of peptide transporters from both intestine and kidney, from a number of different species, has allowed the protein(s)' structure and its arrangement and orientation in the plasma membrane to be elucidated. The structure of rabbit PepT1 was proposed by Fei *et al.* (1994) following cloning and expression of the protein. However, all of the cloned mammalian peptide transporters have the same predominant structural features, which are retained throughout distinct species.

The peptide transporters possess 12 hydrophobic sequences, each of a sufficient length to span the bilayer as an α-helix; these are designated transmembrane domains (TM) (figure 1.6). This structure is typical of a number of other solute transporters e.g. SGLT1 (Hediger *et al.*, 1987). These 12 TM domains were predicted from hydropathy analysis of the primary amino acid sequences of the protein, but it couldn't be unequivocally proven. Confirmation of the number and orientation of the TM's and adjoining loops was only made in 1998 by Covitz *et al.* This group inserted a small epitope tag into various points throughout the protein structure. A combination of monoclonal antibodies and immunofluorescence confocal microscopy was used to determine whether the connecting loops and/or amino/carboxyl termini were located on the extracellular or intracellular surface of the bilayer. The predicted orientation originally proposed by Fei *et al.* (1994) was ascertained to be correct.

The TM domains are connected by loops of varying length, in particular there is a large hydrophilic loop present between TM 9 and 10. This extracellular loop was subsequently found in other peptide transporters that were cloned in the following years and its presence makes this protein distinct from those of previously reported organic solute transporters. Although the main structural features of the peptide transporters are found in both isoforms in all species, specific differences are apparent, such as the number and location of putative glycosylation sites, PKA and PKC sites, etc.

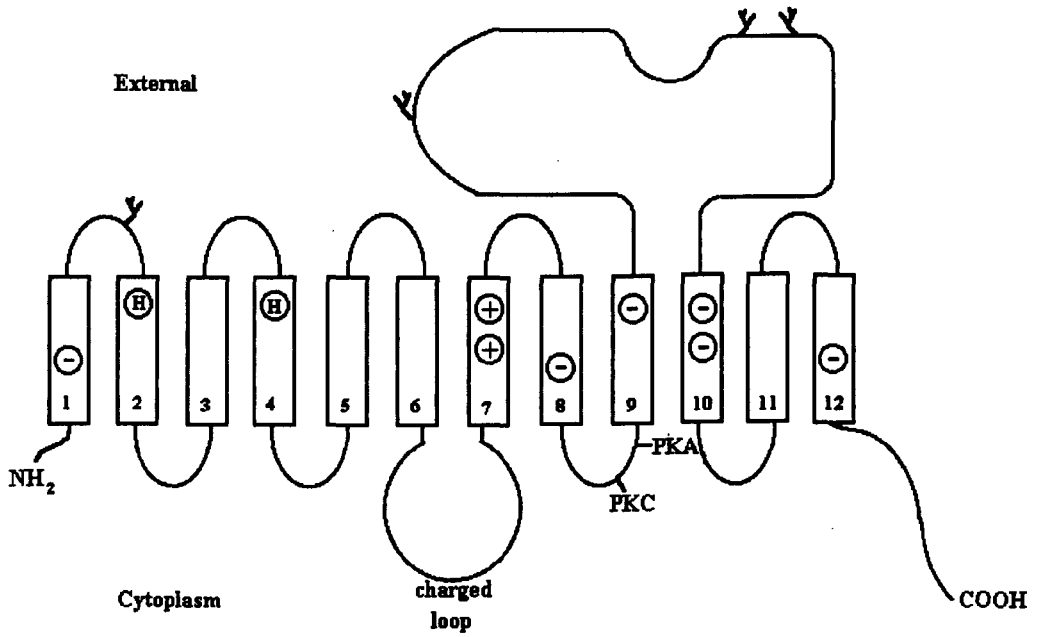

Figure 1.6

Schematic diagram showing the membrane model of the peptide transporter located in the apical membrane of rabbit small intestine (PepT1). Boxes represent the 12 transmembrane (TM) domains interconnected by intra- and extra-cellular loops of varying length. H; histidine residue, PKA and PKC show the regions postulated as the sites for phosphorylation by protein kinases, charged residues in the TM domains are shown, and branches represent putative *N*-glycosylation sites. Adapted from Meredith & Boyd (1995).

1.4.1.1 Species differences in PepT1 structure

The primary sequence of rabbit PepT1 contains four putative *N*-linked glycosylation sites (N-x-S/T) (Asn_{50}, Asn_{439}, Asn_{498}, Asn_{513}), a potential protein kinase C regulatory site (Ser_{357}) and a PKA site (Thr_{362}) (see figure 1.6). The authors proposed, on the position of these specific sites, that the amino and carboxyl terminals would be intracellular (Fei *et al.*, 1994). The large extracellular loop in rabbit PepT1 consists of 202 amino acids and contains three of the four potential glycosylation sites. Another notable loop (intracellular) connects TM 6 and 7 and contains a high density of cationic amino acids (>25%) suggesting a possible interaction with another protein within the cytosol. The apparent molecular weight of the rabbit PepT1 protein is 71 kDa; it is thought that at least 11 kDa is due to core glycosylation of the protein, indicated by endoglycosidase H treatment.

Human PepT1, cloned by Liang *et al.* (1995), was predicted to consist of 708 amino acids and have a molecular weight of ~79 kDa, with an isoelectric point of 8.6. In comparison to rabbit PepT1 it has seven putative *N*-linked glycosylation sites and two PKC sites (Ser_{357} and Ser_{704}), but no PKA site.

The cDNA isolated and cloned from rat small intestine (Saito *et al.*, 1995) encoded a protein of 710 amino acids with a molecular weight of ~75 kDa. The primary sequence of the protein possesses 5 potential *N*-linked glycosylation sites (Asn_{415}, Asn_{439}, Asn_{510}, Asn_{532}, Asn_{539}), a PKC site (Ser_{357}) and a PKA site (Thr_{362}). A comparison of key points and similarities between cloned rat, rabbit and human PepT1 structure and sequence are described in table 1.4.

1.4.1.2 Species differences in PepT2 structure

In contrast to human PepT1, hPepT2 only has 3 putative *N*-linked glycosylation sites, but five PKC regulatory regions and no PKA site (Liu *et al.*, 1995). It was demonstrated to have a 50% identity and 70% similarity to hPepT1, although it was 21 amino acids longer. The similarity between the two proteins was much higher in the TM domains, than in the large extracellular loop or either termini.

A summarisation of key structural and functional features of rat PepT2 are described in table 1.5, in a direct comparison with rat PepT1. Sequence analysis (Saito *et al.*, 1996) shows that rat PepT2 (81 kDa) has an 83% amino acid identity to hPepT2. In addition it is interesting to note that two PKA sites (Thr_{12} & Thr_{727}) and

	RAT	RABBIT	HUMAN
cDNA	2,921 bp	2,746 bp	2,127 bp
Molecular weight	~75 kDa	71 kDa	~79 kDa
Amino acid residues	710	707	708
N-linked glycosylation sites	5	4	7
PKA motifs	**Thr_{362}**	**Thr_{362}**	-
PKC motifs	**Ser_{357}**	**Ser_{357}**	**Ser_{357}**, Ser_{704}
Amino acid sequence identity			
Total	77% to rabbit	81% to human	83% to rat
Hydrophilic loop	58% to rabbit		69% to rat
Pattern of expression	Small intestine > kidney cortex	Small intestine > kidney cortex, liver > brain	Small intestine > kidney cortex > liver, placenta & pancreas
Reference	Saito *et al.* (1995)	Fei *et al.* (1994)	Liang *et al.* (1995)

Table 1.4

A comparison of the structural features of the cloned H^+/peptide transporter PepT1 isolated from rat, rabbit and human small intestine. Amino acid residues shown in bold type are conserved residues between species forming PKA/PKC motifs.

	PepT1	PepT2
CDNA	2,921 bp	3,938 bp
Structure		
Molecular weight	~75 kDa	81 kDa
Amino acid residues	710	729
N-linked glycosylation sites	Asn_{415}, Asn_{439}, Asn_{510}, Asn_{532}, Asn_{539}	Asn_{435}, Asn_{448}, Asn_{528}, Asn_{587}
PKA motifs	Thr_{362}	Thr_{12}, Ser_{33}, Thr_{727}
PKC motifs	Ser_{357}	Ser_{376}, Ser_{640}, Thr_{708}
Homology	48%	
Essential residues	His_{57} & His_{121}	His_{87} & His_{142}
Pattern of expression	**Small intestine** > kidney cortex	**Kidney** medulla > kidney cortex > brain, lung & spleen
Function		
Driving force	H^+ gradient, membrane potential	H^+ gradient, membrane potential
Substrate	Di-/tri-peptides, β-lactam antibiotics, bestatin, ACE inhibitors	Di-/tri-peptides, β-lactam antibiotics, bestatin
Substrate affinity		
K_m for Gly-Sar (mM)	1.1	0.11

Table 1.5

A comparison of the structural and functional features of the cloned H^+/peptide co-transporters, PepT1 and PepT2, isolated from rat small intestine and kidney, respectively. Data taken from Saito *et al.* (1995 & 1996), Terada *et al.* (1996 & 1997a,b).

two PKC sites (Ser_{376} & Ser_{640}) are conserved in the transporter between the two species.

Rabbit PepT2 has a molecular weight of approx. 107 kDa (with core glycosylation) and it possesses five potential *N*-linked glycosylation sites and four PKC motifs (Boll *et al.*, 1996). It shows a 47% identity to rabbit PepT1; again, the majority of the sequence identity is found in the TM domains, the extracellular loop only showing a 21% match.

1.4.1.3 Additional structural features

It is well known that membrane potential has a considerable effect on peptide transport, as a consequence Meredith & Boyd (1995) predicted that the portion of the protein that lies inside the plane of the bilayer would carry a net negative charge. Fei *et al.* (1994) also predicted a negative charge of the membrane field region of the protein, after consideration of all the charged amino acids in the proposed TM. A charge of –2 to –4 was stated, depending on the degree of protonation of the amino acid residues.

Within the transmembrane regions of the transporter, amino acids such as proline and glycine are prevalent. These are generally classed as 'helix-breaking' amino acids and may act as hinges to allow the flexibility required for the transport of the unusually diverse range and size of substrates (Meredith & Boyd, 1995). These 'hinges' are present in all TMs except TM 12, at an average number of two per TM.

1.4.2 Essential amino acid residues of the peptide transporter(s)

Specific amino acid residues within the transporter protein(s) have essential roles, for example in substrate recognition (binding and/or transport), proton interaction/translocation. The precise residues can be identified by chemical modification followed by uptake/transport studies to determine their role in the transport process. Such modifying agents include those which specifically react with histidine or tyrosine residues, and those which interact with thiol-containing amino acid residues, e.g. cysteine and methionine.

1.4.2.1 Histidine residues

Histidyl residues are predominantly focused upon when studying transport systems because the imidazole group of its side chain has a *p*K value of 6.5, which is very close to physiological pH. This particular characteristic of histidine confers its ability of accepting and releasing H^+ very easily under physiological conditions. Therefore, it is likely that these residues are involved in binding and translocation of H^+ in PepT1 and PepT2.

In many ion coupled transport processes, the systems are activated by the ability of the coupling ion to increase the affinity of the transporter for their respective substrates, for example, Na^+/proline cotransporter, H^+/leucine cotransporter (Brandsch *et al.*, 1997). However, this is not the case with the intestinal H^+/peptide transporter. MacKenzie *et al.* (1996) proposed an ordered transport model in which protons bind first, followed by substrate binding and translocation. In this system the cotransported H^+ was found to activate peptide transport by increasing the maximal velocity (V_{max}), but it had no significant effect on substrate affinity (Ganapathy *et al.*, 1984). This suggestion was confirmed by investigations conducted by Miyamoto and co-workers (1986), on the renal isoform, whereby treatment of BBMV with DEPC caused a reduction in V_{max} of Gly-Sar transport without affecting K_m. The results indicated that DEPC inhibits peptide transport in a non-competitive manner by covalently modifying histidine residues and this, in turn, results in a reduction in the number or availability of active transport proteins in the membrane.

However, the following years brought conflicting results concerning the influence of H^+ and/or DEPC on the kinetic parameters of PepT1, from many different groups. In 1989, Kato *et al.* published data that agreed with Miyamoto's group, demonstrating that modification of histidine residues resulted in a decrease in V_{max}, but no change in substrate affinity. This was later confirmed by Thwaites *et al.* (1993b) on experiments with Caco-2 cells. However, Kramer and co-workers (1988) disputed these conclusions, reporting that DEPC treatment lead to an increase in affinity for cephalexin transport without influencing the maximal velocity of transport.

The previous studies also revealed that pre-incubation with substrates prevented the DEPC-induced inhibition (Miyamoto *et al.*, 1986; Kato *et al.*, 1989;

Kramer *et al.*, 1988; Terada *et al.*, 1998). However, substrate protection only prevailed when the substrate in question had a free α-amino group, suggesting a direct interaction of histidyl residues with this group (Kramer *et al.*, 1988; Terada *et al.*, 1998), possibly in the role of a proton donor/acceptor capacity.

Site-directed mutagenesis studies identified individual histidine residues required for efficient peptide transport. Terada *et al.* (1996) demonstrated that His_{57} and His_{121}, located in TM 2 and 4 respectively of rat PepT1, are absolutely essential for transport. Interestingly, the corresponding residues are conserved in human (Liu *et al.*, 1995), rabbit (Boll *et al.*, 1996) and rat (Saito *et al.*, 1996) kidney transporters. Similar experiments performed by Leibach's group (Fei *et al.*, 1997) on cloned human transporters confirmed the requirement of His_{57} in PepT1, plus His_{87} in PepT2, as being obligatory for transport. But, in contrast to Terada *et al.* (1996) postulated that His_{121} in PepT1, and the equivalent in PepT2 (His_{147}) were not absolutely critical.

The studies so far indicate that the essential histidine residues are localised in the substrate binding site of the transporter(s) and may be involved in intrinsic transport activity, although their precise roles have not yet been elucidated.

1.4.2.2 Thiol residues

Amino acid residues containing thiol (sulphydryl) groups are also thought to be located at or near the substrate binding site of the H^+-coupled peptide transporter and therefore may be involved in substrate interaction/translocation. Thiol groups have the potential to undergo oxidation-reduction reactions in response to a proton gradient across the membrane (Miyamoto *et al.*, 1986) and these reactions may induce changes in substrate affinity, specifically due to regulation by a dithiol and a disulphide situated in the binding site. A number of thiol-oxidising agents inhibited Gly-Sar transport in rabbit renal BBMVs, for example, NBD-Cl (7-chloro-4-nitrobenz-2-oxa-1,3-diazole), NEM (*N*-ethylmaleimide) and PCMBS (*p*-chloromercuri-benzenesulfonic acid). Preincubation with substrates protected these groups from modification and preserved the transport ability of the protein (Miyamoto *et al.*, 1986).

In contrast, the role of thiol groups in PepT1 transport is unclear. Kato *et al.* (1989) and Kramer *et al.* (1990a) demonstrate a lack of effect of PCMBS and NEM,

respectively, on substrate transport by rabbit PepT1. However, treatment of Caco-2 cells expressing hPepT1 with PCMBS resulted in a reduction in transport (Inui *et al.*, 1992). This latter study implicated sulphydryl groups located at the external surface of the intestinal peptide transporter as being directly involved in translocation, in an undefined way.

1.4.2.3 Tyrosine residues

A role for tyrosine residues in transport activity has only been implicated in PepT1. Studies on rabbit PepT1 and PepT2 demonstrated that acetylation of tyrosine by *N*-acetylimidazole lead to a concentration-dependent inhibition of PepT1 transport, but had no effect on PepT2 activity (Kramer *et al.*, 1990a). Furthermore, a recent study by Yeung and co-workers (1998) constructed a computer model to create half of a putative channel formed by a number of TMs in PepT1 to illustrate key charged and aromatic residues that were oriented into the channel and may be involved in peptide transport. They specifically identified Tyr_{167} and subsequent site directed mutagenesis of this residue confirmed its absolute requirement for efficient transport. They hypothesised that its phenolic side chain might be a ligand to the α-amino group of the substrates. Graul and Sadée (1997) performed multiple sequence alignment and demonstrated Tyr_{167} to be conserved in peptide transporters from bacteria, fungi, yeast, plant, rabbit and human.

In conclusion, specific residues have been directly implicated as having an essential role in peptide transport. However, further work is required to clarify exactly which residues are important and to determine if tissue and/or species differences occur.

1.4.3 Substrate transport

The intestinal and renal oligopeptide carriers transport the same solutes; small peptides and peptidomimetic drugs, but their affinities and specificities for the substrates are slightly different. Expression of the transporter proteins in various heterologous systems, in addition to whole tissue and membrane vesicles studies, has provided an insight into the similarities and differences of their substrate requirements. These will be discussed in the following sections.

1.4.3.1 Maximum size of oligopeptides

In contrast to other solute transporters, e.g. for amino acids or sugars, the substrate-specificity of the peptide transport system is extremely broad. Oligopeptides consisting of either two or three amino acids are accepted as substrates; there are potentially 400 dipeptides and 8000 tripeptides (excluding D-isomers), which can be composed of either acidic, neutral or basic amino acids, all of which are transported efficiently. The molecular weight of the peptide substrates range from 102 Da (Gly-Gly) to 576 Da (Trp-Trp-Trp) (Meredith & Boyd, 1995). The broad substrate specificity of PepT1 was initially implied due to studies by Das & Radhakrishran (1975) who showed that over 30 dipeptides and three tripeptides were able to inhibit the uptake of Gly-Leu into monkey or human jejunal strips. This inhibition was also shown to be competitive, indicating they shared the same transport system.

Tetrapeptides were shown not to be efficient substrates of the transporters. Boyd & Ward (1982) first conducted investigations showing the ability of peptides to induce a depolarisation of the brush-border membrane of *Necturus* small intestine. Di- and tri-Gly caused large membrane depolarisations, whereas tetra-Gly or free glycine induced no response (figure 1.7). Both PepT1 and PepT2 have been subsequently shown to have this same basic substrate requirement, i.e. peptides composed of only two or three amino acids will be transported efficiently (Boll *et al.*, 1996).

Molecular volume is not the determining factor in whether a peptide substrate is to be transported, acceptance as a substrate is entirely dependent on chain length (Matthews, 1991). The fact that certain antibiotics with a molecular weight of many hundred are transported efficiently shows the unimportance of large molecular volume, providing the substrate is suitable for transport (Matthews, 1991).

1.4.3.2 Stereospecificity of substrates

Early studies by Burston *et al.* (1972) provided initial evidence that peptides containing L- and D-amino acids were substrates for the peptide transporter, although L-containing peptides were transported to a relatively greater extent. Experiments by Boyd & Ward (1982) also demonstrated that L-amino acid-containing peptides were better substrates; in comparison to L-Leu-L-Leu, when D-Leu-D-Leu was exposed to

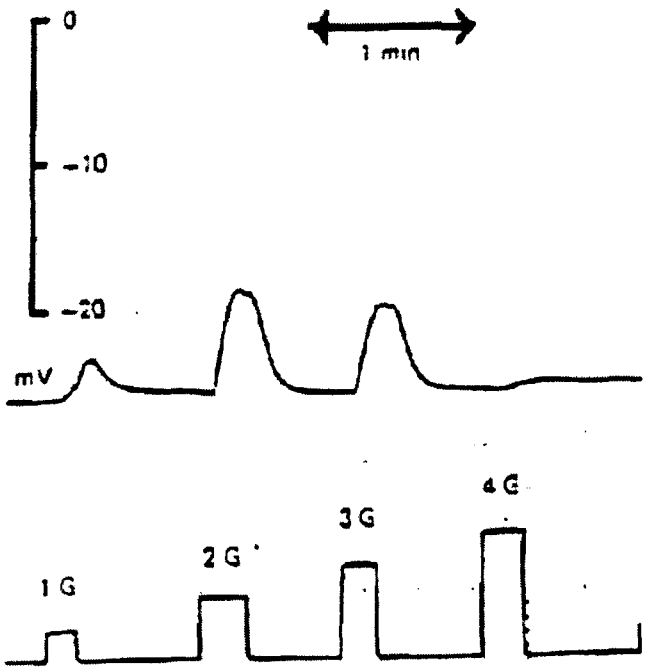

Figure 1.7

Effect of glycine (G) and glycine oligopeptides (2G, 3G, 4G) on the potential of the brush-border membrane of *Necurus* small intestine (upper trace); the lower trace indicates the presence of a substrate. Source: Boyd & Ward (1982).

the apical membrane of *Necturus* small intestine no change in membrane potential was observed. In addition, the side chains of β-lactam antibiotics also contain an asymmetric carbon atom, and the L-isomers of these drugs are better substrates than D-isomers (Leibach & Ganapathy, 1996). A more recent investigation by Lister *et al.* (1995) has shown that peptides containing mixed L- and D-amino acid isomers are actively transported. In this systematic study, the transport of all the possible (eight) dipeptides that can be formed from both L- and D-isomers of phenylalanine and alanine was investigated in isolated loops of rat small intestine (table 1.6). The study had many advantages over previous investigations; including (1) net transmural peptide transport was measured for each of the distinct substrates; (2) HPLC was used to detect the intact peptide and the individual amino acids, which allowed the extent of hydrolysis to be monitored, in addition to the transport rate; and (3) because the peptides were composed of the same amino acid residues direct comparisons between the individual isomers could be made. The results are summarised in table 1.6. Briefly, dipeptides composed of only L-amino acids were transported with the highest efficiency, but were also subject to rapid intracellular hydrolysis. In contrast, dipeptides containing only D-amino acids were extremely hydrolysis-resistant, but were also very poorly transported. This latter finding highlights the very low paracellular transport rate for dipeptides in the native epithelium, because peptide transport was studied in the presence of a high concentration of luminal glucose (28 mM). Pappenheimer & Reiss (1987) suggested that the passive flow of non-hydrolysed peptides by solvent drag through paracellular channels, induced by the active co-transport of glucose and Na^+, is quantitatively important in peptide absorption. The data from Lister *et* al. (1995) indicates this not to be the case and demonstrates that the absorption of peptides from the lumen is an active process. Mixed stereoisomers, where the D-amino acid was located at the N-terminus (D-Phe-L-Ala, D-Ala-L-Phe), were actively transported by the intestine, in particular D-Phe-L-Ala was largely transported intact showing considerable resistance to intracellular hydrolysis. However, if the D-amino acid was located at the C-terminus the dipeptide was not transported to any appreciable extent.

Peptide	Absorption	Hydrolysis	Serosal appearance
L-Ala-L-Phe	++++	++++	0
L-Ala-D-Phe	++++	++++	0
D-Ala-L-Phe	+++	+++	+
D-Ala-D-Phe	minimal	minimal	minimal
L-Phe-L-Ala	++++	++++	0
L-Phe-D-Ala	++	++	0
D-Phe-L-Ala	+	minimal	+
D-Phe-D-Ala	0	minimal	minimal

Table 1.6

Stereospecificity study examining the fate of eight dipeptides of Phe and Ala when perfused through the lumen of rat small intestine (reproduced from Lister *et al.*, 1995); + represent relative transport rates.

1.4.3.3 Charged substrates

Although peptides containing basic, neutral and acidic amino acids are accepted as substrates by the peptide transporters, the charge of the structure affects the efficiency by which it is transported. Moreover, it is the nature and position of the charge within the peptide structure that influences its transport ability (Meredith & Boyd, 1995). Hidalgo and co-workers (1995) reported that there was no difference in interaction of linear dipeptides with the peptide transporter, regardless of the net charge but, despite this view, other groups corroborate the charge dependence of transport.

1.4.3.3.1 Distinct pH-dependence in the transport of charged peptides

It appears that differently charged peptides vary in their dependence on medium pH for transport. A general conclusion is that anionic/zwitterionic substrates are transported with a relatively higher efficiency at a more acidic pH (~5.5), whereas cationic substrates are more rapidly transported at a slightly higher pH (~6.5) (Temple *et al.*, 1995; Wenzel *et al.*, 1996; Amasheh *et al.*, 1997; Steel *et al.*, 1997). Collectively, the investigations indicate distinct pH optima for differently charged substrates, whether peptides or β-lactam antibiotics. For example, the presence of an inwardly-directed proton gradient has a distinct effect on the transport of differently charged peptides when compared to transport in the absence of the gradient; transport of D-Phe-L-Ala (a neutral peptide) is stimulated, but not as much as transport of D-Phe-L-Glu (an anionic peptide). In contrast, however, transport of D-Phe-L-Lys (a cationic peptide) is not altered. In the absence of a pH gradient, the initial rate of substrate entry into vesicles is entirely dependent on charge; relative transport rates are as follows: cationic > neutral > anionic. In conclusion, the H^+-dependence of transport is not identical for all substrates. The differences in transport due to medium pH and charge are thought to be due to differences in affinity for the binding site, rather than in intrinsic activity of the transporter (Steel *et al.*, 1997).

In addition to the direct effect of proton gradient on transport, the external pH has also been shown to affect the membrane potential-dependence of transport in a substrate specific way (Wenzel *et al.*, 1996). For example, zwitterionic antibiotics were demonstrated to lose their membrane potential dependence when pH_o was

reduced from 6.5 to 5.5, whereas the transport of anionic substrates was independent of membrane potential. The reason for this is not clear, further studies are needed to clarify the exact mechanisms involved.

1.4.3.3.2 Distinct H^+ flux coupling ratios of charged substrates

Wenzel and co-workers (1996) proposed that the most plausible explanation for the differences in the pH-dependence of transport of differently charged substrates is that a discrete flux coupling ratio for H^+-mediated transport occurs, which is entirely due to the net charge of the substrate. The results from previous studies (Temple *et al.*, 1995; Steel *et al.*, 1997) corroborated this hypothesis, although Amasheh *et al.* (1997) stated that extracellular H^+ affects the affinities of charged substrates for the transporter and that H^+ binding itself is affected by charged substrates. It was stated (Wenzel *et al*, 1996; Temple *et al.*, 1995; Steel *et al.*, 1997) that anionic peptides are transported in conjunction with two protons, whereas neutral peptides are coupled with one proton and cationic peptides also with one proton, if any at all. This means that the H^+-dependence of transport is not universally fixed for all substrates, but depends specifically on the charge of the transported substrate. In this way, the total charge translocated into the cell remains constant despite the varying anionic, neutral or cationic nature of the substrate itself. The extra proton transported with anionic substrates would primarily function to compensate for the substrates negative charge and the remaining proton, common to all substrates, would drive transport across the membrane in the normal way.

As mentioned in section 1.4.2.1, PepT1 has two histidine residues located in TM domains 2 and 4 (His_{57} and His_{121} in rabbit) which are conserved in the two isoforms in many species. Temple *et al.* (1995) proposed that protonation of both of these residues is essential for the transporter to bind anionic peptides and this does not occur unless the external pH is less than pH 6.5. However, neutral peptides only require one residue to be protonated and a cationic peptide can bind in the absence of an associated proton. Temple and co-workers (1996) devised a model for peptide transport and suggested that the carrier was negatively charged (C^-). They suggested that the charged nature of the carrier protein depended entirely on the pH of the external (luminal) medium, i.e. when pH_o is neutral (7.4) the empty carrier is returned to the external (luminal) surface of the apical membrane possessing a

negative charge (C^-), but if pH_o is more acidic (5.5), the carrier will return in a neutral state (C^-H^+). It is evident that cationic substrates would be able to bind at a higher efficiency to the carrier at a more neutral pH than neutral/anionic substrates. The study also states that H^+ binding is rate limiting for transport, not the return of the empty carrier to the luminal surface.

Elucidation of the precise nature of the transport of differently charged substrates will aid in the design of drugs that will be efficiently absorbed across the apical membrane of the intestine at the pH of the acidic microclimate located adjacent to the brush-border *in vivo*.

1.4.4 Substrate binding site

1.4.4.1 Localisation of the substrate binding site

It is thought that the differences observed between PepT1 and PepT2 in their relative substrate specificities and/or affinities were very likely due to variations in the structure of the substrate binding domain of the two proteins. Chimeras can be generated between closely related family members in order to identify the structural features responsible for these functional properties of the transporters.

Döring *et al.* (1996) constructed a chimeric cDNA from rabbit (CH1Pep) consisting of the N-terminal region of PepT2 (amino acid residues 1-401) and the C-terminal region of PepT1 (residues 402-707), including the large extracellular loop between TM 9 and 10. The cDNA was expressed in *Xenopus* oocytes and its transport characteristics were compared to the parent isoforms. The studies showed that all of the important phenotypic functions of PepT2 were located in its amino terminal region, including its pH-dependence, substrate specificity and its high affinity component. The extracellular loop and carboxy terminal regions were not implicated in these features. However, it was thought that they might be involved in trafficking of the protein or in regulation of transport, due to the fact that PepT2 possesses two additional PKC sites in its C-terminal tail that are not present in PepT1.

In contrast to this study, Fei and co-workers (1998b) reported that the substrate binding domain was located within TM domains 7, 8 and 9 (the C-terminal half of the transporter), as a result of experiments with a number of human PepT1/rat PepT2 chimeras. They also postulated that His_{57} in TM2 might lie in close proximity

to this suggested binding site within the 3-D topology of the transporter and so was also implicated in substrate interaction.

Investigations with rat PepT1/PepT2 chimeras (Terada *et al.*, 2000) also indicated that the H^+ binding site and substrate recognition site were located in the N-terminal halves of the transporters, i.e. in TM 1-6, in agreement with Döring *et al.* (1996). Their results correlated with previous investigations, which showed that histidine residues (57 & 121 in PepT1) were the binding site of the α-amino group of substrates (Terada *et al.*, 1998), and with studies by Yeung *et al.* (1998) which implicated a tyrosine residue in TM 5 of hPepT1 having an essential role. In addition, Terada *et al.* (2000) expressed the possibility that both the N- and C-terminal halves of PepT2 may be involved in determination of substrate affinity, although the C-terminal region of PepT1 does not appear to play the same role. As such, the region influencing substrate affinity is not necessarily the substrate-binding site. The variances observed between theirs and Döring's work compared with the study by Fei *et al.* were attributed to species differences (Fei's group used chimeras constructed from human and rat transporters). As a result of this major difference in the results, Terada *et al.* (2000) postulated that TM 7-9 of rat PepT2 are the critical regions for substrate affinity, rather than the actual binding site.

1.4.4.2 Template for the substrate binding site

Bailey *et al.* (2000) generated a template for the substrate binding site of PepT1 by examining the binding and translocation data of virtually all substrates published so far. They proposed that the simple model would provide an indication of whether potential substrates would be transported by PepT1 with high, medium or low efficiency, and may eventually aid in the design of efficiently absorbable drugs. The model has the following features in 3-D topology, described from the N- to the C-terminus, but only 4 are depicted in figure 1.8a (indicated by #):

(1) a strong attachment site for the amino terminal NH_3^+ group (#1)

(2) a planar backbone from N- to C-termini (optimum 6 Å)

(3) a hydrogen bond to the carbonyl group of the first peptide bond (#2)

(4) alkylation of N_2 is accepted

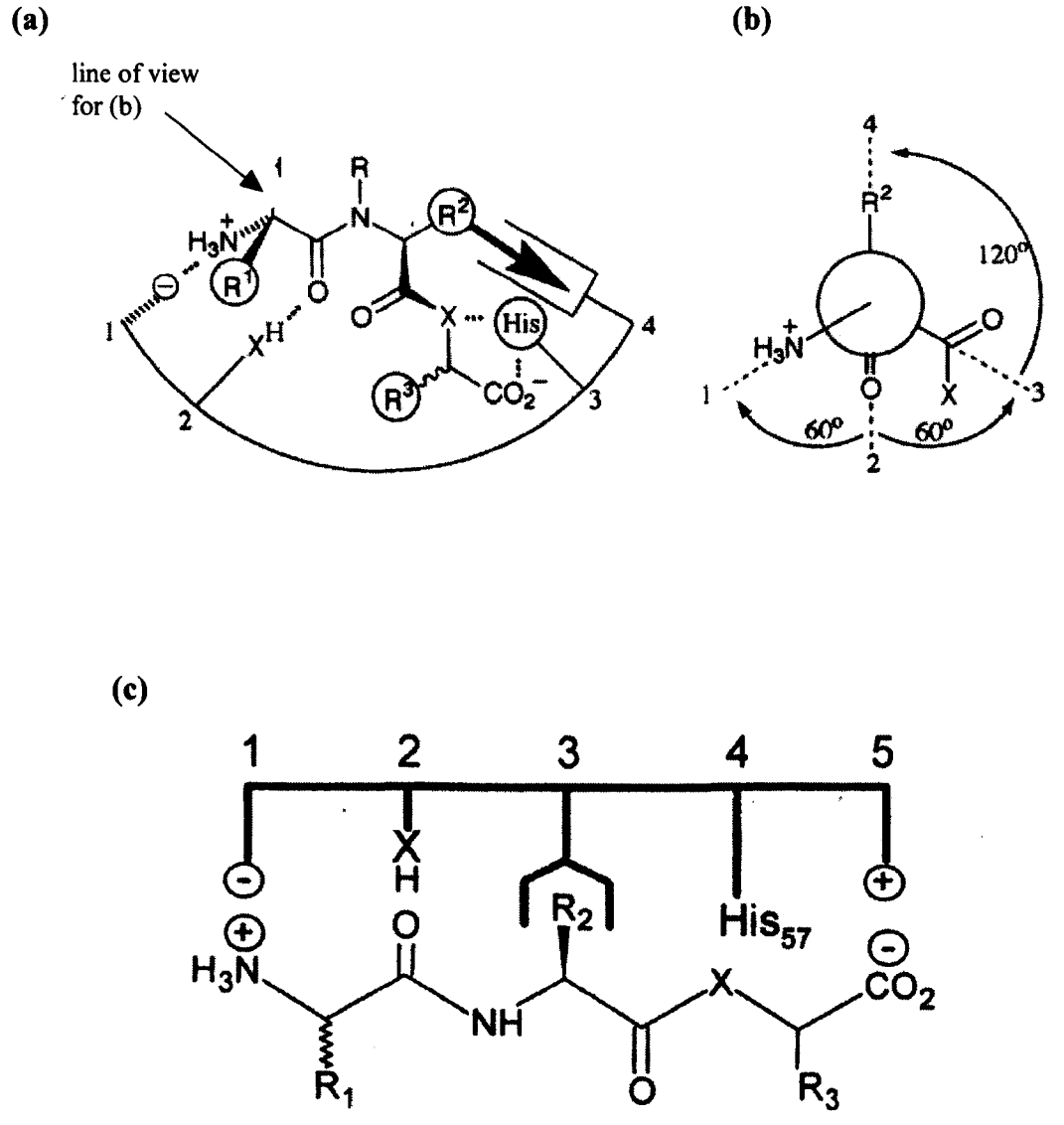

Figure 1.8

The substrate binding template proposed by Bailey *et al.* (2000) shows the layout of the 4 main binding features (see section 1.4.4.2) (a) and their orientation (b), viewed as indicated in (a). A refined model is shown in (c), designating certain features for specific roles within the 3-D structure (Meredith *et al.*, 2000).

(5) specific orientation of three groups at the second residue (usually L isomer)
(6) a hydrophobic pocket (#4)
(7) a carboxylic acid binding site (#3)
(8) potential space for the side chain of the third residue (if a tripeptide)
(9) a second carboxylic acid binding site (#3)

Binding to the active site is maximised by a combination of all of the above factors, i.e. it is an aggregate of all features that determines whether a substrate binds with high or low affinity. Substrates with a high affinity for the binding site are able to adopt the correct conformation to fit into the 3-D pocket without paying a high energetic price.

The same group (Meredith *et al.*, 2000) refined this model by designating certain features for specific roles within the 3-D structure. The revised model is shown in figure 1.8b. Overall, it is thought that the N terminus is the primary binding site for the substrate and that interaction of a tripeptide, in comparison to a dipeptide, occurs through accommodation of the additional C terminus within an extended model (#3 on the initial template). In this way the amino terminus has a fixed location in the binding site, whereas binding of the carboxyl terminus is relatively flexible within the defined space. Specifically, it is thought that Glu_{595} anchors the N terminus and histidine residues are involved in binding of the C-terminus (His_{57} for dipeptides, His_{121} for tripeptides).

1.4.5 Exploitation of PepT1 for efficient drug delivery

The specific requirements for potential substrates of the peptide transporters are not fully understood, although all of the substrates studies so far bear steric resemblance to the backbone of physiologically occurring di- and tripeptides. PepT1 has the potential to be exploited for the efficient absorption of orally active peptidomimetic drugs and could be used to aid rational drug design by the modification of compounds with good pharmacological activity, but poor bioavailability, to allow uptake via PepT1 from the intestine following oral administration. However, in order for this to become a reality, a comprehensive understanding of the pharmacophoric pattern required for interaction of substrates

with the active site of PepT1 is needed. This pharmacophoric pattern of atoms, or groups of atoms, mutually oriented in space can be defined by studies using a set of structurally similar compounds showing affinity for the transporter. The compounds used to study peptide transporters are not peptides, but generally cephalosporins (figure 1.9). This is due to a relatively low conformational flexibility, which means that they are expected to have a few energy minima through which they can interact with the active site, although they resemble the planar backbone of tripeptides. Peptides possess freely rotatable bonds and therefore lack the rigid structure required for this investigation.

The requirement of a free N-terminal α-amino group of substrates has been most extensively studied and all groups unanimously agree that it is not required for transport by PepT1 (Bai *et al.*, 1991,1992b; Oh *et al.*, 1993; Yuasa *et al.*, 1993; Li *et al.*, 1996; Raessi *et al.*, 1999). In contrast, substrates without a C-terminal carboxyl group are not transported (Bai *et al.*, 1992b; Hidalgo *et al.*, 1995). β-amino acids at either side of the peptide bond are compatible with the transporter, whereas γ-amino acids are not (Bai *et al.*, 1992b). Interestingly, it has been demonstrated that a peptide bond is not an absolute requirement for a substrate; Temple *et al.* (1998) first reported the translocation of a compound lacking a peptide bond (4-amino-phenylacetic acid). Other examples of such transported compounds are ω-amino fatty acids (Döring *et al.*, 1998), L-valine ester compounds (Sawada *et al.*, 1999) and Ac-Phe (Meredith *et al.*, 2000). However, though PepT1 can tolerate many diverse substrates, it appears as though it can differentiate between the two possible configurations of a solute; thus Brandsch and co-workers (1998) revealed that only the *trans* isomer of Ala-Pro was accepted as a substrate.

As mentioned in section 1.4.3.1, it is thought that the chain length of a substrate is the determining factor in whether it will be transported, not molecular volume. Li *et al.* (1996) showed that although PepT1 can accommodate a range of distances between the N and C termini of 5.5 and 9 Å, the optimum is 5.5 Å; any increase reduces affinity of the substrate for the transporter. This group extended their study to explain the differences between transport of L and D isomers of peptides (Li *et al.*, 1998). In this latter paper they suggested that inclusion of a D-amino acid at the C-terminus of a dipeptide (L-Val-D-Val) decreased the distance between the amino and carboxyl termini more dramatically than a D-amino acid at the N terminus (D-Val-L-Val). This may account for the low affinity of these mixed

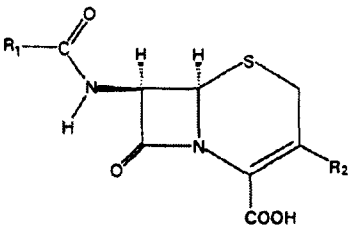

Cephalosporins	R^1	R^2
*Cefaclor		
*Cefadroxil	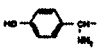	
Cefamandole		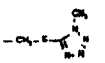
Cefamandole Nafate		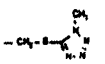
Cefazolin		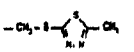
Cefoperazone	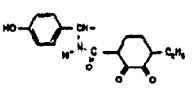	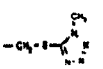
Cefotaxime	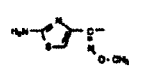	
Cefoxitin		
Cefsulodine		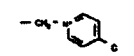
Ceftazidime	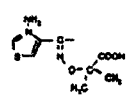	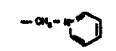
Cefuroxime	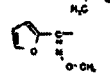	
*Cephalexin		
*Cephalogylycin		
Cephaloridine		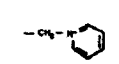
Cephalothin		
Cephapirin	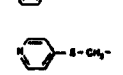	
*Cephradine		

Figure 1.9

The structure of cephalosporins used to determine the substrate requirements of the peptide transporters. Source: Raessi *et al.* (1999).

stereoisomers (N terminal L-amino acid, C terminal D-amino acid) for the transporters (as described in section 1.4.3.2). The postulated minimum distance of 5 Å also partially explains a general low affinity of free amino acids. Döring *et al.* (1998) suggested a minimum distance between the two head groups for efficient transport, but stated that at least four methylene groups are required between the N-and C-termini, which corresponds to a distance of 500-630 pm. They also contrasted their results with another group (Brandsch *et al.*, 1998) to explain the *cis/trans* discrimination by PepT1. Döring *et al.* (1998) postulated that it may not be the absolute conformation of the structure that determines transport, but the associated changes in spacial location and/or separation of the head groups, i.e. *cis* bond substrates are excluded because the N to C distance is too short to interact with important groups in the binding domain. Li *et al.* (1998) reported that the distance between the amino terminus and the second peptide bond (in a tripeptide) is also important.

There are contrasting results concerning the transport of linear and cyclic peptides; Mizuma *et al.* (1998) reported the translocation of cyclic peptides, whereas Hidalgo *et al.* (1995) suggested that cyclisation of peptides reduces transport.

Certain groups have published data which demonstrate a differential recognition and transport of substrates by the intestinal and renal peptide transporters (Ganapathy M. E. *et al.*, 1995; Terada *et al.*, 1997a, b). These data suggest that PepT2 has a higher affinity for β-lactam antibiotics with an α-amino group than PepT1 does, whereas PepT1 appears to prefer β-lactam antibiotics without an α-amino group.

Overall, certain substrate requirements of the peptide transporters have been defined, but further studies are needed to obtain a complete understanding of what exactly is required for maximum bioavailability of potential pharmacologically active compounds, i.e. for efficient interaction with both the intestinal and renal transporters.

1.5 PEPTIDE TRANSPORT AT THE BASOLATERAL MEMBRANE

Although extensive functional and molecular information on peptide transport at the apical membrane of many tissues in a number of different organisms is now available, the importance of the basolateral membrane peptide transporter has been overlooked thus far. Previously is was thought that peptides were not transported intact into the circulation, but hydrolysed to their constituent amino acids prior to entry into the portal blood (Matthews, 1975). It is now accepted that peptides are transported intact into the bloodstream; recent studies have demonstrated that approx. 50% of plasma amino acids are in the form of peptides, the majority as di- and tri-peptides. In addition, orally active β-lactam antibiotics are also efficiently absorbed through the intestinal wall, in spite of their low lipophilicity and resistance to hydrolytic breakdown. Despite this revelation, leading workers still doubted the existence of a basolateral transporter, as a distinct protein to the apical transporter. For example, Fei *et al.* (1994) suggested, as a result of hybrid depletion studies, that PepT1 was responsible for all Gly-Sar uptake activity in *Xenopus laevis* oocytes injected with rabbit small intestinal mRNA.

However, in recent years its existence has been postulated and subsequent studies have provided proof of this, in addition to revealing certain features regarding its mechanism and function. Walker *et al.* (1998) performed experiments which proved that there was a separate transporter, which was not PepT1, at the basolateral membrane. Using hPepT1-specific antibodies, they immunolocalised hPepT1 expression exclusively to the apical membranes of human enterocytes *in vivo* and *in vitro* (Caco-2 cells). Ogihara and co-workers (1996) demonstrated the same in rat small intestine.

However, very little is actually known about this area of peptide transport, despite the huge amount of pharmaceutical interest in the exploitation of peptide transporters as a whole to achieve intact and efficient drug delivery after oral administration. This section will review the (finite) knowledge about this physiologically and therapeutically important peptide carrier.

1.5.1 Mechanism of peptide transport

It must first be stated that although we do have a basic understanding of the function of the basolateral peptide transporter, the membrane protein has not been identified to date.

The results concerning the mechanism of this transporter are conflicting; some groups have reported that transport is stimulated by the presence of a H^+ gradient, much in the same way that PepT1 functions, whereas other have postulated it is a facilitative transporter. H^+-stimulated transport has been demonstrated in BLMV isolated from rabbit intestine (Dyer *et al.*, 1990) and in Caco-2 cells (Thwaites *et al.*, 1993a, b). These studies have shown that although the basolateral transporter does not appear to have an optimum pH for transport, in the same way that PepT1 does, transport is stimulated by a more acidic pH. In addition, Dyer and co-workers (1990) revealed an inhibitory effect of proton ionophores (CCCP and TTFB) on H^+-stimulated uptake in BLMV. Thwaites *et al.* (1993a) demonstrated that Gly-Sar only induced intracellular acidification across the BLM in the presence of a proton gradient.

Other groups (Saito *et al.*, 1993; Terada *et al.*, 1999; Matsumoto *et al.*, 1994) reported that because the effect of external pH at the basolateral membrane was less pronounced than that observed at the apical membrane, transport was due to a facilitative component. Matsumoto *et al.* (1994) indicated a major difference in transport between PepT1 and the basolateral transporter associated with a pH gradient; FCCP had a dramatic effect on apical transport but did not affect basolateral transport to any appreciable extent, implying it is unlikely that a H^+ gradient is coupled to this transporter.

It is evident that further work is required to elucidate the precise driving force and mechanism of the basolateral peptide transporter.

1.5.2 Transport kinetics

Despite the conflicting views about the mechanism of transport, all of the investigations performed so far collectively agree that basolateral transport is due to a single carrier mediated system (for example, Dyer *et al.*, 1990; Terada *et al.*, 1999). For the majority of the substrates studied, transport has been shown to be saturable

and conform to Michaelis-Menten kinetics. The single exception to this was ceftibuten (Matsumoto *et al.*, 1994) in which transport was linear, even up to 20 mM.

Kinetic studies have revealed an important distinction between apical and basolateral transport; a lower K_m value coupled with a higher V_{max} value of PepT1 for substrates demonstrates that the apical carrier has a relatively higher affinity for substrates and a considerably higher capacity for transport than the basolateral transporter. The kinetics are summarised in table 1.7. This difference in transport kinetics has physiological relevance, i.e. PepT1 mediates the active transport of substrates against a concentration gradient, which results in accumulation of the substrate within the cell. If the basolateral transporter had a similar high affinity for substrates, it would constantly be saturated by the elevated levels in the cytosol. A corresponding situation is found with glucose transporters; SGLT1 at the apical membrane has a K_m for glucose of 0.8 mM, whereas GLUT2 in the basolateral membrane has a K_m of 15-20 mM (Hediger & Rhoads, 1994).

The substrate specificity of the basolateral peptide transporter is generally thought to be very similar to PepT1 (Saito *et al.*, 1993; Matsumoto *et al.*, 1994). However, during transport inhibition studies by Terada and co-workers (1999) and Thwaites *et* al. (1995) it was shown that there might be a variation in specificity by the two transporters. For example, out of a number of substrates studied, ceftibuten had the highest affinity for PepT1, whereas it had the lowest affinity for the basolateral transporter (Terada *et al.*, 1999).

It has been unequivocally demonstrated that uptake across the apical membrane into the cell (Caco-2) is considerably greater than uptake across the basolateral membrane; the extent ranging from 3 to 10-fold (Inui *et al.*, 1992; Saito *et al.*, 1993; Thwaites *et al.*, 1993b; Terada *et al.*, 1999), depending on the substrate used. A number of groups have shown that efflux across the basolateral membrane occurs at a significantly faster rate than exit at the apical membrane (Inui *et al.*, 1992; Matsumoto *et al.*, 1994), although Thwaites *et al.* 1993b indicated that basolateral efflux is slower than apical efflux. The direction of transport is also important; transport from the apical to basolateral membrane is more rapid than the reverse (basolateral-to-apical) (Inui *et al.*, 1992; Saito *et al.*, 1993; Thwaites *et al.*, 1993b). This preferred undirectionality of transport corresponds to the absorptive process *in vivo*, and so makes physiological sense. However, it cannot be ruled out that the

SUBSTRATE	TRANSPORTER	K_m	V_{max}
Cephradine[1]	PepT1	5.9	1.9
	BLT	9.2	0.7
Bestatin[2]	PepT1	0.34	0.62
	BLT	0.71	0.24
Gly-Sar[3]	PepT1	0.65	13
	BLT	2.1	9.5

Table 1.7

Kinetic parameters collated from distinct studies which compared substrate transport by PepT1 and the basolateral peptide transporter (BLT) in Caco-2 cells. K_m is expressed as mM, V_{max} is expressed as nmol·min^{-1}·[mg protein]$^{-1}$. [1]Matsumoto *et al.* (1994), [2]Saito *et al.* (1993), [3]Terada *et al.* (1999). Results suggest that the basolateral transporter has a lower affinity and lower capacity for transport, relative to PepT1, for all substrates investigated.

basolateral transporter participates in additional transport functions; for example, it may act to clear dipeptides which have been released due to hydrolysis of bioactive peptides directed at the basolateral surface of intestinal cells *in vivo* (Thwaites *et al.*, 1993b).

1.5.3 Essential residues of the transporter

As stated previously, the basolateral membrane peptide transporter of intestinal enterocytes has not yet been identified. Therefore, no structural information is available on the membrane protein. However, the studies performed so far have revealed that sulfhydryl groups located on the external surface of the transporter are essential for function; PCMBS abolishes transport (Inui *et al.*, 1992; Saito *et al.*, 1993).

PepT1 has been shown to possess essential histidine residues thought to be involved in H^+ binding or interaction with the α-amino group of substrates. DEPC also inhibits activity of the basolateral transporter, albeit to a lesser extent than with PepT1 (Terada *et al.*, 1999) and preincubation of the membrane with substrates prevents this DEPC-induced inhibition. Therefore, if the basolateral transporter is eventually proven to be independent of a proton gradient, the histidine residues might be later demonstrated by site-directed mutagenesis to be involved in substrate recognition.

1.5.4 Is basolateral transport the rate-limiting step in peptide absorption?

In the past it was generally believed that transport at the basolateral membrane is the rate-limiting step in absorption (Thwaites *et al.*, 1993a,b; Matsumoto *et al.*, 1994), due to the relative rates of transport at the apical and basolateral membranes. Data regarding the relative affinities and transport capacities of the transporters have also corroborated this view (see table 1.7), i.e. the basolateral transporter has a lower affinity for substrates and lower capacity for transport than PepT1 (Saito *et al.*, 1993; Matsumoto *et al.*, 1994; Terada *et al.*, 1999). However, the data is disputable because most of the studies on basolateral transport have examined uptake into the cell, not the efflux process which occurs *in vivo* during absorption. Hori *et al.* (1988) demonstrated a good correlation between the apparent

absorption rates of a number of cephalosporins, which were estimated by their disappearance from the lumen of an isolated intestinal loop, and their initial uptake rates by intestinal BBMV. They proposed that it is apical transport that is the rate-limiting step in the intestinal absorption of the antibiotics.

It is clear that a considerable amount of work is required to elucidate the structural and functional features of the basolateral peptide transporter. Only when this knowledge equals that of PepT1, or progresses even further with both proteins, can orally active drugs be designed, which will be transported efficiently across the intestine as a whole, to exert their pharmacologic action.

1.6 REGULATION OF INTESTINAL PEPTIDE TRANSPORT

Regulation of peptide transport in the small intestine has received far less attention than regulation of sugar and amino acid transport. Early investigations (see Ferraris *et al.*, 1988) produced inconsistent results, probably due to methodological problems; for example, the effects of the unstirred water layer and the use of hydrolysis-susceptible peptides made transport difficult to measure.

In principle, peptide absorption can be regulated at either the apical or basolateral membrane of the enterocytes. Regulation can occur both in the long-term (days to weeks); adaptation to dietary changes or alterations in the endocrine status of the animal, or in the short-term (minutes to hours); during assimilation of a meal. Long-term regulation usually involves the biosynthesis of new (additional) transporters, and is associated with epithelial turnover. In contrast, short-term phenomena incorporates either the recruitment of transporters from a pre-formed intracellular pool, followed by their membrane insertion, or modulation of the intrinsic activity of the transporters already present in the membrane. The (limited) investigations concerning the regulation of intestinal peptide transport performed thus far have concentrated exclusively on the apical membrane, and dealt largely with long-term adaptation to dietary changes. In contrast, short-term regulation has barely been studied, despite the fact that this information is crucial if we are to understand the fundamental physiological processes that control the absorption of nutrients after a meal. Even such basic information as to how peptides themselves, and other dietary constituents (amino acids in particular), regulate the absorption of peptides

from the lumen of the intestine is unknown. In addition, a comprehensive knowledge of the roles that hormones, and associated intracellular signalling pathways, play in peptide transport is crucial. Not only is this information required to understand the mechanisms behind nutrient absorption following food intake, but also for the efficient transfer of bio-active drugs into the bloodstream when administered by the oral route. In order for the entire transmural transfer processes to be elucidated, knowledge of regulation, not only at the apical membrane, but also at the basolateral membrane, is required.

This section will report the present knowledge of long-term dietary control of peptide transport, and the finite information available for short-term regulation of transport, at the brush-border membrane.

1.6.1 Long-term regulation of peptide transport

At present, the majority of investigations into long-term regulation of peptide transport have been directed at the role of dietary constituents, or lack thereof (fasting/starvation).

1.6.1.1 Adaptation to changes in luminal nutrient levels

One of the initial studies which examined the effect that high- and low-protein diets had on peptide absorption was performed by Ferraris *et al.* (1988), on the uptake of L-carnosine. They discovered that carnosine transport was considerably higher in rats fed a higher protein ration for two weeks and postulated that the mechanism of stimulation might be due to the induction of more transporters at the apical membrane. A study by Erickson *et al.* (1995) found that, coupled with the stimulation in transport activity, there was an increase in PepT1 mRNA levels in the middle and distal sections of the small intestine.

Subsequent investigations by Thamotharan *et al.* (1998), Walker *et al.* (1998) and Shiraga *et al.* (1999) have extended the knowledge of substrate up-regulation of its own transport. It was found that not only does a high protein diet influence the transport activity of PepT1, but certain individual dipeptides also produce the same effect. The increase in transport activity (figure 1.10) is due to a rise in V_{max} of the transporter, without a corresponding change in K_m. There is a concomitant elevation in PepT1 protein expression at the apical membrane (ranging

from 1.72 to 2.2 fold) (figure 1.10), plus an enhancement of mRNA levels (ranging similarly from 1.98 to 3.0 fold) (figure 1.11a,b). Coupled with this, an increase in mRNA half life, from 8.9 to 12.5 h, due to both enhanced stability and transcription (figure 1.11c) was observed. However, these effects were not universal with all substrates; whereas Gly-Sar (Thamotharan *et al.*, 1998; Walker *et al.*, 1998; Adibi, 1997) and Gly-Phe (Shiraga *et al.*, 1999) induced the stimulation in activity, Gly-Gln did not (Shiraga *et al.*, 1999). Therefore, it appears that the effect might be peptide specific.

In addition to the long-term stimulatory effect of dipeptides on peptide transport, there also appears to be an effect of amino acids (Ferraris *et al.*, 1988). Shiraga and co-workers (1999) demonstrated that free phenylalanine (Phe) enhanced transport in a comparable way to Gly-Phe, in contrast glycine (Gly) and glutamine (Gln) did not. As such, the induced stimulation also seems to be amino acid-specific. It was proposed that certain small peptides and amino acids produced from hydrolytic breakdown of large peptides or proteins in the lumen enter the enterocytes, by their individual carriers, to directly stimulate transcriptional activation of the PepT1 gene. However, it is not known whether the effects of peptides and amino acids are by the same, or completely different, mechanisms.

Walker *et al.* (1998) explained the stimulation in transport as the control of mRNA accumulation, rather than translation or post-translational modification of the protein. However, Thamotharan *et al.* (1998) performed experiments with brefeldin, which disrupts the trans-Golgi network (TGN) required for processing of membrane proteins, and showed that substrate stimulation was abolished despite an increase in gene expression. As such they suggested that stimulation in transport was probably due to membrane recruitment of the transporter protein from a newly synthesised pool.

Substrate upregulation of nutrient transporters is known to be an efficient mechanism for ensuring cellular economy in balancing the costs of synthesis and maintenance. It can be concluded that there is a direct effect of nutrient supply on the function of epithelial cells to induce peptide transport, which doesn't involve neural and/or hormonal factor(s). These findings have therapeutic value, i.e. if the bioavailability of a particular drug is low, absorption may be enhanced by

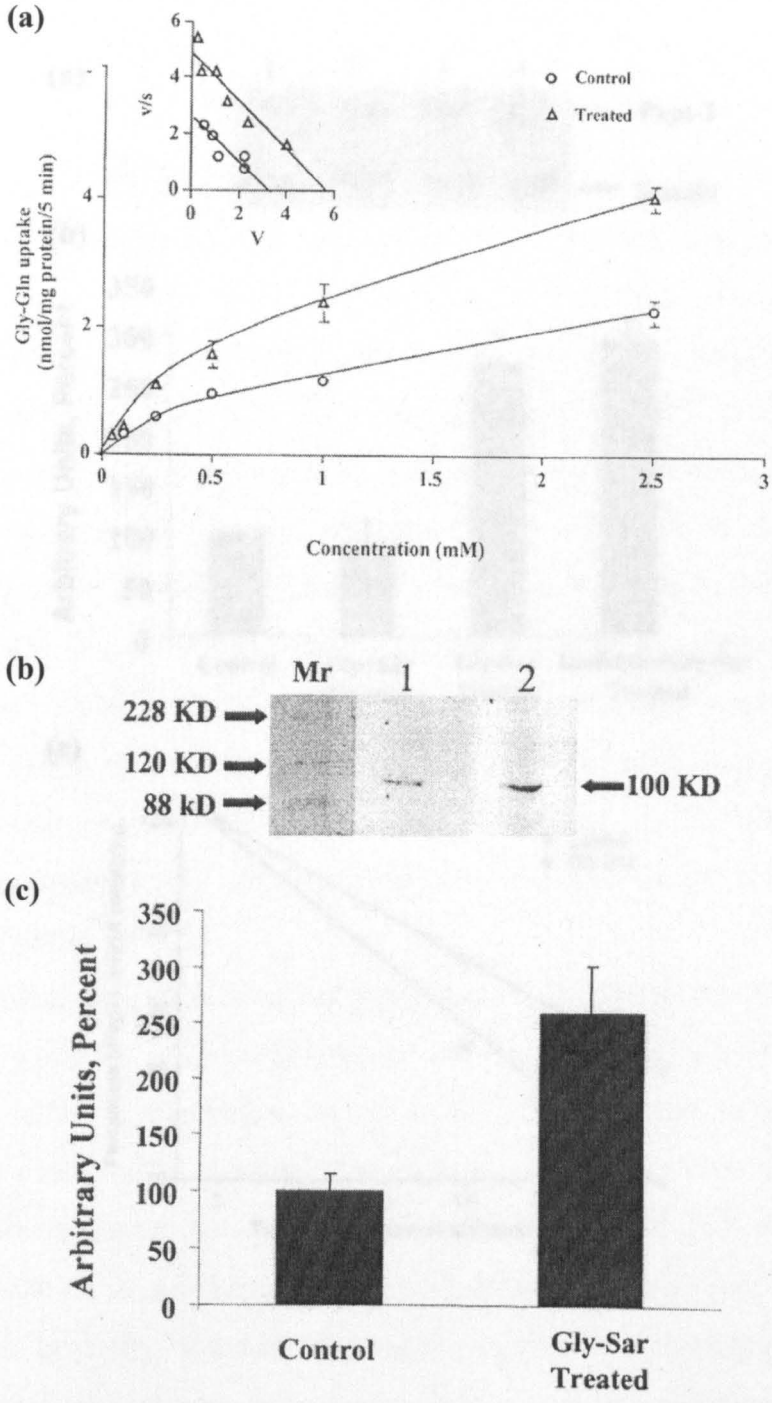

Figure 1.10

Dipeptide stimulation of peptide transport in Caco-2 cells. Pre-treatment of cells with 10 mM Gly-Sar for 24 h induced an increase in transport rate of Gly-Gln (a), and a higher abundance of PepT1 protein mass in apical membranes, demonstrated by SDS-PAGE (b,c). Source: Thamotharan *et al.* (1998).

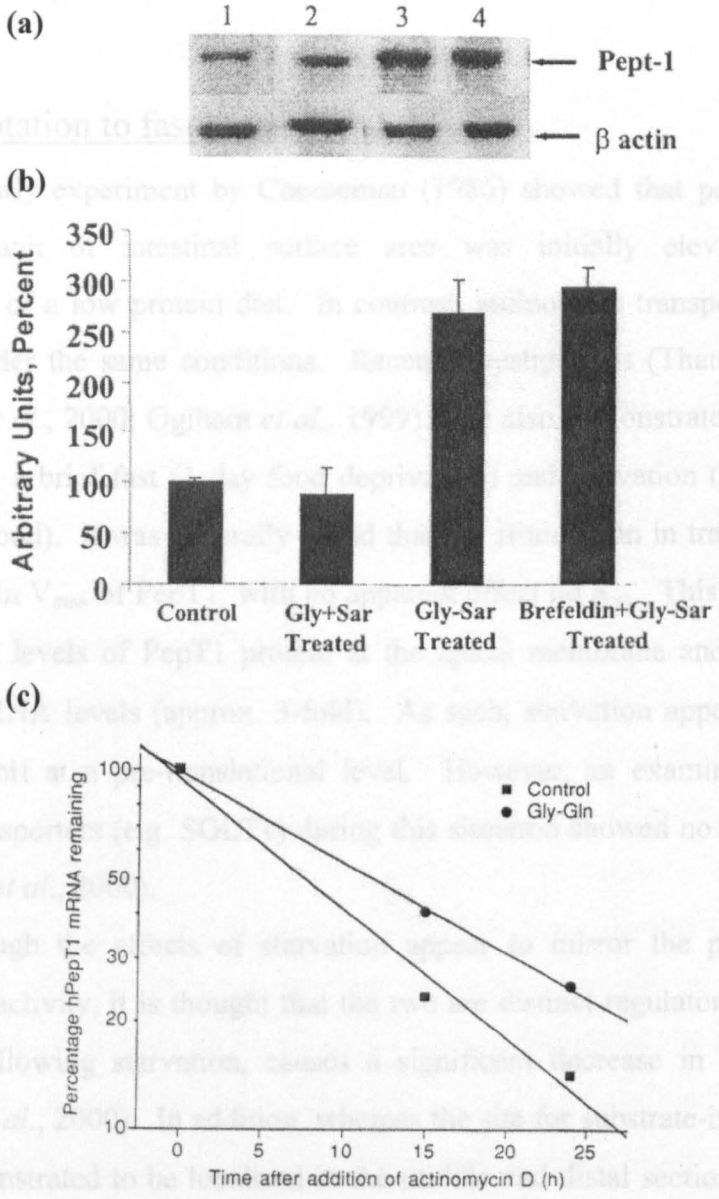

Figure 1.11

Effect of dipeptide pre-treatment of Caco-2 cells on the abundance and half-life of PepT1 mRNA. Pre-treatment of cells with 10 mM Gly-Sar for 24 h induced an increase in PepT1 mRNA abundance (a), demonstrated by densitometric analysis of the Northern blot (b) (Thamotharan *et al.*, 1998). In addition, pre-treatment of cells with 4 mM Gly-Gln for 72 h causes an increase in PepT1 mRNA half-life (c) (Walker *et al.*, 1998).

co-administration with a high protein diet, containing specific dipeptides and amino acids.

1.6.1.2 Adaptation to fasting and/or starvation

An early experiment by Cheeseman (1986) showed that peptide transport activity per unit of intestinal surface area was initially elevated following administration of a low protein diet. In contrast, amino acid transport activity was suppressed under the same conditions. Recent investigations (Thamotharan *et al.*, 1999a; Ihara *et al.*, 2000; Ogihara *et al.*, 1999) have also demonstrated this to be the case following a brief fast (1 day food deprivation) and starvation (more than four days without food). It was generally found that the stimulation in transport was due to an increase in V_{max} of PepT1, with no apparent effect on K_m. This was associated with increased levels of PepT1 protein at the apical membrane and a comparable increase in mRNA levels (approx. 3-fold). As such, starvation appears to enhance peptide transport at a pre-translational level. However, an examination of other membrane transporters (e.g. SGLT1) during this situation showed no such change in activity (Ihara *et al.*, 2000).

Although the effects of starvation appear to mirror the peptide-induced stimulation in activity, it is thought that the two are distinct regulatory mechanisms. Re-feeding, following starvation, causes a significant decrease in PepT1 mRNA levels (Ihara *et al.*, 2000). In addition, whereas the site for substrate-induced activity has been demonstrated to be localised in the middle and distal sections of the small intestine, starvation causes changes in the proximal region (Ihara *et al.*, 2000).

It is generally assumed that these responses to fasting and starvation function to minimise nitrogen loss from the body. From the initiation of fasting, as early as 1 day, mucosal cells are sloughed from the villi into the lumen of the small intestine at a considerable rate. This is indicated by a reduction in the weight of the intestinal mucosa (McManus & Isselbacher, 1970). If these cells were lost, it would contribute to a major loss of nitrogen from the body. However, the remaining cells appear to have an increased efficiency of absorption of small peptides, produced from the hydrolytic degradation of the protein content of the sloughed cells, to maintain the nitrogen levels required. In contrast, glucose and amino acid transport activity are reduced, therefore the effects on peptide transport appear to be paradoxical to

effects on these other nutrient transporters (Thamotharan *et al.*, 1999a). Matthews & Adibi (1976) stated some time ago that the response of the intestinal peptide transporter to nutritional and pathological situations was distinct from the effect on amino acid transport proteins. In this way, one method of absorbing amino nitrogen is better preserved than the other in adversity.

The different responses of nutrient transporters are not unique in dietary situations. Tanaka *et al.* (1998) discovered that injury to cells by 5-fluorouracil had no effect on the amount of PepT1 protein, but seriously affected the levels of sucrase and glucose transporters. In fact, PepT1 mRNA levels were elevated, whereas the mRNA levels of amino acid, glucose and phosphate transporters were depressed.

The biological significance of this starvation-induced enhancement in peptide absorption is not for storage of fuel, because body fat and glycogen are available for calorific use. It probably functions as a precautionary mechanism in the reabsorption of protein during re-feeding. Protein malnutrition is a serious problem because, although protein forms structural and functional tissue, it cannot be stored for future use. Ihara and co-workers (2000) speculated that the stimulation in transport during starvation would act to promote the maximum absorptive ability immediately after a meal is consumed. Therefore, even though upregulation of peptide transport by substrates is moderately slow (i.e. in a time scale of days), the essential nutrients won't be lost by non-absorptive transit through the intestine.

From a clinical viewpoint, the results indicate that if the body were in a malnourished state, peptide feeding in enteral nutrition would have an absorptive advantage over amino acids. From a therapeutic viewpoint, peptidomimetic drugs may be more efficiently absorbed during fasting and/or starvation.

1.6.2 Short-term regulation of peptide transport

As previously mentioned, investigations into short-term regulation of peptide transport are scarce. The studies that have been performed demonstrate an effect of a number of mediators, but no mechanism has been advanced. This area of regulation can be segregated into two distinct groups, regarding the mediator(s) involved; nutrients and hormones, acting through protein kinase cascades.

1.6.2.1 Amino acid regulation

It has been described that certain amino acids in the diet have the ability to up-regulate peptide transport over a period of days (Ferraris *et al.*, 1988; Shiraga *et* al., 1999). A series of experiments by Boyd *et al.* (1996) demonstrated a stimulation of dipeptide transport by specific amino acids in the short-term. In this study the amino acids were infused in the vasculature of the small intestine, rather than being presented in the lumen. The amino acids (Gln and Leu) caused an increase in the transmural transport of D-Phe-L-Gln, but the effect was more pronounced at the basolateral membrane, indicated by reduced intracellular concentrations of substrate. Therefore, a similar mechanism of regulation by amino acids appears to be in force at the basolateral membrane, although it isn't clear from this data at which membrane regulation is predominant, or if both are equal, but due to different processes.

1.6.2.2 Hormonal regulation

Very little is actually known about the regulation of peptide transport by hormones, but a recent study by Thamotharan *et al.* (1999b) implicated insulin as a possible mediator. A physiological concentration (5 nM) of insulin caused a 2-fold increase in Gly-Gln transport, due to an increase in maximal velocity of the transporter with no effect on substrate affinity. This was associated with an increase in the amount of PepT1 protein at the apical membrane, but was not due to changes in mRNA levels. They concluded that insulin acted to increase the membrane population of PepT1 by stimulating its translocation from a pre-formed cytoplasmic pool. Insulin acts through its receptors; an intrinsic protein with tyrosine kinase activity. The exact process by which peptide transport is stimulated by insulin is, as yet, unknown. However, although receptors for insulin are located on both apical and basolateral membranes on enterocytes, they are more concentrated at the basolateral pole. Therefore, insulin might also act to regulate peptide transport at the basolateral membrane.

Another hormone has also been implicated as having a role in the regulation of peptide transport, under specific circumstances; progesterone. Fujita *et al.* (1999) demonstrated that peptide transport is enhanced by treatment of Caco-2 cells with (+)pentazocine, a selective σ1 receptor ligand. σ1 receptors are a subclass of s receptors thought to be involved in the pathogenesis of psychiatric disorders in the

central nervous system. However, they are also expressed in peripheral tissues including the gastrointestinal tract, but little is known regarding their physiological function. (+)pentazocine stimulated peptide transport by increasing V_{max}, coupled with an increase in steady state levels of PepT1 mRNA, although the exact mechanisms are not clear. One physiological implication of this type of regulation might involve progesterone. Progesterone is an endogenous ligand for the σ1 receptor, and its plasma concentration varies dramatically in women depending on their physiological condition, for example during the menstrual cycle. In particular it is known that levels increase considerably in late pregnancy; in this state women require a large amount of nutrition to nurture their foetus. Fujita *et al.* (1999) speculated that these high levels of progesterone might upregulate the intestinal absorption of peptides by interacting with the σ1 receptor, in order to meet these high nutritional demands. At this point it isn't known whether the effect is specific for peptide transport, or if other nutrient transporters are controlled in a similar way.

1.6.2.3 Additional regulatory mechanisms

In addition to the potential role of protein kinase activity modulated by insulin, a role of other kinases has been postulated. PKC regulation of peptide transport was demonstrated by Brandsch and co-workers (1994) using a series of activators and inhibitors. Treatment of Caco-2 cells with PKC activators resulted in a significant inhibition of PepT1 activity due to a decrease in V_{max}, but no change in K_m; inhibitors blocked the inhibitory effect of PKC. In contrast leucine transport was not affected. This regulation could potentially be due to a number of different mechanisms, however, it was demonstrated that a block in *de novo* synthesis or alterations in the transmembrane pH gradient were not involved. It was postulated that regulation of this kind may involve post-translational modifications due to phosphorylation/dephosphorylation of the protein. This could be either a direct effect by PKC itself, or indirect via the action of additional protein kinases or phosphatases. Further work is required to elucidate the precise mechanism.

Muller *et al.* (1996) reported a potential role of PKA, in addition to PKC, in a cAMP-dependent manner. Although an increase in cAMP levels are known to activate PKA, the mechanism by which PKC is activated by cAMP is not clear. Studies in other cell types (Trautwein *et al.*, 1990; Church *et al.*, 1994, see Muller *et*

al., 1996) have indicated that cAMP might act to increase intracellular Ca^{2+} levels due to activation of Ca^{2+} channels; this might form the basis by which PKC regulates transport in this instance.

In summary, it is clear that although initial investigations have demonstrated a variety of ways in which peptide transport appears to be regulated (for instance, dietary and hormonal), both in the long-term and short-term, further work is required in order to determine the precise molecular mechanisms and the physiological/clinical implications.

1.7 AIMS OF THIS THESIS

The wider general aim of this thesis was to investigate oligopeptide transport in rat small intestine. Specifically, attempts to identify the carrier proteins in both the apical and basolateral membranes of jejunal mucosa were made. Protein identification was performed using the technique of photoaffinity labelling, and so the initial aim was to identify a compound, which would specifically interact with the transporters, and could be developed as a potential label. Secondly, direct interaction of the label with the transporter protein(s) had to be demonstrated in order to prove the reliability of the approach. Once the viability of the potential photoaffinity label had been determined, investigations were performed for the specific identification of the carrier proteins.

PepT1 from rat small intestine has previously been cloned and sequenced (see section 1.3.1); therefore the purpose of its identification was not a new concept, but a necessary process to allow investigations in its structural requirements to be performed. The equivalent protein in the basolateral membrane has not been previously identified from any species, or tissue; therefore its identification would be a novel and exciting discovery. Once the protein had been isolated, the primary aim was to obtain structural information with the hope that it could lead to cloning and sequencing of the protein in the near future. Pharmacologically, this protein is equally as important as the apical transporter protein for the efficient absorption of biologically-active peptidomimetic drugs, and clearly its transport properties and substrate requirements need clarification. However, this can only be undertaken if its potential importance is realised and the protein itself has been identified.

A distinct aim of this thesis was to investigate the short-term regulation of transmural peptide transport, i.e. the physiological processes that occur during assimilation of a meal. Limited knowledge regarding the precise mechanisms of transporter regulation has been obtained (see section 1.6); some of these have implicated a potential role of protein kinases and/or phosphatases. Therefore, studies were performed in order to determine the activators/inhibitors, cellular proteins and/or protein kinase pathways involved in peptide transport regulation.

CHAPTER 2: MATERIALS AND METHODS

Animals used in all studies were male Wistar rats bred and supplied by the Animal House of the Biology Department, University of York. They were kept under controlled light conditions of a 12 hour day/night cycle at a constant temperature and ventilation and were fed *ad libitum* on Bantin & Kingman standard rat and mouse diet (Bantin & Kingman Ltd., Humberside, UK.) with free access to water.

All procedures involving animals were performed in accordance with Home Office Regulations under the Animals (Scientific Procedures) Act 1986.

2.1 PROCEDURE FOR THE STUDY OF PEPTIDE TRANSPORT IN THE ISOLATED LUMINALLY AND VASCULARLY PERFUSED RAT JEJUNUM *IN SITU*

The vascular perfusion apparatus and technique used were modified slightly from that originally described by Hanson & Parsons (1976), incorporating certain features described by Bronk & Ingham (1979) and Nicholls *et al.* (1983).

2.1.1 Animals

Rats of 260-280 g bodyweight were used in perfusion studies. At the desired weight, access to food was denied overnight prior to the perfusion, and drinking water was supplemented with 0.5% D-glucose.

2.1.2 Chemicals and materials

Dipeptides (D-Phe-L-Gln, D-Phe-L-Ala) and the photoaffinity label ([4-azido-D-Phe]-L-Ala) were custom-synthesised by Prof. P. D. Bailey and Dr. I. Collier in the Chemistry Department, Heriot Watt University, Edinburgh, U.K.

Amino acids (D-Phe, L-Gln, L-Leu) and bovine serum albumin (BSA) fraction V powder were supplied by Sigma Chemical Co. Ltd., Poole, U.K.

Enzyme inhibitors; rapamycin and wortmannin, were obtained from Calbiochem®.

NaCl, KCl, $MgSO_4$, $NaHCO_3$, $CaCl_2$, D-glucose, methanol, PCA and KOH were supplied by BDH Laboratory Supplies, Poole, U.K. and were of AnalaR® grade.

KH_2PO_4, NaH_2PO_4 and Na_2HPO_4 were supplied by Fisons Scientific Equipment, Loughborough, U.K. and were of Analytical Reagent grade.

Sagatal® (60mg ml^{-1} Pentobarbitone sodium B.P.) general anaesthetic was supplied by Rhone Merieux Ltd., Harlow, UK.

Gas cylinders (95% O_2/5% CO_2) were supplied by BOC Medical Gases, BOC Ltd., Guildford, UK.

Mersilk® 2/0 braided silk suture was supplied by Ethicon Ltd., Edinburgh, UK.

Nalgene tubing (i.d. 1/4", o.d. 5/16") was supplied by Nalge Co., Rochester, New York, USA.

Plastic tubing (i.d. 2.0 mm, o.d. 3.0 mm), silicone tubing (i.d. 3.0 mm, o.d. 5.0 mm) and nylon tubing cannula for vasculature (i.d. 0.75 mm, o.d. 0.94 mm) were supplied by Portex Ltd., Hythe, UK.

Standard PVC manifold pump tubing for peristaltic pumps was supplied by Altec, Alton, UK.

All glassware used to construct the perfusion apparatus and the portal vein cannula were either supplied by the university glassblower or York Glassware Services Ltd., York, UK.

Glucose GOD-Perid® spectrophotometric analysis kits were supplied by Boehringer Mannheim U.K., Lewes, UK.

Variable speed laboratory motor (model S63C) homogeniser was obtained from Tri-R Instruments, Inc.

2.1.3 Solutions

All solutions were made up in diH_2O unless otherwise stated.

Modified Krebs-Ringer bicarbonate saline medium, pH 6.8

A fresh working medium was produced from concentrated stock solutions, which were stored at 4°C, on the day of perfusion. The solution was gassed with 95% O_2/5% CO_2 for 45 min before the subsequent addition of $CaCl_2$.

Component	Final concentration (mM)
NaCl	140.0
KCl	4.5
$MgSO_4$	1.0
Na_2HPO_4	1.8
NaH_2PO_4	0.2
$NaHCO_3$	5.0
$CaCl_2$	1.25

BSA stock solution

A 1 L 10% (w/v) BSA solution containing 0.01% (w/v) streptomycin sulphate was made with modified Krebs-Ringer medium, pH 6.8. The solution was vacuum-filtered through a coarse filter (Whatman 541, 11.0 cm diameter) using a Buchner funnel, bottled in 75 ml aliquots and stored at -20°C.

Luminal and vascular perfusate solutions

Both the vascular and luminal perfusates were based on the modified Krebs-Ringer medium. The vascular perfusate contained 5 mM D-glucose, 5% (w/v) BSA (using the 10% stock solution), 0.005% (w/v) streptomycin sulphate and 0.0035% (w/v) heparin. The luminal perfusate consisted solely of Krebs-Ringer. Substrates were added to the perfusates as required.

Rapamycin stock solution

A 100 μM stock solution was made by dissolving 100 μg into 1.094 ml DMSO. A 4,000-fold dilution into the required perfusate produced a final concentration of 25 nM.

Wortmannin stock solution

A 2 mM stock solution was made by dissolving 1 mg into 1.17 ml diH_20. A 10,000-fold dilution into the required perfusate produced a final concentration of 200 nM.

Solutions for sample treatment and analysis

0.6 M KOH	3.37 g/100 ml
6% (w/v) PCA	17.5 ml/250 ml
HPLC buffer	
21 mM KH_2PO_4	14.29 g/5 L

2.1.4 Perfusion apparatus

The set-up of the perfusion apparatus is shown in a schematic diagram (figure 2.1).

Perfusions were performed at a physiological temperature of 37°C. A constant temperature was maintained inside a closed cabinet by a thermostatically controlled heater and fan. Doors at the front of the cabinet permitted interior access. Within the cabinet the perfusate reservoirs and oxygenator were maintained at 37°C, as was the dissection plate upon which the rat was placed, by circulating heated water through the jackets of the apparatus from an external water bath.

The individual parts of the perfusion apparatus were connected using a combination of nalgene, plastic and silicone tubing. Vascular and luminal perfusates were circulated through the tubing by a 4-channel peristaltic pump.

The luminal perfusate constituted a segmented flow at the rate of 2.0 $ml \cdot min^{-1}$ based on single pass through the isolated region of small intestine. The segmented flow was created by introducing bubbles of gas (95% O_2/5% CO_2) into the

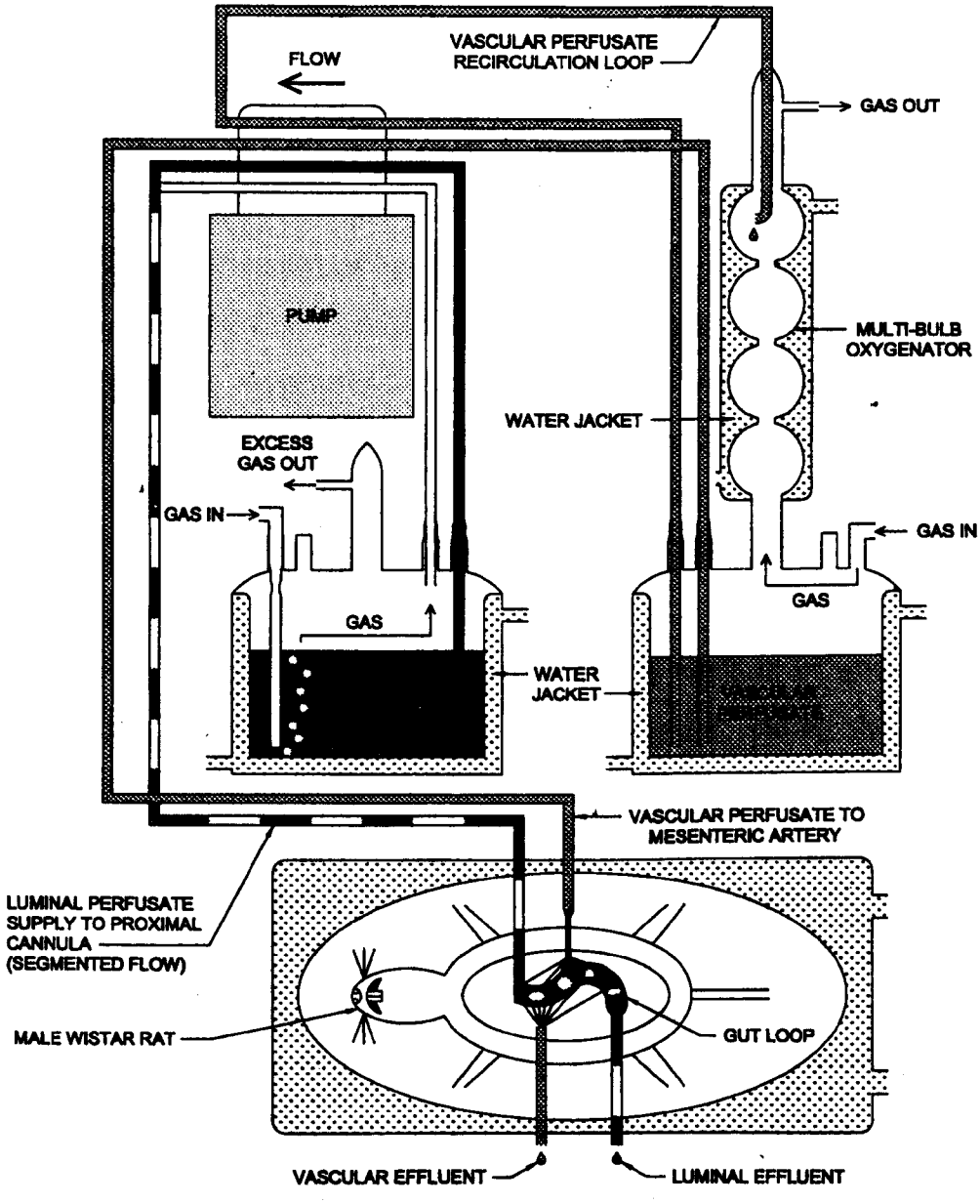

Figure 2.1

Schematic diagram of the apparatus used for luminal and vascular perfusions, *in situ*, of isolated rat jejunum.

luminal circuit using a bubble trap located after the pump. Gas segmentation causes an increase in stirring of the luminal contents (Fisher & Gardner, 1974) and therefore minimises the effects of the stationary, unstirred water layer adjacent to the tissue on the transport of substrates, in addition to an ensuing an improvement in oxygenation of the epithelial cell layer.

The vascular perfusate system consisted of both a single pass and a re-circulated flow (both non-segmented), however the re-circulated flow functions solely for oxygenation of the perfusate, not to perfuse the jejunal mesentery. The dual system was accomplished by pumping perfusate from the reservoir into two separate channels; the first channel recirculated the solution at a rate of 7 $ml \cdot min^{-1}$ through a multi-bulb oxygenator to feed back into the reservoir, whereas the second channel formed a single pass flow to perfuse the superior mesenteric artery of the animal at a rate of 1.5 $ml \cdot min^{-1}$. This arrangement ensured that the vascular perfusate entering the mesenteric cannula was continuously oxygenated via passage through the glass multi-bulb.

An additional external pump permitted compounds to be infused into the luminal and/or vascular perfusates at specific time points during the experiment without interruption to the perfusate flow.

Perfusion of the vascular bed was performed using a nylon tubing cannula via a sharpened distal end. The vascular effluent was collected using a glass 'Z'-shaped portal vein cannula connected to a short length of plastic tubing (i.d. 1.0 mm, o.d. 1.2 mm). In order to attain a negative hydrostatic pressure, the tubing attached to the portal vein cannula was adjusted to lie approximately 3-5 cm below the portal vein, as a result of the unique shape of the cannula. This pressure was sufficient to overcome the frictional resistance associated with flow through a narrow tube.

2.1.5 Operative procedure

A schematic diagram of the dissection is shown in figure 2.2. Bracketed numbers and letters in the text correspond to the placement of ligatures and cannulae, respectively, during the operation.

Prior to surgery the rats were anaesthetised with an intraperitoneal injection of Sagatal® (10 $mg \cdot [100g\ body\ weight]^{-1}$).

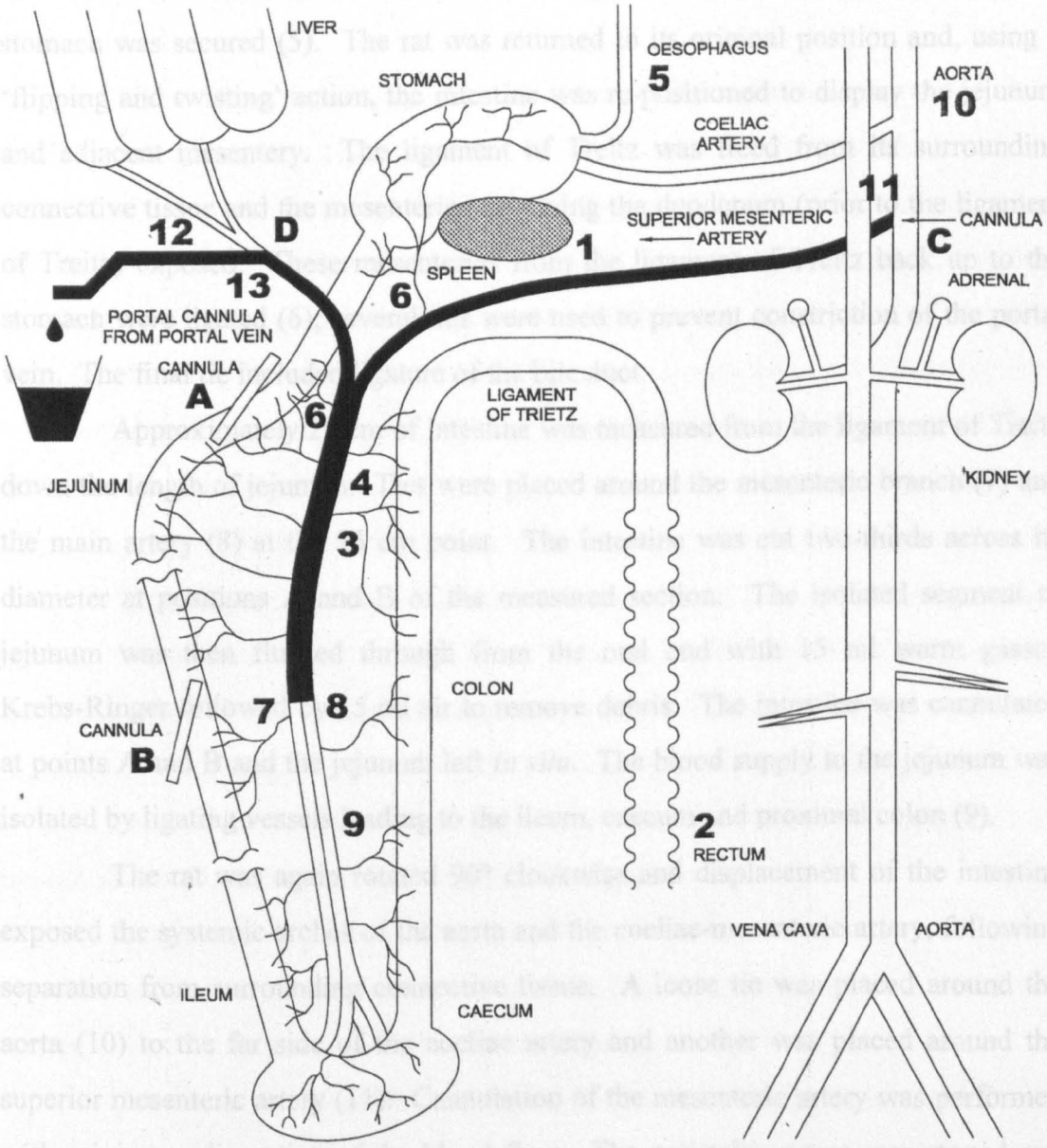

Figure 2.2

Schematic diagram of the operative procedure followed for luminal and vascular perfusions of isolated rat jejunum, *in situ*. Numbers and letters depict the placement of ligatures and cannulae, respectively, and correspond to the text in section 2.1.5.

An incision was made on the midline of the abdomen, followed by a lateral incision at midpoint to open up the abdominal cavity. The spleen (1) was ligated along with the rectum (2), followed by the right colic artery and vein (3 & 4). The rat was rotated 90° clockwise and the vein running parallel to the oesophagus from the stomach was secured (5). The rat was returned to its original position and, using a 'flipping and twisting' action, the intestine was re-positioned to display the jejunum and adjacent mesentery. The ligament of Treitz was freed from its surrounding connective tissue and the mesenteries supplying the duodenum (prior to the ligament of Treitz) exposed. These mesenteries from the ligament of Treitz back up to the stomach were ligated (6); several ties were used to prevent constriction of the portal vein. The final tie included ligature of the bile duct.

Approximately 25 cm of intestine was measured from the ligament of Treitz down the length of jejunum. Ties were placed around the mesenteric branch (7) and the main artery (8) at the 25 cm point. The intestine was cut two-thirds across its diameter at positions A and B of the measured section. The isolated segment of jejunum was then flushed through from the oral end with 15 ml warm gassed Krebs-Ringer followed by 15 ml air to remove debris. The intestine was cannulated at points A and B and the jejunum left *in situ*. The blood supply to the jejunum was isolated by ligating vessels leading to the ileum, caecum and proximal colon (9).

The rat was again rotated 90° clockwise and displacement of the intestine exposed the systemic arches of the aorta and the coeliac-mesenteric artery, following separation from surrounding connective tissue. A loose tie was placed around the aorta (10) to the far side of the coeliac artery and another was placed around the superior mesenteric artery (11). Cannulation of the mesenteric artery was performed with minimum disruption of the blood flow. The peristaltic pump was started and the aorta tied off by tightening of the ligature (10). A small incision was made in the left systemic arch (at the junction of the aorta and superior mesenteric artery) (C) and the cannula inserted immediately. This ligature (11) was gently tightened around the cannula to avoid constriction of the vascular flow. Upon completion of the vascular perfusate circuit, the rat was killed by an overdose of Sagatal into the heart (1 ml).

Rapid cannulation of the mesenteric artery is necessary (within 20 s). and success at the first attempt is crucial, because vascular back pressure and tissue anoxia begin to develop as soon as the animals blood supply is constricted.

Cannulation should also avoid damage to other major blood vessels in the vicinity of the mesenteric artery. Successful cannulation of the artery was indicated by a colour change of the isolated section of jejunum, from pink to white, which demonstrated that it was being supplied by the external reservoir and no longer by the blood supply of the animal.

When the arterial cannula was secured the animal was rotated 180° clockwise to display the hepatic portal vein. Two loose ties were made around the vein (12 & 13) approximately 1.0 cm apart. The upper ligature (12) was tied tightly and a small incision (D) made into the wall of the vein. The portal vein cannula was inserted and the second ligature (13) secured it in place.

Once the flow through the vascular bed was established the luminal circuit was completed by connecting cannulae A and B to the corresponding perfusate tubing. The exposed intestine was kept moistened with a swab soaked in Krebs-Ringer at 37°C to prevent drying of the tissue.

Timed sampling began with completion of both the vascular and luminal circuits. Vascular effluent samples were taken at 1 min intervals every 2 min by collecting fluid in a pre-weighed autoanalyser cup. The flow rate ($ml \cdot min^{-1}$) was monitored by the weight of the sample and venous recovery was calculated. Luminal effluent samples were collected at 1 min intervals every 5 min. All samples were treated as described in section 2.1.6 prior to analysis.

At the end of the experiment, the perfused segment of intestine was removed from the rat and its linear dimensions measured at resting length. The tissue was treated as described in section 2.1.7 prior to analysis.

Following every perfusion, the apparatus and tubing were rinsed with copious amounts of diH_2O to remove any traces of perfusate and/or substrates.

2.1.6 Sample treatment

Treatment of the luminal and vascular samples was identical; de-proteinisation by a 2-fold dilution in 6% PCA followed by centrifugation at 1800 *g* for 2 min. The supernatant was neutralised by a 1.8-fold dilution in 0.6 M KOH and the final sample was rapidly frozen in liquid nitrogen before being stored at –20°C.

2.1.7 Tissue sample treatment

Mucosal epithelial tissue and its underlying muscle were analysed post-perfusion to calculate the extent of substrate accumulation during the transfer process across the intestinal wall.

At the end of the perfusion the section of intestine was opened along its antimesenteric surface and blotted well. A 4 cm section was taken and the mucosal layer removed by scraping gently with a microscope slide. The mucosa was plunged into liquid nitrogen and frozen rapidly before its weight was recorded. The frozen pellet was then homogenised in 1 ml 0.6% PCA with a smooth Teflon® pestle using a variable speed laboratory motor (model S63C) homogeniser on setting 4.5. The remaining muscle layer was also frozen, weighed and homogenised in the same way. The resulting homogenates were centrifuged at 1800 *g* for 2 min, the supernatant neutralised with a 2-fold dilution in 0.6 M KOH and the samples frozen in liquid nitrogen before being stored at –20°C.

Additional sections of the intestine were taken to calculate wet and dry weights of the mucosal and muscle tissue. These tissue scrapes, in conjunction with a whole tissue sample, were heated to dryness for 24 h in a constant temperature oven in a pre-weighed glass vial. This information allowed transport rates to be expressed as $\mu mol \cdot min^{-1} \cdot [g\ dry\ weight]^{-1}$.

2.1.8 Sample analysis

2.1.8.1 Glucose analysis

(a) Solutions

10 mM D-glucose 0.18 g/100 ml

(b) Test Principle

Glucose utilisation by the isolated jejunum was an indication of the viability of the perfusion (see section 3.3); represented by the glucose concentration remaining in the vascular effluent following passage through the jejunal vasculature. Vascular samples were analysed on a Cobas-MIRA robotic analyser (Roche Products Ltd., Welwyn Garden City, UK.) using automated enzymatic analysis. Glucose concentration was measured using a commercially available kit, GOD-Perid® (Boehringer Mannheim) which uses the following test principle:

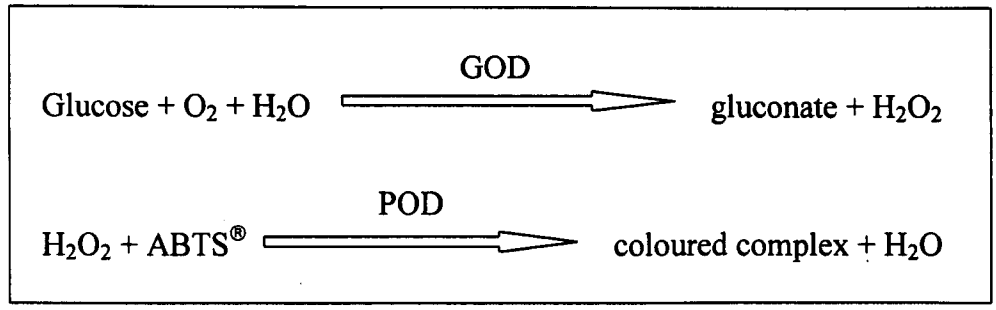

GOD = glucose oxidase
POD = peroxidase
ABTS® = di-ammonium 2,2'azino-bis[3-ethyl-benzothiazoline-6-sulphonate]

The green reaction product has a strong absorbency at 578 nm and the intensity of the coloured complex is directly related to the amount of glucose in the sample. Glucose concentration was calculated using a standard curve of 0-10 mM.

2.1.8.2 HPLC analysis

Vascular and luminal samples, in addition to mucosal and muscle tissue samples, were analysed by HPLC using an automated computer-controlled system (Kontron model 4100) from Kontron Instruments. A 25.0 cm * 4.6 mm column (Jones Chromatography) was used in conjunction with a methanol:H_2O mobile phase. The ratio of methanol to H_2O varied with the dipeptide under analysis, i.e with D-Phe-L-Gln the ratio was 1:9, whereas with the photoaffinity label ([4-azido-D-Phe]-L-Ala) it was 1.5:8.5; both solutions were buffered with 21 mM KH_2PO_4. The mobile phase had a flow rate of 1 $ml \cdot min^{-1}$. Before sample injection, the column was equilibrated with the mobile phase for approx. 15 min using an automatic pump (Kontron 420). Samples contained in 2 ml vials, situated in the sample tray of the autosampler (Kontron 460), were automatically injected onto the column. Dipeptide and amino acid elution were detected at 210 nm using a detector (Kontron 430) for a specified time period depending on the dipeptide under analysis, e.g. D-Phe-L-Gln; 12 min, [4-azido-D-Phe]-L-Ala; 20 min.

Typical elution profiles of D-Phe with D-Phe-L-Gln or [4-azido-D-Phe]-L-Ala are shown in Appendix I. The amount present in each sample was calculated by a comparison of the actual peak area to peaks of known standard concentrations.

2.1.9 Expression of results

Results from these experiments are expressed as the mean ± standard error of the mean (s.e.m.) for *n* number of perfusions.

2.1.9.1 Viability of perfusions determined by glucose utilisation, by the isolated jejunum, from the vascular perfusate

Glucose analysis using the Cobas-MIRA gives the concentration of glucose remaining in the vascular effluent after passage through the jejunal mesenteries. From these values (in mM) the rate of vascular uptake of glucose was determined. The basic calculation is as follows:

At any given time the uptake of glucose is represented as:

$$\Delta C.F$$

where: ΔC is the initial concentration of glucose in the reservoir minus the concentration measured in the effluent sample

F is the flow rate of the perfusate per minute.

However, the most accurate representation of uptake analysis is to express it as the gradient of cumulative uptake under steady state conditions over time. Cumulative uptake (in μmol·[g dry wt]$^{-1}$) is expressed by equation 2.1:

Equation 2.1

$$\sum (\Delta C_n . [\Delta F_n . t] / W$$

where t is the time interval between successive samples

W is the total dry weight of the isolated intestine.

This is represented as a graph showing glucose uptake against perfusion time and is expressed as an uptake rate of μmol·min.$^{-1}$[g dry wt]$^{-1}$.

2.1.9.2 Intestinal transport of a dipeptide as determined by its appearance in the vascular effluent

Graphical representations of the perfusions show the cumulative vascular appearance of dipeptide substrates (*y*-axis) against time (*x*-axis).

The rates of dipeptide transport were calculated as $\mu mol \cdot min.^{-1} \cdot [g\ dry\ wt]^{-1}$. HPLC analysis of vascular samples detected the amount of substrate present and expressed it as a peak area. The concentration of substrate in each sample was calculated by a comparison of the actual peak area to peaks of known standard concentrations. Standards (D-Phe and the dipeptide under study) were analysed at a concentration of 0.01 mM. The equation used to calculate the concentration of peptide (mM) in the samples is as follows:

Equation 2.2:

$$(D/S)*C$$

where: D is the dipeptide peak area
S is the standard peak area
C is the correlation factor; by which sample treatment and dilution of standards are taken into account.

This value (in mM) is then taken through equation 2.1 described in section 2.1.9.1 to calculate the cumulative transport rate of dipeptide and express it as $\mu mol \cdot min^{-1} \cdot [g\ dry\ wt]^{-1}$.

2.1.9.3 Tissue accumulation of peptide and corresponding exit ratio

Additional graphs show accumulations of dipeptide substrates (mM) in mucosal and muscle tissues following the perfusions, plus their corresponding exit ratios. The tissue concentrations of substrate are calculated by equation 2.1. Exit ratios represent the proportion of the substrate that is accumulated in the tissue with respect to its individual transport rate. It is expressed in equation 2.3 as follows:

Equation 2.3:

tissue concentration / final vascular sample concentration

where: the tissue concentration is the concentration of dipeptide (mM) in either the mucosal or muscle tissue
the final vascular sample is the concentration (mM) in the sample taken at 50 min during the perfusion.

2.1.9.4 Statistical analysis

Differences in rates of peptide transport between various conditions were calculated using analysis of variance performed in Excel. The time period analysed was from 20 to 50 min because a steady state of transport was not achieved until approx. 15-20 of perfusion. Differences in tissue concentrations were analysed using unpaired 2-tailed t tests in Excel, assuming equal variances.

2.2 DUAL PREPARATION OF BRUSH-BORDER AND BASOLATERAL MEMBRANE VESICLES FROM RAT JEJUNAL MUCOSA

Brush-border membrane vesicles (BBMV) and basolateral membrane vesicles (BLMV) were prepared from rat jejunal mucosa as previously described by Maenz & Cheeseman (1981) and Corpe *et al.* (1996), with some modifications. The alteration in the method of primary importance was to anaesthetise the rat prior to removal of the intestine. It has been shown that if the rat is killed before dissection, instead of being maintained under anaesthesia, the rate of release/leakage of peptide hydrolase activities increases 4-8 fold (Plumb *et al.* 1987). In addition, if the small intestine is deprived of oxygen, even for as little as 4 min, severe destruction of the villi is observed, including detachment of cells from the mucosal layer, oedema, etc. All changes are characteristic of damage caused by ischaemia (Plumb *et al.* 1987).

2.2.1 Animals

Fed rats of 260-300 g bodyweight were used in vesicle preparation.

2.2.2 Chemicals and materials

Mannitol, imidazole, $MgCl_2$, Tris, EDTA, TCA and ethanol were supplied by BDH Laboratory Supplies, Poole, U.K. and were of AnalaR® grade.

PMSF, Percoll, ATP and ouabain were obtained from Sigma Chemical Co. Ltd., Poole, UK.

The BCA protein assay kit was supplied by Pierce, Warrington, UK.

The alkaline phosphatase assay kit was supplied by Roche Diagnostic Systems.

A polytron GS25 homogenising tube and Kinematica large head homogeniser were obtained from The Northern Media Supply Ltd., North Cave, North Humberside, UK.

A superspeed Sorval centrifuge and SS34 rotor were obtained from Du Pont Instruments, Du Pont (UK) Ltd. Herts. UK.

The L7/L8 ultracentrifuge and SW28 (96E 6426) rotor and the TL100 centrifuge and SN 2291 rotor were obtained from Beckman, PK Services.

Remaining chemicals and materials have been described in previous methods sections.

2.2.3 Solutions

All solutions were made up in diH_2O, unless otherwise stated.

Buffered mannitol, pH 7.5

250 mM mannitol	45.542 g/L
20 mM imidazole	1.362 g/L

50 mM PMSF	8.8 mg/ml ethanol

100 mM $MgCl_2$	2.03 g/100 ml

2.2.4 Membrane vesicle preparation

All preparative steps were carried out on ice or at 4°C.

12 rats were anaesthetised with an intraperitoneal injection of Sagatal® (10 mg·[100g body weight]$^{-1}$). An incision was made on the midline of the abdomen,

followed by a lateral incision at midpoint to open up the abdominal cavity. Approximately 40 cm of small intestine distal to the ligament if Treitz was removed and flushed through with 25 ml ice cold buffered mannitol containing 0.1 mM PMSF. The segments were placed in fresh mannitol/PMSF on ice. Following removal of the jejunum, the rats were killed by the method of exsanguination. The jejunal segment was placed on a chilled glass plate, opened along its antimesenteric surface and the mucosa was isolated by gentle scraping using a microscope slide. This was performed with a total of 4 rats. The mucosal scrapes were combined, its weight noted and placed in buffered mannitol (10 ml/g of scrape) in the pre-chilled Polytron GS25 homogeniser tube. PMSF was added to a final concentration of 0.1 mM. The mucosa was homogenised using a Kinematica homogeniser (large head) on setting 7 for 4 * 30 s pulses, with 20 s rest on ice between each pulse. This dissection and homogenisation procedure was repeated until the jejunal mucosa from all 12 rats had been treated. A homogenate sample for enzyme assays was taken; this was a combined sample from all rats used.

The final homogenate was centrifuged at 2500 *g* for 15 min using the pre-chilled SS34 rotor in the Sorval centrifuge. After centrifugation, the fatty material was removed and the pellet discarded. The supernatant was centrifuged at 21000 *g* for 20 min. A double layer pellet was formed of which the fluffy, white upper layer was rich in basolateral membranes and the hard, dark lower layer was brush-border rich. The vesicle preparation then diverged into two separate protocols performed simultaneously to purify the respective membranes.

2.2.4.1 Basolateral membrane purification

The upper fraction was isolated by **gently** swirling the pellet in buffered mannitol, to dislodge **only** these membranes, and the suspension was transferred to a fresh tube. PMSF was added to a concentration of 0.1 mM. The membranes were resuspended in buffer by 6 strokes in a hand-held glass/Teflon homogeniser. The solution was made up to 38 ml, containing 12% (v/v) Percoll, and the solution gently mixed by inversion. The suspension was centrifuged at 48,000 *g* for 60 min in a Beckman ultraclear (344058) tube using SW28 (96E 6426) rotor in the Beckman L7/L8 centrifuge. This resulted in a self-forming Percoll density gradient in which the basolateral membranes were concentrated in a tight band towards the top of the

centrifuge tube. BLMV were recovered and resuspended/revesiculated in buffered mannitol containing 0.1 mM PMSF using a 21G hypodermic needle and syringe. The Percoll was washed out of the sample by centrifuging the suspension at 48,000 *g* for 30 min in the Sorval. Membranes were recovered and concentrated by centrifugation at 166,000 *g* for 15 min using the TL100 centrifuge and pre-chilled rotor (SN 2291). The final membrane sample was revesiculated as before.

2.2.4.2 Brush-border membrane purification

The inner pellet was resuspended/revesiculated in buffered mannitol plus 0.1 mM PMSF using a 21G needle. $MgCl_2$ was added to a final concentration of 10 mM and solution inverted six times and incubated on ice for 20 min, with gentle agitation at 10 min. Differential centrifugation of the suspension followed at 3,000 *g* for 10 min using the SS34 rotor to pellet unwanted precipitated membranes. Fatty material and the gelatinous pellet were discarded. The supernatant containing pure brush-border membranes was then centrifuged at 27,000 *g* for 30 min. The supernatant was discarded and the pellet resuspended/revesiculated in buffered mannitol plus 0.1 mM PMSF. The vesicle suspension was centrifuged at 27,000 *g* for 30 min. The final pellet was resuspended/revesiculated to a required final concentration in buffered mannitol.

2.2.5 Assays to establish vesicle purity

Final membrane samples and original tissue homogenate (taken after the initial crude intestinal scrape homogenisation) were routinely assayed for protein purification and to ensure that the purified membranes were enriched over the homogenate sample. The enzyme assays chosen were specific marker enzymes for either the brush-border or basolateral membrane;

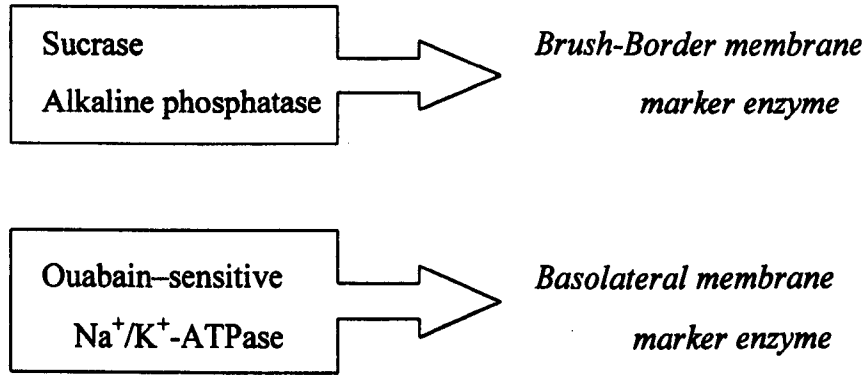

An assay to determine protein concentrations of the membrane samples and homogenate were also performed.

All assays (except the ouabain-sensitive Na^+/K^+-ATPase) were performed on a Cobas-MIRA robotic analyser (Roche Products Ltd., Welwyn Garden City, UK.) which performs automated enzymatic analysis based on user-specific criteria outlined in designated programs.

2.2.5.1 Protein assay

Protein was assayed using a commercially available kit; BCA Protein Assay Kit from Pierce. This kit uses BCA (bicinchoninic acid) for the quantitation of total protein content within a sample using a colorimetric detection method. It involves the biuret reaction in which protein causes the reduction of Cu^{2+} to Cu^+ in an alkaline medium. BCA is highly sensitive to Cu^+; it binds in a 2:1 ratio to form a purple-coloured reaction product. This coloured complex exhibits a high absorbancy at 562 nm that is linear with increasing protein concentrations. The reaction scheme is summarised as follows:

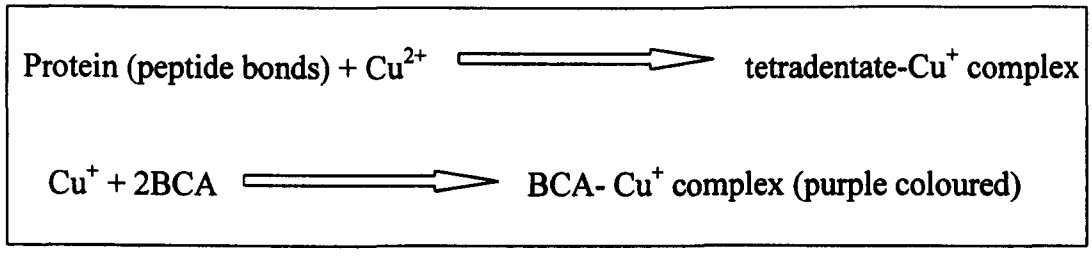

The protein concentration in the samples were calculated based on a standard curve of 0.02-2.0 $mg \cdot ml^{-1}$ BSA.

2.2.5.2 Alkaline phosphatase assay

Alkaline phosphatase (ALP) hydrolyses monophosphate esters to form a phenol and a phosphate ion;

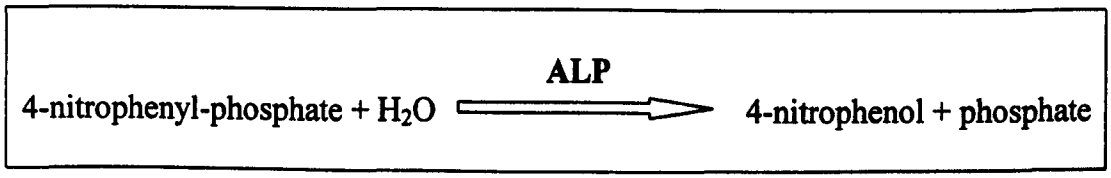

Under alkaline conditions 4-nitrophenol is yellow with a strong absorbency at 405 nm. Its rate of formation is directly proportional to ALP activity within the range studied.

ALP activity is expressed as U·[mg protein]$^{-1}$.

2.2.5.3 Sucrase assay

(a) Solutions

Assay buffer (100 ml)

100 mM imidazole, pH 7.0	0.681 g
100 mM NaCl	0.584 g
60 mM sucrose	2.054 g

10 mM D-glucose	0.18 g/100 ml
0.6M KOH	3.37 g/100 ml
6% (w/v)PCA	17.5 ml/250 ml

(b) Assay

Sample preparation was as follows; an aliquot of membrane/homogenate sample was incubated with 1 ml assay buffer for 15 min at 37°C in an Eppendorf heating block. The reaction was quenched by a 2-fold dilution in 6% PCA followed by centrifugation at 1800 *g* for 2 min. The supernatant was neutralised by a 1.6-fold dilution into 0.6 M KOH. Sucrase activity (mM) was measured by the amount of glucose generated in 15 min at 37°C by membrane samples minus a blank sample (buffered mannitol replacing membranes to eliminate buffer activity).

The reaction scheme and testing protocol are described in section 2.1.8.1.

Sucrase specific activity was calculated using the following equation:

$$[G*(1.0+V)]/[V*15*P]$$

$\mu mol \cdot min^{-1} \cdot (mg\ protein)^{-1}$

G = glucose (mM)
V = volume of sample
P = protein concentration ($mg \cdot ml^{-1}$)

2.2.5.4 Ouabain-sensitive Na^+/K^+-ATPase assay

The ouabain-sensitive Na^+/K^+-ATPase enzyme is located predominantly in the basolateral membrane, with very little or no activity detected in the brush-border (Fujita *et al.*, 1971; Harms *et al.*, 1980). As such, it can be used as a reliable marker to demonstrate the purity of a BLMV preparation.

This assay consisted of two distinct steps. In the initial sample assay, ATP is cleaved in the presence of Na^+, K^+ and Mg^{2+}, with ouabain present or absent as required, to generate inorganic phosphate (P_i). The second detection step measures the amount of P_i produced during the first step using the method of Fiske & Subbarrow (1925); P_i reacts with molybdate to produce phosphomolybdic acid. Phosphomolybdic acid is, in turn, is reduced to a blue coloured reaction product possessing a high absorbency at 680 nm.

(a) Solutions

(A) Assay buffer (100 ml)

200 mM Tris, pH 7.6	2.423 g
10 mM $MgCl_2$	0.2033 g
4 mM EDTA	0.1169 g

(B) 1 M NaCl 5.844 g 100 ml

(C) 0.5 M KCl 3.728 g 100 ml

(D) 30 mM ATP 18.4 mg/ml

(E) 5.714 mM Ouabain 20.8 mg/ml

(F) 30% (w/v) TCA 30 g/100 ml

Phosphate standard stock solution

0.5 mM K_2HPO_4 8.7 mg/100 ml

5N H_2SO_4 3.6 ml of 98% pure S. G. 1.84 acid / 100 ml

2.5% (w/v) ammonium molybdate 2.5 g/100 ml 5N H_2SO_4

0.25% (w/v) F &S reducer 0.25 g/100 ml

(b) Sample assay

100 µl of diluted samples (10-fold dilutions of BBMV and homogenate (H), 100-fold dilution of BLMV) were incubated under the following conditions; without ouabain ('total') or with ouabain ('ouabain-inhibited'), in conjunction with a blank (in which buffered mannitol replaced the membranes). The constituents of each assay is shown in table 2.1.

SOLUTION	TOTAL	OUABAIN	BLANK
A	250	250	250
B	100	-	100
C	20	-	20
D	-	350	-
E	430	200	430

Table 2.1 Constituents of each of the different conditions in the ouabain-sensitive Na^+/K^+-ATPase assay. Volumes are in µl.

Solutions were incubated for 15 min at 37°C; during this time solution D was equilibrated to temperature. 100 µl of pre-warmed solution D was added to each sample which was mixed and incubated for a further 20 min. The reaction was quenched by the addition of 200 µl solution F and the sample centrifuged at 1800 *g* for 2 min.

(c) P_i detection

A standard curve of 0-0.5 mM phosphate was constructed. Standards and sample were analysed in the same way; the solution was as follows:

- 750 µl diH_2O
- 175 µl 2.5% (w/v) ammonium molybdate
- 75 µl 0.25% (w/v) F &S reducer
- 100 µl of assayed sample

The solution was mixed and incubated at room temperature for 15 min. Samples were then read at A_{680}.

Absorbance of the blank assay was subtracted from the membrane samples and P_i concentration in the sample was calculated using the phosphate standard curve. The specific activity of ATPase within the sample was calculated using the following equation;

$$[[(x*1.2*(60/20))/0.1]*D]/P$$

$\mu mol.\cdot h^{-1}\cdot(mg\ protein)^{-1}$

x = P_i concentration (mM)
D = dilution factor
P = protein concentration ($mg\cdot ml^{-1}$)

The difference in UV absorbancy, and therefore the difference in specific activity, between samples incubated ± ouabain represent the ouabain-sensitive Na^+/K^+-ATPase located at the basolateral membrane.

2.2.5.5 Enrichment factors of marker enzymes

Enrichment factors for all marker enzymes were calculated in both basolateral and brush-border membranes to demonstrate purity of the vesicle preparation and is represented by the ratio of activity in pure membranes to activity present in the crude homogenate.

2.3 IDENTIFICATION OF PEPTIDE TRANSPORTERS BY PHOTOAFFINITY LABELLING OF INTESTINAL MEMBRANE PROTEINS USING [4-AZIDO-3,5-^{3}H-D-PHE]-L-ALA

Membrane vesicles were labelled with the photolabile dipeptide derivative [4-azido-3,5-^{3}H-D-Phe]-L-Ala. Labelling was performed within two possible environments; in the absence of substrates (unprotected) and in the presence of a high concentration of a particular substrate (protected). The substrates used for protection studies were either a dipeptide (D-Phe-L-Gln) or its constituent amino acids (D-Phe and L-Gln). Potential differences in label incorporation by membrane proteins would demonstrate substrate-specific labelling and indicate the preferred nature of the substrate with which the protein interacts.

2.3.1 Photoaffinity labelling of membrane vesicles

2.3.1.1 Chemicals and materials

The photoaffinity label (custom-synthesised by Prof. P. D. Bailey and Dr. I. Collier in the Chemistry Department, Heriot Watt University, Edinburgh, U.K.) was tritiated to form ([4-azido-3,5-^{3}H-D-Phe]-L-Ala) by Zeneca.

Amino acids (D-Phe, L-Gln, L-Leu), MES and bestatin were supplied by Sigma Chemical Co. Ltd., Poole, U.K.

Xenon arc lamp (Wotan 250 W) positioned 22 cm from the sample cuvette.

Remaining chemicals and materials have been described in previous methods sections.

2.3.1.2 Solutions

All solutions were made up in diH_20 unless otherwise stated.

[4-azido-3,5-^{3}H-D-Phe]-L-Ala in 35% aqueous ethanol was supplied as a 42 μM stock solution (37 MBq/ml; 888 GBq/mmol.)

Labelling buffer

50 mM MES, pH 5.5	0.976 g/100 ml
16.7 mM D-Phe-L-Gln	4.912 mg/ml MES
16.7 mM D-Phe	2.77 mg/ml MES
16.7 mM L-Gln	2.43 mg/ml MES
20 μM bestatin	6.89 mg/ml MES

2.3.1.3 Labelling protocol

Transport by PepT1 has been shown by a number of groups to be optimum at pH 5.5-6.0 (reviewed in Meredith & Boyd, 1995). In addition, the limited studies conducted on the basolateral peptide transporter have shown that although transport does not have an optimum pH, it is maximal at a slightly acidic pH (Saito *et al.* 1993; Thwaites *et al.* 1993a; Matsumoto *et al.* 1994; Terada *et al.* 1999). As such, prior to photoaffinity labelling, vesicles were equilibrated at pH 5.5 by repeated wash and centrifugation steps. 200 μg membrane vesicles were re-suspended in 1 ml MES, pH 5.5 in a Beckman 1.5 ml centrifuge tube and centrifuged at 106,000 *g* in the TL100 ultracentrifuge for 10 min at 4°C. This process was repeated 3 times. It ensured that potential substrates would have a higher affinity for the transporters, and therefore maximised potential interactions.

The pellet from the final wash and centrifugation step was resuspended in the appropriate experimental solution;

'unprotected':		MES, pH 5.5
'protected':	either	16.7 mM D-Phe-L-Gln
	or	16.7 mM D-Phe & 16.7 mM L-Gln

at a concentration of 1 $mg \cdot ml^{-1}$ and incubated at room temperature for 15 min with gentle agitation. Subsequent steps were all performed in the absence of light.

[4-azido-3,5-^{3}H-D-Phe]-L-Ala (740 KBq) was added to the vesicle suspension at a final concentration of 4.2 μM. The solution was vortexed and incubated at room temperature for a further 10 min. The sample was then transferred

to a quartz cuvette and this was placed in a cuvette stand positioned 22 cm from the Xenon arc lamp. The sample was irradiated with intense UV light for 20 s to stimulate covalent binding of the azide moiety to proteins. The sample was then transferred to another pre-chilled 1.5 ml Beckman tube. The quartz cell was washed with two additional 300 µl aliquots of MES, which were combined with the original sample. The initial wash and centrifugation steps were performed again on the labelled sample to eliminate any unbound/loosely bound label remaining in solution. The final pellet was subjected to either SDS-PAGE (section 2.3.2) or IEF (section 2.3.3) in rod gels to resolve the membrane proteins based on either their molecular mass or isoelectric point, respectively.

For photoaffinity labelling studies in the presence of bestatin, vesicles were incubated with 20 µM bestatin for 30 min prior to the labelling procedure in the same way as the substrate protection studies.

2.3.2 SDS-polyacrylamide gel electrophoresis of photoaffinity labelled membrane vesicles

SDS-PAGE was used to resolve the vesicle membrane proteins as a function of their relative molecular weights. SDS is an anionic detergent that binds to proteins in a ratio of 1.4:1. This not only causes complete disruption of the proteins secondary and tertiary structures, but SDS also masks the charge of the proteins due to the formation of anionic complexes, all of which possess an equal negative charge per unit mass. In the presence of a reducing agent, e.g. β-mercaptoethanol, the polypeptides form flexible rod shapes and so the relative mobility of a protein within an SDS-PAGE gel is directly proportional to its molecular weight.

2.3.2.1 Chemicals and materials

SDS, glycerol and glycine were obtained from BDH Laboratory Supplies, Poole, U.K. and were of AnalaR® grade.

β-mercaptoethanol, TEMED, APS, bromophenol blue and pre-stained molecular weight markers were supplied by Sigma Chemical Co. Ltd., Poole, UK.

Acrylamide/Bisacrylamide solution (37.5:1) was obtained from Protogel.

Optiphase Scintillation Cocktail (Ultima-Gold™ XR) was obtained from Packard.

A gel slicer with razor blades positioned exactly 3 mm apart was custom-made in the Biology Dept., University of York

Remaining chemicals and materials have been described in previous methods sections.

2.3.2.2 Solutions

All solutions were made up in diH_2O unless otherwise stated.

Gel buffers (100 ml)

1.5 M Tris	18.165 g
8 mM EDTA	0.297 g

Stacking gel was titrated to pH 6.8 with HCl

Resolving gel was titrated to pH 8.9 with HCl

30 mM Tris-HCl, pH 7.8	0.363 g/100 ml
10% (w/v) SDS	10 g/100 ml

Sample buffer (10 ml in 30 mM Tris-HCl, pH 7.8)

9% (w/v) SDS	0.9 g
6% (v/v) β-mercaptoethanol	0.6 ml

Tracker dye (10 ml in 30 mM Tris-HCl, pH 7.8)

15% (v/v) Glycerol	1.5 ml
0.05% (w/v) bromophenol blue	0.005 g

Tank buffer (2.4 L)

40 mM Tris	9.0 g
0.38 M glycine	43.2 g
0.1% (w/v) SDS	3.0 g

1% (w/v) APS	0.1 g/10 ml

Extraction buffer (1 L)

0.1% (w/v) SDS	1.0 g
50 mM Tris-HCl, pH 7.5	6.057 g

2.3.2.3 Casting of the gels

Gels were cast in glass tubes (i.d. 5 mm) based on a discontinuous system; the 10% resolving gel formed 10 cm of the total length and the 5% stacking gel was 1.5 cm in length. The bottoms of the tubes were covered with numerous layers of Parafilm to; a) prevent leakage of the gel solution during polymerisation, and b) to prevent entry of air through the slightly porous film which may affect polymerisation. The resolving and stacking gel monomer solutions were prepared as shown in table 2.2. Values shown are per 12 gels cast.

	5% STACKING	**10% RESOLVING**
Tris/EDTA	12.6 ml	12.6 ml
Acrylamide/Bis	8.4 ml	16.6 ml
10% SDS	0.5 ml	0.5 ml
diH_2O	23.8 ml	15.4 ml
TEMED	50 µl	50 µl
1% (w/v) APS	5.0 ml	5.0 ml

Table 2.2 Constituents of gel monomer solutions used to cast SDS-PAGE rod gels

The resolving gel solution (without TEMED and APS) was degassed using a vacuum pump and Buchner funnel for 15 min. Polymerisation was initiated by the addition of 50 µl TEMED and 5.0 ml 1% (w/v) APS. The solution was gently mixed to avoid the introduction of air and then pipetted directly into the top of the glass tube towards the wall to prevent the formation of air bubbles during polymerisation. Once the solution reached the 10 cm mark, the gel was overlaid with isopropanol to ensure an even interface between the two gel solutions. The resolving gel was allowed to polymerise for approx. 30 min at room temperature. Upon completion of polymerisation, the isopropanol was poured off and the surface of the gel was washed with copious amounts of ddH_2O, before blotting any excess water. The degassed

stacking gel solution was pipetted on top of the resolving gel and again overlaid with isopropanol. The gels were left to polymerise and their surfaces washed in the same way as before, prior to being positioned in the electrophoresis tank. The upper and lower reservoirs were filled with tank buffer, ensuring leakage from the upper chamber did not occur. The gels could be stored in the tank at 4°C for approx. one week or until required.

2.3.2.4 Sample preparation and electrophoresis

The pellet from the final spin of the PAL procedure was resuspended in 70 µl freshly made sample buffer and the proteins denatured by incubation at 70°C in an Eppendorf heating block for 2 min. The sample was left to cool to room temperature prior to the addition of 35 µl tracker dye. Samples were loaded individually onto rod gels in conjunction with a sample of pre-stained molecular weight markers. Gels were electrophoresed overnight (approx 16 h) at a constant voltage of 90 V at 4°C.

2.3.2.5 Detection of a labelled protein

Following electrophoresis, the gels were extruded from the glass tubes by injection of diH_2O between the two surfaces using a hypodermic needle and syringe. The stacking gel was removed and the resolving gel sectioned into 3 mm pieces using the razor blade slicer. The slices were stored individually in labelled 1.5 ml Eppendorf tubes and mashed dry using a custom-made Teflon® pestle. 1 ml extraction buffer was added to each crushed slice, the solution was vortexed and samples were incubated overnight at 18°C with gentle rotation to allow passive extraction of the proteins from the gel.

The following day, samples were microfuged at 1800 *g* for 5 min and 100 µl supernatant was removed and added to 3 ml Optiphase scintillation fluid in 6 ml capacity Pony™ vials. The samples were vortexed and subjected to scintillation counting using a Tri-Carb® liquid scintillation analyser, model 1900CA.

2.3.2.6 Expression of results

Efficiency of scintillation counting of [4-azido-3,5-^{3}H-D-Phe]-L-Ala

Each individual scintillation counter is different in its efficiency for counting and this efficiency is also compound-dependant. To obtain the results from PAL experiments in 100% form, the counting efficiency of the label was calculated using equation 2.4:

Equation 2.4

Efficiency = (cpm/dpm)*100

This value was used to correct raw data to obtain a 100% efficiency of results.

Normalisation of data

As described in the protocol section, 20 µl of radioactive label was added to each vesicle suspension and this is equivalent to 740 kBq of radioactivity. However, minor inherent errors in the pipette may result in slightly more or less actually being used. Whereas this wouldn't have a dramatic impact on labelling results *per se*, a direct comparison between the different conditions couldn't reliably be done. And so, the degree of inhibition by certain substrates could not be calculated accurately. So, the exact amount of label added to the vesicles was measured by taking a sample of supernatant following the first centrifugation step after labelling and counting it. The total amount in the whole sample could then be calculated. An average of total counts between experiments performed simultaneously was used to normalise the data to one final initial radioactivity content added to the vesicles, using the following equation (2.5):

Equation 2.5

Normalised data = (peak dpm * mean total dpm) / actual total dpm

The data, following manipulation by these two equations, are shown in graphical form of radioactive label incorporation expressed as dpm (y axis) versus gel slice number (x axis). Therefore, peaks of radioactivity represent specific label incorporation by a protein.

Conversion of dpm to Becquerels

The results obtained from scintillation counting (in dpm) were converted to actual radioactivity for additional calculations. The following information was required for this:

- 1mCi = 2.2 x 10^{12} dpm
- 1mCi = 37 MBq

therefore,

- 37 MBq = 2.2 x 10^{12} dpm
- 1 dpm = 0.0168 Bq

Calculation of the amount of label specifically bound to a membrane protein

The amount of label covalently attached to specific membrane proteins are expressed both as the percentage of the initial amount applied and the actual amount in picomoles. The percentage of label incorporation was calculated in the following way (equation 2.6):

Equation 2.6

Bq contained in the peak / total Bq added to vesicles

The volume of label added to the vesicles was 20 µl; this is equivalent to a total of 42 µM. However, a 10-fold dilution of the label into the vesicle suspension gave a final concentration of 4.2 µM. This information was used to calculate the amount of dipeptide label covalently attached to a protein. The amount of label added to the vesicles is expressed as;

$$\mathbf{2 \times 10^{-5} * 4.2 \times 10^{-5} = 8.4 \times 10^{-10}}$$

A total of 840 pmoles of label added to the membrane vesicles. Using the percentage incorporation calculated in equation 2.6 it is possible to calculate the amount of label (in femtomoles) bound to a particular protein.

2.3.3 Isoelectric focusing (IEF) of photoaffinity labelled membrane proteins

Isoelectric focusing separates proteins solely on the basis of their isoelectric point (pI). Proteins isolated from the first dimension (SDS-PAGE) required re-solubilisation in a high concentration of urea and non-ionic detergent to displace the SDS and disrupt the anionic complexes so that the proteins were able to regain their native charge. A pH gradient was formed using commercially available ampholytes and within this gradient proteins have either a positive, negative or zero net charge based on the pH of their surroundings. Under the influence of an electric field proteins migrate to a point where their net charge is zero, i.e. at their pI. IEF concentrates proteins at their pI and separates on the basis of very small charge differences (<0.01 pH unit).

2.3.3.1 Chemicals and materials

Triton X-100, urea, NaOH and H_3PO_4 were supplied by Sigma Chemical Co. Ltd., Poole, U.K.

Ampholytes (Bio-Lyte® 5/7, Bio-Lyte® 3/10) were supplied by Bio-Rad.

Remaining chemicals and materials have been described in previous methods sections.

2.3.3.2 Solutions

All solutions were made up in diH_20 unless otherwise indicated.

10% (w/v) Triton X-100 10 g/100 ml

IEF sample buffer

9.5 M urea	5.7 g
2% (v/v) Triton X-100	2.0 ml (of 10% stock)
5% (v/v) β-mercaptoethanol	0.5 ml
1.6% (v/v) 5-7 ampholytes	0.16 ml
0.4% (v/v) 3-10 ampholytes	0.04 ml

Solution was warmed in a water bath to dissolve the urea, made up to a total of 10 ml and stored at -80°C.

IEF sample overlay buffer

9.0 M urea	5.41 g
0.8% (v/v) 5-7 ampholytes	80 µl
0.2% (v/v) 3-10 ampholytes	20 µl
bromophenol blue	trace

Solution is warmed in a water bath to dissolve the urea, made up to a total of 10 ml and stored at -80°C.

Upper electrolyte buffer (pH 2.2)

20 mM NaOH	0.8 g/L

Lower electrolyte buffer (pH 12.2)

100 mM H_3PO_4	0.68 ml/L

10% (w/v) APS	1.0 g/10 ml

2.3.3.3 Casting of the IEF gels

Gels were cast in the same glass tubes as the SDS-PAGE gels (i.d. 5.0 mm) and were 10 cm total in length (IEF gels are a continuous system). The bottoms of the tubes were wrapped in Parafilm as before (section 2.3.2.3) and the monomer solution was mixed as shown in table 2.3. This produced enough solution to cast five gels.

FINAL CONCENTRATION	AMOUNT
9.2 m urea	13.75 g
4% (v/v) T (acrylamide)	3.325 ml of 37.5:1 stock
0.1% (v/v) Triton X-100	3.0 ml of 10% stock
2.5% (v/v) 5-7 ampholytes*	625 µl
2.5% (v/v) 3-10 ampholytes*	625 µl
diH_20	4.925 ml
TEMED	25 µl
10% (w/v) APS	25 µl

Table 2.3 Constituents of the gel monomer solution used to cast IEF rod gels

*A total volume of 5% ampholytes were used, but the proportions of the samples could be altered to create the gradient required. The proportions indicated here produced a non-linear gradient pH 3-10.

The solution (without inclusion of the catalysts) was heated gently in a water bath to dissolve the urea. Polymerisation was initiated by adding 25 µl 10% (w/v) APS and 25 µl TEMED. The solution was pipetted into the glass tubes to the 10 cm mark and overlaid with isopropanol. Gels were allowed to polymerise at 37°C for approx. 2 h. Upon completion of polymerisation, the gel surfaces were washed with diH_20 and the tubes positioned in the tank. Gels were equilibrated by adding 30 µl of IEF sample buffer to their surface for 15 min at room temperature.

Electrolytes were degassed in Buchner funnels using vaccum pumps for 30 min before pouring into their respective chambers. All air bubbles surrounding the gels were removed using a Pasteur pipette.

2.3.3.4 Sample preparation and electrophoresis

Samples (either from the first dimension; SDS-PAGE, or original samples from PAL) were incubated in IEF sample buffer at room temperature for 15 min. Samples from the SDS-PAGE gels were diluted so that the concentration of SDS was less than 0.25% and its ratio to Triton X-100 was at least 1:8. SDS interferes with

IEF because the negatively charged complex it forms with the proteins disrupts their focusing process. The urea and Triton X-100 ensured the proteins remained in solution and this solubility was enhanced by the presence of ampholytes in the buffer. Ampholytes help to minimise protein aggregation caused by charge-charge interactions. Under no circumstances should the sample in the urea buffer be heated because this could introduce considerable charge heterogeneity of the proteins due to carbamoylation of the proteins by isocyanate formed from the decomposition of urea.

Before the samples were loaded onto the gels, a pre-electrophoresis stage created the pH gradient of the ampholytes within the gels. The step-wise procedure was as follows:

- 200 V for 10 min
- 300 V for 15 min
- 400 V for 15 min

Once this step was complete, samples were loaded onto the gel surface.

Gel loading was a little more difficult than with SDS-PAGE gels because the buffer doesn't contain glycerol to give the sample a lower density than the electrolyte; the sample was overlaid with another buffer with an intermediate density to prevent its diffusion from the surface of the gel. This had to be done immediately after sample loading to ensure the sample was in direct contact with the gel surface.

Electrophoresis began with another stepwise process that primarily functioned to prevent overheating of the gels due to the high voltages employed in this technique. The procedure was as follows:

- 500 V for 10 min
- 750 V for 15 min
- 1000 V for 8 h

The gels were electrophoresed at a constant voltage for 8 h at room temperature. An indication that IEF was complete was shown by a very low final current, typically less than 1 mA. This demonstrated that the proteins had reached their pI and that there was very little ionic movement within the system.

2.3.3.5 Detection of a labelled protein

Once the voltage had been switched off, slicing of the IEF gels was performed quickly because a loss of current resulted in the highly focused proteins starting to diffuse away from their pI.

Sectioning of the IEF gels was a little more difficult than with SDS-PAGE gels due to a lower acrylamide content, as such the custom-made slicer could not be used satisfactorily. Gels were sliced using a scalpel blade into 2 mm sections. The pH of each individual slice was measured using a flat bulb electrode and pH meter; the flat bulb ensured direct contact of the electrode with the surface of the gel. The gel slices were crushed and the protein extracted in the same way as described in section 2.3.2.5. Scintillation counting to detect labelled proteins was also performed in the same way.

2.3.3.6.Expression of results

Results from IEF of photoaffinity labelled proteins are graphically represented as radioactive incorporation (y-axis) against the pH gradient throughout the length of the gel (x-axis). This permitted the pI of a labelled protein to be measured.

2.3.4 Papain digestion of membrane vesicles prior to photoaffinity labelling

Digestion of BBMV using papain was employed to solubilise all known hydrolases located in that membrane. BBMV have a right side out orientation, i.e their outer surface is the outer surface of the enterocyte which faces the intestinal lumen. Brush-border hydrolases have an asymmetric orientation within the membrane, i.e. the bulk of the molecule is exposed at the luminal surface (Kenny & Maroux, 1982). As such, papain treatment can hydrolyse these proteins from the membrane whilst conserving the integrity of the lipid bilayer structure. Papain digestion was conducted prior to labelling of BBMV in order to prevent incorporation of the label by the hydrolases during PAL.

2.3.4.1 Chemicals and materials

Papain was commercially available as a 23 $mg \cdot ml^{-1}$ suspension in sodium acetate from Sigma Chemical Co. Ltd., Poole, U.K. Cysteine, HEPES and dithiothreitol were also supplied by Sigma.

Remaining chemicals and materials have been described in previous methods sections.

2.3.4.2 Solutions

All solutions were made up in diH_2O unless otherwise stated.

Potassium phosphate buffer, pH 6.2

Consisted of 2 stock solutions;

(A) 50 mM KH_2PO_4	0.68 g/100 ml
(B) 50 mM K_2HPO_4	0.871 g/100 ml

A working buffer of pH 6.2 contains 40.75 ml solution A and 9.25 ml solution B.

Hepes/mannitol buffer, pH 7.5 (100 ml)

1 mM HEPES	0.026 g
100 mM mannitol	1.822 g

50 mM cysteine	79 mg/10 ml phosphate buffer
3 mM DTT	46 mg/100 ml phosphate buffer

2.3.4.3.Papain digestion protocol

All steps were performed at 4°C unless otherwise stated.

200 µg BBMV were centrifuged in the TL100 at 106,000 *g* for 10 min to pellet the membranes. The vesicles were equilibrated at pH 6.2 by repeated wash and centrifugation steps as described in section 2.3.1.3 but using the potassium phosphate buffer. The pellet from the final spin was resuspended in potassium phosphate buffer at a concentration of 5 $mg \cdot ml^{-1}$.

Papain was required at a concentration of 39 $mg \cdot ml^{-1}$ in potassium phosphate buffer, so 39 mg of the commercial suspension (169.6 µl) was pelleted by centrifugation at 240,000 *g* in the TL100. Papain was activated by resuspension of the pellet in 100 µl potassium phosphate buffer containing (final concentration) 5 mM cysteine and 0.03 mM DTT and incubated for 15 min on ice. Activated papain was then added to the vesicle suspension at the concentration required, e.g.

- 0.5 $mg \cdot ml^{-1}$ = 0.51 µl papain
- 0.25 $mg \cdot ml^{-1}$ = 0.26 µl papain

The sample was vortexed and incubated at 37°C for the required time period of digestion.

Following digestion, the reaction was quenched in one of two different ways;

(i) chilled to 4°C (Ganapathy *et al.*, 1981)

(ii) 5-fold dilution with ice-cold HEPES/mannitol buffer, pH 7.5 (Berteloot *et al.* 1980).

The suspension was centrifuged at 106,000 *g* for 45 min. The membrane pellet was then equilibrated to pH 5.5 with 50 mM MES as described in section 2.3.1.3 and the photoaffinity labelling procedure was performed exactly as before.

2.4 ISOLATION AND PURIFICATION OF AN INDIVIDUAL MEMBRANE PROTEIN

Proteins can be isolated using two-dimensional electrophoresis (2-DE) with immobilised pH gradients (IPGs). However, during each of the distinct steps a certain amount of the initial protein is lost. These sequential losses are summarised as follows:

- IEF 30-35% loss
- Equilibration 40-45% loss
- SDS-PAGE 43-48% loss

(taken from Celis & Bravo, 1984)

At the end of the procedure as much as half of the initial protein applied to the IEF strip may be lost. If the protein of interest is a minor component of the sample, there won't be a sufficient amount remaining at the end to be used for sequence analysis. As such, in order to ensure a satisfactory yield of a specific membrane protein, it was necessary to employ a scaled-up protein isolation procedure using the rod gels prior to the 2-D purification step.

2.4.1 Identification of a protein by photoaffinity labelling

Samples (200 μg) of membrane vesicles were photoaffinity labelled following the protocol previously described (section 2.3.1) and the radioactive membranes were subjected to SDS-PAGE in rod gels as previously described (section 2.3.2.). A total of 10 samples could be run due to the structure of the electrophoresis system.

Following resolution, the gels were sliced, crushed and the proteins extracted as before. The labelled samples were subjected to scintillation counting to determine which slice number contained the radioactively labelled protein.

2.4.2 Isolation of a specific protein using SDS-PAGE slab gels

The slice(s) containing the labelled protein from all gels were run on 10% slab gels in a Mini-Protean® II dual slab gel kit (Bio-Rad) to determine precisely which samples contained the protein of interest only, without contamination from other proteins of similar molecular weight.

A discontinuous system was employed in the slab gels following standard Bio-Rad protocols. Gel solutions and buffers were as described in section 2.3.2, however, gels were cast between two glass plates (inner plate 7.3*10.2 cm, outer plate 8.3*10.2 cm) to form a gel of dimensions 7.0 cm in length by 8.0 cm in width. PVC (polyvinyl chloride) spacers determined the thickness of the gel (0.75 mm). Teflon® combs formed the sample loading wells within the stacking gel.

From each of the required samples, 15 μl of supernatant was added to 2 μl β-mercaptoethanol and 7 μl tracker dye, and vortexed. 20 μl of the final samples were loaded onto the gel, in conjunction with a sample of pre-stained molecular weight markers. Gels were electrophoresed at a constant voltage (100 V) for approx. 2-3 h until the required resolution was attained.

2.4.3 Silver staining

Protein bands were visualised by silver staining of the gels following the standard Bio-Rad protocol, based upon a photochemical process outlined by Merril (1981), described below.

2.4.3.1 Solutions

All solutions were made up in diH_2O unless otherwise stated.

Fixative (100 ml per gel)

40 % (v/v) methanol	40 ml
10 % (v/v) acetic acid	10 ml

Oxidiser

This was supplied as a 10x concentrated solution and had to be diluted prior to use.

Silver reagent

This was supplied as a 10x concentrated solution and had to be diluted prior to use.

Stop solution (100 ml per gel)

5% (v/v) acetic acid	5 ml

Developer

This was supplied as a dry chemical blend (115 g).

One bottle was dissolved in 3.6 L.

2.4.3.2 Staining protocol

All steps were performed on an orbital shaker table to ensure contact of the gel with solutions at all times.

Immediately following the electrophoretic run, the gel was separated from the glass plates, the stacking gel removed and the resolving gel placed in fixative solution for 30 min. The gel was then transferred to oxidiser for a further 5 min

followed by repeated washing in several changes of diH_20 for 15 min. The gel was then immersed in silver reagent for 20 min before another rapid wash (<30 s) in diH_20. The gel was submerged in developer to visualise the protein bands; the appearance of a brown precipitate indicated the need for fresh developer. The bands were imaged as dark lines on a pale background. When the required intensity was achieved, image development was quenched by immersing the gel in stop solution.

2.4.4 Protein isolation and concentration

Silver staining of the gels allowed the final step of isolation of the desired protein from an initial complex mixture. A preliminary step was to calculate the approximate molecular weight of the radioactively labelled protein using the pre-stained molecular markers to construct a standard curve based on their relative distances travelled through the gel. The gel was analysed using an imaging system (AlphaEase™ version 3.3, Alpha Innotech Corporation) in which the positions of the standards in the gel were manually indicated along with their known molecular weights. The AlphaEase™ Stand Alone Software constructed a calibration curve which it then used to calculate the molecular weight of the labelled protein who's position in the gel was also indicated. Once the apparent molecular weight of the labelled protein had been calculated, all samples containing this protein were isolated.

The isolated protein samples were then concentrated from an approx. 800 µl initial individual volume (per sample) to a combined final volume of 50 µl. This was performed using a NANOSEP™ Microconcentrator (Pall Filtron Corporation). Samples were pipetted into the device which was spun at 1800 *g* in a bench top angled centrifuge at 4°C. The final sample was stored at -80°C.

2.4.5 Determination of protein content in the pure sample

Prior to analysis, the amount of protein contained in the final sample required elucidation. This was achieved using BSA as an indicator of protein content within a band formed by SDS-PAGE in slab gels when silver stained. A calibration curve (50-400 ng) was constructed within the gel.

The spot densitometry program on the AlphaEase™ was used to measure the pixels associated with the IDV (integrated density value) of the stained BSA bands.

The IDV of an individual protein is proportional to the amount stained, up to a saturation point. Although BSA would stain slightly differently to the isolated protein, it was still a reliable marker for calculating the amount of protein present in a band. To ensure an accurate estimate was achieved, only values lying within the linear range were used. Determination of the protein content within a known volume permitted the total amount, plus the protein concentration, to be calculated. This information was useful at a later date when performing analysis of the protein.

2.5 TWO-DIMENSIONAL ELECTROPHORESIS OF MEMBRANE PROTEINS USING AN IMMOBILISED pH GRADIENT

Two-dimensional electrophoresis (2-DE) is a powerful method for the analysis of protein mixtures from biological samples. The two distinct steps have been briefly described in sections 2.3.2 and 2.3.3.; this technique using carrier ampholytes was first introduced by O'Farrell in 1975, however due to various problems, such as low reproducibility, the technique wasn't widely used. Its application has only become significant in the past few years as the result of a number of developments. The major improvement in technique was to replace the carrier ampholyte gels with immobilised pH gradient (IPG) gels; IPGs have permitted extremely high resolution with very small initial quantities of protein. As such, this 2-DE procedure was used to isolate an individual labelled protein with which to perform sequence analysis to aid in its identification.

2.5.1 Chemicals and materials

Urea (Electran), Resolytes 4-8 and glycerol (~87%) were supplied by BDH Laboratory Supplies, Poole, U.K. and were of AnalaR® grade.

Thiourea, DTE (BioChemika), SDS and sodium thiosulphate were supplied by Fluka.

CHAPS, iodoacetamide, and brilliant blue G-colloidal stain were supplied by Sigma Chemical Co. Ltd., Poole, UK.

Agarose and the Protein II xi cell for the second dimension were supplied by Bio-Rad.

Immobiline dry strips non-linear pH 3.5-10.0 (18 cm), IPG strip holders (18 cm), IPG rehydration tray, IPG cover fluid and the IPGphor™ isoelectric focusing system were obtained from Amersham Pharmacia Biotech.

Remaining chemicals and materials have been described in previous methods sections.

2.5.2 Solutions

All solutions were made up in diH_2O unless otherwise stated.

Sample/rehydration buffer (100 ml)

7 M urea	42.04 g
2 M thiourea	15.22 g
4% (w/v) CHAPS	4.0 g
65 mM DTE	5.0 g
0.8% (v/v) Resolytes 4-8	0.8 ml
bromophenol blue	trace

Solution was aliquoted and stored at –20°C.

Equilibration stock solution (100 ml)

50 mM Tris-HCl, pH 6.8	0.61 g
6 M urea	36.03 g
30% (v/v) glycerol	30.0 ml
2% (w/v) SDS	2.0 g

Solution was stored at 4°C.

Equilibration solution 1 (per 10 ml stock solution)

1% (w/v) DTE	10.0 mg

Equilibration solution 2 (per 10 ml stock solution)

4% (w/v) iodoacetamide	40.0 mg
bromophenol blue	trace

SDS-PAGE gel monomer solution (10% gel)

1.5 M Tris-HCl, pH 8.8	13.25 ml
Acrylamide/bisacrylamide (37.5:1)	17.7 ml
Sodium thiosulphate	0.042 g
diH_20	21.5 ml
TEMED	26.5 µl
10% (w/v) APS	0.53 ml

Second dimension electrolyte buffer (2 L)

25 mM Tris	6.06 g
198 mM glycine	29.72 g
0.1% (w/v) SDS	2.0 g

0.5% (w/v) agarose	0.05 g/10 ml electrolyte buffer

2.5.3 First dimension: Isoelectric focusing

2.5.3.1 Sample loading

The IPG ceramic holders were used for both gel rehydration/sample loading and IEF.

At this stage in the protein isolation procedure, the required protein in the concentrated sample was not completely pure, i.e other proteins with similar molecular weights may have been extracted from the rod gels simultaneously. So, in order to be able to specifically identify the protein of interest in the final 2-DE gel, a sample of radioactively labelled protein was subjected to 2-dimensional electrophoresis.

Immediately before re-swelling of the gel strip, an aliquot of rehydration buffer was thawed out to room temperature. The 50 µl labelled protein sample (obtained from the concentration step in section 2.4.4) was combined with this; a total rehydration solution volume of 350 µl was used for an 18 cm IPG strip. This 7-fold dilution factor ensured that the SDS contained in the primary sample was reduced to less than 0.25% and was present in a ratio of 8:1 non-ionic detergent : SDS.

The 350 µl rehydration sample was pipetted into the ceramic holder by 'spotting' the solution along its length and air bubbles were removed. The IPG strips were stored at –20°C until required; at room temperature the protective cover from the gel was removed and the strip was placed gel-side down into the ceramic holder, over the rehydration solution, with the pointed (anodic) end at the pointed end of the holder. Positioning the strip was achieved by lowering the anodic end into the slot first and gently sliding the gel over the buffer, ensuring good contact between the ends of the gel strip and electrodes. Once in position, the strip was overlaid with approx. 3 ml of IPG cover fluid by pipetting it drop-wise at one end of the holder until half of the strip was covered, and then repeating this at the other end until the whole strip was overlaid. The cover was placed onto the ceramic boat; pressure blocks on the underside of the lid maintained continuous contact between the strip and the electrodes in the holder as the gel re-swelled.

2.5.3.2 Rehydration and isoelectric focusing

Rehydration and IEF of the strip were performed on the IPGphor at 20°C. The ceramic boat holding the gel strip was placed onto the plate of the IPGphor ensuring its correct orientation by using the guidemarks. The safety lid of the IPGphor was closed; at least two of the three pressure pads on the underside of the lid was required to touch the cover of the ceramic boat in order to gain efficient contact between the holder electrodes and the electrode areas of the IPGphor plate.

The rehydration step was incorporated into a standard user-defined program on the IPGphor. A summary of the rehydration/IEF program for an 18 cm strip is as follows;

- Rehydration 22 h
- IEF: 'step 'n' hold' gradient 300-3,500 V 3 h
- 3,500 V 3 h
- 5,000 V ~ 15 h

The low initial voltage, combined with 'step 'n' hold' gradients, functioned to minimise overheating of the gel strip and prevent sample aggregation. Subsequent to the build up of voltage, the system was maintained at 5,000 V for a necessary time

period to give a volt-hour product of 100,000; this was generally about 15 h. Each step defined in the protocol was controlled by the IPGphor, therefore the system could be left unattended until the IEF was complete.

After strip rehydration, tracking of the bromophenol blue in the re-swelled gel indicated that IEF had been initiated and that a current was flowing. But, clearing of the dye front from the gel wasn't a sign that IEF was complete because it leaves the gel well ahead of protein focusing. Focusing was achieved when the specified number of volt hours was reached.

2.5.4 Equilibration of the focused IPG strip

Equilibration was performed in the rehydration tray. Equilibration solutions 1 and 2 were made using the stock solution immediately before use.

After completion of IEF, the strip was removed from the ceramic boat and rinsed thoroughly with diH_20 before placing it into a groove in the rehydration tray gel-side upwards. Approx. 3 ml of equilibration solution 1 was pipetted over the strip and incubated for 12 min. This solution was removed by pipetting it out of the groove and 3 ml equilibration solution 2 was added for a 5 min incubation period.

Immediately after equilibration was finished the gel strips were loaded onto the second dimension (SDS-PAGE) slab gels.

2.5.5 Second dimension: SDS-PAGE

The second dimension slab gels were cast prior to strip equilibration. The gels used were of a large format (18 cm * 16 cm * 1 mm) to be run in the Protein II xi cell (Bio-Rad). The procedure used for casting of the gels was as described in section 2.3.2 but with the solutions specified in section 2.5.2, except that this slab gel was a continuous system (no stacking gel) and the gel solution was overlaid with water-saturated butanol instead of isopropanol during polymerisation. The other difference was that the gels were polymerised in the dark for 2 h. Once the gels were cast, the butanol was removed and replaced with electrolyte buffer and stored at 4°C until required.

Prior to strip loading, the electrolyte was removed. The 0.5% (w/v) agarose solution was mixed, heated in a microwave oven and poured on top of the slab gel. The strip was loaded onto the surface of the gel through the hot agarose solution,

using a spatula to push it between the glass plates and attain complete contact with its surface. The orientation of the strip was noted; the acidic end (pointed) was placed at the left side of the slab gel when facing it during loading. The agarose solution cooled and solidified to hold the strip in full contact with the slab gel.

The slab gels were placed in the tank and electrophoresed at 40 mA per gel until the required resolution was achieved. The gels were maintained at 4°C by recirculating chilled water around the tank by an external bath.

After the second dimension, the gels were removed and the protein spots visualised by an appropriate stain. Care was taken to note the correct orientation of the gel by notching the upper acidic corner.

2.5.6 Staining of the 2-D gel with brilliant blue G-colloidal

2.5.6.1 Solutions

All solutions were made up in diH_2O unless otherwise stated.

Fixative (500 ml per gel)

7% (v/v) glacial acetic acid	35 ml
40% (v/v) methanol	200 ml

Brilliant blue G-colloidal stain (1 x working solution)

Add 800 ml to contents of the bottle and mix thoroughly

Colloidal stain (500 ml per gel)

20% (v/v) methanol in 1x working solution	100 ml

Destaining solution 1 (500 ml per gel)

10% (v/v) glacial acetic acid	50 ml
25% (v/v) methanol	125 ml

Destaining solution 2 (500 ml per gel)

25% (v/v) methanol	125 ml

2.5.6.2 Staining protocol

After the electrophoretic run was complete, the gels were stained using a brilliant blue G-colloidal stain. Initially they were fixed for 1 h in fixative solution on an orbital shaker table. The staining solution was made immediately before use and added to the gels after the fixing stage. The gels remained in stain overnight with gentle agitation. They were then immersed in destaining solution 1 for 10-30 s before being transferred to solution 2 to rinse excess stain from their surface. This solution was replaced after 30 s and was used to store the gels in until it was photographed and/or used for further analysis.

2.6 IN GEL TRYPTIC DIGEST OF AN INDIVIDUAL MEMBRANE PROTEIN ISOLATED BY 2-DIMENSIONAL ELECTROPHORESIS

Once an individual protein had been isolated by the 2-DE procedure, an initial step in its identification was to establish whether it had previously been documented, or whether it was novel. The most rapid method of protein identification that could be performed with relative ease was to do an enzymatic digest of the protein using trypsin and then use the resulting peptide fingerprint in database searches. Trypsin is a highly specific serine protease that exclusively cleaves the peptide backbone at the carboxylic side of lysine and arginine residues to produce a series of peptide fragments. These fragments constitute a unique fingerprint of a particular protein and are therefore collectively designated a 'peptide fingerprint'. Molecular mass searching using this fingerprint is a powerful and accurate tool in protein identification.

2.6.1 Chemicals and materials

Sequencing grade modified trypsin was obtained from Promega.

AmBic, formic acid and TFA were supplied by Sigma Chemical Co. Ltd., Poole, UK.

Acetonitrile was supplied by BDH Laboratory Supplies, Poole, UK.

A Speed Vac® Plus vaccum centrifuge (model SC110A) was obtained from Savant.

Remaining chemicals and materials have been described in previous methods sections.

2.6.2. Solutions

All solutions were made up in diH_2O unless otherwise stated.

Wash buffer A (10 ml)

25 mM AmBic	19.77 mg
50% (v/v) acetonitrile	5.0 ml

Digest stock solution (100 ml)

25 mM AmBic	197.7 mg
1mM $CaCl_2$	14.7 mg

Tryptic digest buffer (in digest stock solution)

0.0125% (w/v) trypsin	12.5 µg/ml

Wash buffer B (10 ml)

5% (v/v) formic acid	0.5 ml

Analysis buffer (10 ml)

0.1% (v/v) TFA	10 µl
50% (v/v) acetonitrile	5.0 ml

2.6.3. Digest protocol

Protein digestion followed staining of the 2-DE gels with brilliant blue G-colloidal stain. All protein spots that were visualised in the 2-DE gel containing the photoaffinity labelled membrane protein at the approximate molecular weight were excised, crushed and added to 3 ml Optiphase scintillation fluid in 6 ml capacity Pony™ vials. The samples were vortexed and subjected to scintillation counting using a Tri-Carb® liquid scintillation analyser, model 1900CA. This enabled the

precise spot containing the radiolabelled protein to be determined. Once this had been elucidated, the corresponding spot in a second 2-D gel was excised and subjected to tryptic digestion. Excision of the spot was performed carefully so as not to include any of the surrounding gel.

The excised spot was chopped into small pieces (approx. 1 mm^2) and contained in a 1.5 ml capacity Eppendorf tube. The gel pieces were washed in 500 µl wash buffer A three times for 10 min at room temperature with gentle agitation. The pieces were then dried down completely in the Speed Vac® Plus; this process usually took approx. 30 min but required constant monitoring of progress. The dried gel pieces were then re-swelled in tryptic digest buffer; just enough solution was added to cover the gel. This rehydration step took about 3-5 min and functioned to draw trypsin into the gel. Tryptic digest buffer was added to the re-swelled gel in an appropriate volume to keep the gel submerged during the digestion. The volume of buffer was determined by the size of the gel spot and the amount of protein it contained, plus the ratio of trypsin to protein required; trypsin was used in at least a 1:100 ratio with protein. The gel pieces were incubated in digest buffer overnight at 37°C in an incubation room, not a heating block. Following digestion, excess solution was removed and stored on ice. The gel was washed three times in very small volumes of wash buffer B for 30 min with gentle agitation. Extraction of peptides was carried out in small volumes to avoid the adsorption of peptides to the sides of the tube. After each wash period, the solution was removed, combined with the initial digest solution from the overnight incubation and stored on ice. The final collated sample was spun to dryness in the vaccum centrifuge. The precipitate was washed by resuspension in 100 µl diH_20, before being spun to dryness again. This last wash step was repeated and the final dried sample was stored at 4°C until analysis.

2.7 MALDI-TOF MASS SPECTROMETRIC ANALYSIS OF PEPTIDE FRAGMENTS PRODUCED FROM TRYPTIC DIGEST OF A PROTEIN

When analysing an unknown protein the simplest and most rapid method for its unequivocal identification with high sensitivity and accuracy is to analyse the masses of the tryptic peptides using MALDI-TOF (matrix assisted laser desorption/ionisation time of flight) mass spectrometry. The peptide mass fingerprint can then be used to search databases to find a positive match for the protein, providing that the unknown protein is contained within the databases.

2.7.1 Chemicals and materials

C_{18} ZipTips were obtained from Millipore.

Acetone was supplied by BDH Laboratory Supplies, Poole, UK.

α-cyano-4-hydroxycinnamic acid (4-HCCA) and trifluoroacetic acid (TFA) were supplied by Sigma Chemical Co. Ltd., Poole, UK.

The stainless steel sample plate, the MALDI-TOF (Voyager DE-STR) and the calibration standards (Cal2) were obtained from PerSeptive Biosystems, PE Applied Biosystems, Cheshire.

Remaining chemicals and materials have been described in previous methods sections.

2.7.2 Concentration and desalting procedure using C_{18} ZipTips

The final dried peptide sample was washed to removed salts and buffers that may be present; this clean-up procedure results in better spectra from mass spectrometric analysis.

2.7.2.1 Solutions

All solutions were made up in diH_2O

100% Acetonitrile

Wash solution B (100 ml)

0.1% TFA	100 µl

MALDI-TOF elution buffer (100 ml)

50% acetonitrile	50 ml

Q-TOF elution buffer (100 ml)

0.1% TFA	100 µl
50% methanol	50 ml

2.7.2.2 Procedure

The sample was cleaned up using the ZipTip immediately prior to analysis, to prevent polymers from the Eppendorf tubes an/or tips contaminating the pure sample.

The dried peptide sample was resuspended in 10 µl 50% acetonitrile prior to the ZipTip clean-up. The tip was washed with 10 µl 100% acetonitrile by drawing up and down several times: this was then repeated twice. The tip was then washed once with 10 µl 50% acetonitrile, followed by three times with 10 µl 0.1% TFA (the acidic pH of TFA promoted maximum binding of the peptides to the mini column). The resuspended sample was then drawn up and down through the tip several times to ensure complete binding of the peptides. The bound peptides were washed with 0.1% TFA, by drawing 10 µl through the tip three times; at this point all washes were retained. The peptides were eluted in either 50% acetonitrile (MALDI-TOF analysis) or 0.1% TFA in 50% methanol (Q-TOF analysis), in a volume of 2 µl. If the sample was found to be too concentrated in this small volume, appropriate dilutions could be made during analysis.

2.7.3 MALDI-TOF analysis of peptide fragments

2.7.3.1 Solutions

All solutions were made up in di$H_2$0 unless otherwise stated.

Resuspension buffer (10 ml)

0.1% (v/v) TFA	10 µl
50% (v/v) acetonitrile	5.0 ml

Saturated matrix solution (in resuspension buffer)

100% (w/v) 4-HCCA	10 $mg \cdot ml^{-1}$

2.7.3.2 Sample plate preparation

A stainless steel 100-position sample plate was used for peptide fragment analysis. Prior to sample loading the plate was cleaned to ensure it was contaminant-free. This was achieved by washing the surface with methanol and a lint-free lab tissue. The plate was rinsed with diH_2O, followed by acetone and allowed to air dry.

2.7.3.3 Matrix and sample preparation

A variety of matrix compounds are available for sample analysis, however, the matrix used for peptide analysis was α-cyano-4-hydroxycinnamic acid (4-HCCA). A saturated matrix solution was made by dissolving 10 mg 4-HCCA in 1 ml 50% (v/v) acetonitrile, 0.1% (v/v) TFA. The solution was mixed well by vortexing and any undissolved matrix was pelleted out of solution by centrifugation at 1800 *g* for 5 min. The supernatant was used for sample analysis. A 100% solution was required so that the matrix was present in molar excess of the peptides. The matrix solution was made in the same solvent as that used to re-dissolve the dried peptides; the organic solvent was present to prevent aggregation of the peptides and TFA functioned to maintain the pH below 4 to preserve the matrix crystallisation properties.

The sample was prepared for analysis on the plate using the dried droplet recipe; 0.5 µl of sample (following ZipTip clean-up) was spotted onto the plate, and 0.5 µl of saturated matrix solution was added to this. The drops were mixed well by

pipetting the combined sample/matrix solution up and down the tip several times. The mixed sample was allowed to crystallise by drying in a constant stream of room temperature air. During this time the peptides were incorporated into the crystallising matrix to produce peptide-doped crystals.

2.7.3.4 Sample analysis

In conjunction with every sample analysed, a multi-point calibration was performed. This was conducted using one of a number of commercially available calibration mixtures; Cal2 (PerSeptive). The mixture contains a number of proteins with known molecular masses, all of which only occur in one isoform. The mixture was chosen based on the molecular weight range under study. The components of Cal2 are shown in table 2.4.

PROTEIN	CALIBRATION PEAKS (Da)		CHARGE
	Monoisotopic	Average	
Angiotensin 1	1,296.6853	1,297.51	+1
ACTH (clip 1-17)	2,093.0867	2,094.46	+1
ACTH (clip 18-39)	2,465.1989	2,466.72	+1
Insulin (bovine)	2,865.8083	2,867.80	+2
ACTH (clip 7-38)	3,657.9294	3,660.19	+1
Insulin (bovine	5,730.6087	5,734.59	+1

Table 2.4 Peptide constituents of the Cal2 calibration mixture and their associated molecular masses.

The calibration mixture was applied to the sample plate with matrix in the same way as the peptide mixture. Analysis of the standards provided an external calibration of the MALDI-TOF. The aim of the calibration step was to get mass peak data identical, or as close to as possible, to the masses shown in table 2.4. Only when this was achieved could reliable interpretation of the sample peak masses be performed.

The calibration was performed prior to sample analysis because, although not essential, peaks masses could be assigned immediately once the calibration file had been specified. An absolute requirement of the calibration was that every time

the vacuum seal on the MALDI was broken, i.e. to load additional samples, a new calibration step had to be performed due to small changes in internal pressure that had probably occurred.

Standards and samples were analysed in linear or reflector mode; linear analysis was performed initially because it had a higher degree of sensitivity, i.e. it was able to detect peptides of low abundance. However, it only measured the average masses of the peptides. If a good spectrum were gained with this method, then the sample was analysed in reflector mode to obtain an improved mass resolution and accuracy of the peptide data by measuring the monoisotopic masses of the peaks. If reflector data was obtained, this was used in database searches, due to a higher degree of accuracy.

The sample plate was loaded into the ion source region, which is at a high internal pressure, and allowed to equilibrate. In this region, under vacuum, the solvent was removed, leaving co-crystallised peptide molecules homogeneously dispersed within matrix molecules. A pulsed nitrogen laser (337 nm) was used to ionise the molecules; an intermediate intensity (approx. 2000) was initially used, which was altered accordingly due to the strength of the signals detected. The relationship between the peptide ion current and laser intensity has been shown to be highly non-linear; a threshold level is required initially to produce the ions, the abundance of which increases rapidly to a maximum level with increasing laser power. However, the system as a whole is thought to function more efficiently when laser intensity is close to the threshold. The laser was pulsed to avoid thermal decomposition of the peptide molecules. Samples were analysed in delayed extraction (DE) mode with a low mass gate of 400 Da, to eliminate peaks produced from the matrix, and the system was set to analyse positive ions exclusively.

The basic principle by which the MALDI-TOF analyses peptide molecules is as follows. When the laser hits the surface of the crystals the energy is transferred to the matrix which, in turn, sublimes and carries the intact peptides into the vapour phase, while simultaneously ionising them, i.e. peptides are desorbed from the probe surface. The peptide fragment ions, all possessing equal kinetic energies, are accelerated down the field-free drift region by the electric field towards the anode and to reach the detector. Therefore, the time it takes for the ions to travel from the ion source to the detector is entirely dependent on the mass of the ion, i.e small ions reach the detector before larger ions. Once the ions hit the detector, the impact signal

is converted into digitized data. Data accumulated from successive laser shots are summed to yield a time of flight (TOF) mass spectrum, which is more accurate and has a better signal-to-noise ratio than data from single shots alone. The TOF spectrum represents the detector signal versus time. The mass of an ion is calculated by the following equation:

$$T \approx (m / z)\, 1 / 2$$

whereby the time of flight for a molecule (t) is proportional to its mass (m) and charge (z) to travel the distance.

This relationship, in conjunction with the Cal2 peak data of known m and z, is used to calibrate the spectra, calculate the ion masses and convert the data into a conventional mass spectrum of a mass-to-charge ratio. Fortunately, the laser ionisation technique employed in MALDI-TOF predominantly produces singly protonated ions; therefore the mass-to-charge ratio is the true mass plus 1 Da. The data system not only collates all the accumulated data, but also controls all instrument parameters and data processing and manipulation to produce an output of peptides masses (m / z) on the *x* axis against signal intensity i.e. abundance of the peptide, on the *y* axis.

2.8 Q-TOF MASS SPECTROMETRIC ANALYSIS OF PEPTIDE FRAGMENTS PRODUCED FROM TRYPTIC DIGEST OF A PROTEIN

In addition to the peptide map that can be obtained from MALDI-TOF analysis of the tryptic digested protein, other sequence information can also be retrieved and used to increase the power of searching when identifying a protein from databases. This type of analysis was performed in order to gain a partial sequence from one or more of the peptide fragments generated from the digest. The Q-TOF (quadrupole time-of-flight) mass spectrometer (Micromass UK. Ltd) used for this analysis is located in the Biochemistry department of the University of Leeds; analysis of my samples were performed by Dr. Alison Ashcroft.

Briefly, the Q-TOF is an electrospray tandem mass spectrometer. As opposed to the MALDI-TOF, where sample is analysed by desorption from a sample plate, in the Q-TOF minute volumes of sample (2-3 μl) are sprayed into the instrument through a fine needle over a period of 20-30 min. As its name indicates, tandem mass spectrometers consist of two consecutive analysers; in the case of the Q-TOF, a quadrupole followed by a TOF analyser. Once sprayed into the instrument, at high vaccum, the solvent rapidly evaporates providing a constant stream of peptide ions.

The sample is initially analysed using only the TOF system, to identify multiply-charged ions, which is indicative of a peptide fragment. These charged ions differ by half of a mass unit, and it is these ions which are of interest to me; they are selected using the quadrupole mass analyser for further analysis.

The principle purpose of Q-TOF analysis of my samples was to obtain a partial sequence of at least one of the peptide fragments to use in protein identification. By selecting a particular peptide ion, the ion beam enters the quadrupole, which in turn is tuned to permit only the transit of those ions with the selected mass-to-charge ratio. These specified ions enter a cell, in which fragmentation occurs due to collision of the ion with an inert gas, usually argon. Fragmentation can cause cleavage at any of the bonds within the peptide structure but, under conventional conditions, is predominantly restricted to the backbone of the peptide (see section 5.8.5) The generated fragments are accelerated orthogonally by applying a pulsed electric field and their masses determined by the TOF analyser, in the same way as the latter stages in MALDI-TOF analysis.

In order to visualise the partial amino acid sequence from the peptide fragment, it is usual to select the series of y-ions, which sequentially differ by the exact mass of one of the possible twenty naturally occurring amino acid residues. As such, the sequence is read from the intervals between the peaks of the y-ion series to reveal the partial sequence (sequence tag).

2.9 PROTEIN IDENTIFICATION USING ON-LINE DATABASE SEARCHES

Tryptic digest data, in the form of peptide masses analysed and calculated by MALDI-TOF or the sequence tag produced from Q-TOF analysis, were used in on-line database searches in an attempt to identify the protein. Proteins can be unequivocally identified from databases (if its sequence is present) with a relatively limited set of peptide masses (as little as 5-6) when screened against more than 100,000 proteins (Pappin, 1997). In addition, a single sequence tag is adequate for unequivocal protein identification, unless it is present within a conserved domain of several distinct proteins of a family. However, this also means that the tag can be matched to homologous proteins in other species, if required.

A number of database search engines are available on the World Wide Web, the sites relevant to protein identification using tryptic digest fragment data and sequences tags are shown in Appendix II.

2.9.1 Data input and search parameters

Each program functions in essentially the same way, however, detailed instructions for use are provided on individual web sites. The programs scan their respective databases and generate theoretical peptide fragments, based on the specific protease used, for each of the sequences they possess. The molecular masses of these peptides are computed from their primary amino acid sequence. Depending on the type of search specified, these are either average or monoisotopic masses. The program scans all of this theoretical information, in conjunction with actual masses input by the operator, simultaneously comparing both sets of data. If a theoretical fragment lies within a user specified tolerance level of an actual fragment mass, the match is recorded. If the number of matching peptide fragments for a protein exceeds the minimum number of matches required, that protein is added to the list of possible matching proteins.

The following criteria of the unidentified protein are utilised in the search:

- cleavage reagent
- peptide masses (Da)
- mass accuracy
- number of missed cleavages
- modifications during electrophoretic separation and isolation, for example, oxidation of methionine or tryptophan, alkylation of cysteine, etc.

Additional parameters may be included to selectively identify the protein, while excluding false positives:

- species of origin
- estimated molecular mass
- estimated pI
- type of protein anticipated.

All peptides that had a good signal-to-noise ratio were utilised in the search, in conjunction with other fragments that formed distinctive peaks in the spectrum. When a complex spectra, which included the less abundant peaks, was analysed, the mass tolerance was increased due to the possibility that mass accuracy may have been compromised as a result of a low signal intensity (Parker, 1998). However, as with all modifications to search parameters, care needed to be taken to avoid misidentification of the protein if an aspect was altered too aggressively. For example, if a larger mass tolerance was specified it would increase the possibility of matching unrelated proteins, whereas decreasing the tolerance would increase the incidence of missing the crucial match. The main point taken into account during searching was that the smaller the permitted ranges of any of the parameters used produced a higher level of confidence so that if a match was found, it was highly likely to be genuine.

Searching using sequence tags is even simpler; generally only the original protein mass is required, plus the parent peptide which was fragmented (optional) and the defined amino acid sequence.

Different search tools can be used to ensure complete coverage of all the databases available.

2.9.2 Elimination of false peptides

Modified trypsin from Promega, which has been demonstrated not undergo autolysis, was used to digest the isolated protein. However, in order to eliminate any peptides produced from autolytic digestion of trypsin, a theoretical digest of the protein was performed using the MS-Digest program from Prospector (see Appendix II). This generated the masses of peptides that would have been produced if in fact autolysis had occurred. These masses were analysed in conjunction with the isolated protein's masses and any coinciding peptides were not used in the database searches.

This site was also used to perform theoretical digests of other proteins thought to be similar to the isolated protein, in order to establish that they were not the same entity.

CHAPTER 3: INTERACTION OF A POTENTIAL PHOTOAFFINITY LABEL WITH PEPTIDE TRANSPORTERS IN RAT JEJUNUM

3.1 Development and synthesis of the photoaffinity label

Previous investigations of peptide transport by rat jejunum (Lister *et al.*, 1995) have shown that although naturally occurring dipeptides are significantly hydrolysed following apical absorption into the enterocyte, some chemically synthesised peptides have an inherent resistance to hydrolytic breakdown while still being efficiently transported. Results from this study demonstrated that the presence of a D-amino acid at the N-terminus of a dipeptide reduces peptidase activity sufficiently to permit its intact transmural transport; D-phenylalanine (D-Phe) at the amino terminal confers stronger resistance to hydrolysis in comparison to other amino acids, e.g. D-alanine. In particular, one dipeptide was shown to possess an extremely efficient resistance to hydrolysis coupled with a substantial rate of transport at both the brush-border membrane (BBM) and the basolateral membrane (BLM), in comparison to the other peptides studied; this was D-phenylalanyl-L-alanine (D-Phe-L-Ala). This dipeptide was therefore used as a substrate backbone with which to synthesise a potential photoaffinity label for the identification of peptide transporters at both the apical and basolateral membranes of rat small intestine.

The dipeptides and the photoaffinity label used in the work contained in this thesis were custom-synthesised using standard techniques (P. D. Bailey, 1990) by Professor P. D. Bailey and Dr. I. Collier in the Chemistry Department of Heriot Watt University, Edinburgh, UK. Briefly, each peptide was created by condensation of the *N*-tertiary-butyl-oxy-carbonyl-derivative of the N-terminal amino acid with the carboxy-benzyl-L-derivative of the C-terminal amino acid. The products were subjected to a series of acid and alkali washes to eliminate starting materials and by-products, prior to removal of the protecting groups. Finally, the samples were freeze-dried and the purity was demonstrated to be >95% by mass spectrometry, NMR and HPLC. For the photoaffinity label, an azide group (N_3) was attached to position 4 on the phenylalanine ring of D-Phe-L-Ala to confer its extreme

photo-reactivity. This, in turn, would permit highly specific labelling of an active site of a protein to which the dipeptide moiety will selectively bind. The chemical structure of the potential photoaffinity label ([4-azido-D-Phe]-L-Ala) is shown in figure 3.1.

3.2 Aims of the experiments

This study utilised the technique of the isolated, *in situ*, luminally and vascularly perfused rat jejunum (abbreviated to 'vascular perfusion' in subsequent text) to demonstrate a highly specific interaction of the photoaffinity label with the peptide transporters in the BBM and BLM. This particular perfusion approach permitted the application of [4-azido-D-Phe]-L-Ala to both sides of the enterocyte, i.e adjacent to either the apical or the basolateral membrane, whilst maintaining the intact jejunum *in situ*. The blood supply to the jejunum was isolated and replaced with a perfusate of a physiological solution containing substrate(s) if required, in parallel with a separate perfusate (± substrates) in the lumen. Transmural transport of [4-azido-D-Phe]-L-Ala itself was measured, in addition to the effect that it had on the transport rate of another dipeptide (D-Phe-L-Gln). Inhibition of the transport of the second peptide would indicate that the potential label can directly interact with the peptide transporter(s). Substrate inhibition would demonstrate that [4-azido-D-Phe]-L-Ala is an effective substrate and therefore likely to be an efficient label with which to identify the membrane proteins responsible for peptide transport in the jejunum.

The primary aim of these experiments was to demonstrate an unequivocal direct interaction of [4-azido-D-Phe]-L-Ala with the peptide transporters so that it could be used to specifically label the membrane protein(s) to aid in their identification and isolation.

3.3 Viability of the vascular perfusions

Previous investigations using the vascular perfusion method (Hanson & Parsons, 1976; Boyd *et al.*, 1975; Nicholls *et al.*, 1983) have demonstrated that it is an extremely reliable technique for the study of substrate transport by the small intestine (see section 1.2.4). In addition, it is the only preparation that permits direct access of substrates to the basolateral membrane of the mucosa from the vasculature,

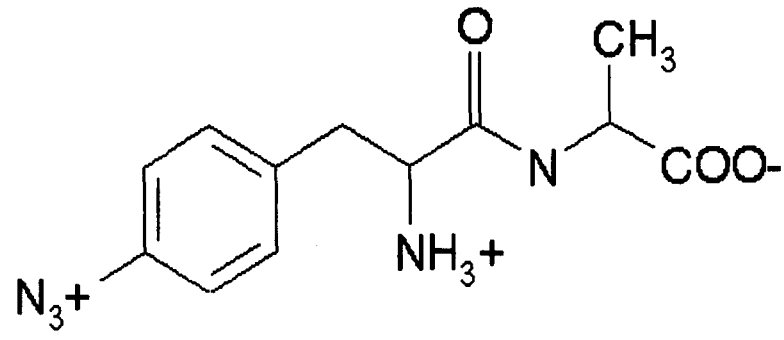

Figure 3.1

Chemical structure of the potential photoaffinity label [4-azido-D-Phe]-L-Ala. For details of synthesis see section 3.1.

in situ. Viability of the intestine subjected to this technique has previously been indicated by an essentially normal histology and absence of oedema in the tissue following the perfusions, in addition to an active transport of substrates and constant oxygen consumption from the vascular perfusate by the intestine during the perfusions.

Rats were starved overnight prior to perfusion and glucose-fed in order to obtain consistent data. Initially, glucose feeding was introduced to lessen the rates of glucose utilisation by the small intestine when rats were maintained on the Bantin & Kingman diet (Kellett & Barker, 1989); however other beneficial effects were soon evident. These advantages included an enhanced sensitivity of the intestine to regulation by endocrine/paracrine mediators and, more importantly, the highly reliable reproducible results that could be obtained.

Viability of the vascular perfusion data included in this thesis was assessed using two factors. Firstly a high portal vein recovery (>90%) of vascular perfusate was achieved. In association with this, a constant vascular flow rate, measured from the portal vein effluent, indicated that the isolated segment of intestine was not under any undue stress. Although a complete (100%) venous recovery was not always attained from a flow rate of 1.5 $ml \cdot min^{-1}$ (pump determined rate), previous investigations (A. Pennington, D Phil thesis, 1992) have demonstrated that flow rates of 1.5 ± 0.2 $ml \cdot min^{-1}$ are acceptable, because the rate of active glucose transfer across the intestine was not affected. Reasons for minor variations in flow rate were not always apparent, but if a continual decline in the portal vein recovery rate was observed, the perfusion was abandoned. A second indication of a viable perfusion was a constant rate of glucose utilisation by the isolated segment of jejunum. This was measured by assaying the glucose concentration remaining in the vascular effluent, after its passage through the mesenteries adjacent to the jejunum, using the GOD-Perid® method performed on the Cobas-MIRA automated analyser. The concentration of glucose remaining in the effluent samples was used to calculate the rate of uptake of glucose by the jejunum, expressed as $\mu mol \cdot min^{-1} \cdot [g \text{ dry wt.}]^{-1}$ (equation 1, section 2.1.9.1). A typical example of glucose uptake during the course of a vascular perfusion with a dipeptide is shown in figure 3.2.

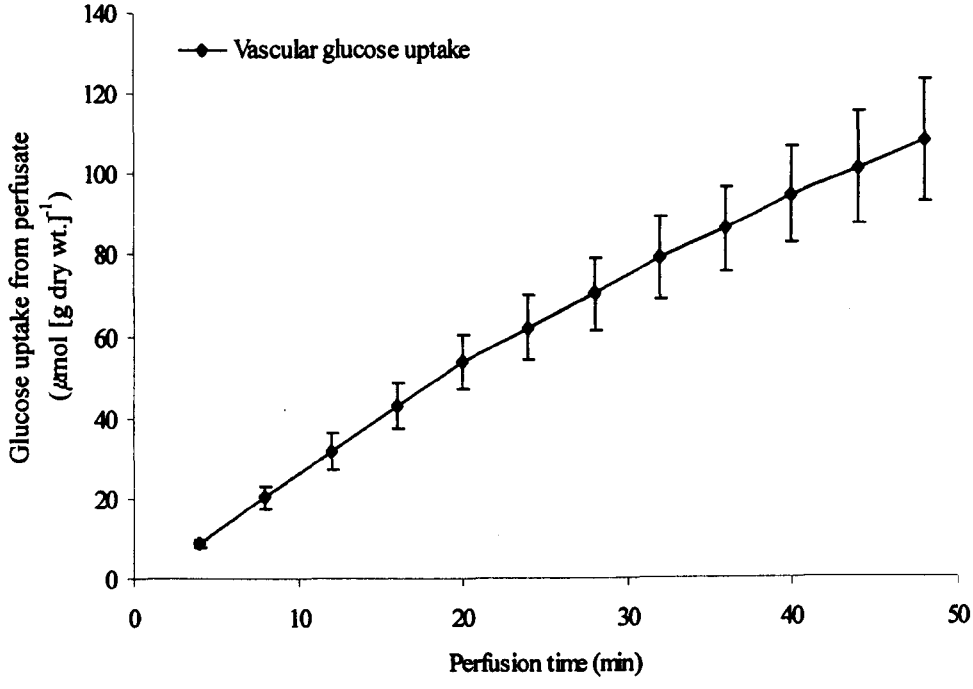

Figure 3.2

A representative time course showing the uptake of glucose from the vasculature during a typical series of vascular perfusions with a dipeptide. Data points represent the mean ± s.e.m. (n = 5). A steady state of uptake was achieved at 15-20 minutes, and so the time period analysed was between 20 and 50 minutes. The rate of glucose uptake for this period is 2.24 ± 0.33 μmol·min^{-1}·[g dry wt.]$^{-1}$.

3.4 Transmural transport of [4-azido-D-Phe]-L-Ala across the jejunum

In order to establish whether it would be worthwhile to develop [4-azido-D-Phe]-L-Ala as a photoaffinity label, initial experiments were performed to investigate if it was accepted as a substrate by the intestinal peptide transporters. This was investigated by determining whether it was transported intact across the intestine, from the lumen to the serosa, at a reasonably efficient rate. Vascular perfusions in which the jejunal lumen was perfused with either D-Phe-L-Gln or [4-azido-D-Phe]-L-Ala, both at a concentration of 1 mM, were conducted. The cumulative rate of dipeptide appearance in the vasculature was measured (which demonstrated transmural transport), together with the accumulation in mucosal and muscle tissues during the perfusion for both substrates. In addition, exit ratios of substrate accumulation/transport were calculated. A summary relating the physiological significance of exit ratios to the activity of peptide transporters and their interaction with substrates is shown in table 3.1.

D-Phe-L-Gln is transported efficiently through the intestine, demonstrated by its rate of intact cumulative appearance in the vascular effluent (0.244 ± 0.022 $\mu mol \cdot min^{-1} \cdot [g\ dry\ wt.]^{-1}$ s.e.m.) (figure 3.3(I)). Previous perfusion studies with D-Phe-L-Gln (Bronk *et al.*, 1995) formed the basis of its utilisation as a representative dipeptide to demonstrate peptide transport through the jejunum *in situ*. Other studies (Lister *et al.*, 1995) had shown that the presence of a D-amino acid at the N-terminal of a mixed dipeptide confers hydolysis resistance, but does not substantially reduce transepithelial transport across rat small intestine *in vitro*. The usefulness of D-Phe-L-Gln was due to its rapid transport rate, relative to other D-amino acid-containing dipeptides, and inherent resistance to hydrolysis both at the apical membrane and within the cytosol.

Transport of the photoaffinity label was compared to D-Phe-L-Gln in order to assess its suitability as a substrate for the peptide transporters. Figure 3.3(I) shows that [4-azido-D-Phe]-L-Ala is transported through the intestine at a rate that is 10-fold faster than that of D-Phe-L-Gln (2.66 ± 0.62 $\mu mol \cdot min^{-1} \cdot [g\ dry\ wt.]^{-1}$, $P < 0.001$). In addition, it accumulates to a lesser extent in the mucosa (4.88 ± 0.93 mM compared to 7.95 ± 0.92 mM, $P < 0.05$), although its muscle concentration is over 2-fold higher (5.68 ± 0.35 mM compared to 2.18 ± 0.35 mM,

EXIT RATIO	PHYSIOLOGICAL SIGNIFICANCE	IMPLICATIONS IN TRANSMURAL TRANSPORT	IMPLICATIONS IN INHIBITION STUDIES
↑	**Peptide accumulates to a high level in the tissue with respect to its transport rate**	**Peptide interacts with PepT1 more efficiently than with BLT**	**(1) Peptide transport is stimulated at the BBM , relative to the BLM** **(2) Peptide transport is inhibited at the BLM, relative to the BBM**
No change	**Peptide accumulates to the same extent in the tissue with respect to its transport rate, i.e. if there is an increase in rate, there is an associated increase in accumulation, and vice versa**	**Peptide interacts with PepT1 and BLT with an equal efficiency**	**Peptide transport occurs to the same degree at both the BBM and BLM**
↓	**Peptide accumulates to a lower extent in the tissue with respect to its transport rate**	**Peptide interacts with BLT more efficiently than with PepT1**	**(1) Peptide transport is stimulated at the BLM, relative to the BBM** **(2) Peptide transport is inhibited at the BBM, relative to the BLM**

Table 3.1
A brief explanation of the tissue exit ratios calculated in the vascular perfusion studies and their physiological relevance in the study of transmural peptide transport of a single substrate and in transport inhibition studies. It should be noted that this is a simplified account of mucosal tissue analysis used to reflect the activities of the peptide transporters at the BBM and BLM. Inclusion of transport rates and actual tissue concentrations gives a more detailed view, but is too complex to be contained in this summary table. BLT; basolateral transporter.

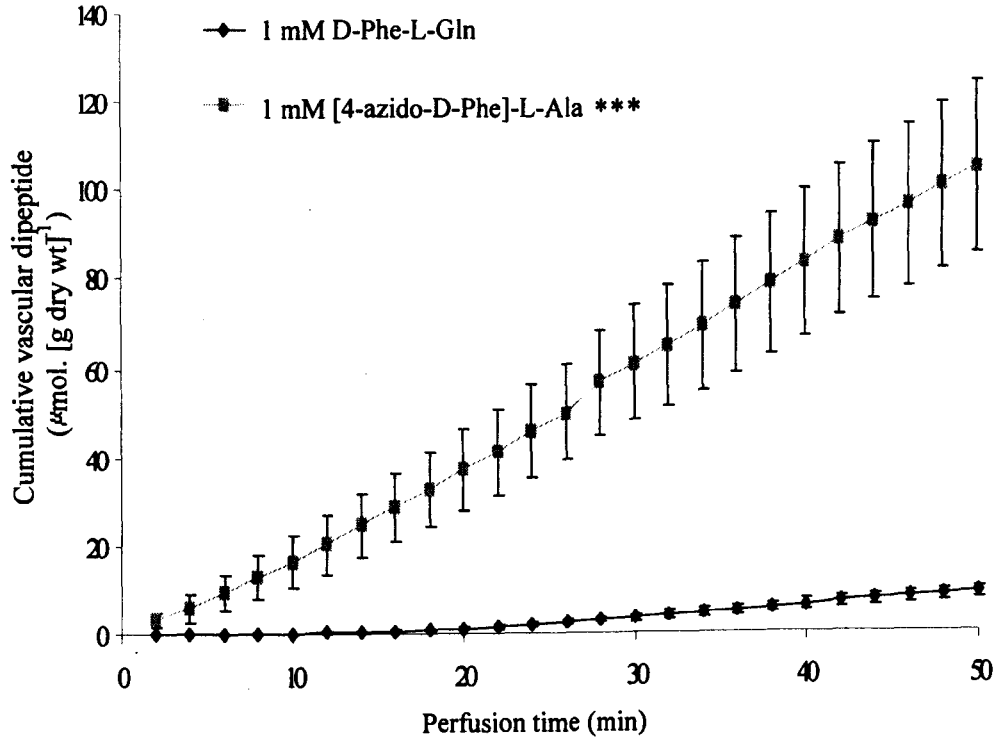

Figure 3.3 (I)

A comparison of the transmural transport rates of D-Phe-L-Gln and [4-azido-D-Phe]-L-Ala, at 1 mM concentration, from the lumen to the serosa of the jejunum. Data points represent the mean ± s.e.m. (n = 5) *** $P < 0.001$ depicts a significant difference in transport rates.

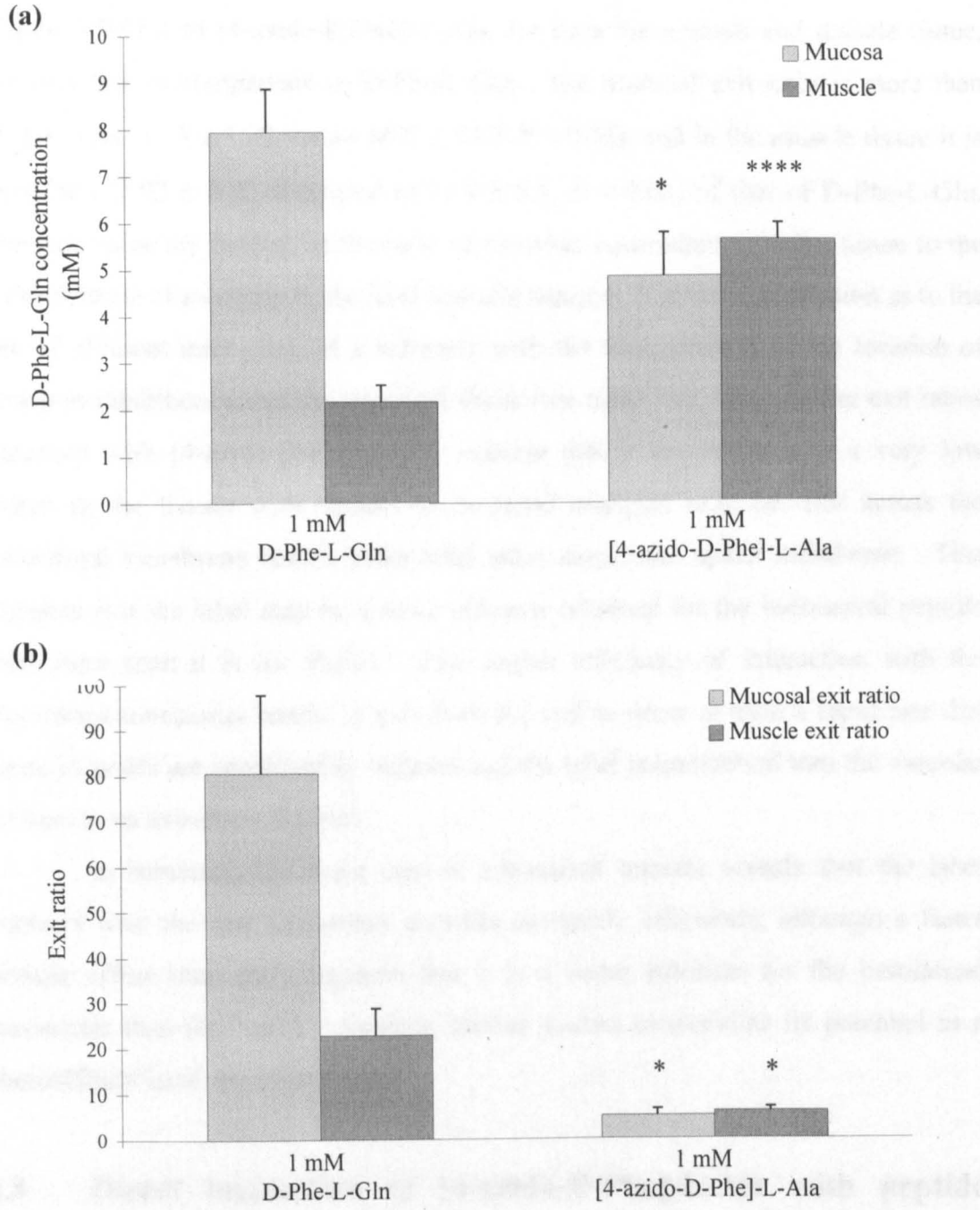

Figure 3.3 (II)

Tissue accumulations (a) and exit ratios (b) of D-Phe-L-Gln and [4-azido-D-Phe]-L-Ala following perfusion, at a concentration of 1 mM, from the lumen to the serosa of the jejunum (see figure 3.3 (I)). Bars represent the mean ± s.e.m. (n = 5). * $P < 0.05$, **** $P < 0.0001$ depict significant differences.

$P < 0.0001$), than that observed with D-Phe-L-Gln (figure 3.3(IIa)). The exit ratios (figure 3.3(IIb)) of [4-azido-D-Phe]-L-Ala, for both the mucosa and muscle tissue, are very low in comparison to D-Phe-L-Gln. The mucosal exit ratio is more than 15-fold less (5.15 ± 1.33 versus 80.7 ± 17.2 $P < 0.05$), and in the muscle tissue it is only 26% (5.93 ± 0.82 compared to 22.8 ± 5.9, $P < 0.05$) of that of D-Phe-L-Gln. The exit ratios are defined as the ratio of substrate concentration in the tissue to the concentration of substrate in the final vascular sample. It gives an indication as to the site of efficient interaction of a substrate with the transporter(s) or the location of transport inhibition within the intestinal tissue (see table 3.1). The smaller exit ratios observed with [4-azido-D-Phe]-L-Ala indicate that it accumulates to a very low extent in the tissues with respect to its rapid transport rate, i.e. exit across the basolateral membrane occurs faster than entry across the apical membrane. This suggests that the label may be a more efficient substrate for the basolateral peptide transporter than it is for PepT1. This higher efficiency of interaction with the basolateral transporter results in exit from the cell to occur at such a rapid rate that mucosal levels are considerably reduced and the label is transferred into the vascular effluent at an extremely fast rate.

In summary, the rapid rate of transmural transfer reveals that the label interacts with the two transporter proteins extremely efficiently, although a faster cellular efflux than entry suggests that it is a better substrate for the basolateral transporter than for PepT1. As such, further studies to elucidate its potential as a photoaffinity label were performed.

3.5 Direct interaction of [4-azido-D-Phe]-L-Ala with peptide transporters

Initial perfusions have demonstrated that the label is transported across the enterocyte intact and at a considerable rate to suggest it is an effective substrate for both intestinal peptide transporters. This work was progressed to show a direct interaction of the label with the membrane proteins responsible for peptide transport. This was achieved by performing transport inhibition studies in which the jejunal lumen was perfused with a substrate (1 mM D-Phe-L-Gln, the control) in conjunction with the label, which was included in either the luminal or the vascular perfusate at a concentration of 2.5 mM. Inhibition of D-Phe-L-Gln transport in the presence of

[4-azido-D-Phe]-L-Ala would indicate a direct interaction of the label with the peptide transporters, due to substrate-specific competition for the binding site. The results from these perfusions are shown in figure 3.4 (I & II).

Addition of the label to the vasculature has no effect on the basic rate of D-Phe-L-Gln transport (0.234 ± 0.025 compared to 0.244 ± 0.022 $\mu mol \cdot min^{-1} \cdot [g\ dry\ wt.]^{-1}$) (figure 3.4 (I)), nor is there any change evident in substrate accumulation in mucosal or muscle tissue (figure 3.4 (II). However, if the label is perfused through the lumen of the jejunum, in conjunction with the substrate, a significant reduction in the rate of D-Phe-L-Gln transport is observed (0.146 ± 0.016 $\mu mol \cdot min^{-1} \cdot [g\ dry\ wt.]^{-1}$ versus control, $P < 0.001$). This is associated with an enhanced accumulation of substrate in the mucosal layer (12.8 ± 1.44 mM versus control, $P < 0.05$). A relatively larger mucosal exit ratio, although not statistically significant, supports the detected increased mucosal concentration of substrate, with respect to the substantially lower transport rate. Collectively, these results indicate that the label does not inhibit basolateral exit of the substrate from the cell by interaction with an extracellular site of the membrane protein. Inhibition of transport following inclusion of the label in the lumen might implicate PepT1, but an increased level of substrate in the mucosa indicates that inhibition is occurring at the endofacial site of the basolateral transporter more predominantly than at the apical membrane. Competition of the label with the substrate for the same intracellular active site of the basolateral transporter therefore prevents exit of the substrate from the cell. Thus, there seems to be an asymmetry in binding of the label to the basolateral transporter.

These findings were further investigated by performing washout experiments using the 'perturbation' method in which the intestine is loaded with substrate from the lumen and its washout into the vascular bed is monitored (Boyd & Parsons, 1978). During the initial 30 min of these perfusions, the lumen of the intestine was perfused with 1 mM D-Phe-L-Gln and then the substrate was removed from the solution and the perfusion continued with a substrate-free medium for an additional 30 min (figure 3.5). In the inhibition experiment, [4-azido-D-Phe]-L-Ala was perfused through the vasculature at a concentration of 2.5 mM from the 30 min time point, when the substrate was removed, for the remaining 30 min to determine whether its presence would inhibit washout of the substrate into the vascular effluent. The vascular appearance of substrate per min was measured throughout the 60 min

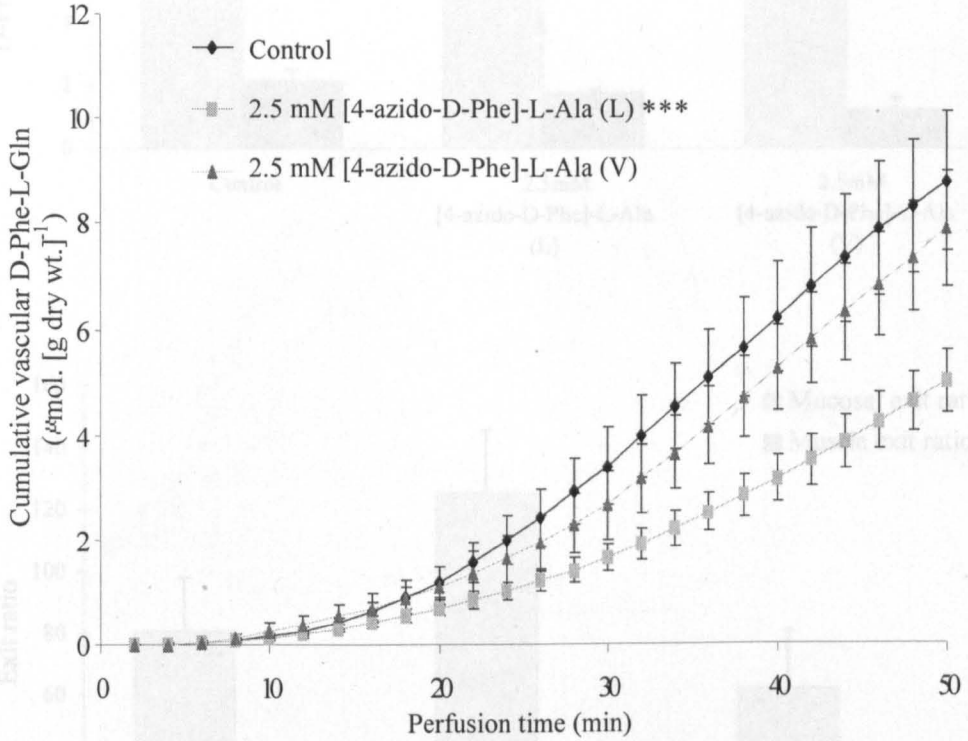

Figure 3.4 (I)

Direct interaction of [4-azido-D-Phe]-L-Ala with intestinal peptide transporters as demonstrated by its effect (at 2.5 mM) on the transmural transport rate of 1 mM D-Phe-L-Gln (control) from the lumen to the serosa. Data points represent the mean ± s.e.m. (n = 5). *** $P < 0.001$ depicts a significant difference in transport rate against the control.

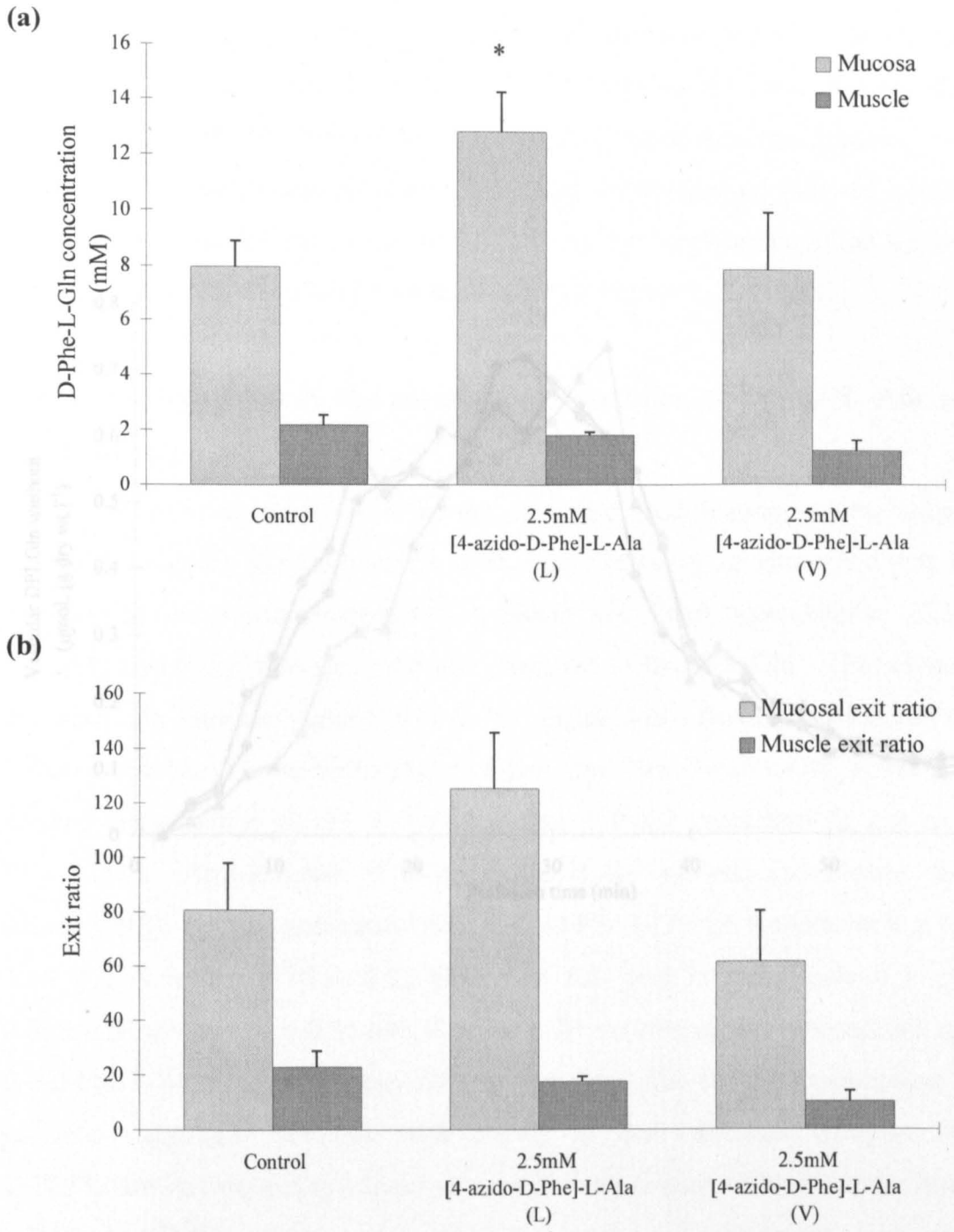

Figure 3.4 (II)

Effect of [4-azido-D-Phe]-L-Ala, present at 2.5 mM in either the lumen or the vasculature of the jejunum, on tissue accumulation (a) and exit ratio (b) of D-Phe-L-Gln following vascular perfusion at 1 mM from the lumen to the serosa of the jejunum. Bars represent the mean ± s.e.m. (n = 5). * $P < 0.05$ depicts a significant difference against the control.

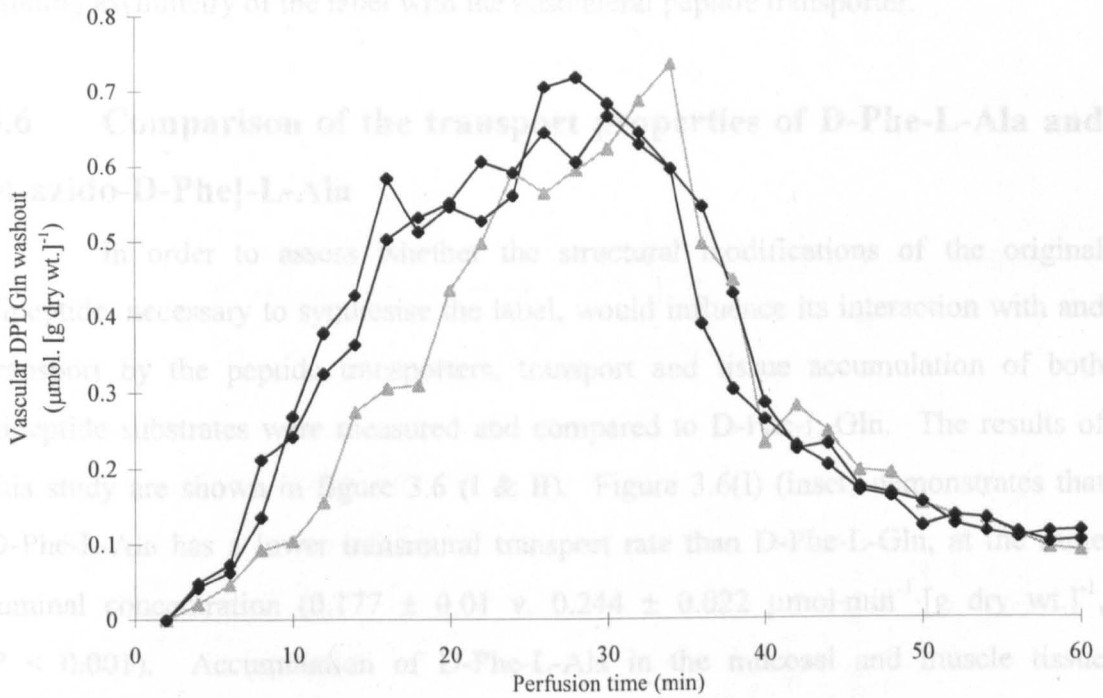

Figure 3.5

Perturbation experiments demonstrating that [4-azido-D-Phe]-L-Ala does not inhibit substrate mucosal efflux when presented to the serosal face of the basolateral membrane. 1mM D-Phe-L-Gln was perfused through the lumen from 0-30 min and then removed from the perfusate (control; diamonds) for the remaining 30 min. Inhibition of substrate efflux into the serosa was investigated by perfusing [4-azido-D-Phe]-L-Ala at a concentration of 2.5 mM through the vasculature from 30-60 min (triangles).

perfusion of the two conditions and the results are shown in figure 3.5. It is evident from these perfusions that the presence of the label on the vascular side of the intestine has no effect on the washout of a second dipeptide from the mucosa.

This evidence (see figure 3.5) strengthens the conclusions from the results of the previous vascular perfusions and reinforces the implication of an apparent binding asymmetry of the label with the basolateral peptide transporter.

3.6 Comparison of the transport properties of D-Phe-L-Ala and [4-azido-D-Phe]-L-Ala

In order to assess whether the structural modifications of the original dipeptide, necessary to synthesise the label, would influence its interaction with and transport by the peptide transporters, transport and tissue accumulation of both dipeptide substrates were measured and compared to D-Phe-L-Gln. The results of this study are shown in figure 3.6 (I & II). Figure 3.6(I) (inset) demonstrates that D-Phe-L-Ala has a lower transmural transport rate than D-Phe-L-Gln, at the same luminal concentration (0.177 ± 0.01 v. 0.244 ± 0.022 $\mu mol \cdot min^{-1} \cdot [g\ dry\ wt.]^{-1}$, $P < 0.001$). Accumulation of D-Phe-L-Ala in the mucosal and muscle tissue (figure 3.6(II)) is also significantly lower than D-Phe-L-Gln (in the mucosa it is only 3.16 ± 0.59 mM v. 7.95 ± 0.92 mM, $P < 0.01$ and in the muscle it is only 0.56 ± 0.07 mM v. 2.18 ± 0.35 mM, $P < 0.01$). The corresponding mucosal exit ratio for D-Phe-L-Ala is approximately 50% of that for D-Phe-L-Gln, corroborating the previous suggestion that that with respect to their different transport rates D-Phe-L-Ala accumulates to a lesser extent within the tissue. Collectively the results indicate that D-Phe-L-Ala is a less efficient substrate for both peptide transporters than D-Phe-L-Gln, but this may be more pronounced at the apical membrane, resulting in the overall lower rate of transport.

A comparison of the original dipeptide (D-Phe-L-Ala) and the peptide-derivative label shows that D-Phe-L-Ala is transported at a much lower rate than [4-azido-D-P]-L-Ala (0.177 ± 0.01 v. 2.657 ± 0.279 $\mu mol \cdot min^{-1} \cdot [g\ dry\ wt.]^{-1}$, $P < 0.001$). In conjunction with this is a similar mucosal concentration of substrate (3.16 ± 0.59 mM v. 4.88 ± 0.93 mM) coupled with a significantly higher mucosal exit ratio (38.9 ± 5.8 v. 5.15 ± 1.33, $P < 0.01$). This suggests that D-Phe-L-Ala is accumulating to a larger extent in the mucosa than the label, with respect to its

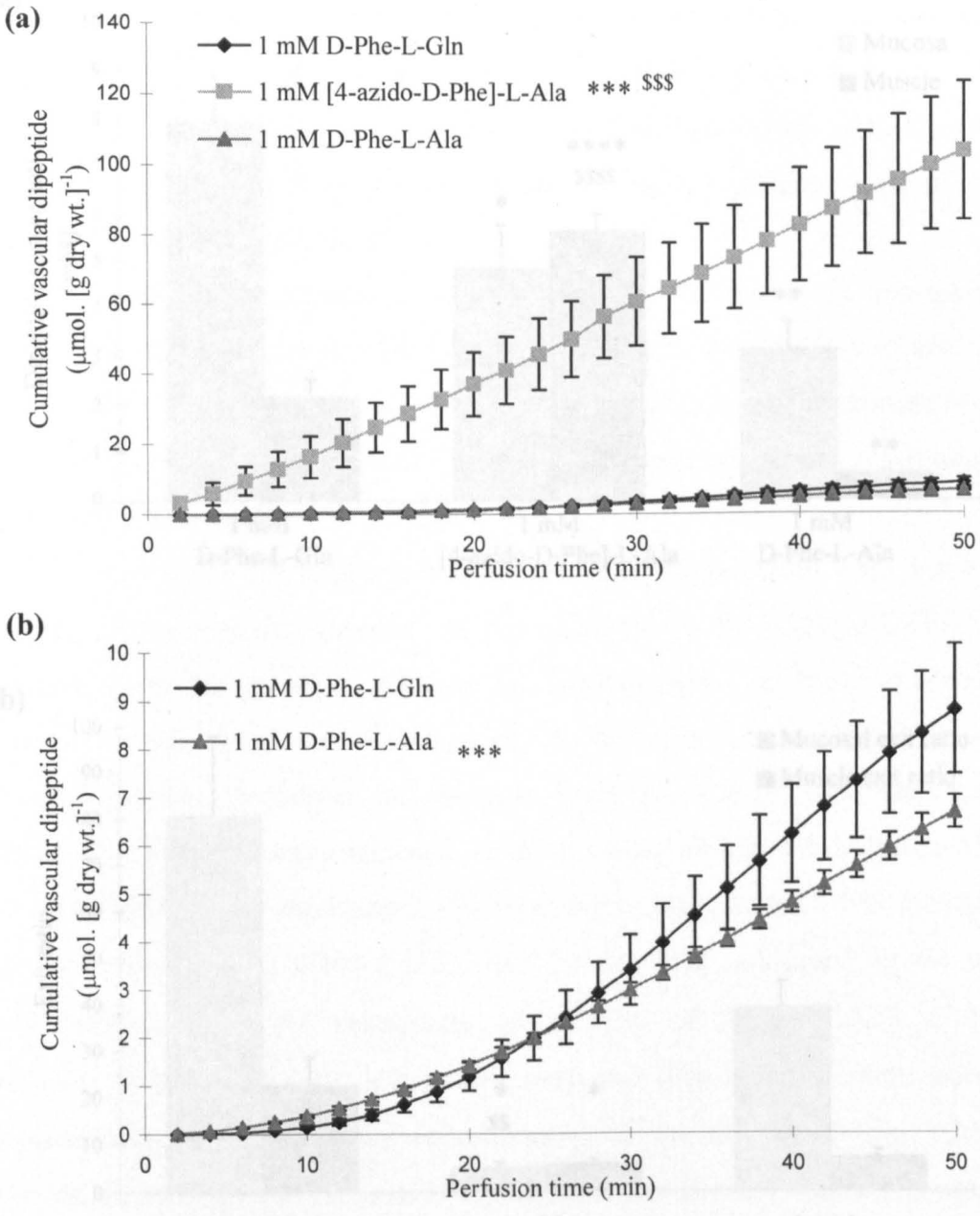

Figure 3.6 (I)

A comparison of the transmural transport rates of D-Phe-L-Gln, D-Phe-L-Ala and [4-azido-D-Phe]-L-Ala, at 1 mM concentration, from the lumen to the serosa of the jejunum. Data points represent the mean ± s.e.m. (n = 5). *** $P < 0.001$ and $^{\$\$\$}$ $P < 0.001$ depict a significant difference in transport rate against 1 mM D-Phe-L-Gln and D-Phe-L-Ala, respectively.

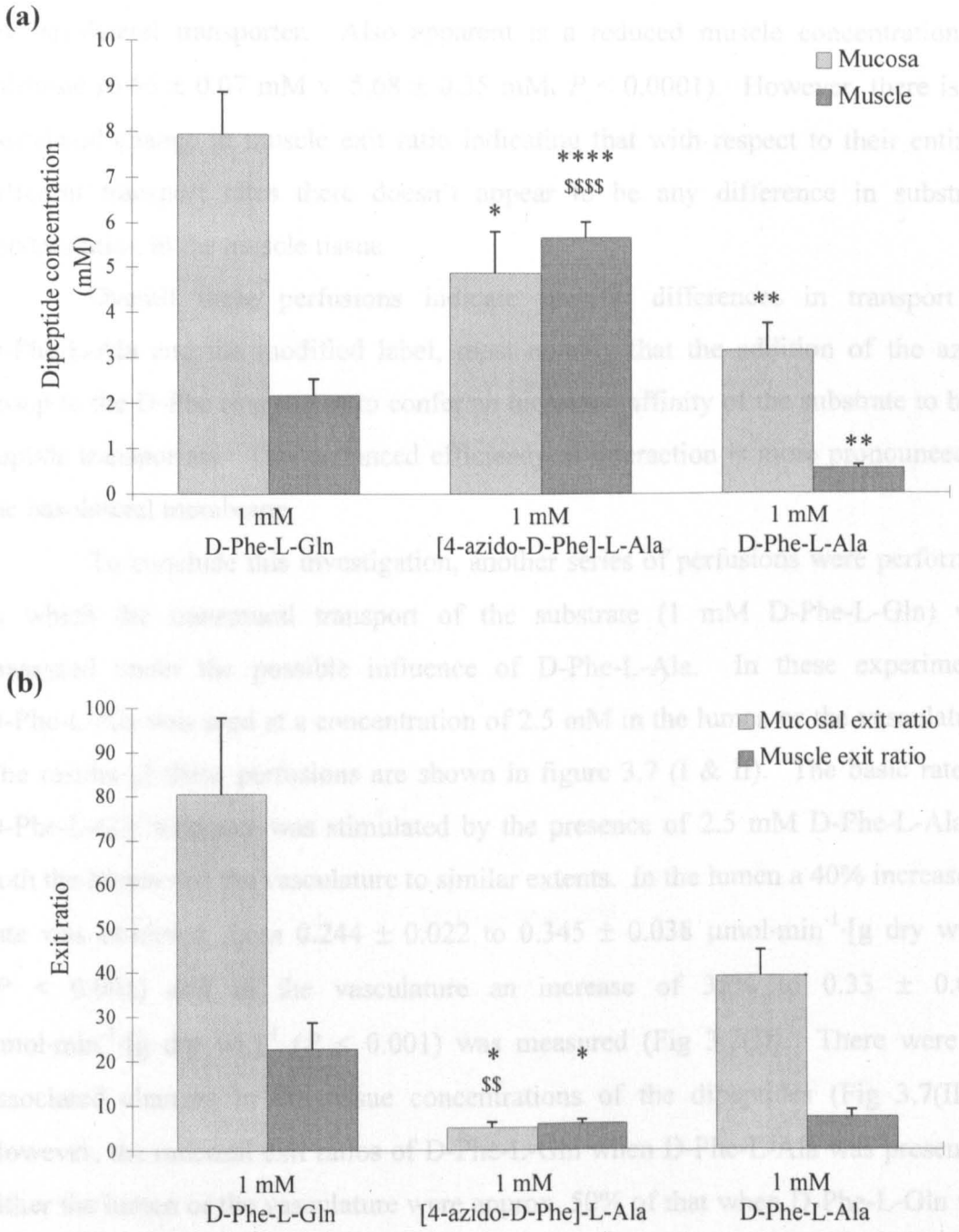

Figure 3.6 (II)

Tissue accumulations (a) and exit ratios (b) of D-Phe-L-Gln, D-Phe-L-Ala and [4-azido-D-Phe]-L-Ala following perfusion, at a concentration of 1 mM, from the lumen to the serosa of the jejunum (see figure 3.6 (I)). Bars represent the mean ± s.e.m. (n = 5). * $P < 0.05$, ** $P < 0.01$, **** $P < 0.0001$, and $^{\$\$}$ $P < 0.01$, $^{\$\$\$\$}$ $P < 0.0001$, depict significant differences against 1 mM D-Phe-L-Gln and 1 mM D-Phe-L-Ala, respectively.

considerably lower rate of transport, implying it has a lower level of interaction with the basolateral transporter. Also apparent is a reduced muscle concentration of substrate (0.56 ± 0.07 mM v. 5.68 ± 0.35 mM, $P < 0.0001$). However, there is no associated change in muscle exit ratio indicating that with respect to their entirely different transport rates there doesn't appear to be any difference in substrate accumulation in the muscle tissue.

Overall these perfusions indicate specific differences in transport of D-Phe-L-Ala and the modified label, most notably that the addition of the azide group to the D-Phe ring seems to confer an increased affinity of the substrate to both peptide transporters. This enhanced efficiency of interaction is more pronounced at the basolateral membrane.

To conclude this investigation, another series of perfusions were performed in which the transmural transport of the substrate (1 mM D-Phe-L-Gln) was measured under the possible influence of D-Phe-L-Ala. In these experiments D-Phe-L-Ala was used at a concentration of 2.5 mM in the lumen or the vasculature. The results of these perfusions are shown in figure 3.7 (I & II). The basic rate of D-Phe-L-Gln transport was stimulated by the presence of 2.5 mM D-Phe-L-Ala in both the lumen and the vasculature to similar extents. In the lumen a 40% increase in rate was observed, from 0.244 ± 0.022 to 0.345 ± 0.038 $\mu mol \cdot min^{-1} \cdot [g\ dry\ wt.]^{-1}$ ($P < 0.001$) and in the vasculature an increase of 35% to 0.33 ± 0.036 $\mu mol \cdot min^{-1} \cdot [g\ dry\ wt.]^{-1}$ ($P < 0.001$) was measured (Fig 3.7(I)). There were no associated changes in the tissue concentrations of the dipeptides (Fig 3.7(IIa)). However, the mucosal exit ratios of D-Phe-L-Gln when D-Phe-L-Ala was present in either the lumen or the vasculature were approx. 50% of that when D-Phe-L-Gln was perfused alone (Fig 3.7(IIb)), although not significant. This indicates that the effect of D-Phe-L-Ala, present either in the lumen or the vasculature, was to stimulate peptide exit from the mucosa across the basolateral membrane.

It was initially assumed that D-Phe-L-Ala may have an inhibitory effect on D-Phe-L-Gln transport because, although it has been shown to be a relatively less efficient substrate for both transporters, they share the same system and would therefore be competing for the same active site(s). But this is not the case. The increase in transmural transport rate without a corresponding increase in tissue levels suggests that D-Phe-L-Ala may be stimulating D-Phe-L-Gln transport at both the

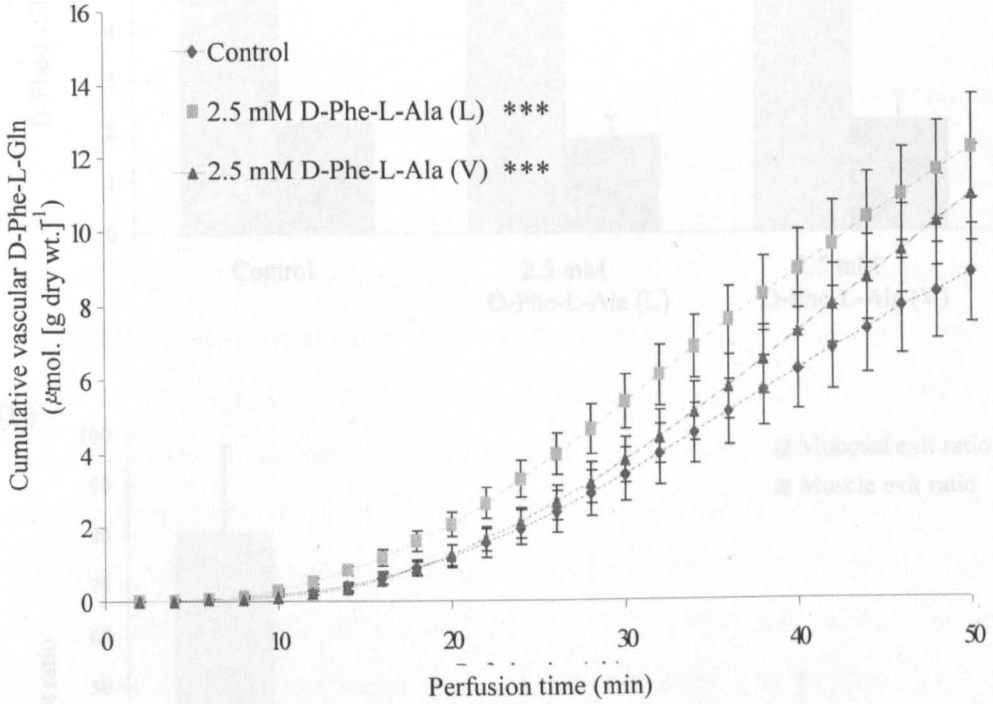

Figure 3.7 (I)

Effect of D-Phe-L-Ala, present at 2.5 mM in either the lumen or the vasculature of the jejunum, on the transmural transport rate of 1 mM D-Phe-L-Gln from the lumen to the serosa. Data points represent the mean ± s.e.m. (n = 5). *** $P < 0.001$ depicts significant differences against the control (1 mM D-Phe-L-Gln).

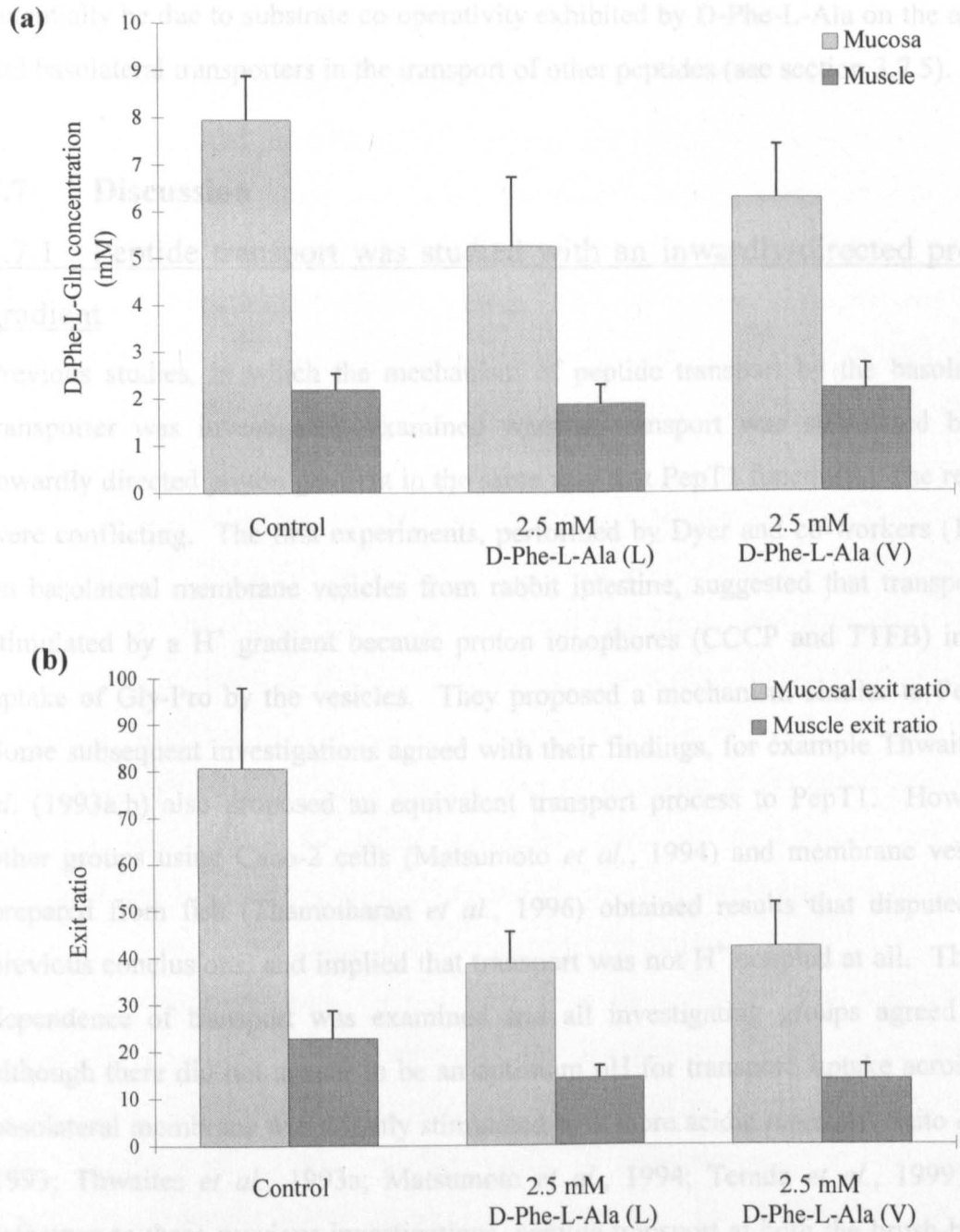

Figure 3.7 (II)

Effect of D-Phe-L-Ala, present at 2.5 mM in either the lumen or vasculature of the jejunum, on tissue accumulation (a) and exit ratio (b) of D-Phe-L-Gln following vascular perfusion at 1 mM from the lumen to the serosa of the jejunum. Bars represent the mean ± s.e.m. (n = 5).

apical and basolateral membrane to the same degree. This stimulation in rate may potentially be due to substrate co-operativity exhibited by D-Phe-L-Ala on the apical and basolateral transporters in the transport of other peptides (see section 3.7.5).

3.7 Discussion

3.7.1 Peptide transport was studied with an inwardly-directed proton gradient

Previous studies, in which the mechanism of peptide transport by the basolateral transporter was investigated, examined whether transport was stimulated by an inwardly directed proton gradient in the same way that PepT1 functions. The results were conflicting. The first experiments, performed by Dyer and co-workers (1990) on basolateral membrane vesicles from rabbit intestine, suggested that transport is stimulated by a H^+ gradient because proton ionophores (CCCP and TTFB) inhibit uptake of Gly-Pro by the vesicles. They proposed a mechanism similar to PepT1. Some subsequent investigations agreed with their findings, for example Thwaites *et al.* (1993a,b) also proposed an equivalent transport process to PepT1. However, other groups using Caco-2 cells (Matsumoto *et al.*, 1994) and membrane vesicles prepared from fish (Thamotharan *et al.*, 1996) obtained results that disputed the previous conclusions, and implied that transport was not H^+ coupled at all. The pH dependence of transport was examined and all investigating groups agreed that, although there did not appear to be an optimum pH for transport, uptake across the basolateral membrane was slightly stimulated by a more acidic medium (Saito *et al.*, 1993; Thwaites *et al.*, 1993a; Matsumoto *et al.*, 1994; Terada *et al.*, 1999). In reference to these previous investigations, peptide transport at both the brush-border and basolateral membrane was studied, using the vascular perfusion technique, in the presence of an inwardly directed H^+ gradient. The solutions used to perfuse the lumen of the intestine and its adjacent vasculature were of a slightly acidic pH of 6.8, which created the proton gradient, whilst keeping the perfusate medium physiologically viable.

3.7.2 Interaction of the photoaffinity label with PepT1 and the basolateral transporter

Vascular perfusions demonstrated that the photoaffinity label is transported at an extremely rapid rate through the intestine as a whole, with respect to the other D-amino acid-containing peptides used in this study. As such, it appears to be a very effective substrate for the peptide transporter proteins located in both the apical and basolateral membranes. In addition, the label does not accumulate in mucosal tissue to a significant level, although a high concentration was observed in muscle, which suggests that it interacts with the basolateral transporter protein with an even greater efficiency than it does with PepT1.

Additional perfusions examining substrate inhibition between D-Phe-L-Gln and [4-azido-D-Phe]-L-Ala have demonstrated that the label does not inhibit peptide transport from the serosal side of the basolateral membrane. However, an increased mucosal accumulation of D-Phe-L-Gln implies that it does inhibit transport at the endofacial surface of the basolateral transporter to a relatively higher degree than a potentially lower level of inhibition that may be occurring at the apical membrane. Transport inhibition at the apical membrane cannot be seen directly with this technique due the overwhelming inhibition observed at the basolateral membrane. However, its occurrence should not be completely discounted.

Investigations with Caco-2 cells have demonstrated that inhibition on cellular uptake of substrates by various peptide-like compounds is more pronounced at the apical membrane in comparison to the basolateral membrane (Saito *et al.*, 1993; Terada *et al.*, 1999). In other words, the substrates seem to have a lower affinity for the serosal face of the basolateral transporter than they do for the luminal surface of PepT1. In addition, kinetic analysis of the basolateral transporter and PepT1 has shown that all the substrates studied had a lower K_m and higher V_{max} for PepT1 (Saito *et al.*, 1993; Matsumoto *et al.*, 1994; Terada *et al.*, 1999). Therefore, it appears that the basolateral transporter has a lower affinity and lower capacity for peptide uptake into the cell from the extracellular medium, in contrast to a higher affinity and capacity when performing the role of peptide transfer out of the cell (Inui *et al.*, 1992), although this area is not absolutely clear and is disputed by other groups (Thwaites *et al.*, 1993b), who state that the opposite is true. A conceivable explanation as to why transport inhibition by [4-azido-D-Phe]-L-Ala was not seen

when included in the vascular perfusate (asymmetric interaction) is described in section 3.7.3.

In contrast to basolateral uptake, PepT1 has a higher capacity for solute transport into the cell. This may form the basis for a possible explanation as to why the label isn't seen to inhibit D-Phe-L-Gln transport at the brush-border membrane, i.e. both substrates may be transported simultaneously without any deleterious effects on their rates. Or, as mentioned previously, inhibition may be occurring but cannot be detected due to the scale of inhibition located at the basolateral membrane. Despite the fact that transport inhibition at the brush-border could not be directly observed, it should not be concluded that the label does not interact with PepT1 (its efficient binding is proven by its rapid transmural transfer rate). In addition, previous experiments with PepT1-expressing *Xenopus* oocytes (Boyd *et al.*, personal communication) demonstrated significant inhibition of D-Phe-L-Gln transport by [4-azido-D-Phe]-L-Ala. As such, [4-azido-D-Phe]-L-Ala is an extremely effective substrate but its presence may be required in a higher concentration in order to observe any inhibitory effects at the apical membrane that can be detected over-and-above the inhibition that is occurring at the basolateral membrane.

If the 'transport capacity' theory is extrapolated to the basolateral membrane, wherein the transporter has a lower affinity and capacity for transport in comparison to PepT1, D-Phe-L-Gln transport would be impaired by the excess presence of the label. The label has been shown to be a more efficient substrate for the basolateral transporter than D-Phe-L-Gln and will therefore predominantly bind and its own transport will override that of D-Phe-L-Gln.

3.7.3 Asymmetrical binding of [4-azido-D-Phe]-L-Ala to the basolateral peptide transporter

There is an asymmetry in binding of [4-azido-D-Phe]-L-Ala to the basolateral peptide transporter, i.e. it inhibits D-Phe-L-Gln transport when present at the endofacial side of the protein but not when at its exofacial surface. This is demonstrated by studies whereby the presence of [4-azido-D-Phe]-L-Ala in the luminal perfusate caused a 40% reduction in rate of D-Phe-L-Gln transport coupled with a considerable increase in mucosal tissue concentration, indicating that peptide transport was predominantly inhibited at an intracellular site of the basolateral

transporter. In contrast, [4-azido-D-Phe]-L-Ala had no effect on the rate of D-Phe-L-Gln transport or on its accumulation in the tissues when included in the vascular perfusate. This lack of effect was reinforced by the perturbation experiments, in which the presence of [4-azido-D-Phe]-L-Ala on the serosal side of the intestine did not affect the washout of D-Phe-L-Gln from the intestine.

Previous investigations using Caco-2 cells have shown that efflux across the basolateral membrane occurs at a much faster rate than uptake into the cell across this membrane (Inui *et al.*, 1992), although other groups state that uptake exceeds exit (Thwaites *et al.*, 1993b). Other studies have demonstrated that uptake across the basolateral membrane is lower than uptake across the BBM, (Saito *et al.*, 1993; Thwaites *et al.*, 1993a, b; Terada *et al.*, 1999) and that efflux across the BLM exceeds exit by the BBM (Inui *et al.*, 1992; Matsumoto *et al.*, 1994). In addition, these groups have also shown that the direction of transmural transport is important. Transport from the BBM to the BLM (corresponding to the absorptive process *in vivo*) occurs preferentially in the enterocyte as opposed to the reverse (Inui *et al.*, 1992; Saito *et al.*, 1993; Thwaites *et al.*, 1993b). Nevertheless, net secretion of peptides by the intestine can occur under optimal conditions. Collectively, this information can be used to explain the asymmetry in binding of the label to the basolateral transporter. For example, the perfusion data imply that the label has a very low affinity for the basolateral transporters extracellular surface, but this may not actually be the case. Uptake by the basolateral membrane has been previously demonstrated to be lower than efflux (Inui *et al.*, 1992). This suggests that the label isn't unable to interact with the active site on the exofacial surface; a higher concentration of the label may be required to observe an inhibition of substrate transport that is predominantly occurring more rapidly in the opposite (absorptive) direction. In other words, the asymmetrical interaction of the label with the basolateral transporter, indicated by this data, correlates with the unidirectionality of the absorptive process; it binds with higher affinity to the transporters endofacial active site, to which peptides bind during their exit from the enterocyte into the bloodstream.

3.7.4 Modifications to the D-Phe-L-Ala structure confers an increased affinity for the peptide transporters

Pursuing the observed differences in transport rate of D-Phe-L-Gln and the potential photoaffinity label, it was decided to determine whether the modification to the D-Phe-L-Ala structure performed for label synthesis alters its interaction with the transporters. D-Phe-L-Ala was perfused through the lumen at 1 mM concentration and its transport rate and accumulation was compared with that of D-Phe-L-Gln and the label (Fig. 3.6 (I & II)). D-Phe-L-Ala is transported at a lower rate than D-Phe-L-Gln and accumulates to a lesser extent in the jejunal tissue layers. Reduced exit ratios, coupled with a lower rate of transport, implies that D-Phe-L-Ala is probably a less effective substrate for both transporters, although this is more pronounced at the apical membrane due to entry at a lower rate. However, this may be coupled with, to a certain extent, that D-Phe-L-Ala is a better substrate than D-Phe-L-Gln for the basolateral transporter and exits the cell more rapidly once inside. The rate of D-Phe-L-Ala transport is also considerably less than that of the azide label (more so than compared to D-Phe-L-Gln). However, exit ratios demonstrate that its mucosal accumulation is much higher when taking into account their respective transport rates. Therefore, the addition of the positively charged azide group to D-Phe-L-Ala appears to increase its affinity for the peptide transporters, most notably at the basolateral membrane. This must be due to their charge differences because the azide group is very small and would not have any effect on transport on the spacial arrangement of the substrate, as the transporters have been shown to accept an extremely diverse range of substrates of various shapes and sizes.

A few studies have been published which have scrutinised the effects of charge on the transport of dipeptides. A general conclusion is that anionic and zwitterionic peptides are transported more efficiently at a pH of approx. 5.5, whereas transport of cationic peptides is maximised at a slightly higher pH ~6.5 (Temple *et al.*, 1995; Wenzel *et al.*, 1996; Steel *et al.*, 1997; Amasheh *et al.*, 1997). Therefore, differently charged substrates have different pH dependences/optima. These variations in transport rate at different pHs are thought to be due to a difference in affinity of the substrate for the transporter rather than the transporter's intrinsic activity (Steel *et al.*, 1997). The same studies have demonstrated that differently

charged peptides have distinct flux-coupling ratios for H^+-mediated transport. Anionic peptides are transported in conjunction with two protons, whereas neutral peptides are coupled with one proton and cationic peptides also with one proton, if any at all. In this way H^+ dependence is not fixed but rather depends on the charge carried by the transported peptide. As such, the total charge translocated into the cell remains constant despite the varying anionic, neutral or cationic nature of the substrate itself. PepT1 has two histidine residues (His_{57} and His_{121}) located on transmembrane domains 2 and 4, respectively; protonation of both residues is essential for the transporter to bind anionic peptides and this does not occur unless $pH_o < 6.5$ (Temple *et al.*, 1995). Transport of a neutral peptide requires a single residue to be protonated but a cationic peptide can bind in the absence of an associated H^+. Temple *et al.* (1996) proposed a model for the binding of substrate and H^+ for PepT1 that stated that the empty carrier is negatively charged (C^-). The charged state of the carrier is entirely dependent on the external pH, i.e. when pH_o is 7.4 the empty carrier is returned to the external surface of the membrane with a negative charge (C^-) but if pH_o is 5.5 the carrier is returned in a neutral state (C^-H^+). It is therefore evident that cationic peptides would bind more efficiently at a higher pH than neutral peptides. The study also states that H^+ binding is rate limiting for transport, not the return of the empty carrier to the external surface. Collectively these studies suggest that at pH 6.8 (the pH of the perfusate medium used in vascular perfusions) the positively charged [4-azido-D-Phe]-L-Ala would be transported more efficiently than the zwitterionic D-Phe-L-Gln or D-Phe-L-Ala because it doesn't necessarily require co-binding of a proton. This possible higher affinity for the transporter(s) may form the basis for the more rapid transfer rate. It isn't known what causes a faster transport rate at the basolateral membrane due to a lack of knowledge in that area. However, the studies previously mentioned (Dyer *et al.*, 1990; Thwaites *et al.*, 1993a, b; Saito *et al.*, 1993; Terada *et al.*, 1999) imply that basolateral transport could be H^+-coupled and so the same process may also occur in this membrane.

3.7.5 Stimulation of substrate transport by D-Phe-L-Ala

The results obtained when investigating the effects of D-Phe-L-Gln transport in the presence of D-Phe-L-Ala (Fig. 3.7 (I & II)) were suprising. It appears

that absence of the azido group on the D-Phe ring confers an innate ability to stimulate D-Phe-L-Gln transport through the intestine, or rather the addition of the azido group to D-Phe-L-Ala diminishes this stimulatory ability and converts the peptide structure into an inhibitor. Stimulation of transmural D-Phe-L-Gln transport by D-Phe-L-Ala is similarly observed when D-Phe-L-Ala is present in either the lumen or the vasculature of the jejunum. But, there are no corresponding changes in tissue concentrations of substrate. The first observation made from the perfusion data is that, although the label, at a concentration of 2.5 mM, doesn't appear to interact with the exofacial surface of the basolateral transporter, it seems as though D-Phe-L-Ala can.

It was expected that D-Phe-L-Ala would inhibit D-Phe-L-Gln transport in the same way that the label does, because both dipeptides would be competing for the same active site on the membrane protein(s). However, D-Phe-L-Ala appears to be enhancing transport of D-Phe-L-Gln at both the apical and the basolateral membrane (the stimulation being more predominant at the basolateral membrane, implied by smaller exit ratios). The process by which one molecule stimulates binding of another distinct molecule to an enzyme can be classified as allosteric control. An allosteric enzyme, which can be stimulated in this way, is described as exhibiting 'positive substrate cooperativity'. In this process, at low substrate concentrations only a few substrate molecules bind to the enzyme's active site (with relatively poor affinity), but as more substrate binds, the positive cooperativity effect increases the ability of the enzyme to bind additional substrate by increasing its affinity. An allosteric activator decreases the level of cooperativity required, by reducing the K_m, and therefore acts to increase substrate binding. An indication that an enzyme is under allosteric control is that a sigmoidal curve is formed when plotting a graph of substrate concentration against its activity. To determine whether this was true with peptide transporters, the rate of D-Phe-L-Gln transfer to the vasculature was measured at different luminal concentrations. The results of this are shown in figure 3.8. It is evident that there is a sigmoidal (or S-shaped) curve depicting transport rate when the substrate is D-Phe-L-Gln.

The process by which D-Phe-L-Ala stimulates D-Phe-L-Gln transport at both the apical and basolateral membrane may be a factor of allosteric control of the peptide transporters. This control appears to be more predominant at the basolateral

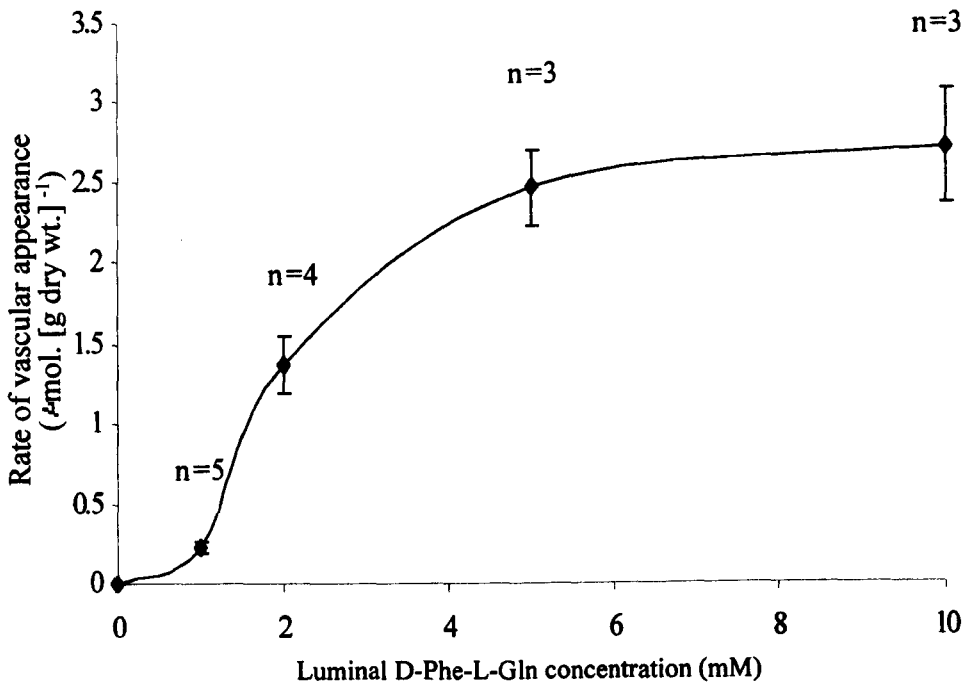

Figure 3.8

Relationship between D-Phe-L-Gln concentration and its rate of transfer to the serosa. D-Phe-L-Gln was perfused through the lumen at a specified concentration for 40 minutes. The sigmoidal curve is indicative of allosteric control. Data points represent the mean ± s.e.m (n values are depicted on the specific points on the graph). Data was obtained from the Bronk laboratory (personal communication).

membrane implied by reduced mucosal exit ratios of D-Phe-L-Gln in the presence of D-Phe-L-Ala. This suggests that D-Phe-L-Ala appears to interact with the basolateral transporter more efficiently than it does with PepT1, or that it exerts more control at this membrane, or that the basolateral transporter is more sensitive to regulation. Previous studies with Caco-2 cells have shown that preincubation with one dipeptide causes stimulation in the transport of a distinct dipeptide (Thamotharan *et al.*,1998; Walker *et al.*, 1998; Shiraga *et al.*, 1999). This stimulation is a result of an increase in V_{max} of transport with no change in K_m, and is associated with an increase in PepT1 mRNA levels and mRNA stability in the cell, in addition to an enhancement of PepT1 protein abundance at the apical membrane. As such, it seems to be a result of transcriptional control to provide a larger population of transporters at the membrane to increase absorption. However, this stimulation only follows at least 24-72 hours preincubation with the dipeptide. In addition, it is only caused by particular dipeptides, i.e. Gly-Sar (Thamotharan *et al.*, 1998) and Gly-Phe (Shiraga *et al.*, 1999) have been shown to cause a stimulation in transport, whereas Gly-Gln did not have the same effect (Shiraga *et al.*, 1999). This implies that the effect may be peptide-specific. The mechanism of stimulation in transport described in these studies cannot really be used to explain the stimulation in D-Phe-L-Gln transport observed with D-Phe-L-Ala in the perfusions presented here, due to the shorter time periods of exposure to peptide. However, Sharp *et al.* (1996) demonstrated that there was an additional rapid regulatory response of SGLT1 to jejunal glucose, that preceded the onset of increased protein expression at the brush-border membrane in rat, which occurred within 30 min of exposure. This same response may be equivalent as to what is being observed with peptide transport in these present perfusions. However, these perfusions alone cannot unequivocally discriminate which process of activation is occurring (if any).

Further work is required to elucidate the stimulation/inhibition of D-Phe-L-Gln transport by the modified dipeptide and the original structure.

3.8 Conclusions

(1) [4-azido-D-Phe]-L-Ala is transported at a significantly more rapid rate than D-Phe-L-Gln, but accumulates to a lesser extent in mucosal tissue and a higher extent in muscle. Therefore, [4-azido-D-Phe]-L-Ala appears to be a more effective substrate for the peptide transporters at both the BBM and BLM than D-Phe-L-Gln, but has a relatively more efficient interaction with the basolateral transporter than with PepT1.

(2) Inhibition of substrate transport by [4-azido-D-Phe]-L-Ala at the brush-border membrane (PepT1) is not apparent from these perfusion experiments. However, previous data (Boyd *et al.*, personal communication) have demonstrated transport inhibition in PepT1-expressing *Xenopus* oocytes, indicating a direct interaction of the label with the transporter protein.

(3) [4-azido-D-Phe]-L-Ala inhibits transport at the endofacial active site of the basolateral transporter, but not by interaction with its exofacial surface. Therefore, it has an asymmetrical interaction for the transporter that agrees with previous studies concerning the unidirectionality of transport, which corresponds to the absorptive process *in vivo*.

(4) Addition of the azide group to D-Phe-L-Ala increases its rate of transmural transport. This enhanced affinity is probably due to the presence of a positive charge, i.e. cationic peptides are more efficiently transported at slightly higher pH's (pH 6.8).

(5) D-Phe-L-Ala stimulates substrate transport at both membranes, but more predominantly at the BLM. The peptide transporters may be under allosteric control. Further work is required to confirm this theory.

In summary, although certain discrepencies concerning the nature of inhibition/stimulation in substrate transport by peptide transporters are observed with

the vascular perfusions, the main aim of the investigation has been fulfilled. It has been demonstrated unequivocally thet [4-azido-D-Phe]-L-Ala is able to interact specifically with the peptide transporters at both the apical and basolateral membranes in rat jejunum in a substrate-specific way. [4-azido-D-Phe]-L-Ala is therefore a potentially good reagent to be used for photoaffinity labelling in the identification of the membrane proteins responsible for peptide transport in rat jejunal mucosa.

CHAPTER 4: PHOTOAFFINITY LABELLING OF PEPT1 IN RAT JEJUNAL BRUSH-BORDER MEMBRANE VESICLES USING [4-AZIDO-3,5-^{3}H-D-PHE]-L-ALA

4.1 Tritiation of [4-azido-D-Phe]-L-Ala to allow its detection

The radioactive form of the photoaffinity label is shown in figure 4.1. [4-azido-D-Phe]-L-Ala was custom-synthesised using standard techniques (P. D. Bailey, 1990) by Professor P. D. Bailey and Dr. I. Collier in the Chemistry Department of Heriot Watt University, Edinburgh, UK (see section 3.1 for details). The D-Phe ring was tritiated at positions 3 and 5 to permit detection of the label and, therefore, to allow the detection of a protein to which it may bind to. Attachment of the tritium groups (^{3}H) to form [4-azido-3,5-^{3}H-D-Phe]-L-Ala was performed by Zeneca.

4.2 Purity of BBMV prepared from rat jejunum

Brush-border membrane vesicles prepared from rat jejunal mucosa were routinely analysed by enzyme assays to assess their purity and enrichment in comparison to the initial crude homogenate sample. Assays were performed for enzymes that are highly specific for the apical membrane; sucrase and alkaline phosphatase. In addition, an enzyme specific for the basolateral membrane was also assayed (ouabain-sensitive Na^+/K^+-ATPase) to eliminate the possibility of cross-contamination. The results of the assays are shown in figure 4.2. The data demonstrate that the BBMV used were consistently of a high purity with negligible contamination by other membranes.

4.3 Feasibility of using [4-azido-3,5-^{3}H-D-Phe]-L-Ala to identify PepT1 in membrane vesicles

As mentioned previously, the potential label has been shown to have a high affinity for PepT1 in the apical membrane of intact jejunum, i.e. it is transported at a very rapid rate from the lumen to the serosa during vascular perfusions. This unidirectionality of transport corresponds to the absorptive process *in vivo*. The label

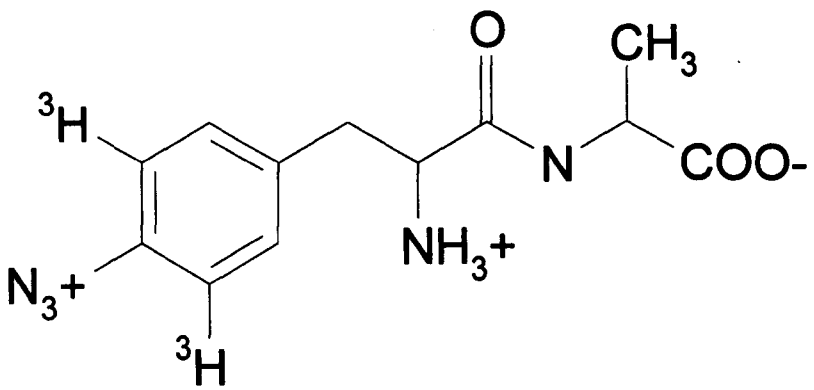

Figure 4.1

Chemical structure of the radioactive photoaffinity label [4-azido-3,5-^{3}H-D-Phe]-L-Ala. The hydrolysis resistant dipeptide, D-Phe-L-Ala, was synthesised by standard techniques (P. D. Bailey, 1990) prior to the addition of the azido group (N_3) to position 4 of the D-Phe ring. The label was tritiated at positions 3 and 5 of the D-Phe ring by Zeneca to permit its detection by scintillation counting.

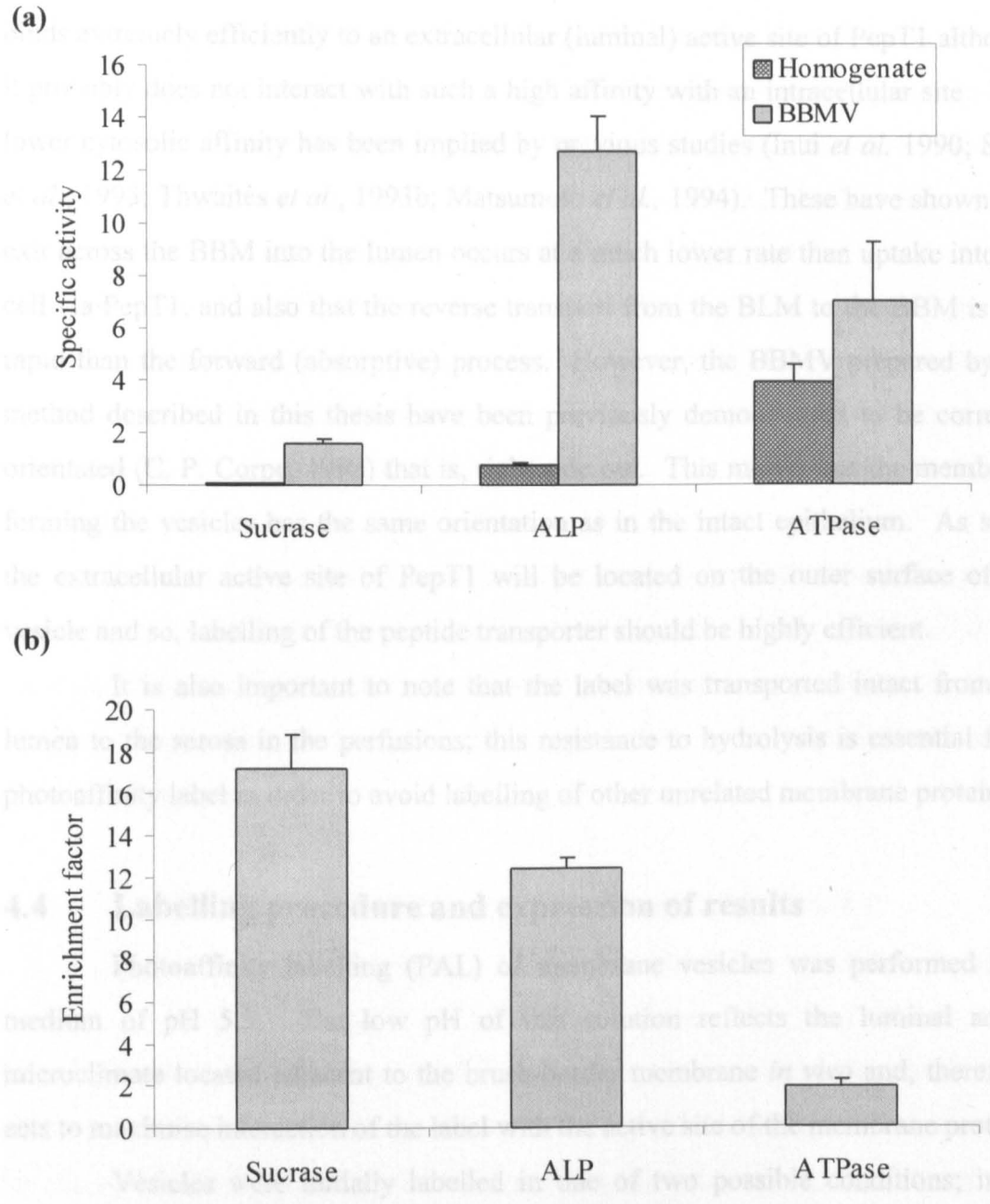

Figure 4.2

Purity of BBMVs were assessed by assaying enzymes specific for a given membrane in the intestinal enterocyte. Assays were performed for sucrase and ALP (BBM markers) and ouabain-sensitive Na^+/K^+-ATPase (BLM marker). The specific activity of the enzymes in the homogenate and BBMV are shown (a) and are expressed as follows: sucrase, $\mu mol \cdot min^{-1} \cdot [mg\ protein]^{-1} \cdot$; ALP, $U \cdot [mg\ protein]^{-1}$; ATPase, $\mu mol \cdot hr^{-1} \cdot [mg\ protein]^{-1} \cdot$. Also shown is the enrichment of each enzyme in BBMV as compared to the original crude homogenate (b). Bars represent the mean ± s.e.m. (n = 6).

binds extremely efficiently to an extracellular (luminal) active site of PepT1 although it probably does not interact with such a high affinity with an intracellular site. This lower cytosolic affinity has been implied by previous studies (Inui *et al.* 1990; Saito *et al.*, 1993; Thwaites *et al.*, 1993b; Matsumoto *et al.*, 1994). These have shown that exit across the BBM into the lumen occurs at a much lower rate than uptake into the cell via PepT1, and also that the reverse transport from the BLM to the BBM is less rapid than the forward (absorptive) process. However, the BBMV prepared by the method described in this thesis have been previously demonstrated to be correctly orientated (C. P. Corpe, 1993) that is, right side out. This means that the membrane forming the vesicles has the same orientation as in the intact epithelium. As such, the extracellular active site of PepT1 will be located on the outer surface of the vesicle and so, labelling of the peptide transporter should be highly efficient.

It is also important to note that the label was transported intact from the lumen to the serosa in the perfusions; this resistance to hydrolysis is essential for a photoaffinity label in order to avoid labelling of other unrelated membrane proteins.

4.4 Labelling procedure and expression of results

Photoaffinity labelling (PAL) of membrane vesicles was performed in a medium of pH 5.5. The low pH of this solution reflects the luminal acidic microclimate located adjacent to the brush-border membrane *in vivo* and, therefore, acts to maximise interaction of the label with the active site of the membrane protein.

Vesicles were initially labelled in one of two possible conditions; in an 'unprotected' or 'protected' environment. Unprotected vesicles were labelled directly in the absence of substrate, whereas protected vesicles were pre-incubated in a high concentration of a substrate for 15 min prior to labelling. The substrates used were either a dipeptide (D-Phe-L-Gln) or its equivalent free amino acids (D-Phe and L-Gln), all at a concentration of 16.7 mM. This protection was used to provide information regarding the type of substrate with which a labelled protein would interact, i.e. it would demonstrate substrate-specific labelling by inhibition of label incorporation.

[4-azido-3,5-^{3}H-D-Phe]-L-Ala was added to the vesicles at a final concentration of 4.2 μM and a total radioactivity content of 740 kBq (20 μl volume). When exposed to light, the azido group becomes extremely reactive and will form a covalent attachment to a number of different bonds within close vicinity. The low

concentration ensures that the level of non-specific labelling is kept to an absolute minimum and that label incorporation is due to a substrate/active site interaction.

Results from PAL experiments are presented as graphs of gel slice number on the *x*-axis (which corresponds to a decrease in molecular weight from left to right) against radioactivity detected by scintillation counting (dpm) on the *y*-axis. A peak in the data indicates that the label has covalently attached to a membrane protein. Results from unprotected vesicles are shown in conjunction with substrate-protected studies. These collated data are normalised to the same initial radioactivity content of the sample to allow results of the different labelling conditions to be directly compared.

Label incorporation by a membrane protein is expressed as the percentage of radioactivity bound, with respect to the initial radioactivity content, and also shown is the percentage inhibition caused by substrate preincubation/enzymatic treatment of vesicles. Finally the amount of [4-azido-3,5-^{3}H-D-Phe]-L-Ala actually bound to the protein is calculated.

4.5 Photoaffinity labelling of BBMV to identify PepT1

BBMV were photoaffinity labelled with the peptide derivative [4-azido-3,5-^{3}H-D-Phe]-L-Ala in the presence or absence of either D-Phe-L-Gln or its constituent amino acids, on the basis that compounds which compete with the label for binding should decrease the extent of specific labelling. The results are shown in figure 4.3. There appears to be a high level of incorporation of the label by a membrane protein shown to have an apparent molecular weight of approx. 130 kDa when analysed by slab gel SDS-PAGE (data not shown). Binding of the radioactive label to this protein is strongly inhibited by pre-incubation with the dipeptide but not by the amino acids. The dipeptide inhibits 56% of label binding (table 4.1 and figure 4.4) whereas the amino acids provide very little protection (6%). It is also interesting to note that incubation with the dipeptide and the amino acids collectively confers slightly more inhibition than the dipeptide alone (62%).

The pattern of label incorporation seen in figure 4.3 was highly reproducible and the data collectively suggests that the predominantly labelled 130 kDa protein specifically interacts with dipeptides but not with amino acids.

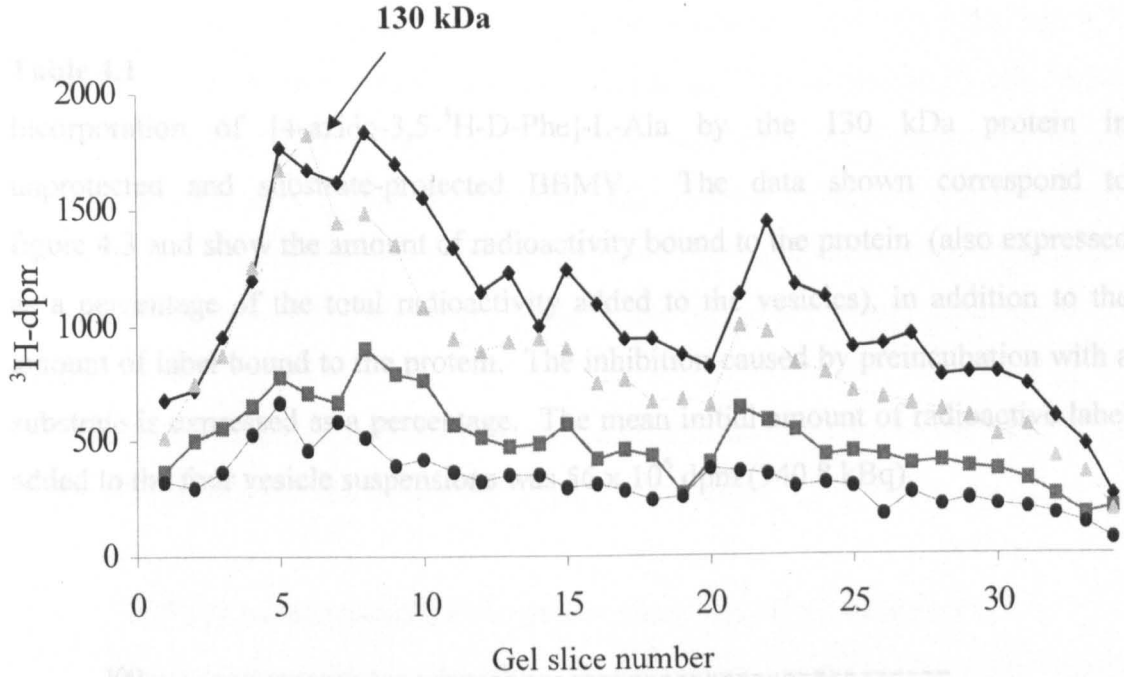

Figure 4.3

Representative result of photoaffinity labelling of BBMV at pH 5.5 with [4-azido-3,5-^{3}H-D-Phe]-L-Ala. Labelling was performed under four different conditions; unprotected (diamonds) and protected by 16.7 mM D-Phe-L-Gln (squares), D-Phe and L-Gln at 16.7 mM (triangles) or both peptide and amino acids (circles). The *x*-axis of gel slice number represents a decrease in molecular weight from left to right, down the rod gel, and the *y*-axis shows label incorporation by a membrane protein. A peak demonstrates that a protein has bound the radioactive label.

	Protein-bound ^{3}H-dpm	Bq	% label bound	Total label bound	% inhibition
Unprotected	1775	29.82	0.0032	27 fmoles	
D-Phe-L-Gln	780	13.1	0.0014	12 fmoles	56%
D-Phe & L-Gln	1677	28.17	0.003	25 fmoles	6%
D-Phe-L-Gln, D-Phe & L-Gln	668	11.22	0.0012	10 fmoles	62%

Table 4.1

Incorporation of [4-azido-3,5-^{3}H-D-Phe]-L-Ala by the 130 kDa protein in unprotected and substrate-protected BBMV. The data shown correspond to figure 4.3 and show the amount of radioactivity bound to the protein (also expressed as a percentage of the total radioactivity added to the vesicles), in addition to the amount of label bound to the protein. The inhibition caused by preincubation with a substrate is expressed as a percentage. The mean initial amount of radioactive label added to the four vesicle suspensions was 56 x 10^6 dpm (940.8 kBq).

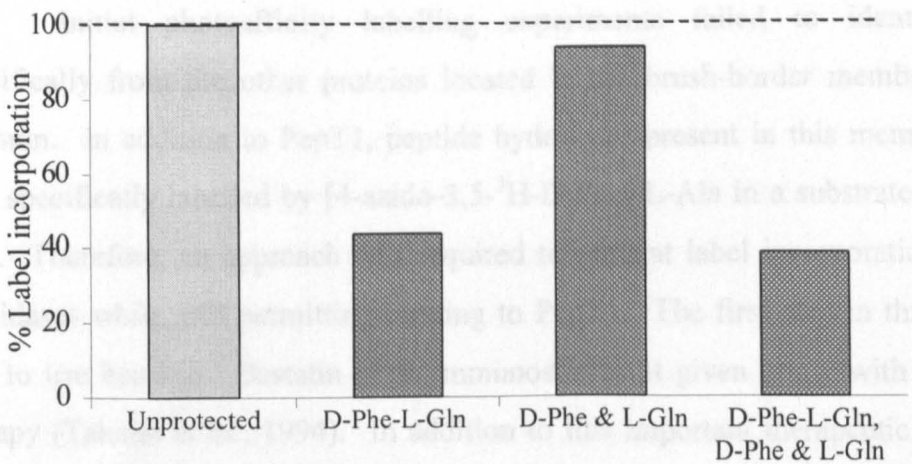

Figure 4.4

Inhibition of [4-azido-3,5-^{3}H-D-Phe]-L-Ala binding to the 130 kDa protein as a result of pre-incubation with substrates (at 16.7 mM). Unprotected labelling (in the absence of substrates) is taken to be 100% incorporation. The degree by which the substrates inhibit labelling indicates the preferred nature of substrate with which the membrane protein interacts.

The amount of [4-azido-3,5-^{3}H-D-Phe]-L-Ala covalently bound to the 130 kDa protein is very low; in the unprotected vesicles only 27 fmoles from an initial 840 pmoles specifically binds, i.e just 0.0032% (table 4.1). However, the low level of incorporation suggests that the covalent attachment of the label to the membrane protein should be very specific and that the highly reactive azido group is not forming a bond with random proteins with which the dipeptide backbone does not interact.

It is evident that not only is there predominant labelling of the 130 kDa protein, but also there is a considerable amount of label incorporation by other BBM proteins. Labelling of all proteins appears to be inhibited by the dipeptide but not the amino acids, albeit to varying extents. The high molecular weight proteins (approx. slice numbers 4-11 in figure 4.3) are thought to be peptide hydrolases associated with the apical membrane, but the nature of the lower molecular weight proteins are not known.

Due to the extent of label incorporation by many proteins in the BBMV it is impossible from these data to identify PepT1 individually.

4.6 Effect of bestatin on singular identification of PepT1

Initial photoaffinity labelling experiments failed to identify PepT1 specifically from the other proteins located in the brush-border membrane of the jejunum. In addition to PepT1, peptide hydrolases present in this membrane were also specifically labelled by [4-azido-3,5-^{3}H-D-Phe]-L-Ala in a substrate-inhibitable way. Therefore, an approach was required to prevent label incorporation by these peptidases while still permitting binding to PepT1. The first step in this approach was to use bestatin. Bestatin is an immunostimulant given orally with anti-cancer therapy (Takano *et al.*, 1994). In addition to this important therapeutic use, it is a potent inhibitor of exopeptidases, dipeptidases and several aminopeptidases, except aminopeptidase A (Wilkes & Prescott, 1985), in the apical membrane. It has also been shown to be a transportable substrate of the intestinal peptide transporter (Kramer *et al.*, 1990b). However, a considerably higher concentration is required for interaction with PepT1 than with the peptidases; the concentration being three orders of magnitude higher (10 mM compared to ~ 10 μM) (Kramer *et al.*, 1990b; Takano *et al.*, 1994). Due to the differences in affinity of the distinct membrane proteins, it was thought that preincubation of BBMV with a low concentration of bestatin

(20 μM) would inhibit label incorporation by the peptidases and aid in the distinct labelling of PepT1.

Figure 4.5 shows the results of these experiments. It is evident that the presence of bestatin has no effect on blocking label incorporation by the BBM peptidases, in particular it only inhibits 6% of label binding (table 4.2, figure 4.6) to the 130 kDa protein principally detected in figure 4.3. A similar low extent (or lack) of inhibition was observed as an overall effect throughout the membrane as a whole. However, D-Phe-L-Gln again has a dramatic effect and completely abolishes label incorporation by all proteins, especially by the 130 kDa protein (87.5% inhibition).

The amount of label attachment to the unprotected 130 kDa protein is comparable with the initial experiments; only 31 fmoles is covalently bound to the protein (0.0037% of the initial 840 pmoles). Again this low level of incorporation indicates a highly specific interaction of [4-azido-3,5-^{3}H-D-Phe]-L-Ala with all proteins.

The overall result of these experiments is that PepT1 cannot be individually identified due to a lack of inhibition of peptidase labelling by bestatin.

4.7 Papain treatment of BBMV to digest peptide hydrolases

Because of the failure in identifying PepT1 by using bestatin to block hydrolase labelling, another approach to inhibit label incorporation by these proteins was required. The study was progressed by treating the vesicles with papain prior to labelling. Papain has been demonstrated to cleave, and solubilise, the extracellular domain of hydrolases from the bilayer structure of the membrane whilst preserving the integrity of the vesicles (Berteloot *et al.*, 1980; Ganapathy *et al.*, 1981; Kenny & Maroux, 1982). Other studies have shown that papain treatment of BBMV (at a concentration of 0.5 mg·ml^{-1}) causes a stimulation of peptide transport by PepT1 (Ganapathy *et al.*, 1981; Inui *et al.*, 1984). This stimulation in peptide transport was associated with peptidase digestion from the apical membrane and, as such, was due to an increase in enrichment of PepT1 transport activity.

Vesicles were initially digested with 0.5 mg·ml^{-1} papain (0.21 U ml^{-1} enzyme activity) using a method previously described (Louvard *et al.*, 1975; Ganapathy *et al.*, 1981) in which the reaction was quenched by chilling the digestion mixture to 4°C. The results from papain digestion of BBMV are shown in figure 4.7

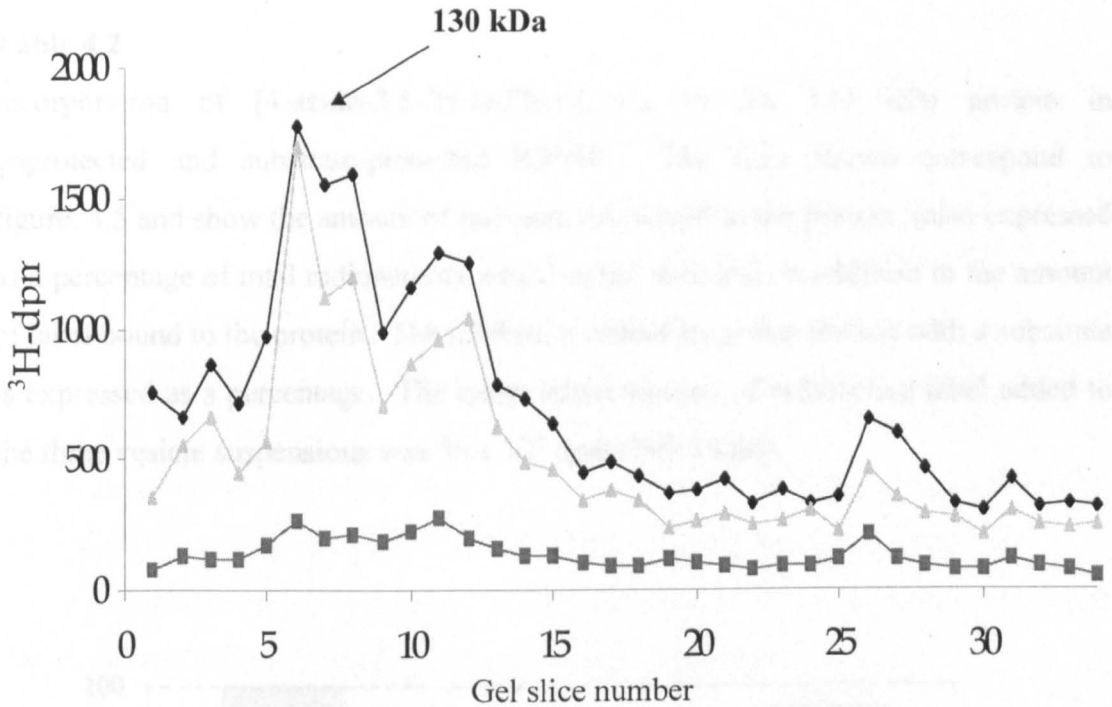

Figure 4.5

Representative result of photoaffinity labelling of BBMV at pH 5.5 with [4-azido-3,5-^{3}H-D-Phe]-L-Ala. Vesicles were preincubated with 20 μM bestatin (triangles) in an attempt to block labelling of brush-border peptide hydrolases to allow specific labelling of PepT1. Also shown are labelling of unprotected vesicles (diamonds) and vesicles protected by 16.7 mM D-Phe-L-Gln (squares). The *x*-axis of gel slice number represents a decrease in molecular weight from left to right, down the rod gel, and the *y*-axis shows label incorporation by a membrane protein. A peak demonstrates that a protein has bound the radioactive label.

	Protein-bound ^{3}H-dpm	Bq	% bound	Total label bound	% inhibition
Unprotected	2083	34.99	0.0037	31 fmoles	
D-Phe-L-Gln	251	4.22	0.0005	4 fmoles	87.5%
Bestatin	1980	33.26	0.0035	29 fmoles	6%

Table 4.2

Incorporation of [4-azido-3,5-^{3}H-D-Phe]-L-Ala by the 130 kDa protein in unprotected and substrate-protected BBMV. The data shown correspond to figure. 4.5 and show the amount of radioactivity bound to the protein (also expressed as a percentage of total radioactivity added to the vesicles), in addition to the amount of label bound to the protein. The inhibition caused by preincubation with a substrate is expressed as a percentage. The mean initial amount of radioactive label added to the three vesicle suspensions was 56 x 10^6 dpm (940.8 kBq).

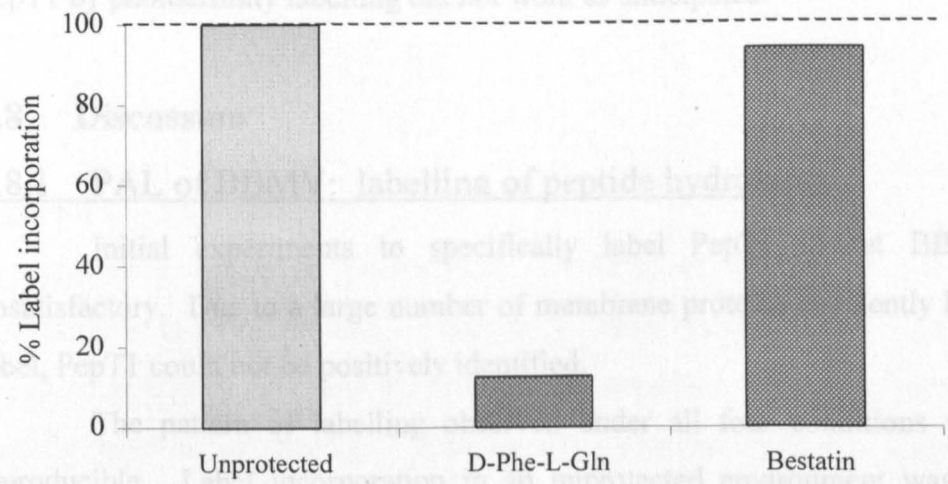

Figure 4.6

Extent of [4-azido-3,5-^{3}H-D-Phe]-L-Ala binding to the 130 kDa protein as a result of pre-incubation with D-Phe-L-Gln (at 16.7 mM) or bestatin (at 20 μM). Unprotected labelling (in the absence of additional compounds) is taken to be 100% incorporation.

and figure 4.8. It is immediately apparent that digestion of the vesicles in this way completely abolishes label incorporation by all brush-border membrane proteins, not just the hydrolases.

It was thought that simply chilling the digestion mixture to 4°C did not quench the reaction fully. So, another digestion was performed with the same papain concentration but the reaction was stopped by a 5-fold dilution in a mannitol/HEPES buffer, pH 7.5 (as described by Berteloot *et al.*, 1980). Figures 4.7 and 4.8 show the results of this experiment. Again it is evident that the digestion was too aggressive and did not leave PepT1 in the membrane able to bind the label. A third experiment utilised half of the original papain concentration (0.25 $mg \cdot ml^{-1}$) in an attempt to reduce the extent of digestion. This, again, resulted in complete inhibition of labelling throughout the whole of the membrane.

Louvard and co-workers (1975) suggested that freezing the vesicles accelerated solubilisation by papain so, experiments using previously frozen and freshly prepared vesicles were performed. Traces of radioactive label incorporation were again practically identical to the data already presented (data not shown).

Overall, papain digestion of BBMV performed to specifically identify PepT1 by photoaffinity labelling did not work as anticipated.

4.8 Discussion

4.8.1 PAL of BBMV: labelling of peptide hydrolases

Initial experiments to specifically label PepT1 in rat BBMV were unsatisfactory. Due to a large number of membrane proteins covalently binding the label, PepT1 could not be positively identified.

The pattern of labelling observed under all four conditions was highly reproducible. Label incorporation in an unprotected environment was also very similar to that seen in a series of studies performed by Kramer and co-workers in which BBMV from rat (1987), rabbit (1988, 1990c) and pig (1990b) were labelled with photolabile derivatives of known PepT1 substrates. The 130 kDa molecular weight protein predominantly labelled by [4-azido-3,5-^{3}H-D-Phe]-L-Ala in this study corresponds to the protein of 127 kDa that was identified by Kramer's group. In Kramer's investigations, pre-incubation of vesicles with other (non-radioactive) PepT1 substrates caused a clear concentration-dependent decrease in the extent of

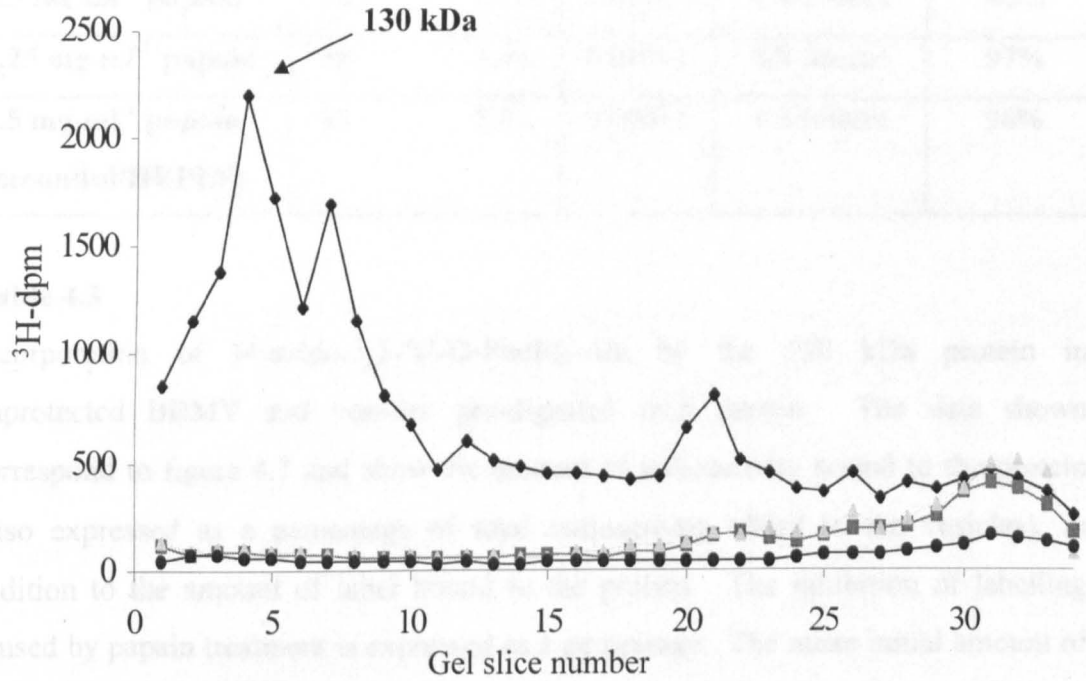

Figure 4.7

Representative result of photoaffinity labelling of BBMV at pH 5.5 with [4-azido-3,5-^{3}H-D-Phe]-L-Ala. Prior to labelling vesicles were incubated with papain in an attempt to digest the brush-border peptidases out of the bilayer to allow specific labelling of PepT1. Vesicles were digested with 0.5 mg·ml^{-1} papain (triangles) and 0.25 mg·ml^{-1} papain (circles) and the reaction quenched by chilling to 4°C, or they were digested with 0.5 mg·ml^{-1} and the reaction quenched by a 5-fold dilution in a mannitol/HEPES buffer (squares). Also shown is unprotected labelling of BBMV (diamonds). The *x*-axis of gel slice number represents a decrease in molecular weight from left to right, down the rod gel, and the *y*-axis shows label incorporation by a membrane protein. A peak demonstrates that a protein has bound the radioactive label.

	Protein-bound ^{3}H-dpm	Bq	% bound	Total label bound	% inhibition
Unprotected	2196	36.89	0.0038	32 fmoles	
0.5 mg·ml^{-1} papain	98	1.65	0.00017	1.4 fmoles	96%
0.25 mg·ml^{-1} papain	62	1.04	0.00011	0.9 fmoles	97%
0.5 mg·ml^{-1} papain (mannitol/HEPES)	85	1.43	0.00015	1.3 fmoles	96%

Table 4.3

Incorporation of [4-azido-3,5-^{3}H-D-Phe]-L-Ala by the 130 kDa protein in unprotected BBMV and vesicles pre-digested with papain. The data shown correspond to figure 4.7 and show the amount of radioactivity bound to the protein (also expressed as a percentage of total radioactivity added to the vesicles), in addition to the amount of label bound to the protein. The inhibition of labelling caused by papain treatment is expressed as a percentage. The mean initial amount of radioactive label added to the four vesicle suspensions was 58 x 10^6 dpm (974.4 kBq).

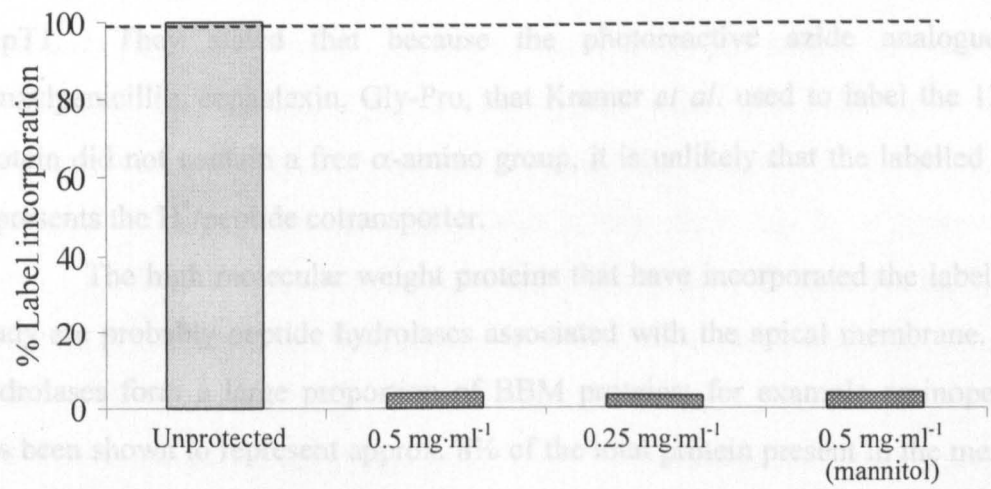

Figure 4.8

Effect of papain digestion on [4-azido-3,5-^{3}H-D-Phe]-L-Ala binding to the 130 kDa protein. Unprotected labelling (in the absence of papain treatment) is taken to be 100% incorporation.

labelling of this protein, whereas bile acids, sugars and amino acids had no effect. They therefore suggested that it could be a component of the peptide transport system. Even so, they examined whether certain hydrolases of this molecular weight were contributing to label binding, e.g. aminopeptidase N, dipeptidyl peptidase IV. Immunoprecipitation studies indicated that these hydrolases were not a part of the transport system and so they postulated that the 127 kDa protein was directly involved in the transfer of oligopeptides and peptide-like drugs across the enterocyte BBM. Further studies by this group were to reconstitute the 127 kDa protein into proteoliposomes (Kramer *et al.*, 1992). This resulted in specific binding of β-lactam antibiotics and dipeptides to the protein, in addition to observing a stereospecific transport activity. A longitudinal examination of the small intestine revealed that the 127 kDa protein was present throughout its entire length (Kramer *et al.*, 1998). This protein was demonstrated to be highly glycosylated; treatment with various de-glycosylating enzymes produced a lower molecular weight of the protein (95-100 kDa). This apparent heavy glycosylation, coupled with the fact that when subjected to 2-D electrophoresis the protein did not focus into a sharp spot (Kramer *et al.*, 1990d), but was evenly distributed over a pH range of approx. 1 unit (pH 5-6), implies that it is a microheterogenous glycoprotein.

In reference to the previous papers by Kramer and co-workers, Daniel & Adibi (1993) conducted investigations into the substrate-specific requirements of PepT1. They stated that because the photoreactive azide analogues, i.e. benzylpenicillin, cephalexin, Gly-Pro, that Kramer *et al.* used to label the 127 kDa protein did not contain a free α-amino group, it is unlikely that the labelled protein represents the H^+/peptide cotransporter.

The high molecular weight proteins that have incorporated the label in this study are probably peptide hydrolases associated with the apical membrane. These hydrolases form a large proportion of BBM proteins; for example aminopeptidase has been shown to represent approx. 8% of the total protein present in the membrane (Desnuelle, 1979). Their molecular weights range from 170 kDa of aminopeptidase A, through 130 kDa (aminopeptidase N, dipeptidyl peptidase IV), to 93 kDa of endopeptidase (Kenny & Maroux, 1982). Because they are peptide hydrolases they specifically interact with peptides, and therefore, in conjunction with PepT1, will also bind the photolabile dipeptide.

4.8.2 Distinct molecular weight of PepT1

The molecular weight of the protein predominantly labelled by the modified dipeptide (130 kDa) does not correlate with molecular weights of PepT1 that have previously been published. Fei *et al.* (1994) and Daniel *et al.* (1996) both identified PepT1 in rabbit small intestine with an apparent molecular weight of 71 kDa. Investigations with rat brush-border membranes identified a protein of 75 kDa (Saito *et al.*, 1995; Ogihara *et al.*, 1996), thought to be only 63 kDa without glycosylation (Saito *et al.*, 1995). Studies in human tissue by Liang and co-workers (1995) identified a protein of 78.81 kDa molecular weight, deduced from its primary amino acid sequence, whereas Dantzig *et al.* (1994) postulated that a protein of 92 kDa (designated HPT-1) is associated with hPepT1. A later study by Fei's group in 1997, on Caco-2 cells, identified a 120 kDa protein that they hypothesised as being PepT1.

It is evident that there are variations in the apparent molecular weight of PepT1 and these are due to the diversity of animal species under study, but in addition it may also be due to discrepancies in technique by the different groups. It may be that a functional transport protein isolated from an intact tissue, which is the case in this present study, has a different subunit composition, or molecular weight, from a transporter that has been functionally expressed by injection of its cDNA into oocytes. This may explain the apparent differences in the molecular weight of the protein that has been labelled by [4-azido-3,5-^{3}H-D-Phe]-L-Ala in this study to previously published results. Although moderately higher molecular weights have been described (120 kDa by Fei *et al.*, 1997), these were found in human tissue. The molecular weight consistently recorded for smaller animals, in particular rat, is approx. 70-75 kDa. The detected protein in this study may be a dimer of these proteins previously documented. However, this is unlikely because the BBMV were subjected to SDS-PAGE in the presence of a reducing agent (β-mercaptoethanol) and therefore all bonds between potential subunits of proteins would have been destroyed by the denaturing conditions employed. Therefore, although the 130 kDa protein has been predominantly labelled by [4-azido-3,5-^{3}H-D-Phe]-L-Ala it may in fact be a protease, or possibly a regulator of peptide transport. PepT1 was not resolved because of extensive labelling of other proteins. Its presence, individually, at 75 kDa, could not be individually identified by this method.

4.8.3 Inhibition of label interaction with peptidases by bestatin

Although peptidases located in the BBM are not directly involved in peptide transport, they bind peptide structures and have been shown in the initial studies to interact with the photoaffinity label. A step was taken in an attempt to eliminate specific label incorporation by these peptidases by incubating vesicles with bestatin (at 20 μM concentration) prior to labelling. The results, however, were disappointing. Bestatin did not inhibit labelling of the peptidases to any appreciable extent and so PepT1 could not be specifically identified.

The concentration of bestatin added to the vesicles was comparable to that described in previous papers, for example, Wilkes & Prescott (1985) performed a series of hydrolase-inhibition experiments using bestatin at increasing concentrations. Their results showed that the extent and rapidity of inhibition increased as a result of bestatin concentration. Complete inhibition was achieved with 19.1 μM after only 5 min incubation. Other values published for bestatin are that rabbit aminopeptidases are inhibited with an IC_{50} value of 5 μM (Takano *et al.*, 1994) and half-maximal inhibition of aminopeptidase N is seen with approx. 10 μM bestatin (Kramer *et al.*, 1990b). Therefore, at a bestatin concentration of 20 μM a certain degree of label inhibition should have occurred.

In addition to being an inhibitor of peptide hydrolases, bestatin is also a substrate for PepT1. However, a higher concentration is required for interaction with the peptide transporter than with the peptidases. A half-maximal inhibition of cephalexin uptake into BBMV was observed with an IC_{50} of approx. 10 mM bestatin (Kramer *et al.*, 1990b); this concentration is three orders of magnitude higher than that described for peptidases. A separate study has measured transport of bestatin into membrane vesicles and demonstrated that uptake consisted of two saturable components (Takano *et al.*, 1994). A high affinity component was understood to be due to binding of bestatin to aminopeptidases on the surface of the vesicles, whereas a low affinity component was a result of specific uptake by PepT1 into the intravesicular space. At the low concentrations used in this study, bestatin should have bound preferentially to the hydrolases leaving PepT1 free to be photoaffinity labelled.

The lack of effect by bestatin might be due to its incubation time with the membrane vesicles. Studies by Wilkes & Prescott (1985) imply that bestatin is an

inhibitor that gains equilibrium with peptidases to form a tightly bound enzyme-inhibitor (E-I) complex in a time dependant manner. Mechanisms have been proposed suggesting an initial collision complex followed by a slow conformational change that takes approx. two hours to achieve. These induced changes may involve the formation of ligands between zinc (in the peptidase active site) and bestatin, possibly via α-hydroxy and carboxyl groups. These findings indicate that it may be feasible to increase the incubation time of vesicles with bestatin to 2 h for PepT1 identification.

4.8.4 Papain digestion of peptidases

Papain digestion of the vesicles was no more successful than the use of bestatin. Membrane surface constituents that are known to be detached from, or loosely attached to, the lipid core can be solubilised either by proteolytic digestion or by treatment with detergents. Hydrolases are asymmetrically orientated within the brush-border membrane, i.e. the bulk of the molecule (including the catalytic site) is exposed at the luminal surface (Kenny & Maroux, 1982) and are therefore on the extravesicular side of BBMV. They are composed of 3 domains; a large hydrophilic region protruding out of the cell, a hydrophobic region plunged into the lipid core of the bilayer and a small cytoplasmic tail located inside the cell (which constitutes only 2.5-5% of its total mass) (Desnuelle, 1979). The mechanism of hydrolase solubilisation is not known but proteases such as papain are thought to split a limited number of bonds at the hydrophilic/hydrophobic junction at the membrane surface, therefore shaving off the extracellular part and leaving the hydrophobic part in the bilayer. Untreated BBMV have a regular array of knobs on their external surface, shown by negative staining preparations (Kenny & Maroux, 1982). After papain treatment the surface of the vesicles are smooth; this has been interpreted as correlating with the release of the susceptible hydrolases. Not all hydrolases are released from the membrane at the same rate, for example aminopeptidase N and dipeptidyl peptidase IV are readily solubilised whereas aminopeptidase A and γ-glutamyltransferase are released more slowly (Kenny & Maroux, 1982). These differences in rate of release from the membrane has been attributed to bond accessibility, i.e. how deep the enzyme is buried within the membrane lipids, in addition to several structural parameters. These include the geometry of fit of papain

at the surface of the membrane and the primary structure of the accessible region of the susceptible polypeptide chain.

Previous studies using papain digestion of BBMV have demonstrated that it causes a stimulation of peptide transport by PepT1 (Ganapathy *et al.*, 1981; Inui *et al.*, 1984). This increase in transport correlates with protein removal during digestion; a 42% stimulation in Gly-L-Pro transport corresponded to the solubilisation of 45% of protein in the apical membrane, resulting in a 2.5-fold enrichment in specific transport activity (Ganapathy *et al.*, 1981). A similar occurrence was seen in the study by Inui (1984); a 2-fold enhancement in specific activity of cephalexin transport closely matched the extent of protein removal using papain (40-50% digestion). It was suggested (Ganapathy *et al.*, 1981) that the stimulation in peptide transport might be the result of a reduction in the thickness of the unstirred water layer adjacent to the apical membrane, implied by a substantial decrease in extravesicular space.

Although peptide transport was demonstrated to have remained intact following papain digestion of BBMV in previous studies using an identical method, it is apparent that papain digestion in this study completely abolished label incorporation, not only by the hydrolases but also by PepT1. This could possibly be due to an incubation time that was too prolonged. The previous studies (Ganapathy *et al.*, 1981; Inui *et al.*, 1984) used BBMV prepared from rabbit small intestine, whereas this study used rat jejunal BBMV. This species difference may contribute to the discrepancies resulting from papain digestion observed, although it isn't likely.

4.8.5 pH-dependence of label interaction with PepT1

A possible reason why PepT1 does not appear to be incorporating the photoaffinity label to a great extent may be due to the pH at which labelling is performed (pH 5.5), although pH 5.5-6.5 was generally thought to be the optimum for transport of all peptides. Previous photoaffinity labelling studies by Kramer and co-workers (1987, 1988, 1990b,c) were performed at a pH of 7.4, and they also failed to specifically identify PepT1 at the correct molecular weight. Separate studies (Temple *et al.*, 1995; Wenzel *et al.*, 1996; Steel *et al.*, 1997; Amasheh *et al.*, 1997) suggest that cationic peptides (such as the label) have a higher affinity for PepT1 at a pH of approx. 6.5. Therefore, photoaffinity labelling at the same pH at which the

vascular perfusions were performed (pH 6.8) may reveal stronger labelling of PepT1. Labelling was originally conducted in a buffer of pH 5.5 because of the simplicity of its contents, i.e MES only, titrated with HCl. A physiological buffer at pH 6.8 is an option for future work.

In conclusion, PepT1 could not be specifically identified by the approaches to photoaffinity labelling described in this chapter.

4.9 Conclusions

(1) The pattern of [4-azido-3,5-^{3}H-D-Phe]-L-Ala incorporation by brush-border membrane proteins was highly reproducible.

(2) A large number of proteins in the apical membrane were specifically labelled by [4-azido-3,5-^{3}H-D-Phe]-L-Ala. Labelling is inhibited by a dipeptide but not by free amino acids.

(3) Incorporation of [4-azido-3,5-^{3}H-D-Phe]-L-Ala by membrane proteins is highly specific; only approx. 0.003% of the initial amount actually forms a covalent attachment.

(4) One protein is predominantly labelled (130 kDa), but it is probably not PepT1.

(5) The high molecular weight proteins that have been labelled are probably hydrolases associated with the apical membrane.

(6) PepT1 cannot be distinguished from other labelled proteins by pre-incubation with bestatin (to block peptidase labelling) or by papain digestion (to solubilise peptidases from the membrane).

Overall, photoaffinity labelling of BBMV could not individually identify PepT1.

CHAPTER 5: IDENTIFICATION OF A CANDIDATE PEPTIDE TRANSPORTER IN THE BASOLATERAL MEMBRANE

5.1 Purity of BLMV prepared from rat jejunum

Basolateral membrane vesicles prepared from rat jejunal mucosa were routinely analysed by enzyme assays to assess their purity and enrichment in comparison to the initial crude homogenate sample. An assay was performed for an enzyme that is highly specific for the basolateral membrane (ouabain-sensitive Na^+/K^+-ATPase) in addition to assays for two marker enzymes of the apical membrane (sucrase and alkaline phosphatase), to assess the possibility of cross-contamination. The results of the assays are shown in figure 5.1. The data demonstrate that the BLMV used for photoaffinity labelling experiments were consistently of a high purity with negligible contamination by brush-border membranes.

5.2 Viability of using [4-azido-3,5-^{3}H-D-Phe]-L-Ala to identify the basolateral peptide transporter in membrane vesicles

[4-azido-3,5-^{3}H-D-Phe]-L-Ala has been shown to interact directly with the basolateral peptide transporter by experiments using the technique of isolated, *in situ*, luminally and vascularly perfused jejunum (see chapter 3). The label was transported intact through the intestinal wall at a very rapid rate, suggesting a high affinity for peptide transporters in both the apical and basolateral membranes of the cell. In addition, it accumulates to a very low extent in the mucosal tissue, with respect to its rapid transport rate (implied by small exit ratios), indicating that it might be a more efficient substrate for the basolateral transporter than it is for PepT1.

These initial studies demonstrated that the label was a substrate for the basolateral peptide transporter. Subsequent perfusions unequivocally showed that the label interacts directly with the active site of the transporter protein (see chapter 3). In these transport inhibition experiments, the presence of [4-azido-3,5-^{3}H-D-Phe]-L-Ala in the luminal perfusate, and subsequent transport into the enterocyte, resulted in inhibition of dipeptide exit from the cell, although its presence on the serosal side did not have the same effect. Therefore, there appears to

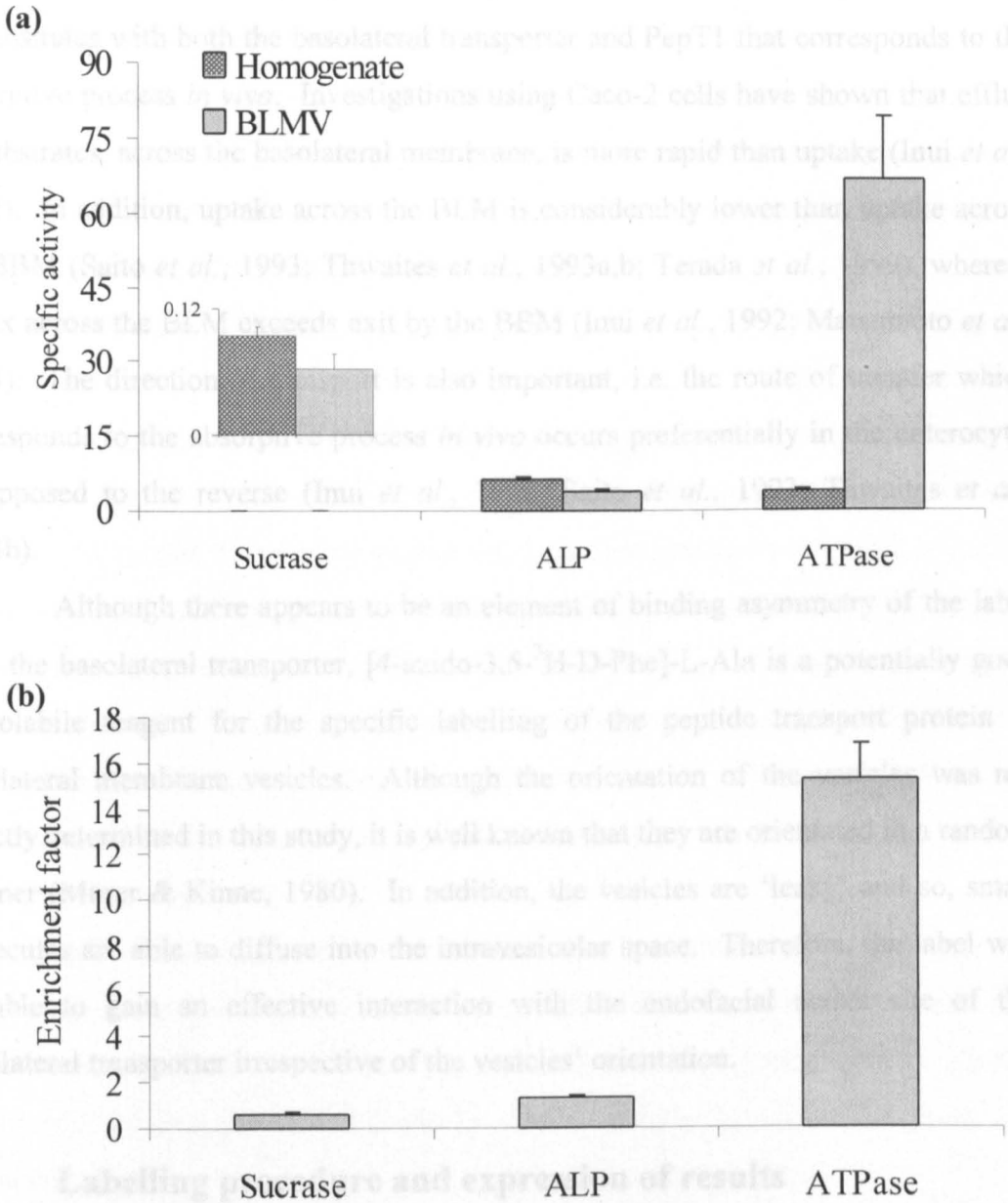

Figure 5.1

Purity of BLMVs were assessed by assaying for enzymes specific for a given membrane in the intestinal enterocyte. Assays were performed for Na^+/K^+-ATPase (BLM marker), sucrase and ALP (BBM markers). The specific activity of the enzymes in the homogenate and BLMV are shown (a) and are expressed as follows: sucrase, $\mu mol \cdot ^{1}min^{-1} \cdot [mg\ protein]^{-1}$; ALP, $U \cdot [mg\ protein]^{-1}$; ATPase, $\mu mol \cdot hr^{-1} \cdot [mg\ protein]^{-1}$·. Also shown is the enrichment of each enzyme in BLMV as compared to the original crude homogenate (b). Bars represent the mean ± s.e.m. (n = 8).

be an asymmetry in binding of the label to the basolateral peptide transporter. Previous studies by other groups have also demonstrated an asymmetry in interaction of substrates with both the basolateral transporter and PepT1 that corresponds to the absorptive process *in vivo*. Investigations using Caco-2 cells have shown that efflux of substrates, across the basolateral membrane, is more rapid than uptake (Inui *et al.*, 1992). In addition, uptake across the BLM is considerably lower than uptake across the BBM (Saito *et al.*, 1993; Thwaites *et al.*, 1993a,b; Terada *et al.*, 1999), whereas efflux across the BLM exceeds exit by the BBM (Inui *et al.*, 1992; Matsumoto *et al.*, 1994). The direction of transport is also important, i.e. the route of transfer which corresponds to the absorptive process *in vivo* occurs preferentially in the enterocyte, as opposed to the reverse (Inui *et al.*, 1992; Saito *et al.*, 1993; Thwaites *et al.*, 1993b).

Although there appears to be an element of binding asymmetry of the label with the basolateral transporter, [4-azido-3,5-^{3}H-D-Phe]-L-Ala is a potentially good photolabile reagent for the specific labelling of the peptide transport protein in basolateral membrane vesicles. Although the orientation of the vesicles was not directly determined in this study, it is well known that they are orientated in a random manner (Murer & Kinne, 1980). In addition, the vesicles are 'leaky' and so, small molecules are able to diffuse into the intravesicular space. Therefore, the label will be able to gain an effective interaction with the endofacial active site of the basolateral transporter irrespective of the vesicles' orientation.

5.3 Labelling procedure and expression of results

Photoaffinity labelling of BLMV was performed in a medium of pH 5.5. The mechanism of peptide transport at the basolateral membrane has not been elucidated, although previous studies have suggested that transport may be enhanced in a slightly acidic medium (pH 5.5-6.0). However, unlike PepT1, there doesn't appear to be an optimum pH (Saito *et al.*, 1993; Thwaites *et al.*, 1993a; Matsumoto *et al.*, 1994; Terada *et al.*, 1999).

Vesicles were labelled in an unprotected or protected environment, following the same procedure whereby BBMV were previously labelled (section 4.5), to elucidate the preferred nature of substrate with which a labelled protein interacts.

The basolateral membrane peptide transporter has been shown to be temperature sensitive (Inui *et al.*, 1992), i.e. transport is abolished at a low temperature (4°C). Vesicles were incubated at 4°C during equilibration to pH 5.5, to prevent proteolytic breakdown of the membrane constituents. However, due to the temperature sensitivity of transport, vesicles were incubated at room temperature for 15 min (with or without substrates), to allow interaction of the label and/or substrates with the active site of the transporter, prior to photolysis.

Photoaffinity labelled membrane proteins were initially resolved either by SDS-PAGE or IEF in rod gels. Proteins separated by SDS-PAGE are presented as graphs of gel slice number (3 mm sections) on the *x*-axis, against radioactivity detected by scintillation counting (dpm) on the *y*-axis. IEF-resolved proteins are also presented as graphs of gel slice on the *x*-axis (2 mm sections), although here they represent the pH gradient throughout the length of the gel, versus radioactivity on the *y*-axis. A peak in either data indicates that the label has covalently attached to a membrane protein. Results from unprotected vesicles are shown in conjunction with substrate-protected studies. These sets of data from the different conditions are normalised to the same initial radioactivity content in the sample to allow results to be directly compared.

Label incorporation by a membrane protein is expressed as the percentage of radioactivity bound, with respect to the initial radioactivity content, and also reported is the percentage inhibition of labelling caused by substrate preincubation. Finally the amount of [4-azido-3,5-^{3}H-D-Phe]-L-Ala covalently bound to the protein is calculated.

5.4 Photoaffinity labelling of BLMV

BLMV were photoaffinity labelled with [4-azido-3,5-^{3}H-D-Phe]-L-Ala in the presence or absence of either D-Phe-L-Gln or its constituent amino acids, on the basis that compounds which compete with the label for binding to the active site of proteins should decrease the extent of labelling. A representative example of the results is shown in figure 5.2. The *x*-axis in this graph represents a decrease in molecular weight, proceeding from left to right, through the length of the rod gel.

A definitive radioactive peak in the data indicates that a membrane protein has been specifically labelled by the dipeptide derivative. However, label binding

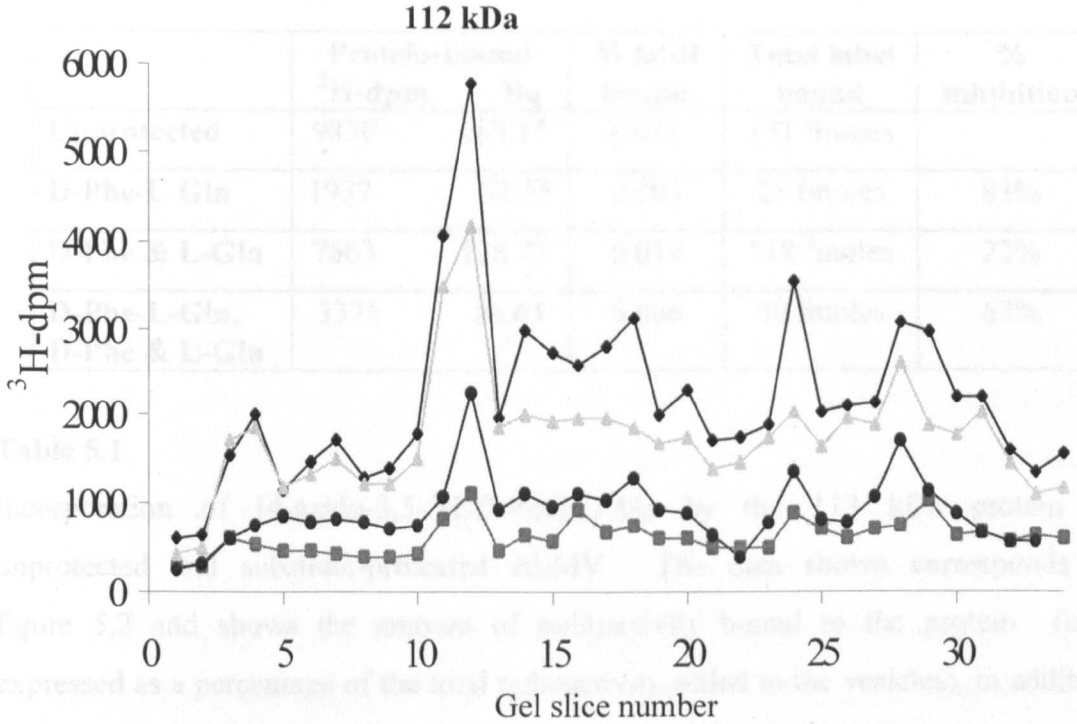

Slice number	Labelling ratio
11	3.63
12	12.64
14	5.1
18	5.1
24	4.98
28	3.0

Figure 5.2

Representative result of photoaffinity labelling of BLMV at pH 5.5 with [4-azido-3,5-^{3}H-D-Phe]-L-Ala followed by SDS-PAGE. Labelling was performed within four different environments; unprotected (diamonds) and protected by D-Phe-L-Gln (squares), D-Phe and L-Gln (triangles) or both peptide and amino acids (circles), all at 16.7 mM. The *x*-axis of gel slice number represents a decrease in molecular weight from left to right, down the rod gel, and the *y*-axis shows label incorporation by a membrane protein. A peak demonstrates that a protein has bound the radioactive label. The labelling ratio represents the proportion of radioactivity bound to an unprotected protein compared to protein protected by the dipeptide:- a large ratio indicates a higher degree of substrate-inhibitable label interaction.

	Protein-bound ^{3}H-dpm	Bq	% label bound	Total label bound	% inhibition
Unprotected	9830	165.15	0.018	151 fmoles	
D-Phe-L-Gln	1937	32.55	0.003	25 fmoles	83%
D-Phe & L-Gln	7663	128.75	0.014	118 fmoles	22%
D-Phe-L-Gln, D-Phe & L-Gln	3371	56.63	0.006	50 fmoles	67%

Table 5.1

Incorporation of [4-azido-3,5-^{3}H-D-Phe]-L-Ala by the 112 kDa protein in unprotected and substrate-protected BLMV. The data shown corresponds to figure 5.2 and shows the amount of radioactivity bound to the protein (also expressed as a percentage of the total radioactivity added to the vesicles), in addition to the amount of label bound to the protein. The inhibition caused by preincubation with a substrate is expressed as a percentage. The mean initial amount of radioactive label added to the four vesicle suspensions was 56 x 10^6 dpm (940.8 kBq).

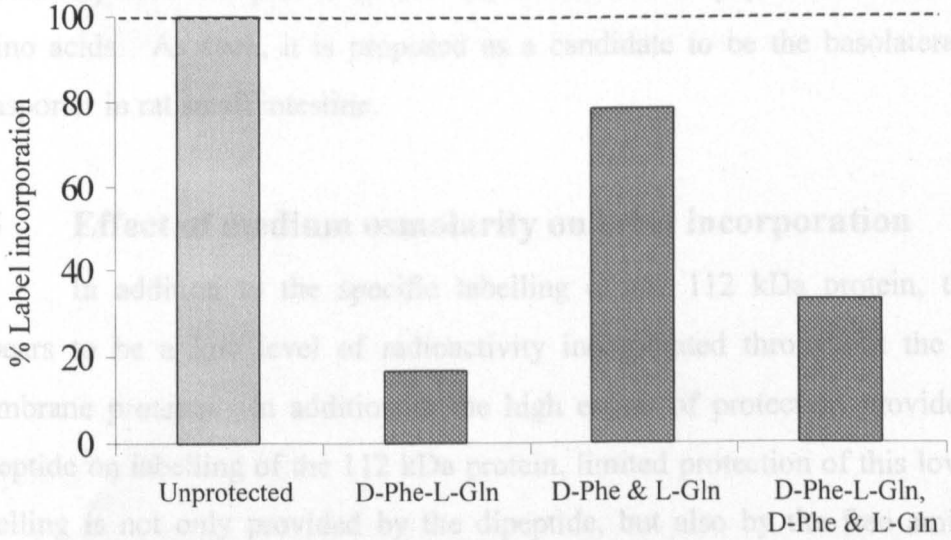

Figure 5.3

Inhibition of [4-azido-3,5-^{3}H-D-Phe]-L-Ala binding to the 112 kDa protein as a result of preincubation with substrates (each at 16.7 mM). Unprotected labelling (in the absence of substrates) is taken to be 100% incorporation. The degree by which the substrates inhibit labelling indicates the preferred nature of substrate with which the membrane protein interacts.

ratios for each of the peaks in figure 5.1 were calculated (shown in the subsequent table) to determine which protein in the membrane demonstrated maximal substrate-inhibitable labelling. Pre-incubation with the dipeptide strongly inhibited label incorporation by the protein contained within slice number 12, but free amino acids had very little effect. The dipeptide inhibits 83% of label binding (table 5.1 and figure 5.3) whereas the amino acids provide very little protection (22%). Interestingly, pre-incubation with both the dipeptide and amino acids provides slightly less protection of labelling than the dipeptide alone (67%). Repetitive analysis over a series of identical experiments of the migration distance of the labelled protein, in comparison to standard molecular weight markers, by silver stained SDS-PAGE slab gels indicates it has a molecular weight of 112 ± 2 kDa (n = 30). A representative example of this data analysis is shown in figure 5.4. It should be noted that a single band is present in the peak sample, suggesting an individual protein species has been photoaffinity labelled.

The pattern of [4-azido-3,5-^{3}H-D-Phe]-L-Ala incorporation by the basolateral membrane is highly reproducible. The 112 kDa protein is dominantly and consistently labelled, plus it specifically interacts with peptides but not with free amino acids. As such, it is proposed as a candidate to be the basolateral peptide transporter in rat small intestine.

5.5 Effect of medium osmolarity on label incorporation

In addition to the specific labelling of the 112 kDa protein, there also appears to be a low level of radioactivity incorporated throughout the range of membrane proteins. In addition to the high extent of protection provided by the dipeptide on labelling of the 112 kDa protein, limited protection of this low level of labelling is not only provided by the dipeptide, but also by the free amino acids, although the reason for this is not clear. It was initially thought that the high concentrations of the substrates used might be the causing factor in inhibition of labelling. This theory was investigated by performing a series of experiments with the vesicles in different medium osmolarity, using mannitol at different concentrations in an unprotected vesicle suspension. The concentrations of mannitol reflected the high substrate concentrations used in the protection studies; 16.7 mM

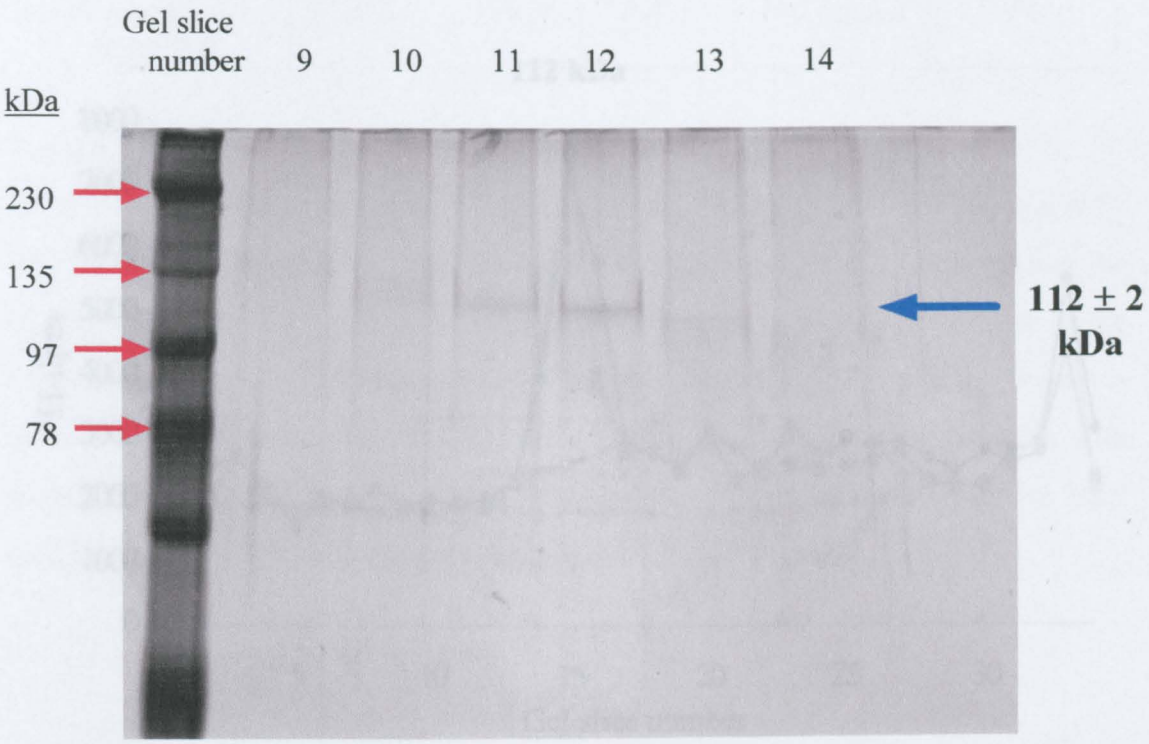

Figure 5.4

SDS-PAGE analysis of samples forming the radioactive peak (slices 11 & 12), plus surrounding gel slices, to determine the molecular weight of the labelled protein. The gel slices coincide with the unprotected BLMV separated by SDS-PAGE in rod gels shown in figure 5.2. Samples were electrophoresed on a 10% gel (70*80*0.75 mm) and the bands visualised by silver staining. Repeated analysis of the labelled protein with reference to known standards indicates an apparent molecular weight of 112 ± 2 kDa (n = 30).

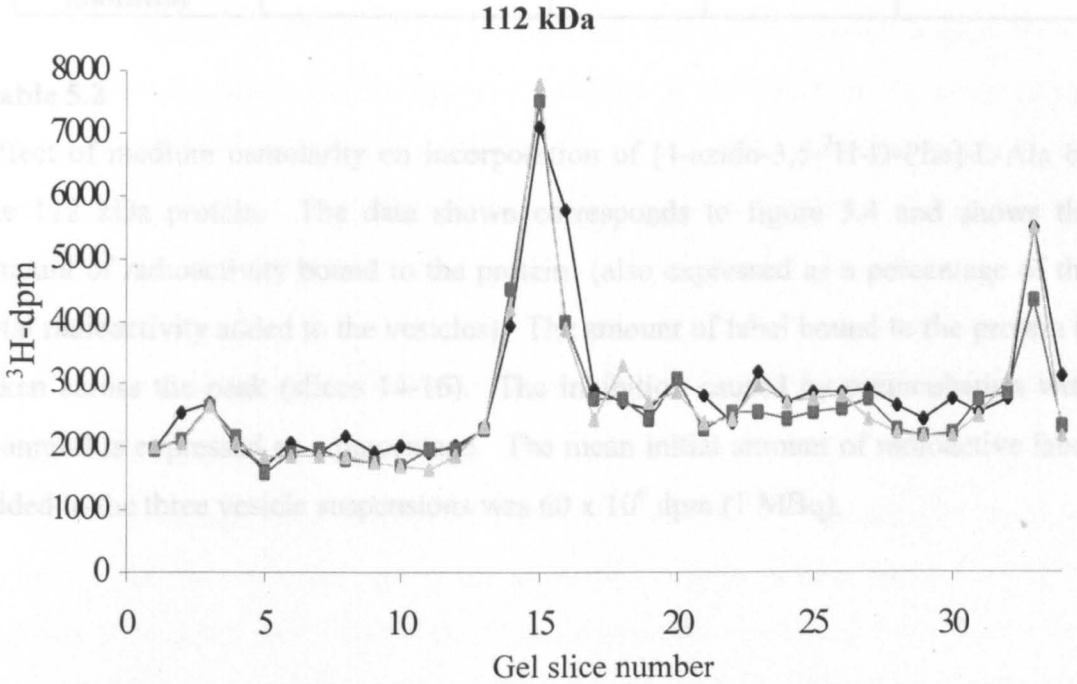

Figure 5.5

The effect of osmolarity on photoaffinity labelling is demonstrated by preincubation of BLMV in mannitol, in equivalent concentrations to that of the substrates shown in figure 5.2. Vesicles were labelled in an unprotected environment (diamonds) and in the presence of 16.7 mM mannitol (squares) or 33.4 mM mannitol (triangles) before SDS-PAGE electrophoresis. The *x*-axis of gel slice number represents a decrease in molecular weight from left to right, down the rod gel, and the *y*-axis shows label incorporation by a membrane protein. A peak demonstrates that a protein has bound the radioactive label.

	Protein-bound ^{3}H-dpm	Bq	% label bound	Total label bound	% inhibition
Unprotected	12,859	216.03	0.021	176 fmoles	
16.7 mM mannitol	11,517	193.49	0.019	160 fmoles	9%
33.4 mM mannitol	11,685	196.31	0.019	160 fmoles	9%

Table 5.2

Effect of medium osmolarity on incorporation of [4-azido-3,5-^{3}H-D-Phe]-L-Ala by the 112 kDa protein. The data shown corresponds to figure 5.4 and shows the amount of radioactivity bound to the protein (also expressed as a percentage of the total radioactivity added to the vesicles). The amount of label bound to the protein is taken across the peak (slices 14-16). The inhibition caused by preincubation with mannitol is expressed as a percentage. The mean initial amount of radioactive label added to the three vesicle suspensions was 60 x 10^6 dpm (1 MBq).

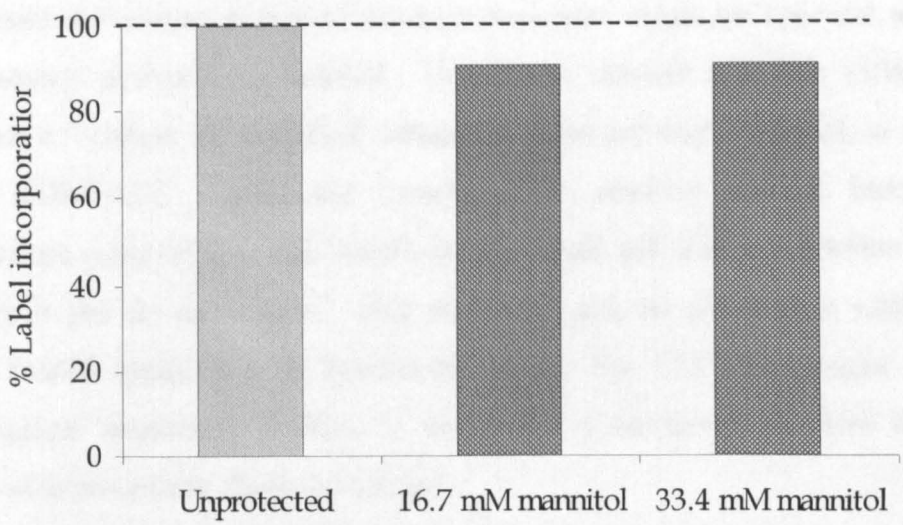

Figure 5.6

Effect of medium osmolarity on inhibition of [4-azido-3,5-^{3}H-D-Phe]-L-Ala binding to the 112 kDa protein. Unprotected labelling is taken to be 100% incorporation. The degree by which the presence of mannitol inhibits labelling is negligible.

representing the dipeptide, and 33.4 mM representing the amino aicds. The results of this study are shown in figure 5.5.

It is evident that incubation of the vesicles in high concentrations of mannitol did not affect labelling of the 112 kDa membrane protein; only 9% inhibition at the 112 kDa protein was observed (figure 5.6, table 5.2). In addition, there was no difference in radioactivity in the remainder of the proteins.

Therefore, medium osmolarity does not affect label incorporation by the 112 kDa protein, and so the inhibition of labelling by the dipeptide must be entirely due to a substrate-active site interaction. These data demonstrate that the abolishment of label incorporation by the 112 kDa protein, due to the presence of the dipeptide, is substrate-specific.

5.6 Two-dimensional electrophoresis of the photoaffinity labelled basolateral membrane protein

Two-dimensional electrophoresis (2-DE) is an extremely powerful technique for the isolation and purification of a single protein from a complex mixture. A single protein band in the silver-stained slab gel (figure 5.4) suggests that the radioactive peak sample contains a single protein species. However, it cannot be assumed that another protein of the same molecular weight isn't present, although not necessarily photoaffinity labelled. In order to achieve complete isolation of the protein of interest, an additional separation technique was employed, in conjunction with SDS-PAGE. Isoelectric focusing (IEF) resolves proteins based on their isoelectric point (pI), i.e. the protein focuses at the pH, within a gradient in a gel, at which it has no net charge. This step was used, in conjunction with the initial SDS-PAGE separation, to specifically isolate the 112 kDa protein from other basolateral membrane proteins in rod gels. Collectively, the two distinct, but step-wise procedures, form a 2-DE gel.

The first dimension in the 2-DE procedure was to identify and separate the radioactively labelled 112 kDa protein from other proteins by the principal method of SDS-PAGE, as before. However, a relatively large quantity of protein was required to take through each of the different steps of the 2-DE process, and so multiple (identical) vesicle suspensions were labelled simultaneously, either in an unprotected state or protected by D-Phe-L-Gln. The membranes were subjected to SDS-PAGE in

rod gels as before, and labelled proteins were detected by scintillation counting. The results from the series of identical unprotected labelling experiments are shown in figure 5.7 (data is not shown for the equivalent dipeptide-protected vesicles).

The samples from the gel slices that contained the 112 kDa protein (from the unprotected and dipeptide-protected vesicles) were pooled individually and concentrated in preparation for the next stage.

The second dimension in the 2-DE gel was IEF. The concentrated aliquots of the unprotected and dipeptide-protected labelled proteins were electrophoresed through an internal pH gradient of 4 to 7, in separate rod gels. A representative example of the results from this step is shown in figure 5.8.

The unprotected radioactively labelled 112 kDa protein focuses at an isoelectric point of 6.5; a sharp definitive peak indicates excellent resolution within the pH gradient. There is another smaller peak, again at pH 6.5, which corresponds to the same 112 kDa protein, which was protected by the dipeptide during labelling. Pre-incubation with D-Phe-L-Gln appears to provide 41% protection of labelling.

Samples were taken from these two discrete peaks and subjected to SDS-PAGE in a 10% slab gel for molecular weight analysis. The silver stained gel is shown in figure 5.9. Protein bands at the correct molecular weight indicate that the 112 kDa protein is present in both peaks.

The two radioactive peak samples contain a single band, suggesting that an individual protein is present after the 2-DE separation. It is very unlikely that two or more proteins in a mixture would possess identical molecular weights and isoelectric points, and therefore it appears that the 112 kDa protein has been successfully isolated as an individual species.

The two steps in the 2-DE procedure were also performed in reverse order, i.e. IEF prior to SDS-PAGE, using combined concentrated samples as before. Similar radioactive peaks at 112 kDa and pI 6.5 were obtained irrespective of the order of the dimensions of separation.

Isoelectric focusing of [4-azido-3,5-^{3}H-D-Phe]-L-Ala was also performed in order to eliminate the possibility of the free label forming the radioactive peak seen in the IEF stage of 2-DE of the labelled protein, although any unbound/loosely bound label would have been washed from the sample during the labelling procedure, or eluted from the preliminary SDS-PAGE gels. The label focuses at a pI of 6.0

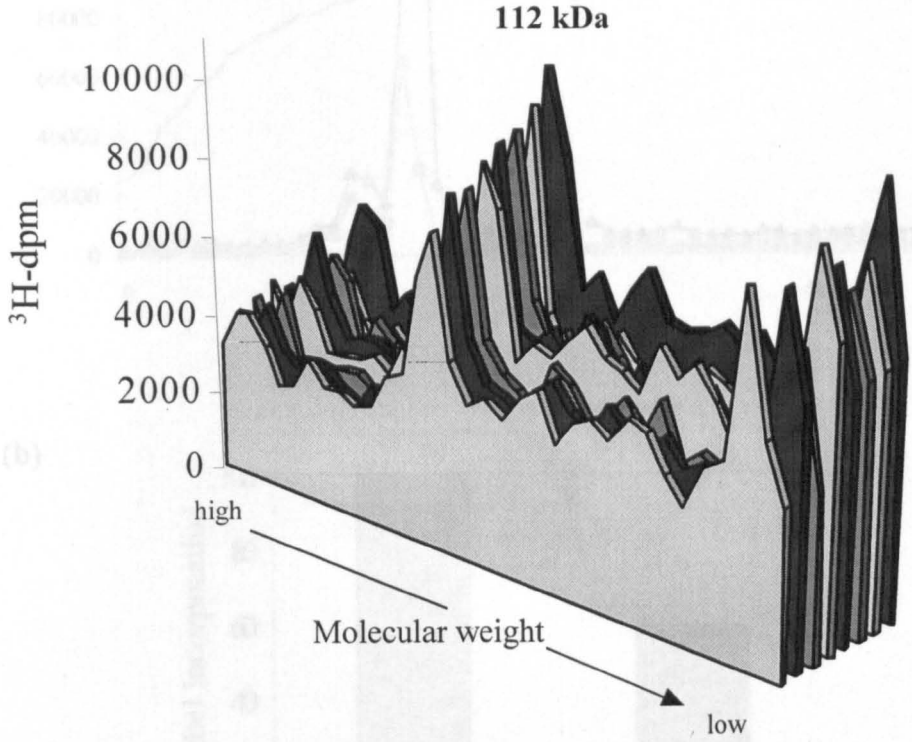

Figure 5.7

SDS-PAGE of a number of identical photoaffinity labelled (unprotected) BLMV. The samples from the peak containing the 112 kDa protein were pooled and concentrated to 50 µl in preparation for the next step in the 2-DE procedure within rod gels.

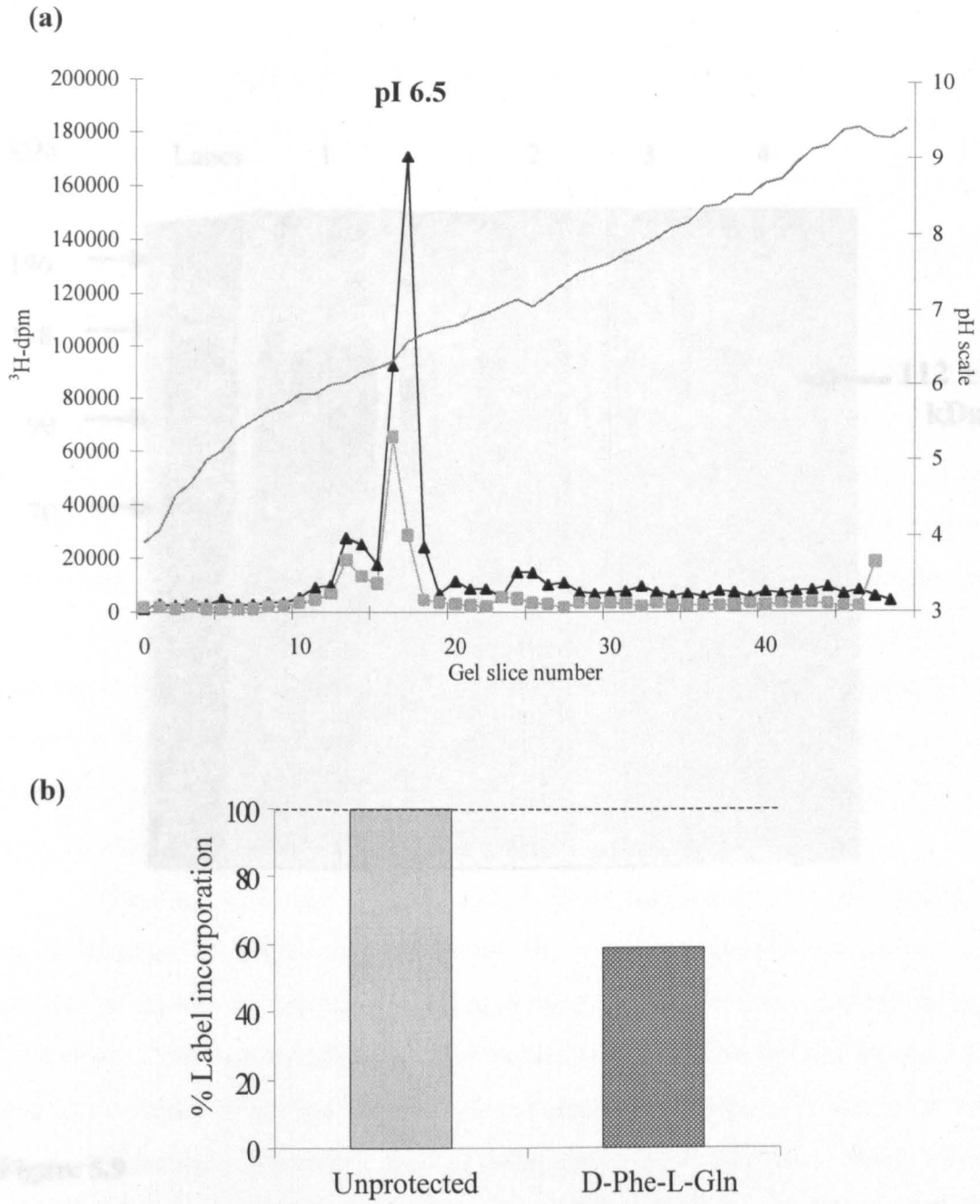

Figure 5.8

Isoelectric focusing (a) of the photoaffinity labelled 112 kDa protein isolated from SDS-PAGE of unprotected BLMV (triangles) and from vesicles protected by 16.7 mM D-Phe-L-Gln (squares). The *x*-axis depicts the gel slice number of the rod gels and the *y*-axis show label incorporation by a membrane protein and the pH gradient throughout the gels (also depicted by the smooth line). A peak represents label binding by a protein. Also shown is the extent of inhibition caused by pre-incubation with the dipeptide (b); unprotected labelling is taken to be 100%.

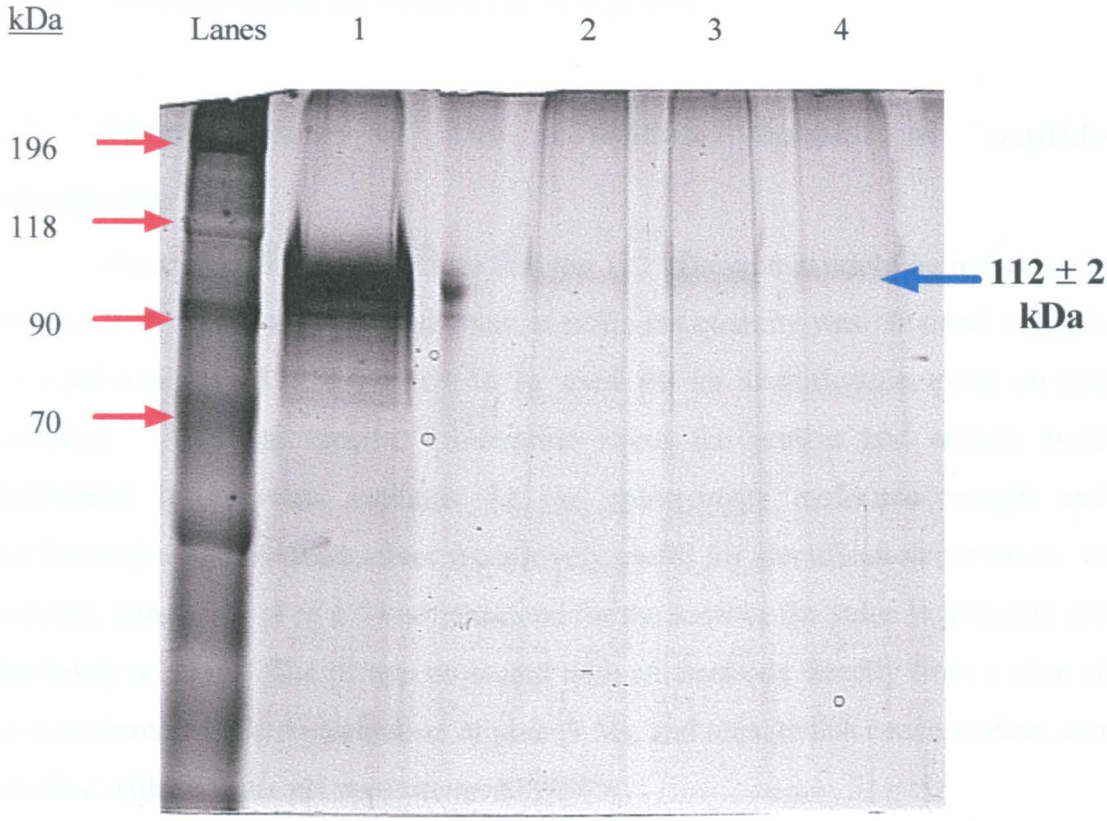

Figure 5.9

SDS-PAGE analysis of the samples forming the final radioactive peak following 2-DE of the labelled 112 kDa protein in rod gels. Lane 1 is an aliquot of the concentrated protein isolated from the first dimension (SDS-PAGE) (see figure 5.7) which was then run in the second (IEF) dimension. Lanes 2-4 are samples forming the peaks obtained from the final IEF stage (see figure 5.8); lanes 2 and 3 are from the peak in the unprotected vesicles, and lane 4 is the peak sample from the vesicles protected by D-Phe-L-Gln. Samples were electrophoresed on a 10% gel (70*80*0.75 mm) and the bands visualised by silver staining. Repeated analysis of the labelled protein with reference to known standards indicates an apparent molecular weight of 112 ± 2 kDa (n = 30).

(figure 5.10), which is considerably different from the pI of the labelled protein. Therefore, the radioactive peak detected in the 2-DE separation of the membrane proteins is entirely due to the labelled 112 kDa protein.

5.7 Identification of the candidate basolateral peptide transporter

Once it had been determined that the 112 kDa protein could be individually isolated from the basolateral membrane, a sufficient quantity was obtained to begin principal analysis of its sequence, to be used for its identification using on-line databases. Although specific information about the protein had already been determined by previous methods, i.e. an approximate molecular weight and isoelectric point, these themselves are not very useful for identification purposes. In addition, although a pI of 6.5 was measured for the protein, the value is probably not absolutely accurate. The pI was measured with an electrode directly from a slice of gel containing a high concentration of urea (9 M), and urea, at this concentration, can interfere with accurate pH measurement.

The most rapid and reliable way to obtain initial sequence information to use in database searches, which requires the minimum quantity of protein and extracts the maximum data possible, is to convert the protein into a peptide mixture for analysis. This was initially attempted on the protein sample isolated by the 2-DE method described in section 5.6, but the presence of contaminants interfered with subsequent analysis. Therefore, another technique of 2-DE was used, which utilised an immobilised pH gradient. This produces a single spot in a second dimension slab gel, containing a pure sample of protein. However, sequence analysis requires a substantial amount of protein, therefore 2-DE was performed using a combined and concentrated sample of relatively pure protein, rather than a crude BLMV sample, to ensure the protein was present in the necessary quantity.

5.7.1 Isolation and purification of the 112 kDa protein from membrane vesicles

The primary step towards sequence analysis was to isolate and purify a labelled sample of the 112 kDa protein, by simultaneous electrophoresis of a number of SDS-PAGE rod gels. Several unprotected photoaffinity-labelled BLMV samples

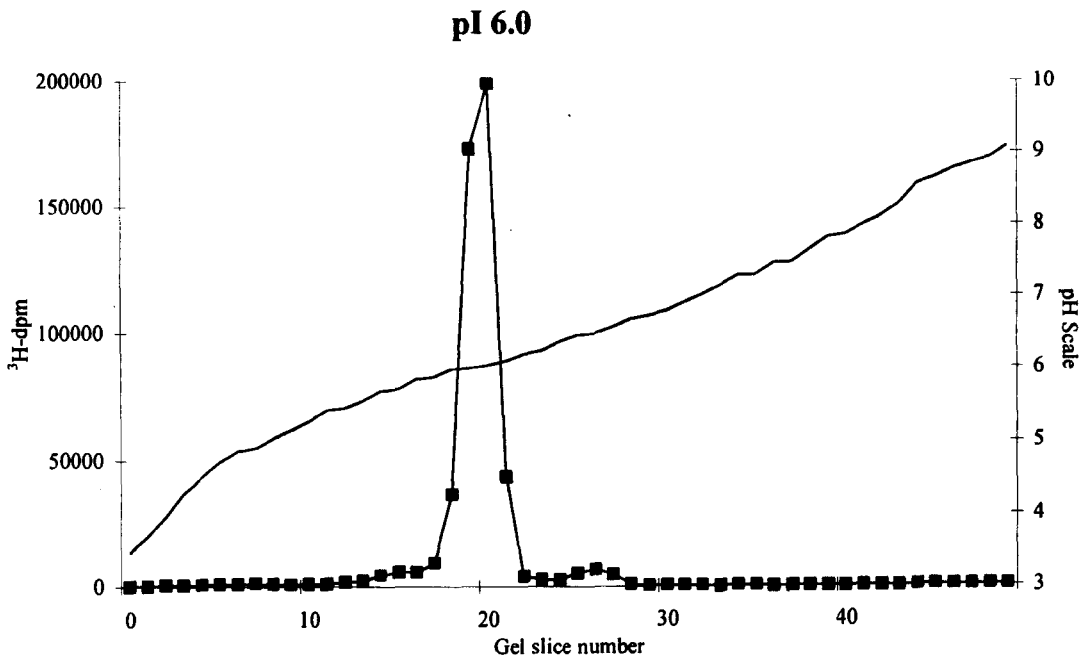

Figure 5.10

Isoelectric focusing of the photoaffinity label ([4-azido-3,5-^{3}H-D-Phe]-L-Ala) in a rod gel. 1 µl of label was electrophoresed through the gel; this is equivalent to 2.2 x 10^6 dpm (37 kBq) of radioactivity. The *x*-axis depicts the gel slice number and the *y*-axis show radioactivity detected and the pH gradient throughout the gel (also depicted by the smooth line). The peak shows the exact pH in the gradient where the label focuses (pI 6.0).

were run simultaneously, as before (section 5.6), to obtain a concentrated protein sample.

The final concentrated aliquot was analysed to determine the amount of protein contained. For this, a calibration curve (50-400 ng) was constructed within a 10% SDS-PAGE slab gel using BSA as the standard, in conjunction with an aliquot (3 µl) of the final protein sample (figure 5.11a). The gel was electrophoresed and then silver stained. The relative density of the BSA protein bands to the 112 kDa protein band was used to calculate the amount present in that small aliquot (figure 5.11b). This value was then extrapolated to the total volume of the protein sample.

The silver stained BSA standard curve was linear in the protein range used ($r^2 = 0.998$). The amount of protein estimated to be in a 3 µl aliquot of the 112 kDa sample was 205 ng. The total volume of the sample was approximately 120 µl, therefore the total amount of protein was 8.2 µg. This is equivalent to 7.32×10^{-11} moles (73 pmoles) of protein. This concentration of protein was extracted from 20 initial rod gels, therefore the amount that was obtained from 200 µg BLMV (starting material for one gel) was approx. 410 ng (3.65 pmoles) of 112 kDa protein. This is equivalent to approx. 0.002% of the total amount of protein located in the basolateral membrane. It is clear that the 112 kDa protein is only a minor constituent of the total basolateral membrane proteins. As such, the highly consistent, and individual, labelling of this small quantity indicates that the interaction of the dipeptide label with the protein is extremely specific.

5.7.2 2-DE of the 112 kDa protein using an immobilised pH gradient

The concentrated, labelled 112 kDa protein sample was subjected to 2-DE in a non-linear pH gradient from 3 to 10 (a non-linear gradient means that the scale between approx. pH 4 to 8 is 'stretched', or more resolved, to allow better separation within this range). This non-linear gradient was used for a more accurate resolution surrounding the measured pI of the labelled protein. The second dimension involved a standard SDS-PAGE separation within a vertical slab gel, followed by staining with Colloidal coomassie blue. The Colloidal stain was used in replacement of silver stain for two main reasons. Firstly, and most importantly, silver staining can interfere with sequence analysis and secondly, it is generally accepted that if the protein spot can be

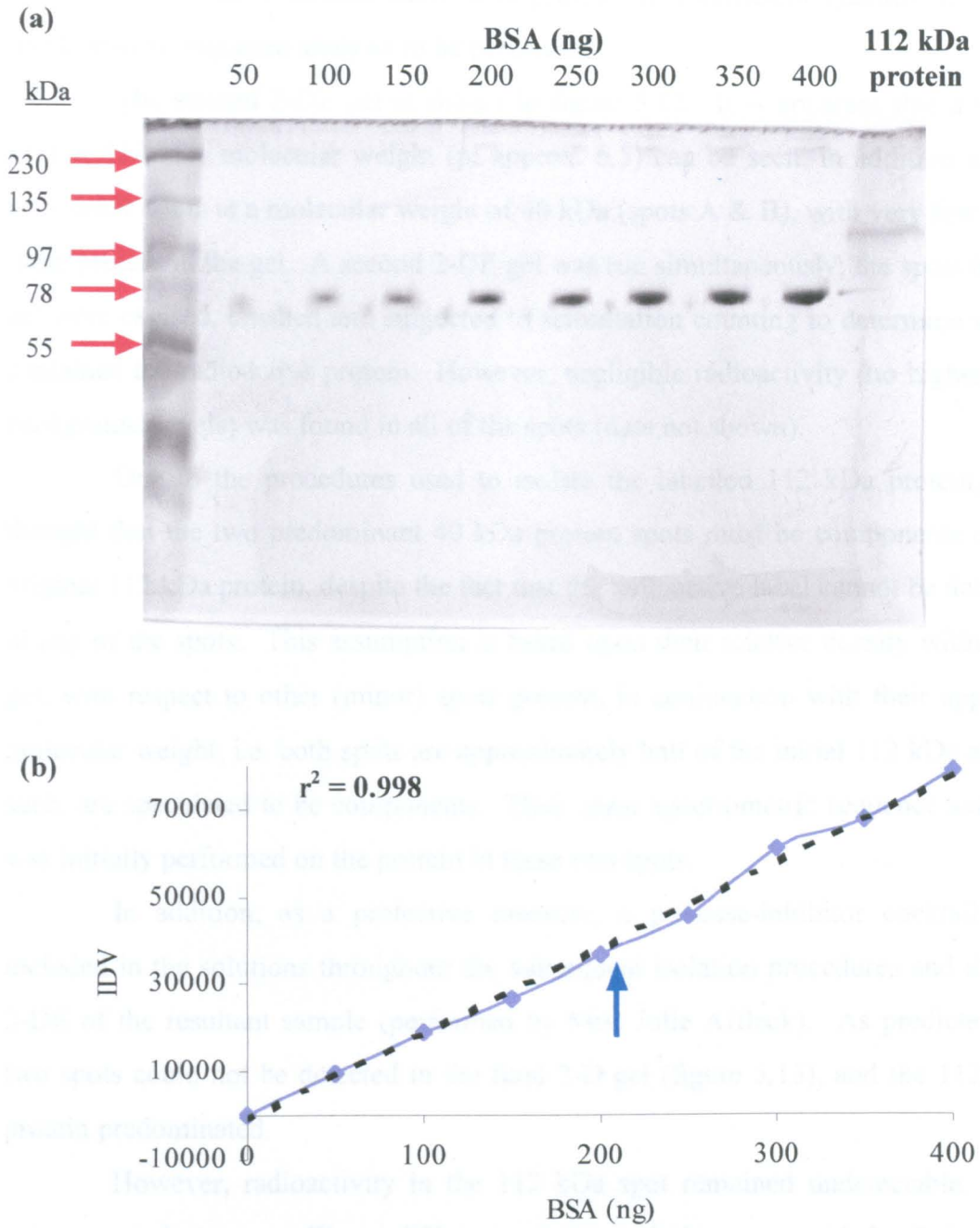

Figure 5.11

The amount of 112 kDa protein in the final concentrated sample was calculated using a calibration curve of BSA in a silver stained SDS slab gel (a). The relative intensity of the BSA bands (b) was used to estimate the amount of 112 kDa protein in the gel by measuring the integrated density value (IDV) using a spot densitometry program in a gel documentation system (AlphaEase™ version 3.3). The standard curve of BSA is shown by the continuous line and the dashed line shows the trendline of the curve. The IDV of the 112 kDa protein aliquot (3 µl), and therefore the amount present in the gel, is indicated by the arrow.

visualised with the Colloidal stain, it is present in a sufficient quantity for mass spectrometric sequence analysis to be performed.

The stained 2-DE gel is shown in figure 5.12. It is apparent that a minor spot at 112 kDa molecular weight (pI approx. 6.5) can be seen, in addition to two very dense spots at a molecular weight of 40 kDa (spots A & B), with very few other spots present in the gel. A second 2-DE gel was run simultaneously; the spots in this gel were excised, crushed and subjected to scintillation counting to determine which contained the radioactive protein. However, negligible radioactivity (no higher than background levels) was found in all of the spots (data not shown).

Due to the procedures used to isolate the labelled 112 kDa protein, it is thought that the two predominant 40 kDa protein spots must be components of the original 112 kDa protein, despite the fact that the radioactive label cannot be detected in any of the spots. This assumption is based upon their relative density within the gel, with respect to other (minor) spots present, in conjunction with their apparent molecular weight, i.e. both spots are approximately half of the initial 112 kDa and as such, are speculated to be components. Thus, mass spectrometric sequence analysis was initially performed on the protein in these two spots.

In addition, as a protective measure, a protease-inhibitor cocktail was included in the solutions throughout the subsequent isolation procedures and during 2-DE of the resultant sample (performed by Mrs. Julie Affleck). As predicted the two spots could not be detected in the final 2-D gel (figure 5.13), and the 112 kDa protein predominated.

However, radioactivity in the 112 kDa spot remained undetectable. The next approach was to utilise a different staining technique to avoid the fixing step that was required for the Colloidal blue stain, which was thought to prevent elution of the protein from the gel prior to scintillation counting. A negative stain (zinc) was performed, but again radioactivity could not be detected, possibly due to quenching by the stain. A final approach to demonstrate that the protein isolated was the intial protein that was specifically labelled from vesicles, was to perform IEF on the IPG strip, section the strip and subject the slices to scintillation counting. A peak of radioactivity was detected at the precise point in the IPG strip that corresponded to the pI at which the 112 kDa protein focused following the second dimension (data not shown).

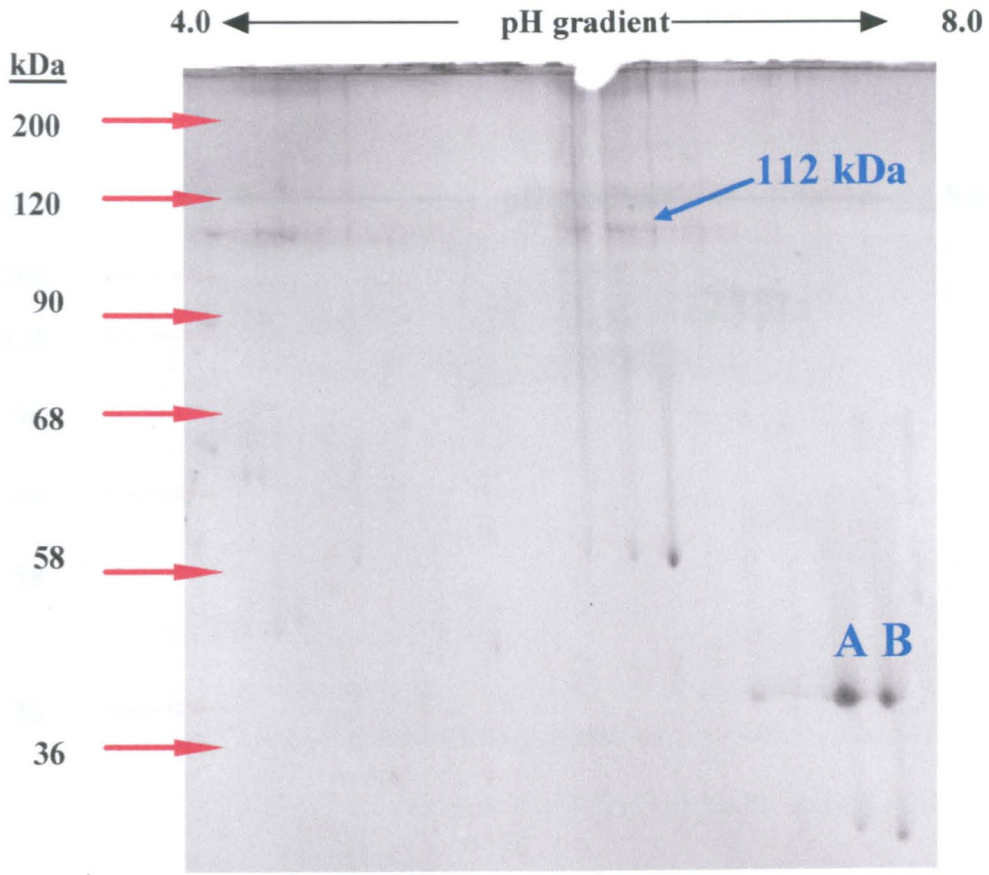

Figure 5.12

Two-dimensional electrophoresis of a concentrated sample of 112 kDa protein from the basolateral membrane. First dimension (*x*-axis); IEF in an immobilised dry strip (IPG, Pharmacia) pH 3-10, non-linear (range from pH 4-8 shown), second dimension (*y*-axis); 12% SDS-PAGE gel, stained with Colloidal Coomassie blue (Sigma). A spot at 112 kDa cannot be detected, but the two 40 kDa spots (A & B) are thought to be proteolytic breakdown products originating from the 112 kDa protein.

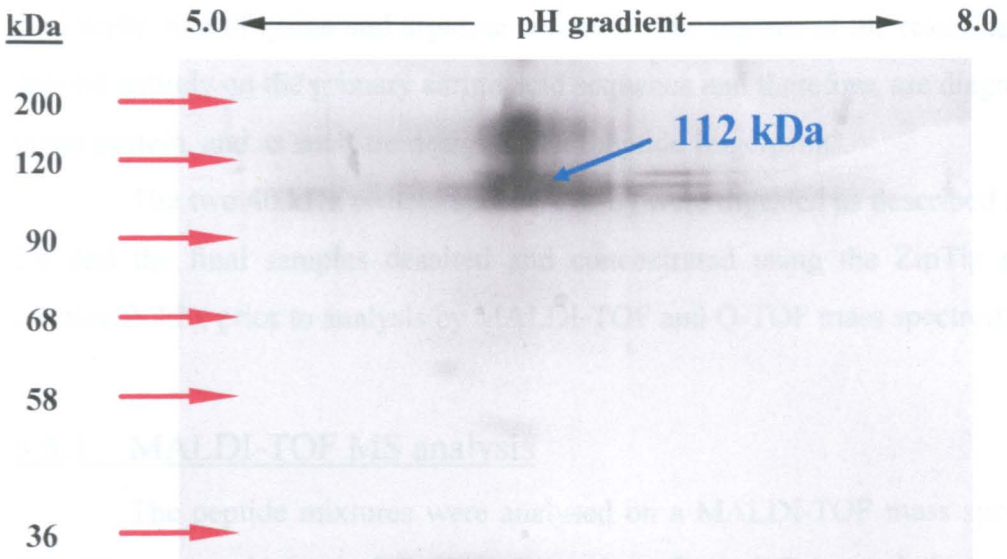

Figure 5.13

Two-dimensional electrophoresis of a concentrated sample of the photoaffinity labelled protein isolated from the basolateral membrane; a protease-inhibitor cocktail was present throughout the isolation and electrophoresis stages to prevent proteolytic breakdown. In reference to figure 5.12, the two proteolytic products (spots A & B at 40 kDa) are not apparent, whilst the major spot at 112 kDa is preserved intact. For details of 2-DE see figure 5.12.

Sequence analysis of the labelled protein could now be performed on a protein at the correct molecular weight.

5.8 Mass spectrometric sequence analysis

As mentioned in section 5.7, the most efficient method of obtaining initial sequence information of a protein is to digest it with trypsin to produce a series of peptide fragments. Trypsin cleaves the polypeptide backbone of proteins at the carboxylic side of lysine and arginine residues. The masses of the resulting peptides depend entirely on the primary amino acid sequence and therefore, are diagnostic of a given protein, and as such are designated a 'peptide fingerprint'.

The two 40 kDa protein spots (A & B) were digested as described in section 2.6 and the final samples desalted and concentrated using the ZipTip procedure (section 2.7.2), prior to analysis by MALDI-TOF and Q-TOF mass spectrometry.

5.8.1 MALDI-TOF MS analysis

The peptide mixtures were analysed on a MALDI-TOF mass spectrometer (PE Biosystems Voyager DE-STR) located at Central Science Laboratory, Sand Hutton, York, with the invaluable help and tuition from Dr. David Ashford (Biology department, University of York).

The peptide mixture was analysed in reflector mode using delayed extraction, which together provided a greater resolution and, therefore, higher degree of accuracy in the data; usually better than ± 0.5 Da in the mass range studied. The excellent resolution of the data allows the detection of the isotopic peaks of the peptides rather than an average mass, i.e. the ^{13}C content of the peptide can be observed. An example of an isotopic peak pattern from one of the peptide fragments (2066.28 Da in spot A) is shown in figure 5.14. A close examination of the individual peptide peaks provides confidence that the component isotopic peaks are well resolved, the monoisotopic peak is correctly defined and the data is therefore accurate. Use of the monoisotopic peak masses in database searches is considerably more reliable than using the average masses of the peptides.

The main spectrum resulting from MALDI-TOF analysis of spot A is shown in figure 5.15, and the spectrum for spot B in figure 5.16, although additional spectra were also obtained (data not shown). Analyses of different dilutions were performed

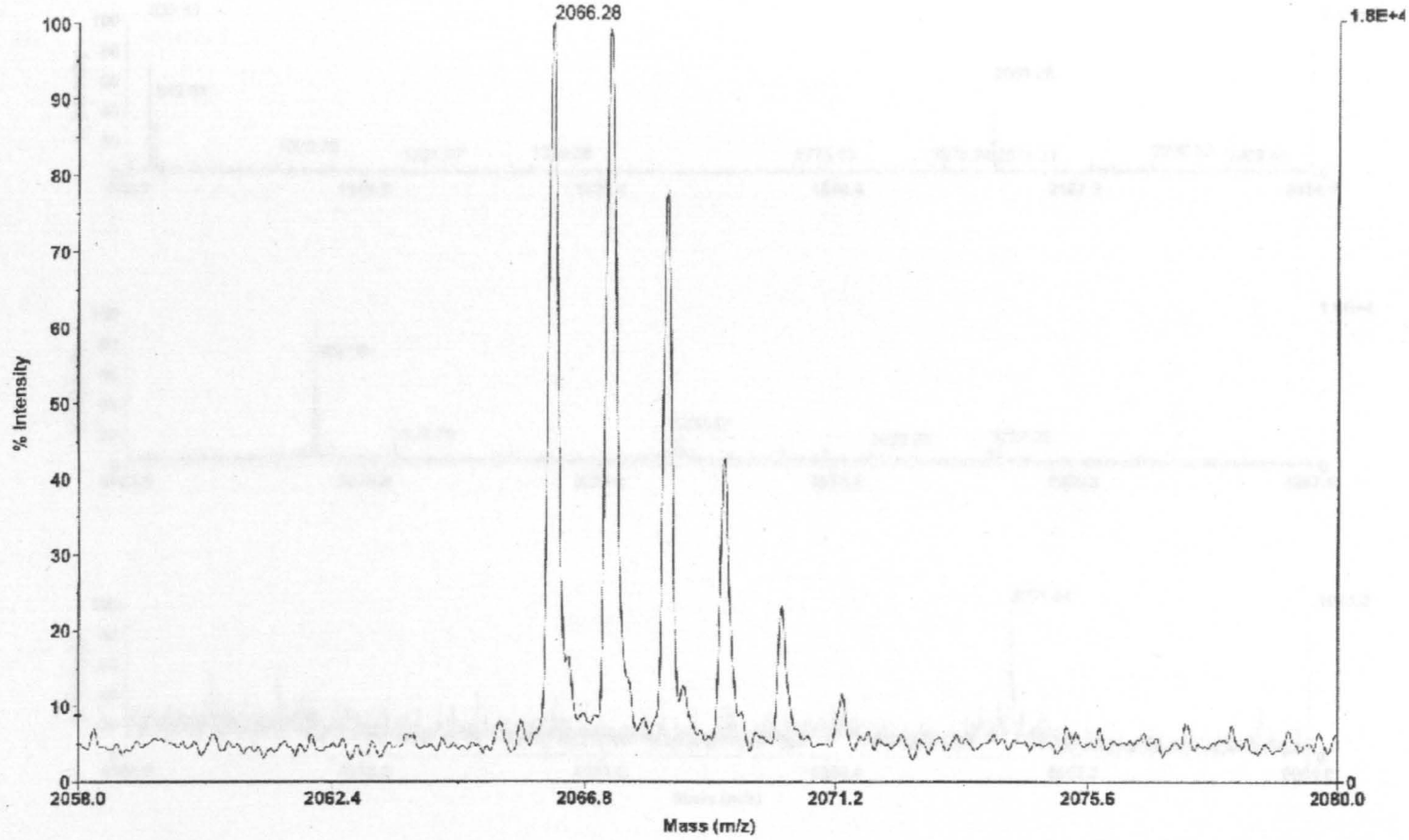

Figure 5.14

Analysis of tryptic peptides in reflector mode by MALDI-TOF MS provides very high resolution, enough to observe the isotopic peaks of a single peptide (2066.28 Da from spot A). The isotopic peaks represent the ^{13}C content of the peptide and sequentially differ in mass by 1 Da. The monoisotopic peak mass is used in database searches for the accurate identification of proteins.

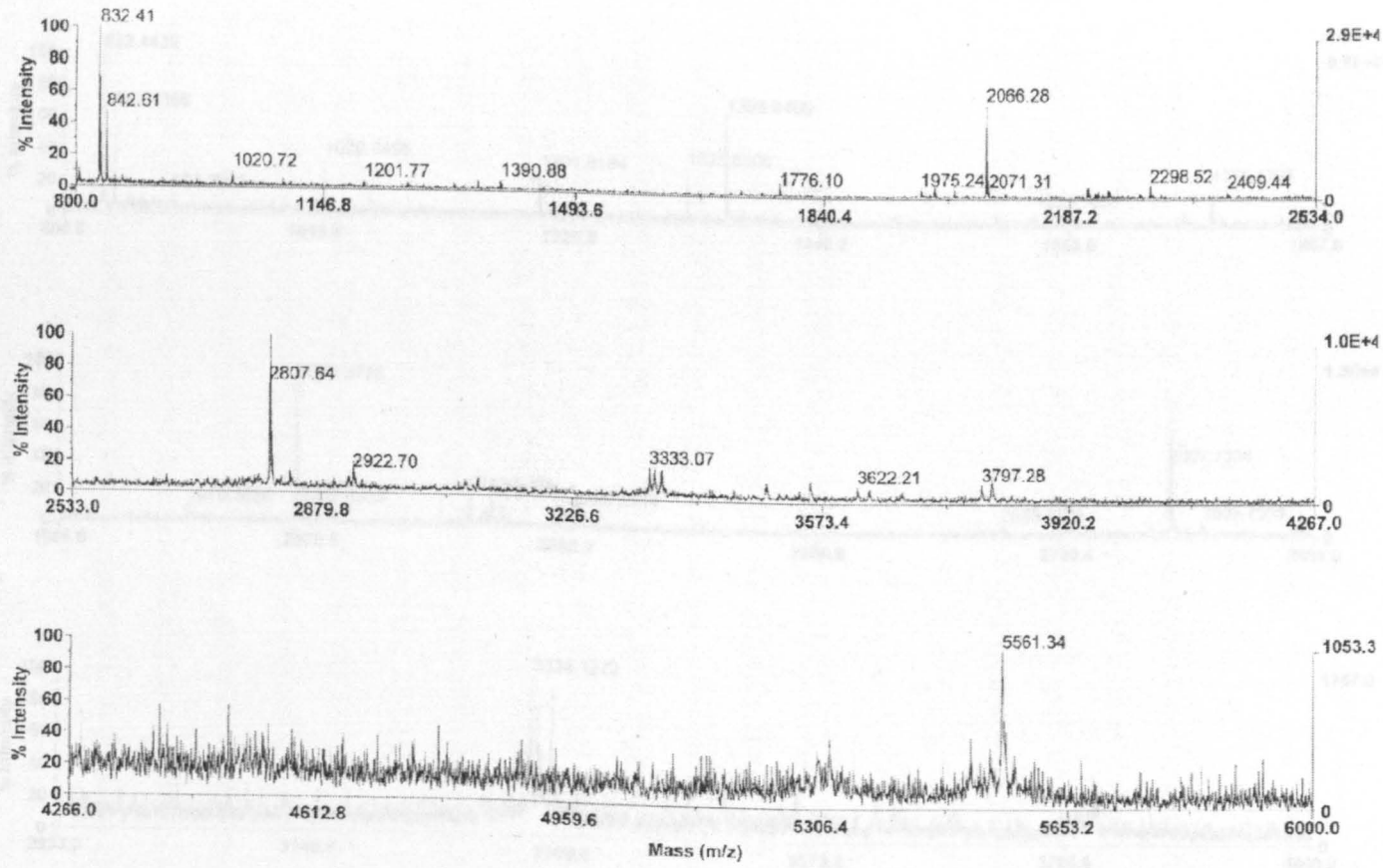

Figure 5.15

MALDI-TOF MS analysis, in reflector mode, of the tryptic digest products of spot A (see figure 5.12). The *x*-axis represents the mass-to-charge ratio and the *y*-axis shows the peak intensity. Each peak signifies an individual peptide; not all peptides are labelled due to spatial limitations, a complete list of all peptides detected from spot A is given in table 5.3.

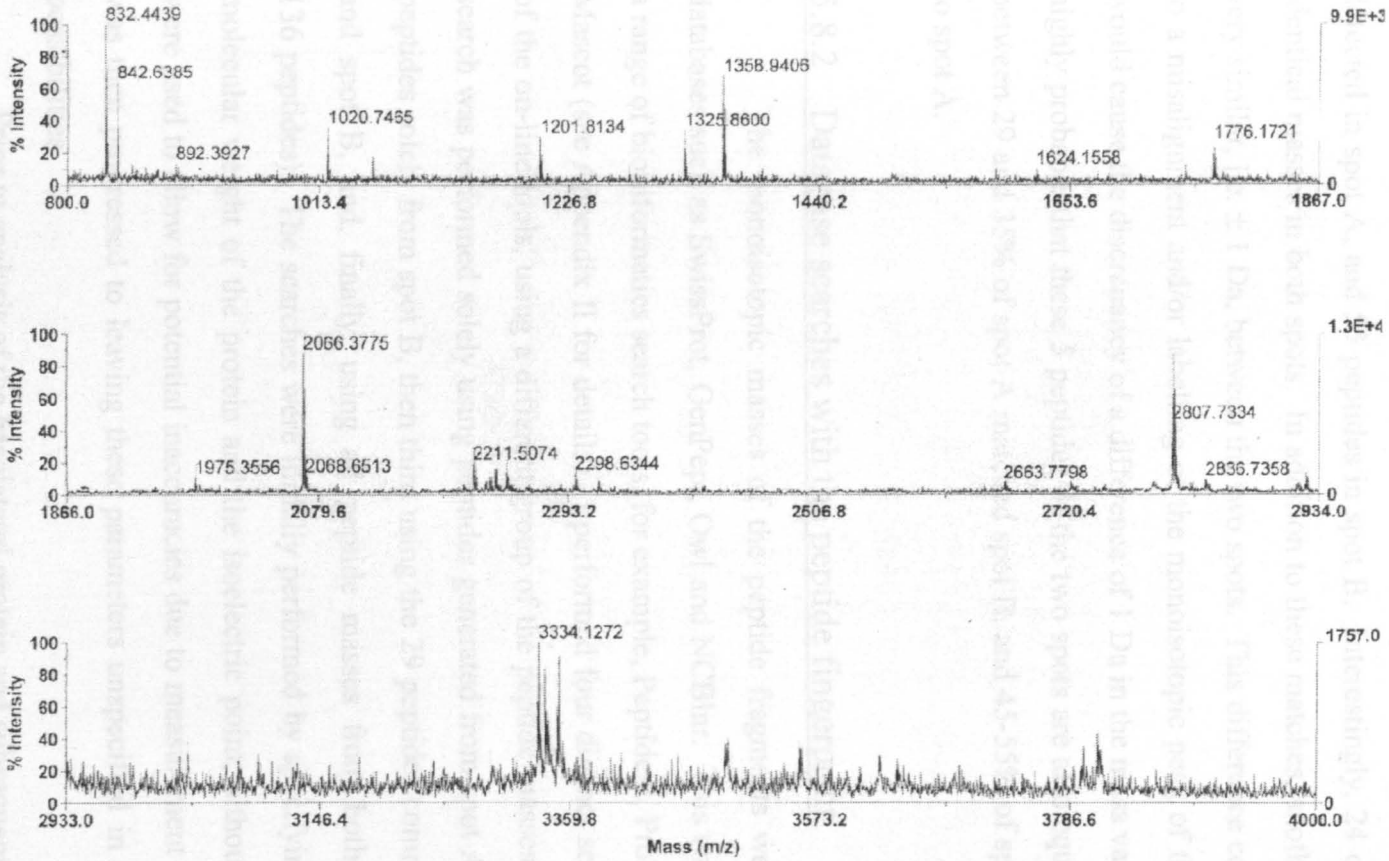

Figure 5.16

MALDI-TOF MS analysis, in reflector mode, of the tryptic digest products of spot B (see figure 5.12). The *x*-axis represents the mass-to-charge ratio and the *y*-axis shows the peak intensity. Each peak signifies an individual peptide; not all peptides are labelled due to spatial limitations, a complete list of all peptides detected from spot B is given in table 5.3.

to maximise detection of all peptide fragments present in the samples. Only the most intense peptide peaks are labelled on the spectra due to spatial limitations, i.e. a close association of adjacent peaks, but a summary of all the peptide masses generated from digestion of spots A and B are shown in table 5.3. A total of 83 peptides were detected in spot A, and 53 peptides in spot B. Interestingly, 24 of the peptides had identical masses in both spots. In addition to these matches, another 5 peptides were very similar, i.e. ± 1 Da, between the two spots. This difference could have been due to a misalignment and/or labelling of the monoisotopic peak of the peptides, which would cause the discrepancy of a difference of 1 Da in the mass values. As such, it is highly probable that these 5 peptides of the two spots are also equivalent. Therefore, between 29 and 35% of spot A matched spot B, and 45-55% of spot B corresponded to spot A.

5.8.2 Database searches with the peptide fingerprint

The monoisotopic masses of the peptide fragments were used to search databases such as SwissProt, GenPept, Owl and NCBInr. This was performed using a range of bioinformatics search tools, for example, PeptIdent, ProFound, MS-Fit and Mascot (see Appendix II for details). I performed four distinct searches within each of the on-line tools, using a different group of the peptide masses in each. The first search was performed solely using peptides generated from spot A, the second using peptides solely from spot B, then third using the 29 peptides common to both spot A and spot B, and, finally, using all peptide masses from both spots (a total of 136 peptides). The searches were initially performed by specifying the approximate molecular weight of the protein and the isoelectric point, although large variances were used to allow for potential inaccuracies due to measurement from gels, and this was then progressed to leaving these parameters unspecified in order to search all possibilities.

Prior to analysis of the basolateral protein and subsequent database searches, the same procedure was performed on a known protein to determine the reliability and precision of the combined techniques in its identification; the protein used was BSA. The monoisotopic peptide masses generated from an in-gel digest of BSA (data not shown) were used in searches to define the optimum parameters required to obtain an accurate positive match, which could then be extrapolated to searches for

Peptides found in spots A & B	Peptides found in spot A		Peptides found in spot B
832. 4	908.4851	2706.584	834.5177
842.6	922.5296	2721.606	844.6521
1020.7	924.4205	2777.684	855.3453
1058.7	949.5595	**2791.004**	870.3359
1201.8	970.4833	2826.665	876.4318
1325.8	1003.535	3334.151	892.414
1358.8	1008.403	3340.328	992.82
1776.1	1011.627	3352.034	1427.941
1975.3	1046.702	3364.307	1624.156
1994.3	1062.865	3541.405	1717.921
2066.3	1091.483	3555.375	1732.056
2211.4	1093.502	3622.213	1752.245
2239.5	1261.54	3797.279	1784.338
2241.5	1359.69	**3809.218**	1824.251
2298.5	1390.883	3811.422	1830.806
2664.7	1565.118	3813.444	2068.651
2792.5	1644.933	3887.454	**2225.532**
2807.7	1995.339	3892.575	**2230.591**
2824.7	2023.276	3895.775	**2242.461**
2836.7	2071.312	3912.823	2285.442
2922.8	2094.357	3928.884	2300.589
3333.1	2203.413	3947.711	2319.53
3339.3	2214.471	3955.775	**2790.709**
3350.2	2214.471	3959.746	2793.022
	2226.428	3962.136	2808.068
	2231.618	3979.499	2914.97
	2233.573	3999.232	2925.857
	2241.515	5561.339	3097.109
	2409.443	5562.716	**3810.479**
	2565.624		

Table 5.3

Monoisotopic masses of peptide fragments (in Da) of the protein contained within spots A & B (see figure 5.12), generated by in-gel tryptic digestion, followed by MALDI-TOF MS analysis in reflector mode. The first column shows the peptides common to both spots, and the bold type depicts additional closely matching peptides between spots A & B (± 1 Da).

the unknown basolateral membrane protein. From the 32 peptide masses detected by MALDI-TOF, approx. 50% of these were positively matched to BSA in the databases. In addition, although some peptides corresponded to other (unrelated) proteins, these matched with a considerably lower probability, typically less than half of that specified for BSA. The two main parameters which can be changed to alter the precision of the search are: (1) the number of missed cleavages, and (2) the mass tolerance level. Increasing either of these parameters resulted in a greater degree of error and increased the probability of matching false positives. By utilising BSA as a standard protein it was found that the values which resulted in the predominant identification of BSA, with the lowest matches to other proteins, was to use one missed cleavage and a mass tolerance of ± 0.5 Da.

Initially these values were specified in searches for spots A & B and this did not achieve a positive match to any rat protein. The parameters of all searches were then widened to a considerable extent, but, again, no proteins from rat tissue were positively identified. In progression, the animal species searched was also expanded to include all taxa, in an attempt to identify potential homologues, but again no probable matches were obtained.

A small number of the peptide fragments matched to various proteins in the databases, which is approximately 12-24% of the total number of peptides, depending on the degree of accuracy in the search. However, no individual protein showed a substantial probability for positively matching, or a probability that exceeded the rest (as was found with BSA). In addition, the proteins identified from the database were mostly from a tissue distinct to the small intestine. As such, I could not identify the protein from the database searches using the peptide fingerprint data, even incorporating the widest possible search parameters.

5.8.3 Elimination of peptides generated by autolysis of trypsin

The commercially available trypsin (Promega) used for the digests had been modified to prevent autolysis (section 2.7), therefore, no trypsin peptides should have been generated during the in-gel digestion procedure. In addition, the database searches did not match porcine trypsin to the peptide fingerprint. However, to ensure that no tryptic peptides were associated with the real peptides, I performed a theoretical digest of porcine trypsin using the MS-Digest program (Appendix II).

This bioinformatics tool can perform a digest of any known protein sequence contained within the databases by analysing the primary sequence, identifying potential cleavage sites for trypsin and generating theoretical peptides of a defined mass. The user can specify the number of missed cleavages permitted during the digestion; I performed the digest with 0, 1 and 2 missed cleavages, to cover the entire spectrum. Potential modifications to amino acid residues under the preparative conditions employed, for example, oxidation of methionine or reduction of cysteine during gel electrophoresis, was also specified.

However, only two trypsin peaks corresponded to the actual peptides; these peptides were common to both spots. Therefore, 'false' peptides originating from trypsin would not interfere with the searches, to any appreciable extent, in preventing a positive match to be found to spot A or B, if present in the database.

5.8.4 Is the photoaffinity labelled 112 kDa protein PepT1?

The peptide fingerprint profiling did not identify PepT1 as a match for the protein from either of the spots, or a combination of both. Despite this, I performed a theoretical digest of rat PepT1 using the MS-Digest program and compared the generated peptides with those of spots A and B.

A comparison of the two fingerprints revealed that only five fragments matched, i.e. only 4% of the peptides from spots A and B corresponded to PepT1 (figure 5.17). The molecular mass of the peptides and their membrane location within the rat PepT1 sequence are shown in table 5.4.

5.8.5 Q-TOF MS analysis

The peptide fingerprint data from spots A and B did not correspond to any other protein contained within the databases. The next step was to obtain additional information about the protein's sequence. In particular, a partial amino acid sequence of one of the peptide fragments is very useful, and can be used solely to unequivocally identify the parent protein from databases, or in conjunction with the peptide fingerprint to provide confidence to potential matches.

Q-TOF MS analysis was kindly performed by Dr. Alison Ashcroft at the Department of Biochemistry, University of Leeds. However, due to a lower tolerance of the Q-TOF for contaminants, in comparison to the MALDI-TOF, we were only

```
1    MGMSKSRGCF GYPLSIFFIV VNEFCERFSY YGMRALLVLY FRNFLGWDDD   50
51   LSTAIYHTFV ALCYLTPILG ALIADSWLGK FKTIVSLSIV YTIGQAVISV  100
101  SSINDLTDHD HDGSPNNLPL HVALSMIGLA LIALGTGGIK PCVSAFGGDQ  150
151  FEEGQEKQRN RFFSIFYLAI NAGSLLSTII TPILRVQQCG IHSQQACYPL  200
201  AFGVPAALMA VALIVFVLGS GMYKKFQPQG NIMGKVAKCI RFAIKNRFRH  250
251  RSKAFPKRNH WLDWAKEKYD ERLISQIKIM TKVMFLYIPL PMFWALFDQQ  300
301  GSRWTLQATT MTGKIGTIEI QPDQMQTVNA ILIVIMVPIV DAVVYPLIAK  350
351  CGFNFTSLKK MTVGMFLASM AFVVAAIVQV EIDKTLPVFP SGNQVQIKVL  400
401  NIGNNDMAVY FPGKNVTVAQ MSQTDTFMTF DVDQLTSINV SSPGSPGVTT  450
451  VAHEFEPGHR HTLLVWGPNL YRVVKDGLNQ KPEKGENGIR FVSTLNEMIT  500
501  IKMSGKVYEN VTSHSASNYQ FFPSGQKDYT INTTEIAPNC SSDFKSSNLD  550
551  FGSAYTYVIR SRASDGCLEV KEFEDIPPNT VNMALQIPQY FLLTCGEVVF  600
601  SVTGLEFSYS QAPSNMKSVL QAGWLLTVAI GNIIVLIVAE AGHFDKQWAE  650
651  YVLFASLLLV VCIIFAIMAR FYTYINPAEI EAQFDEDEKK KGVGKENPYS  700
701  SLEPVSQTNM
```

Figure 5.17

Primary amino acid sequence of rat PepT1 (SwissProt accession number P51574). Potential cleavage sites for trypsin, i.e. at the carboxylic sides of lysine and arginine residues (except if adjacent to a proline), are underlined. The five sequence fragments which match the masses of peptides from spots A and B (figure 5.12) are shown in red type; bold type indicates an overlap between two adjacent peptide fragments. (Original in colour).

Mass (Da)	Amino acid location	Membrane location	Matching spot	Number of missed cleavages
970.5587	250-257	Loop; TM 6 & 7	A	2
992.4723	563-571	Loop; TM 9 & 10	B	0
1830.9345	491-506	Loop; TM 9 & 10	B	2
2793.2943	503-527	Loop; TM 9 & 10	B	1
3809.8898	283-314	TM 7 to loop	A & B	2

Table 5.4

Peptide masses generated from an *in silico* digestion of rat PepT1, using the MS-Digest program, which correspond to peptides produced from in gel tryptic digestion of spots A & B, thought to be components of the candidate basolateral peptide transporter. Only one matching peptide is produced from zero missed cleavages, the majority result from 2 missed cleavages; the probability of the peptides being exact matches is reduced with an increasing number of missed cleavages.

able to gain sequence information from spot A. The TOF spectrum produced from analysis of spot A, performed initially to detect the peptide fragments, is shown in figure 5.18. The peptide fragments are identified from the spectrum as multiply-charged peaks, in particular one doubly-charged fragment of spot A had a mass of 876.44 Da (a total mass of 1750.9 Da); this was used for partial sequence analysis.

In order to reveal a section of its sequence, the peptide had to be fragmented; this was achieved by collision with argon (an inert gas). Fragmentation can cause cleavage at any of the bonds within the peptide structure but, under conventional conditions, is predominantly restricted to the backbone of the peptide; y- and b-ions are the most predominant products of this fragmentation (figure 5.19). The spectrum produced from fragmentation of the doubly-charged 876.44 Da peptide is shown in figure 5.20. The fragmentation spectrum is difficult to interpret completely, but the upper m/z region displays a simple fragmentation pattern which is typical of doubly-charged tryptic peptides (Shevchenko *et al.*, 1996b). The partial amino acid sequence, using the y-series ions, is read in a reverse direction from the spectrum, which corresponds to the direction from the amino to carboxyl ends of the peptide (see figure 5.19 & 5.20). Amino acid residues are easily assigned based on the mass difference between adjacent peaks (Appendix III). A partial sequence of 9 amino acids was obtained using the stretch of sequence ions; six of the residues are definite and the remaining three are thought to be highly probable (> 99% certain) (shown in brackets):

NH_2- / -Thr-Ser-Asn-Phe-Val-Thr-(Ala-Thr-Ser)- / -COOH

A peptide sequence tag consists of this amino acid sequence combined with the distance, in mass units, to the N and C termini of the peptide. Full details of the sequence tag are shown in table 5.5. The sequence tag was used to search databases in an attempt to identify the protein contained within spot A on the 2-DE gel. The searches were performed with either the six definite residues, or using the complete nine residue sequence, on tools such as TagIdent, ProteinInfo, PeptideSearch, MOWSE and Mascot (Appendix II); both full length sequence databases and expressed-sequence tag (EST) databases were searched. A number of potential matches for the sequence was identified with the 9 amino acid residues (see

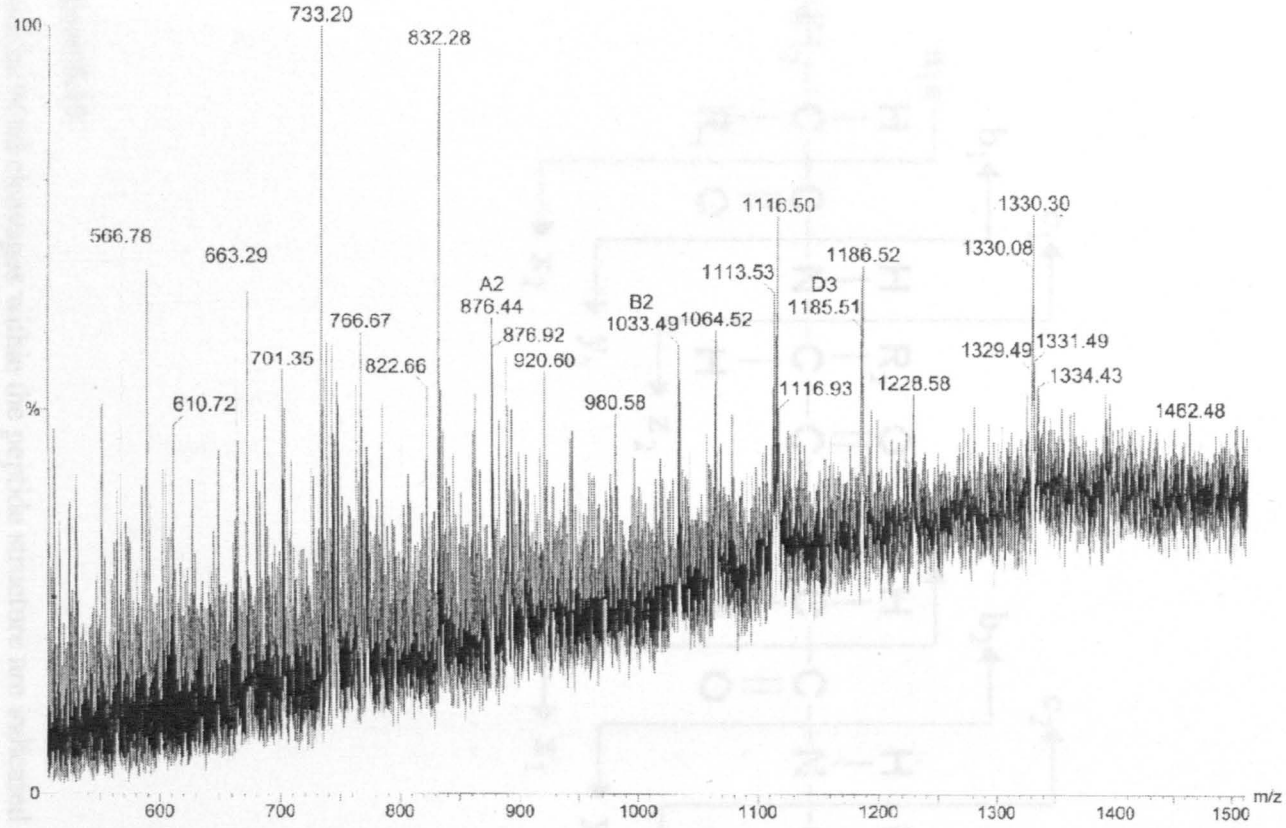

Figure 5.18

Q-TOF analysis of the tryptic digest fragments of spot A (see figure 5.12) initially performed to identify potential peptides with which to fragment to obtain a partial sequence. The peptide chosen for fragmentation is the doubly-charged 876.44 Da peptide.

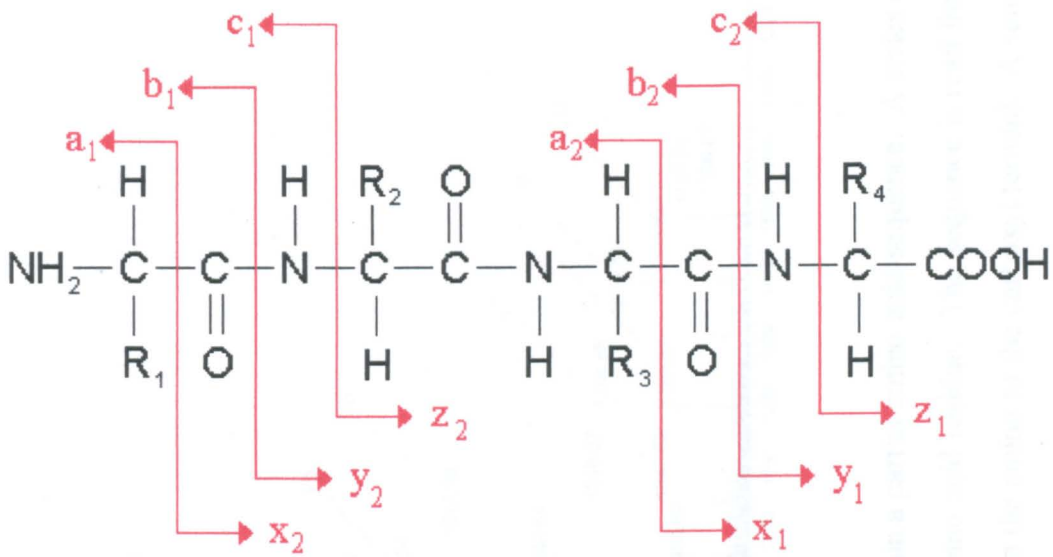

Figure 5.19

Potential bond cleavages within the peptide structure are indicated in red type. Q-TOF fragmentation of the peptide leads to the formation of distinct ion series; if the charge is retained on the N-terminus, the ions formed are of type a_n, b_n and c_n, whereas if the charge is retained on the C-terminus, the x_n, y_n and z_n ions are formed. Ions of the same type, and incremented *n*, differ by the mass of an amino acid residue, minus H_20, (the 'residue mass') at that point in the sequence. A consecutive ion series is used to define amino acid sequence of a peptide.

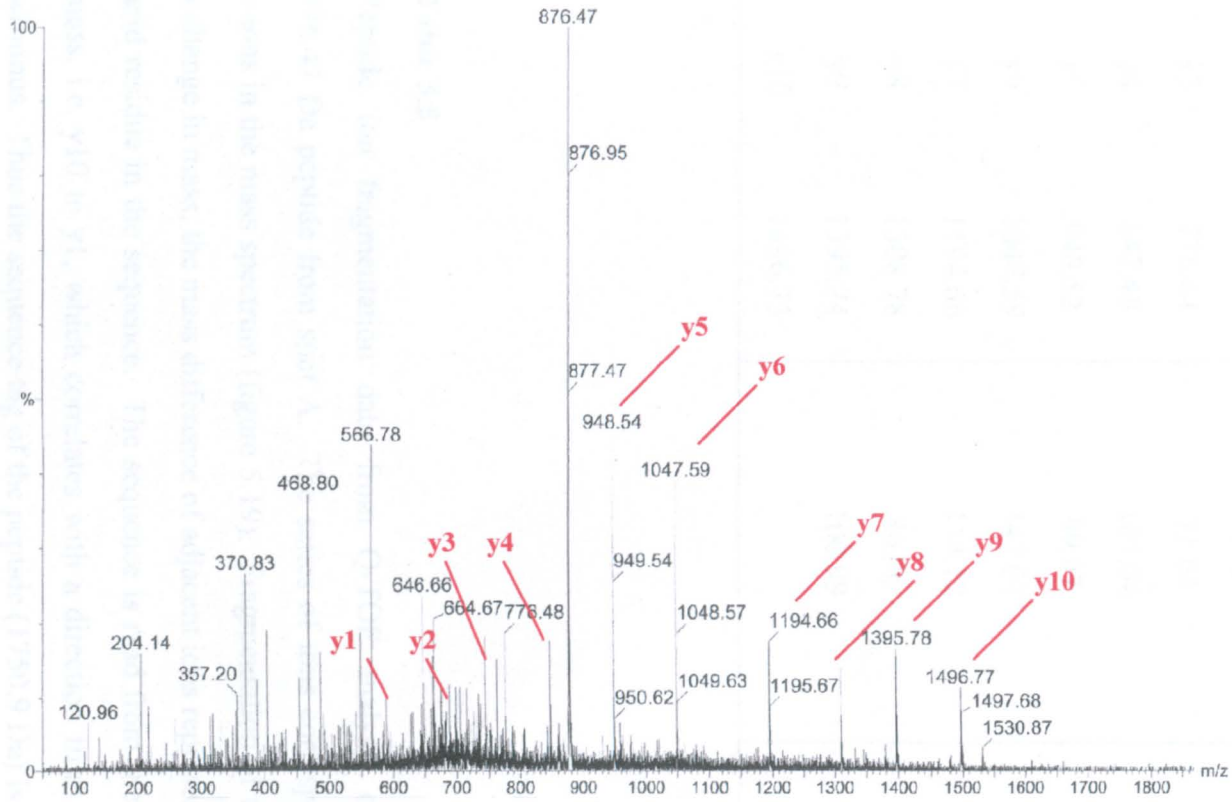

Figure 5.20

Q-TOF fragmentation of the precurser peptide ion (876.44 Da) to obtain a partial amino acid sequence. A series of y-type ions are generated (y1-y10), which differ consecutively by the molecular mass of one amino acid residue. The sequence is read from y10 to y1, to generate a partial sequence of nine amino acids, corresponding to a direction from the amino to the carboxyl termini. A summary of the sequence tag is given in table 5.5.

Fragment ion mass (Da)		Mass difference between adjacent ions (Da)	Corresponding amino acid residue
y1	588.36	87.05	Ser (S)
y2	675.41	101.03	Thr (T)
y3	776.44	71.04	Ala (A)
y4	847.48	101.04	Thr (T)
y5	948.52	99.07	Val (V)
y6	1047.59	147.07	Phe (F)
y7	1194.66	114.12	Asn (N)
y8	1308.78	86.96	Ser (S)
y9	1395.74	100.99	Thr (T)
y10	1496.73		

Table 5.5

Peptide ion fragmentation data from Q-TOF analysis of the doubly-charged 876.47 Da peptide from spot A. The series of ions corresponds to the designated y-ions in the mass spectrum (figure 5.19). Fragmentation of the peptide is shown by a change in mass; the mass difference of adjacent ions represents an individual amino acid residue in the sequence. The sequence is read from the data from high to low mass, i.e. y10 to y1, which correlates with a direction from the amino to carboxyl terminus. Thus the sequence tag of the peptide (1750.9 Da) is as follows;

(1496.73) TSNFVTATS (588.36)

table 5.6). However, these were disregarded because it was highly unlikely that these were the labelled 112 kDa protein because the peptide fingerprint did not match the proteins in the databases, in addition, the complete (9 amino acid) sequence was not found.

Overall, the protein in spots A and B could not be identified by either MALDI-TOF or Q-TOF analysis alone, combined with database searches, or a combination of both mass spectrometric analysis methods. If the basolateral membrane protein was contained within the databases, a positive match would have been found using the data presented here.

5.9 Discussion

5.9.1 Photoaffinity labelling of BLMV to identify the peptide transporter

The pattern of labelling in BLMV is highly reproducible. A single protein of 112 kDa molecular weight is consistently, and predominantly, labelled with [4-azido-3,5-^{3}H-D-Phe]-L-Ala under the conditions employed; indicated by the magnitude of the radioactivepeak and the peptide-protection ratio. Due to the evidence that label incorporation is completely abolished by the presence of a dipeptide, whereas amino acids have very little effect, this extremely specific substrate-protection implies that it is a dipeptide binding protein that does not interact with free amino acids.

The consistency of label incorporation by unprotected basolateral membrane proteins is demonstrated by the data in figure 5.7, where the 112 kDa protein is predominantly labelled in all samples. A minor peak of radioactivity can also be detected at the very end of the rod gel. This minor peak is always present, irrespective of the duration of electrophoresis, therefore it doesn't correspond to any particular molecular weight of protein. As such, the radioactivity is probably not due to a labelled protein but to unbound/loosely bound label adhering to the sides of the glass tube during elution from the bottom of the gel.

The pattern of label incorporation by the basolateral membrane is distinct to that observed with the brush-border membrane (see chapter 4). This corroborates the enzyme assay data in that the two vesicle preparations are extremely pure with negligible cross-contamination.

Protein (organism)	Sequence	% identity
Cell wall protein (*A. thaliana*)	**XSNFVNATS**	87 %
Hypothetical protein (*H. pylori*)	**TATFVTATX**	75 %
GAP-like protein (*H. sapiens*)	**XSNSVTATS**	87 %
Bap gene product (*D. melanogaster*)	**XSSFVTASS**	75 %
CG5891 gene product (*D. melanogaster*)	**TSNSVSATS**	77 %
Breast cancer susceptibility protein (*R. norvegicus*)	**TNSFVTAAS**	66 %
KIAA0495 protein (*H. sapiens*)	**TSKFVSATX**	75 %
Lectin (*R. pseudoacacia*)	**TSTLVTATS**	77 %
Spike protein (*murine hepatitis virus*)	**XSNFVTXTS**	87 %

Table 5.6

Example of results obtained from database searches (using the BLAST program) with the nine amino acid sequence tag generated from Q-TOF fragmentation of a tryptic peptide from the 112 kDa basolateral membrane protein (refer to table 5.5). Matching residues in the partial sequence are represented in bold type. However, although proteins were matched from the sequence tag alone, these were disregarded as a result of peptide fingerprint mismatches. As such, the above proteins are not a positive match for the 112 kDa protein, when taking all sequence data into account.

It is apparent that label binding to proteins in both membranes is very low, suggesting a highly specific interaction. However, a slightly higher label incorporation is seen with the 112 kDa basolateral membrane protein compared to BBM proteins (0.018% v. 0.003%). This difference of label interaction between the two predominantly labelled proteins in the BLM and BBM could be due to the label being a more efficient substrate for the basolateral protein, as indicated by the vascular perfusion experiments (section 3.7.2). However, a relatively higher proportion of the protein in the membrane, compared to PepT1 in the brush-border, may also be a factor. The exact proportion of the peptide transporters in their respective membranes, relative to the total protein content, is not known, however, this potential difference must be acknowledged. However, because interaction with the label by the proteins is extremely specific, and the extent of labelling is very low, the difference between the two is probably not significant.

Another distinction between labelling of the basolateral membrane compared to the brush-border membrane is that D-Phe-L-Gln provides a higher degree of protection to the 112 kDa protein in comparison to all of the proteins labelled in BBMV. This is most likely due to the relatively different affinities and/or transport capacities of the two peptide transporters (Saito *et al.*, 1993; Matsumoto *et al.*, 1994; Terada *et al.*, 1999). The basolateral transporter has been shown to have a lower capacity for transport than PepT1 and therefore the presence of the dipeptide in the suspension, prior to the label, may incur preferential binding. The high concentration of D-Phe-L-Gln would saturate the system and prevent the label (at a considerably lower concentration; 4.2 μM) from interacting with the active site. The higher capacity of PepT1 for transport may mean that both the dipeptide and the label can bind to a limited extent simultaneously. The lower level of transport inhibition at the apical membrane by the label in the perfusion experiments (section 3.7.2) corroborates this theory.

Whereas there are a great number of peptide hydrolases located in the apical membrane, none are found in the basolateral membrane. As such, the preferentially labelled 112 kDa protein is definitely not a peptidase.

The highly specific blocking of labelling by the dipeptide is not due to the high concentrations of substrate employed in this procedure. Examinations into the effect of medium osmolarity on label incorporation demonstrated that inhibition was

entirely due to the structure of the dipeptide substrate, not its presence in such high concentrations.

Collectively, the results from labelling experiments, with reference to the corresponding perfusion data, indicates that the 112 kDa protein is a potential candidate to be the, as yet unidentified, basolateral peptide transporter in rat small intestine.

5.9.2 Isolation of the candidate peptide transporter by 2-DE in rod gels

It appears that a single labelled protein could be isolated from the basolateral membrane simply by SDS-PAGE separation, but it is probable that more than one protein in the basolateral membrane at that molecular weight exists. So, an additional protein separation technique was performed to ensure individual isolation of the 112 kDa protein. Isoelectric focusing separates proteins based on a characteristic which is distinct from their molecular weight. Proteins were electrophoresed through an internal pH gradient, formed by carrier ampholytes within a rod gel, to resolve solely on the basis of their isoelectric point, i.e. the pH at which their net charge is zero. The resolving power of IEF in the rod gels is such that the difference in pH that can be routinely measured between two adjacent slices (of 2 mm) is as accurate as 0.05 of a pH unit.

A step-wise combination of SDS-PAGE and IEF in rod gels demonstrated that only one protein is labelled by [4-azido-3,5-^{3}H-D-Phe]-L-Ala in the basolateral membrane. This labelled protein focused at an isoelectric point of 6.5 and analysis of the final peak samples following the 2-DE separation shows a single band at 112 kDa molecular weight. This implies that an individual protein has been successfully labelled and isolated by a combination of a photoaffinity labelling technique and 2-DE.

There is a discrepancy in the amount of labelled protein loaded onto the IEF gels, and the amount that is present in the radioactive peak following resolution. On average, the 112 kDa protein detected following SDS-PAGE, covalently binds approx. 7800 dpm (131 Bq) of radioactivity (see figure 5.7). A pooled concentrate of eight of these labelled protein samples, subjected to IEF, is therefore approx. 63,000 dpm (1.06 kBq) of radioactivity. However, the peak of radioactivity observed following the second dimension in unprotected vesicles was only 20,000 dpm

(336 Bq), i.e. only 32% of the radioactivity loaded onto the IEF gel was detected following electrophoresis. This loss of labelled 112 kDa protein is potentially due to three factors. Firstly, during the sample concentration step, after SDS-PAGE, a certain amount of protein is lost; this has been discovered by routine analysis to be as high as 50% (data not shown), probably due to adsorption of the protein to the concentrator membrane. Secondly, not all of the protein applied to the surface actually enters the IEF gel, due to the sample overlay procedure employed. Finally, it is possible that not all of the protein in the peak would have been extracted from the gel slice. A combination of all three can be used to explain this substantial loss of protein throughout the procedure. Celis & Bravo (1984) have reported a comparable level of protein loss during a 2-DE procedure, incorporating capillary IEF. It was stated that, during each of the different steps of a 2-DE procedure, a certain amount of the initial protein would be lost. After completion of these 2-DE gel studies, approx. 50% of the initial protein applied to the gel could not be recovered. The higher extent of protein loss observed during the 2-DE separation in rod gels presented here can be attributed to the additional steps of protein extraction and concentration prior to the second dimension.

5.9.3 Preparation of the candidate basolateral peptide transporter for sequence analysis

Although the 2-DE in rod gels provided crucial information about the photoaffinity labelled BLM protein, the techniques did not result in isolation of the protein in a suitable form to permit further analysis. Thus, other methods of preparation were used to achieve isolation of the protein in the form required, i.e. 2-DE to obtain a single spot on a slab gel. However, sequence analysis needed a substantial amount of protein, and so a concentration step preceded 2-D electrophoresis.

The 112 kDa protein was isolated from the basolateral membrane using the SDS-PAGE rod gel procedure and the amount of protein in the final concentrated sample was calculated using a BSA calibration curve in a slab gel. The slab gel was silver stained using the Bio-Rad method; a procedure based on a photographic chemical process, first introduced by Merril *et al.* (1981).

Silver staining was used throughout the photoaffinity labelling and gel electrophoresis studies primarily due to its enhanced sensitivity over many other stains, e.g. Coomassie brilliant blue R-250. This increased sensitivity has many advantages for its use in the isolation and purification of the 112 kDa protein. Firstly, protein loss was kept to an absolute minimum; less of the sample is required for its detection. Secondly, the dilute samples resulting from the protein extraction procedure could be analysed efficiently. And lastly, the purity of the final concentrated protein sample could be visually assessed. The use of silver staining in the BSA calibration gel also has the benefit of linearity between the density of the stain and amount of protein, although care has to be taken because as the density of the protein bands reach saturation, the stain becomes non-linear. However, saturation wasn't reached in the BSA calibration curve in figure 5.11; this curve was linear throughout the range of BSA used, demonstrated by the correlation factor ($r^2 = 0.998$). Despite this, the relationship between the density of the stain and the concentration of the protein is characteristic for each protein, therefore BSA would probably not stain in the same manner as the 112 kDa protein. BSA is widely used as a standard, and studies that have investigated the relationship between staining of different proteins have shown that BSA has an intermediate density curve, i.e. the density does not increase too fast or too slow with concentration (Celis & Bravo, 1984). In addition, BSA was relatively inexpensive for the quantities required and readily available in the laboratory. It was therefore used as a calculated estimate of the approximate amount of protein in the pure sample. Determination of the exact amount of 112 kDa protein in the sample wasn't crucial, as this step was performed solely to determine whether there was enough of the protein present in the sample to continue with further analysis.

In order to obtain a single spot, consisting solely of the photoaffinity labelled 112 kDa basolateral membrane protein necessary to perform initial sequence analysis, a concentrated sample (obtained from SDS-PAGE in rod gels) was subjected to 2-DE using an immobilised pH gradient. The gradient (pH 3 to 10), cast on an 18 cm dry strip, allows excellent resolution to be achieved. A single spot, which contains the protein of interest, can be visualised by simple staining.

However, the pattern of protein spots in the initial slab gel following 2-DE was not as anticipated. As opposed to the expected single spot at approx. 112 kDa

(pI 6.5), two very abundant spots at approx. 40 kDa were also detected. In spite of this, as anticipated, very few other spots were detected in the gel, and those that were present were significantly less dense in comparison to the two 40 kDa spots. The lack of additional spots is due to the protein isolation/concentration procedure; a relatively pure sample of the 112 kDa protein was obtained for 2-D electrophoresis by combining samples from SDS-PAGE, at a specific molecular weight, therefore eliminating the majority of contaminating proteins from the basolateral membrane.

Visualisation of the two dominant 40 kDa spots in the gel, and the presence of a minor spot at 112 kDa, led to the belief that they may be components of the original protein generated by cleavage. However, neither the two dominant 40 kDa spots, nor the remaining minor spots, were found to be radioactive. A lack of radioactivity in both spots suggested that [4-azido-3,5-^{3}H-D-Phe]-L-Ala has become completely detached from the protein.

It was not entirely clear why the 112 kDa protein should be cleaved and the photoaffinity label lost during the 2-DE procedure using the immobilised gradient, whereas the radioactively labelled protein could still be found at 112 kDa following 2-DE in rod gels. The conditions and solutions used for both protocols are very similar, i.e. the same reducing power was used, which might have affected bonding between distinct polypeptides. However, this is very unlikely because if the protein were composed of two separate domains it would have been apparent due to the reducing conditions of SDS-PAGE. The only major distinction between the two different 2-DE procedures is a factor of time. Prior to 2-DE on the immobilised gradient, a period for re-swelling of the dehydrated gel is required; this is performed at 20°C for 22 h. This gel rehydration step is then followed by the isoelectric focusing step, which requires a minimum of 24-36 h for completion, also performed at 20°C. In contrast, although the IEF step in the 2-DE in rod gels is also performed at room temperature, the focusing time is just 8.5 h. During both procedures, at this ambient temperature, breakdown of the protein structure can occur. The prolonged period (7-fold longer) for the immobilised strip rehydration and focusing, allows a greater degree of proteolysis to occur; this is thought to be the predominant reason behind the detection of the two 40 kDa proteins, and loss of the original 112 kDa protein. It also probably caused the loss of radioactivity, due to cleavage of the

portion of protein binding the label and subsequent elution from the bottom of the SDS-PAGE gel.

Despite the proteolytic breakdown of the labelled 112 kDa protein, work on the candidate basolateral peptide transporter was progressed. Due to their predominance in the gel, it is assumed that these two 40 kDa polypeptides were constituents of the 112 kDa protein, and so analysis continued with these two spots.

Subsequent to this work, additional 112 kDa protein was isolated by Mrs. Julie Affleck. As a precautionary measure, a protease-inhibitor cocktail was included in the solutions at all stages of the isolation and 2-DE steps to attempt to prevent proteolysis of the original protein. It can be seen in figure 5.13 that breakdown of the protein was avoided, demonstrated by the presence of a major spot at 112 kDa and a lack of additional spots at 40 kDa. As such, work could then be progressed using the complete protein sequence.

5.9.4 Identification of the candidate basolateral peptide transporter

Conventional means of protein identification have involved sequencing of the primary amino acid structure, for example, by Edman sequencing (Edman & Begg, 1967), providing that the amino terminus is not blocked. Another route is to use the antigenic properties of the protein, i.e. specific antibodies, if available. However, more efficient methods are now available for protein analysis, which are based on mass spectrometry. The use of MS has several advantages, from a greater sensitivity to a high throughput, eliminating the expensive running costs of earlier methods. An enhanced sensitivity, in turn, means that less sample is required for analysis, which creates its own benefits to the worker.

The two MS techniques used for analysis of the candidate basolateral peptide transporter protein are MALDI-TOF (matrix-assisted laser desorption/ionisation time of flight) and Q-TOF (quadrupole time of flight).

5.9.4.1 MALDI-TOF mass spectrometric analysis

MALDI-TOF MS was the principal method used in analysis of the protein, due to certain advantages over Q-TOF, for example, its ease of use and speed of analysis. In addition, it has an inherent high sensitivity and is relatively tolerant towards low levels of contaminants. It was originally developed by Karas and

Hillenkamp (Karas *et al.*, 1988; Hillenkamp *et al.*, 1991), and has been subsequently refined to become an effective and versatile method for the analysis of peptides and proteins. The advantages of this method of analysis are:- (1) samples can be analysed without extensive purification, (2) common biochemical reagents, such as salts, buffers, detergents, etc. at low levels, do not affect analysis, (3) most proteins can be analysed providing they can be dissolved in the appropriate solvents, (4) only a small sample is required, usually between 1-10 pmol and, (5) analysis is complete within a matter of minutes.

MALDI-TOF can be used to measure the molecular mass of a protein with extreme precision, i.e. to 0.01-0.1%, compared to an accuracy of between 5 and 10% by conventional SDS-PAGE methods (James *et al.*, 1993). However, whilst an accurate molecular weight of the protein would have been an achievement, large quantities of protein are required in extremely high concentrations, which would have proven difficult to prepare, and superfluous when the molecular weight was only used in database searches, in which a calculated estimate sufficed.

The MALDI-TOF technique was utilised for the analysis of peptide fragments generated from digestion of the 112 kDa protein using trypsin. Trypsin cleaves peptide bonds at the carboxylic sides of lysine and arginine residues, and so the masses of the peptides produced depend on the primary sequence of the protein. As such, they are individual for a particular protein, and therefore designated a 'peptide fingerprint'. The process of searching databases with these highly specific masses to identify proteins is termed 'peptide fingerprint profiling'.

The ionisation technique of MALDI-TOF predominantly produces singly protonated ions and so the mass-to-charge ratio is the true mass of the peptide plus 1 Da. In the spectra, the mass-to-charge ratio is represented on the *x*-axis and the relative intensity of the peaks on the *y*-axis. An external calibration is used to calculate the masses of the peptide fragments, i.e. peptides of known molecular mass are analysed prior to the sample and utilised by the data software to assign each tryptic peptide a mass value.

The heights of the peptide mass peaks are arbitrary values of the most intense (100%) peptide relative to the rest. The peak intensity is generated by a succession of laser shots, which are summed to yield a time of flight (TOF) mass spectrum that is more accurate, and has a better signal-to-noise ratio, than data from

single shots alone. Therefore, although some peptides appear to be more abundant than others, this may not be so; it may be due to the ability of that particular peptide to 'fly' down the field-free region, relative to the others.

5.9.4.2 Peptide fingerprint of the candidate basolateral peptide transporter

Analysis of the tryptic digestion mixture of spot A from the 2-DE gel detects a total of 83 peptides, with 53 peptides detected from spot B. MALDI-TOF can not detect all of the tryptic peptides present, for a number of reasons, i.e. a few dominant peptides may suppress detection of other less abundant peptides. In addition, some hydrophobic peptides might not be observed due to their low solubility or because of their ability to adsorb to the Eppendorf tubes and/or pipette tips used.

A small number of the peaks in the MALDI-TOF spectrum might represent contaminants from the gel or from the Coomassie stain used to visualise the spots. Other peptides that might be present may also not be from the protein of interest, i.e. human keratins originating from either chemicals and/or sample handling. However, the actual pattern of keratin peptides can not be predicted in the spectrum, and cannot, therefore, be eliminated using a control (Shevchenko *et al.*, 1996a). Additional unidentifiable peaks might result from the unexpected cleavage between Lys/Arg and Pro; this has been attributed to the high enzyme-to-substrate ratios used in *in situ* digestions (Mørtz *et al.*, 1994). However, a positive match from a database only requires a small number of corresponding masses, and so not all peptides are critical. In addition, incomplete maps, although may not unequivocally identify the specific protein, would identify variants or homologues from other species.

Steps can be taken to eliminate contaminating peptides, such as gel components, for example, by electroblotting of the protein onto a hydrophobic membrane (PVDF) or performing the digestion in solution. However, analysis of tryptic peptides from a membrane also has associated problems. These include the loss of some of the protein during transfer, limited or altered protease accessibility to cleavage sites resulting in peptide maps differing from that anticipated, and a preferential release of hydrophilic peptides (Mørtx *et al.*, 1994). Plus, the steps of washing and combining samples from the elution of peptides from the membrane can introduce its own additional background contaminants. In reference to the alternative to digest the protein in solution, previous to the in-gel digestion data presented in this

chapter, work was performed whereby the 112 kDa protein was digested in solution. However, the peptide mixture was not easily analysed and interpreted due to high levels of contamination. In-gel digestion permits washing of the sample to remove the vast majority of the buffers and salts in the high concentrations that can interfere with analysis. Thus, this was the method of choice.

The masses of the peptides shown in figure 5.15, figure 5.16 and table 5.3 were assigned by comparison to known standards in an external calibration; used to improve mass accuracy (Jungblut *et al.*, 1997). Commercial calibration mixtures are generally used (e.g. Cal2 from PerSeptive) because they contain peptides that only occur in one isoform and they do not oxidise easily. Accurate mass assignment depends on a good calibration. It also depends on a good signal-to-noise ratio of the peak; if a signal is weak and noisy, the mass assignment will not be as accurate as for more intense peaks. The signal-to-noise ratio is improved by accumulating data from individual laser shots. Obtaining data using a delayed extraction method (i.e. implementing a time delay between the laser pulse and acceleration of the ion), as performed with spots A and B, also increases accuracy; usually better than 0.5 Da in a mass range up to 5000 Da (Jungblut *et al.*, 1997). Collectively, these steps are taken to maximise precision in data acquisition; a resolution of more than 10,000 is good, however, in these analyses a resolution of > 13,000 was achieved. It is now generally accepted that if the protein, or homologue, is known and its sequence present, the mass fingerprint profile is sufficient for its identification from databases (James *et al.*, 1993).

5.9.4.3 Proteolysis of the candidate basolateral peptide transporter

It was very interesting to discover that 24-29 of the peptides detected in spots A and B had identical masses. This indicates that the two spots probably did originate from one protein. Prior to MALDI-TOF analysis, it was speculated that proteolytic breakdown of the 112 kDa protein during the prolonged IEF procedure resulted in loss of the radioactive label and a lack of detection of a spot at the correct molecular weight. These peptide fragment data corroborate this theory, and suggest that the two 40 kDa spots form the originally labelled protein. It appears as though proteolysis occurred in stages during incubation of the sample at room temperature while performing IEF, i.e. breakdown of the 112 kDa protein to a 40 kDa polypeptide

principally occurred, and then further breakdown of this fragment to a distinct polypeptide would cause the two spots to be formed. The two protein spots possess exactly the same molecular weight, but differ slightly in isoelectric point. The loss of as few as one or two amino acids from the polypeptide sequence can result in a shift of pI to produce a second spot. A considerably greater number of peptides were detected from spot A than spot B. In addition, the more basic spot (spot B) is slightly less abundant than spot A. This collectively suggests that the process of proteolytic breakdown is due to the 40 kDa polypeptide (spot A) being degraded slightly further to form spot B. At some point during proteolysis of the protein, the portion of the polypeptide that formed the active site and therefore bound [4-azido-3,5-^{3}H-D-Phe]-L-Ala was cleaved and eluted from the gel. This must have occurred during the initial breakdown of the 112 kDa protein to the 40 kDa fragment, not during further degradation of spot A to spot B, otherwise radioactivity would still be detected in spot A.

Although the 112 kDa protein spot was not detected from the 2-DE gel, it was assumed that the two 40 kDa spots formed at least part of the original protein, for reasons described above. As such, the peptide fingerprints from both spots were used in database searches for identification of the candidate basolateral peptide transporter.

5.9.4.4 Database searches

Despite the various searches described in section 5.8.2, the peptide fingerprint of the protein isolated from the basolateral membrane did not positively match to any known protein in the databases with any real significance. In addition, only five of the possible 136 peptides produced from the two spots coincided with similar masses of peptides produced from a theoretical digest of rat PepT1.

It is generally accepted that approx. 50% of peptide masses should match in order for a protein to be accepted (Mørtz *et al.*, 1994), which is precisely what was obtained with prior experimentation with BSA. The searches with the peptide masses from spots A and B matched a maximum of 24%, and this only occurred when the search parameters were expanded to include all possible variations and therefore induced a low degree of accuracy within the search. Searches with slightly more precision failed to even reach a match of 20%. Even if the peptide map from

this protein were incomplete, it would be expected to match, or that variants or species homologues would be identified. However, a lack of positive identification suggests it is a novel protein.

Occasionally proteins cannot be identified by MALDI peptide maps, due to detection of only a few peptides (Shevchenko *et al.*, 1996c), and so additional sequence information is required. This was obtained in the form of a partial amino acid sequence of one of the peptide fragments by Q-TOF analysis. The sequence tag (nine amino acids) was also used in database searches to identify the basolateral protein. Identification of proteins using MS fragmentation data has a very high degree of reliability, therefore suggesting that the protein isolated from the basolateral membrane is not contained within either the full length sequence databases, or the EST databases, searched. ESTs are partial sequences (~300 bp) of cDNAs derived from differentiated tissues or cells, whose orientation (5' → 3') and reading frame are usually unknown. As such, they represent portions of expressed genes. The peptide sequence tags are ideally suited for searching these databases in the hope of identifying a gene whose partial sequence, if not the full sequence, has been determined. Only a small amount of correlative sequence is required to achieve identification (Courchesne *et al.*, 1997). Although a number of proteins were found to match the majority of the sequence tag (up to 87%), the complete sequence could not be matched (table 5.6). In addition, the peptide fingerprints of the proteins that did contain a corresponding sequence did not match to the fingerprint(s) of the 112 kDa protein.

It is generally accepted that if a protein has been previously isolated, and its sequence is contained within the databases, a peptide fingerprint or a partial sequence will unequivocally find the match (James *et al.*, 1993). Some proteins can be identified with as little as 5-6 peptide masses, but these are highly specific for that particular protein; in general a considerably higher probability when compared to other proteins is the defining factor for a good match. The fact that the protein was not positively correlated with any other known protein is not due to the reliability of the combined techniques, because prior analysis of BSA by the same methods resulted in its unequivocal identification from all databases. MALDI-TOF and Q-TOF (electrospray ionisation) form a layered approach to protein identification

which, if the protein was contained within the databases, it would be unequivocally identified, if not by one method alone, then undoubtably by a combination of the two.

It is therefore clear that the 112 kDa protein, which has been specifically photoaffinity labelled with a dipeptide analogue, and which is postulated to be a candidate to be the basolateral peptide transporter, has not been previously identified, and as such appears to be a novel protein.

5.9.5 Is PepT1 responsible for the basolateral transport of peptides?

Over the years, studies of peptide transport in the basolateral membrane have been consistently neglected in favour of PepT1. This was probably (initially) due to the fact that physiologically occurring peptides are hydrolysed within the enterocyte before transport of the constituent amino acids out of the cell. However, the demonstration that intact peptides, and peptidomimetic drugs, are transported out of the cell across the basolateral membrane, suggested that there must be a carrier present.

It was then postulated that PepT1 was also responsible for the exit of peptides from the cell, i.e. it was thought that there wasn't a distinct transport protein in the basolateral membrane. During the cloning and expression of rabbit PepT1 by Hediger's group (Fei *et al.*, 1994), hybrid depletion studies performed to block PepT1 expression resulted in a loss of induced Gly-Sar transport activity in *Xenopus laevis* oocytes. As such, they suggested that peptide transport activity in the basolateral membrane is also due to PepT1 expression.

However, at present there is overwhelming evidence proving the existence of a distinct transporter protein at the basolateral membrane. In particular, PepT1 expression has been immunolocalised exclusively to the apical membrane (Ogihara *et al.*, 1996; Walker *et al.*, 1998), in addition to distinct transport characteristics demonstrated by a number of kinetic studies (section 1.5).

The sequence data presented here reinforces the distinction between the two transporters. Only a few (maximum of 5) of the peptide fragments generated from the candidate basolateral peptide transporter correspond to tryptic peptides of rat PepT1. Interestingly, these five peptides are located in just two loops, which connect adjacent transmembrane domains. Sequence comparisons of peptide transporters in both the small intestine and kidney, in a number of animals (in particular rat, rabbit,

human), have shown that the majority of sequence homology is located in the transmembrane domains and cytosolic domains, with only a low level conserved in the extracellular loops. In particular, Paulsen & Skurray (1994) demonstrated that two sequences were not only conserved between peptide transporters, but also found in various other transporters, the only similarity being that they showed a H^+-dependence in the transport of their substrates (section 1.4.3).

The majority of the (limited) matching rat PepT1 peptides to the present data are located in the notably large extracellular loop connecting TM 9 and 10, and the remainder in the intracellular loop adjoining TM 6 and 7. Due to the high degree of homology observed between the peptide transporters cloned thus far, it could be anticipated that the basolateral peptide transporter might show similar sequence similarity, especially in the TM domains. However, not only is there very little corresponding data between the two transporters in the small intestine, but the similarity that is observed is found in the least expected place within the structure. Despite the location of similarity, the fact that only five of the possible 134 peptides that could be generated from rat PepT1 with two missed cleavages, correlate shows that there doesn't appear to be a significant amount of similarity between the two proteins at all.

In addition, the partial sequence of 9 amino acids does not match to any part of the primary sequence of rat PepT1. Therefore, it can be concluded that the 112 kDa protein identified by photoaffinity labelling from the basolateral membrane is definitely not PepT1, and, as such, is a novel protein and a candidate to be the basolateral peptide transporter in rat small intestine.

5.10 Conclusions

(1) Photoaffinity labelling of BLMV produces a highly consistent pattern of [4-azido-3,5-^{3}H-D-Phe]-L-Ala incorporation by membrane proteins, which is distinct to that seen with BBMV.

(2) A single protein is specifically labelled by [4-azido-3,5-^{3}H-D-Phe]-L-Ala, which has a molecular weight of approx. 112 kDa and an isoelectric point of 6.5.

(3) Label incorporation by the 112 kDa protein is completely abolished by preincubation with a dipeptide, but not by free amino acids. Therefore, it is proposed as a candidate to be the basolateral peptide transporter.

(4) The labelled 112 kDa protein can be individually isolated from the basolateral membrane by 2-DE, either in rod gels or using an immobilised gradient, although the latter method results in proteolysis of the protein to form two spots (at 40 kDa) in the final stained gel.

(5) Tryptic digestion of the two 40 kDa spots followed by MALDI-TOF analysis reveals a high degree of similarity between the sequence of the polypeptides (> 50%), suggesting they originated from the same (112 kDa) protein.

(6) The peptide fingerprint of the candidate basolateral peptide transporter did not positively match to any previously sequenced contained within the databases.

(7) A sequence tag of nine amino acids, obtained by Q-TOF analysis of one of the tryptic peptides, also did not fully match to any sequence in either the full length sequence databases or EST databases, although a number of proteins were identified with corresponding sequences (up to 87 % match).

(8) Neither the peptide fingerprint, nor the sequence tag, corresponded to the primary sequence of rat PepT1 to an appreciable extent. This demonstrates that the basolateral peptide transporter is not PepT1, but a distinct protein.

In summary, using the methods described, I have identified, isolated and performed initial sequence analysis on a protein from the basolateral membrane of rat small intestine, which I propose is a candidate to be the, as yet, unidentified peptide transporter. The sequence information obtained thus far collectively indicates that the 112 kDa protein is novel.

CHAPTER 6: SHORT-TERM REGULATION OF PEPTIDE TRANSPORT IN RAT JEJUNAL MUCOSA

6.1 Aims of the experiments

Initial studies in our laboratory (Boyd *et al.*, 1996) demonstrated a stimulatory effect of leucine on peptide (D-Phe-L-Gln) transport in rat small intestine. It has been reported that specific amino acids in the diet have an ability to up-regulate peptide transport, over a period of days (Ferraris *et al.*, 1988; Shiraga *et* al., 1999), due to an increase in the abundance of PepT1 protein at the apical membrane, i.e. long-term regulation (see section 1.6.1). The report by Boyd and co-workers indicated an element of short-term regulation.

Interest in short-term regulation of peptide transport has been limited, despite the fact that this information is crucial if we are to understand the fundamental physiological processes that control the absorption of nutrients after a meal. As such, I decided to investigate the short-term regulatory processes controlling intestinal peptide transport, in particular, to elucidate whether there are different mechanisms of control at the apical and basolateral membranes. The technique used in this study, the luminally and vascularly perfused isolated rat jejunum *in situ* technique, permits some preliminary deductions into the membrane location of regulatory control in intact tissue, because the accumulation of peptide in the mucosal tissue and the corresponding exit ratios can be measured. The exit ratios are defined as the ratio of substrate concentration in the tissue to the concentration of substrate in the vascular effluent sample. It gives an indication as to the relative rate of transport at the two opposing membranes (see table 3.1), therefore allowing the site of inhibition/stimulation to be determined.

6.2 Viability of the vascular perfusions

Assessment of the viability of the vascular perfusions was as described previously in section 3.3. Briefly, the reliability of the data obtained using this technique was appraised using two factors; (1) a consistent, high portal vein recovery (> 90%), and (2) a constant rate of glucose utilisation by the isolated jejunal segment.

6.3 Regulation of peptide transport by leucine

The first step in this study was to reproduce the preliminary experiments of Boyd *et al.* (1996), although the time constraints were altered slightly to permit the infusion of specific drugs, and to observe their effects, in subsequent experiments.

L-leucine was added, at a concentration of 10 mM, at the 20 min time point of the perfusion. It was included in either the luminal or vascular perfusate to determine its effect on the transmural transport of 1 mM D-Phe-L-Gln from the lumen to the serosa of rat jejunum. The results of these perfusions are shown in figure 6.1 (I & II).

It is evident that leucine stimulates the rate of D-Phe-L-Gln transport, irrespective of whether it is present in either the lumen or vasculature of the intestine (figure 6.1(I)). The control transport rate is stimulated by 37% in both cases; from 0.259 ± 0.036 μmol·min.$^{-1}$·[g dry wt.]$^{-1}$ in the control perfusions to 0.356 ± 0.016 μmol·min.$^{-1}$·[g dry wt.]$^{-1}$ ($P < 0.001$) with leucine in the vasculature, and to 0.354 ± 0.041 μmol·min.$^{-1}$·[g dry wt.]$^{-1}$ ($P < 0.001$) with leucine in the lumen.

To ensure that the stimulation in rate is directly due to leucine, the percentage increase in peptide appearance at 20 min (before addition of leucine) was compared to the percentage increase in peptide appearance following leucine stimulation (50 min). When leucine was perfused through the vasculature the increase in cumulative peptide appearance at 20 min was 16% and at 50 min was 25%, therefore an increase in transport is apparent following the addition of leucine. With leucine in the lumen the values were a 20% increase at 20 min and a 27% increase at 50 min, again suggesting that the stimulation is entirely due to leucine. To corroborate this evidence, statistical analysis was performed on the raw data, which indicated no significant difference between the control perfusions and either of the leucine perfusions at the 20 min time point, before a steady state was reached.

However, the precise location of this stimulation can not be deduced from this data alone; the concentration of D-Phe-L-Gln in the mucosa, and the corresponding exit ratios (shown in figure 6.1(II)) provide this additional information. It is apparent that leucine in both the lumen and vasculature causes a significant reduction in the exit ratio of D-Phe-L-Gln from the mucosal tissue; from 91.9 ± 15.07 (control) to 46.66 ± 4.41 ($P = 0.014$) with leucine in the lumen, and to 33.59 ± 7.1 ($P = 0.011$) with leucine in the vasculature. This is associated with a

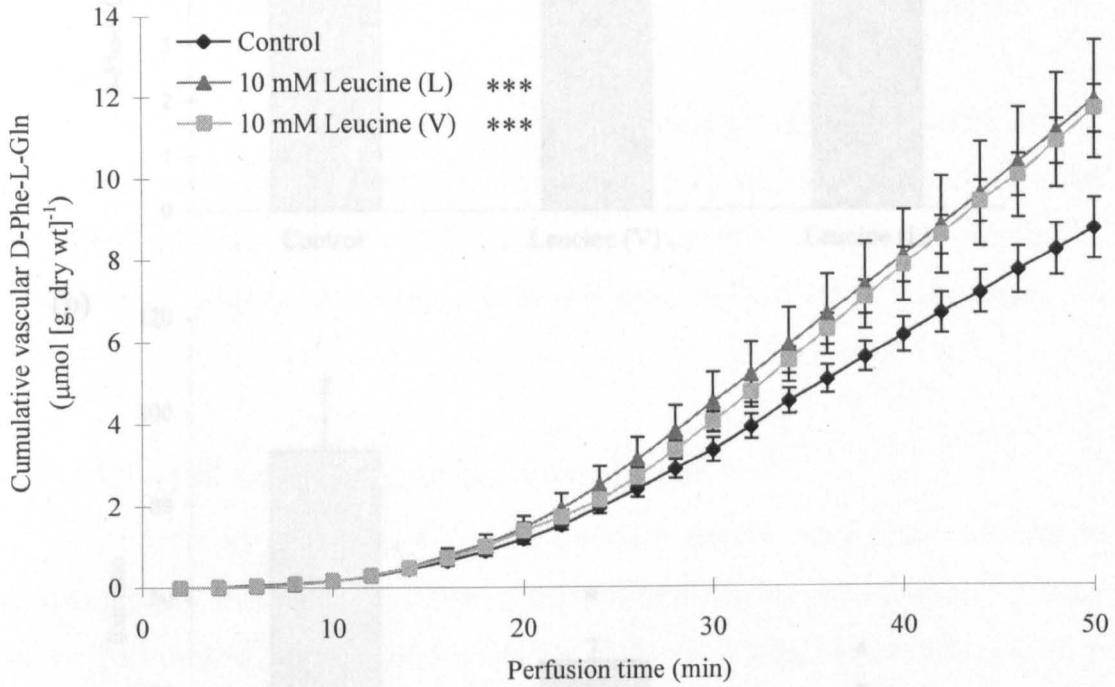

Figure 6.1(I)

Regulation of peptide transport by leucine, demonstrated by its effect on the transmural transport rate of 1 mM D-Phe-L-Gln (control). Leucine, at 10 mM concentration, is present in either the lumen (L) or the vasculature (V). Data points represent the mean ± s.e.m. (control, n = 4; leucine in L & V, n = 6). *** $P < 0.001$ depicts a significant difference in transport rate against the control.

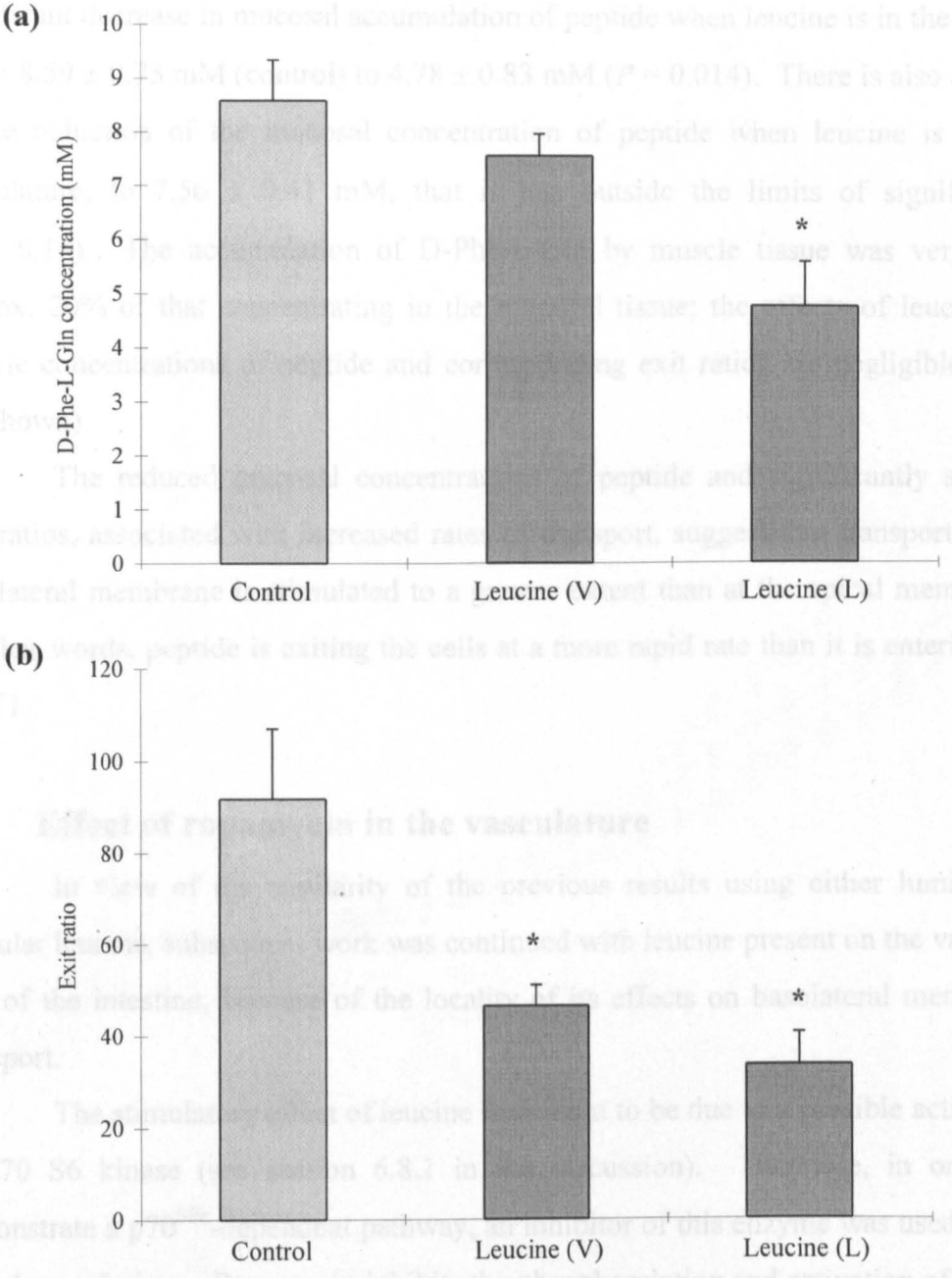

Figure 6.1(II)

Localisation of peptide transport regulation by leucine, demonstrated by its effect on the mucosal accumulation (a) and exit ratios (b) of 1 mM D-Phe-L-Gln. Leucine, at 10 mM concentration, is present in either the lumen or the vasculature of the jejunum. Bars represent the mean ± s.e.m. (control, n = 4; leucine in L & V, n = 6). * $P < 0.05$ depicts a significant difference against the control.

significant decrease in mucosal accumulation of peptide when leucine is in the lumen (from 8.59 ± 0.75 mM (control) to 4.78 ± 0.83 mM ($P = 0.014$). There is also a trend in the reduction of the mucosal concentration of peptide when leucine is in the vasculature; to 7.56 ± 0.41 mM, that is just outside the limits of significance ($P = 0.18$). The accumulation of D-Phe-L-Gln by muscle tissue was very low, approx. 20% of that concentrating in the mucosal tissue; the effects of leucine on muscle concentrations of peptide and corresponding exit ratios are negligible (data not shown)

The reduced mucosal concentrations of peptide and significantly smaller exit ratios, associated with increased rates of transport, suggest that transport at the basolateral membrane is stimulated to a greater extent than at the apical membrane. In other words, peptide is exiting the cells at a more rapid rate than it is entering via PepT1.

6.4 Effect of rapamycin in the vasculature

In view of the similarity of the previous results using either luminal or vascular leucine, subsequent work was continued with leucine present on the vascular side of the intestine, because of the locality of its effects on basolateral membrane transport.

The stimulatory effect of leucine is thought to be due to a possible activation of p70 S6 kinase (see section 6.8.1 in the discussion). Therefore, in order to demonstrate a $p70^{S6k}$-dependent pathway, an inhibitor of this enzyme was used in the vascular perfusions. Rapamycin inhibits the phosphorylation and activation of $p70^{S6k}$ ($IC_{50} = 0.05$ nM), via its action on mTOR (the mammalian target of rapamycin); an upstream regulator of $p70^{S6k}$. It was included in the vascular perfusate (at 25 nM), in conjunction with leucine, to determine its effect on the leucine-stimulation of peptide transport. It was also used in the absence of vascular leucine to assess any potential effects it may have on normal (control) rates of peptide transport. The results of these studies are shown in figure 6.2 (I & II).

It can be seen (figure 6.2(I)) that the presence of rapamycin in the vasculature completely abolishes the leucine-stimulation of peptide transport, from 0.356 ± 0.016 $\mu mol \cdot min.^{-1} \cdot [g\ dry\ wt.]^{-1}$ to 0.245 ± 0.023 $\mu mol \cdot min.^{-1} \cdot [g\ dry\ wt.]^{-1}$ ($P < 0.001$), i.e. back to the control rate of transport ($P > 0.1$). This is also

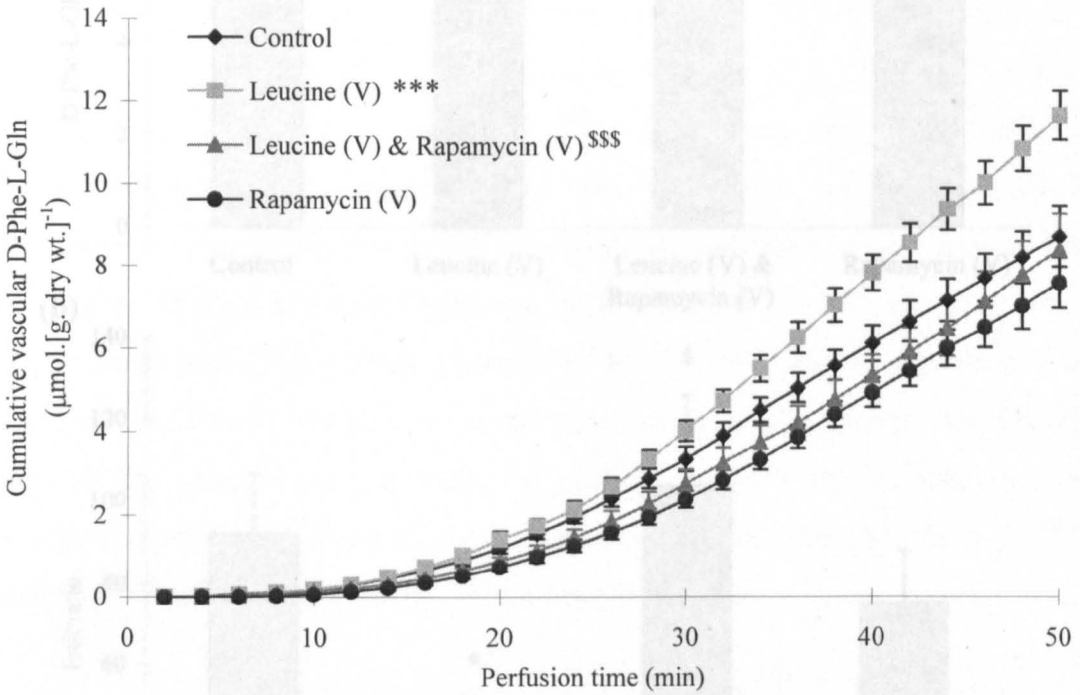

Figure 6.2(I)

Effect of vascular rapamycin (at 25 nM concentration) on the leucine stimulation of 1 mM D-Phe-L-Gln transport, and on control rates of transport, at the basolateral membrane. Data points represent the mean ± s.e.m. (control, n = 4; leucine (V), n = 6; leucine & rapamycin (V), n = 6; rapamycin (V), n = 5). *** $P < 0.001$ depicts a signifiant difference against the control, $^{\$\$\$}$ $P < 0.001$ depicts a significant difference against leucine (V).

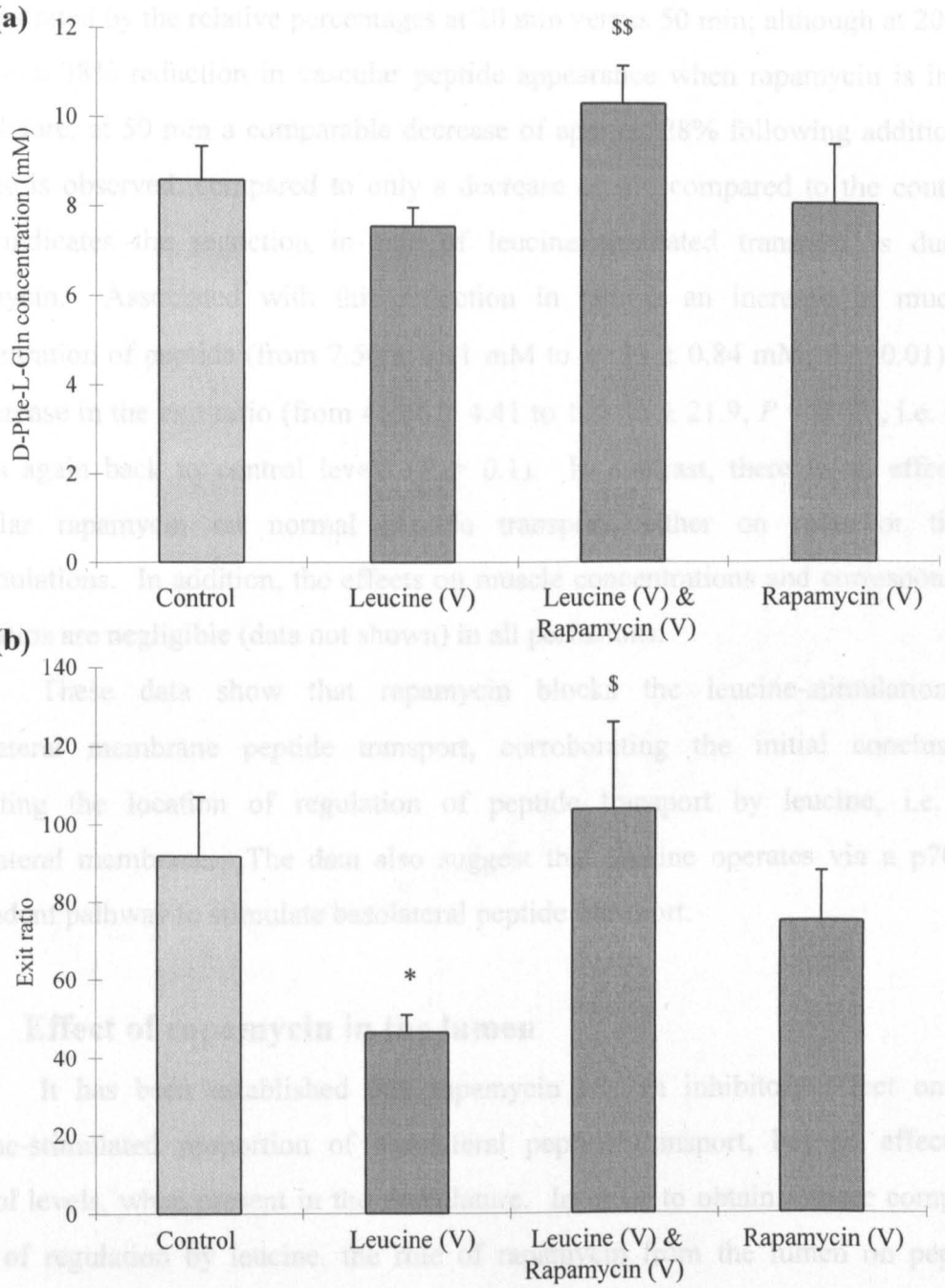

Figure 6.2(II)

Localisation of peptide transport regulation by leucine, demonstrated by the effect of vascular rapamycin on the mucosal accumulation (a) and exit ratios (b) of 1 mM D-Phe-L-Gln. Leucine is present in the vasculature of the jejunum at 10 mM, rapamycin is also in the vasculature at 25 nM, with or without leucine. Bars represent the mean ± s.e.m. (control, n = 4; leucine (V), n = 6; leucine & rapamycin (V), n = 6; rapamycin (V), n = 5). * $P < 0.05$ depicts a significant difference against the control; $^{\$}$ $P < 0.05$, $^{\$\$}$ $P < 0.01$ depict significant differences against 10 mM leucine (V).

demonstrated by the relative percentages at 20 min versus 50 min; although at 20 min there is a 38% reduction in vascular peptide appearance when rapamycin is in the vasculature, at 50 min a comparable decrease of approx. 28% following addition of leucine is observed, compared to only a decrease of 4% compared to the controls. This indicates the reduction in rate of leucine-stimulated transport is due to rapamycin. Associated with this reduction in rate is an increase in mucosal concentration of peptide (from 7.56 ± 0.41 mM to 10.33 ± 0.84 mM, $P = 0.01$) and an increase in the exit ratio (from 46.66 ± 4.41 to 103.86 ± 21.9, $P = 0.03$), i.e. both values again back to control levels ($P > 0.1$). In contrast, there is no effect of vascular rapamycin on normal peptide transport, either on rates or tissue accumulations. In addition, the effects on muscle concentrations and corresponding exit ratios are negligible (data not shown) in all perfusions.

These data show that rapamycin blocks the leucine-stimulation of basolateral membrane peptide transport, corroborating the initial conclusions regarding the location of regulation of peptide transport by leucine, i.e. the basolateral membrane. The data also suggest that leucine operates via a $p70^{S6k}$-dependent pathway to stimulate basolateral peptide transport.

6.5 Effect of rapamycin in the lumen

It has been established that rapamycin has an inhibitory effect on the leucine-stimulated proportion of basolateral peptide transport, but no effect on control levels, when present in the vasculature. In order to obtain a more complete view of regulation by leucine, the role of rapamycin from the lumen on peptide transport was investigated. The previous perfusions were repeated, but rapamycin was included in the luminal perfusate, as opposed to the vascular perfusate with leucine. The results from this series of perfusions are shown in figure 6.3 (I & II).

It is evident that rapamycin, when present in the lumen, appears to have no effect on the rate of leucine-stimulated transport, nor on the mucosal concentration or exit ratios, of D-Phe-L-Gln. A slightly higher (albeit not significant) rate at 20 min (before addition of leucine) (17%) ultimates in a slight reduction (4%) in transport rate at 50 min, demonstrating no effect of luminal rapamycin on the leucine stimulation in rate.

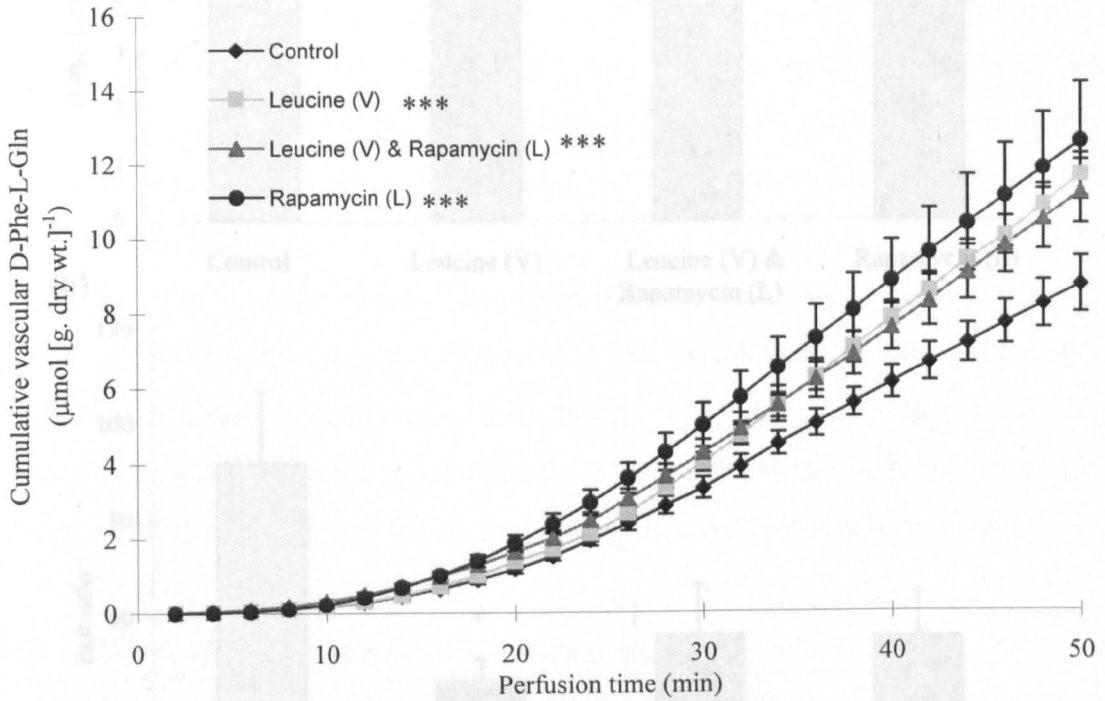

Figure 6.3(I)

Effect of luminal rapamycin (at 25 nM concentration) on the leucine stimulation, and on control rates, of 1 mM D-Phe-L-Gln transport. Data points represent the mean ± s.e.m. (control, n = 4; leucine (V), n = 6; leucine (V) & rapamycin (L), n = 6; rapamycin (L), n = 6). *** $P < 0.001$ depicts a significant difference against the control.

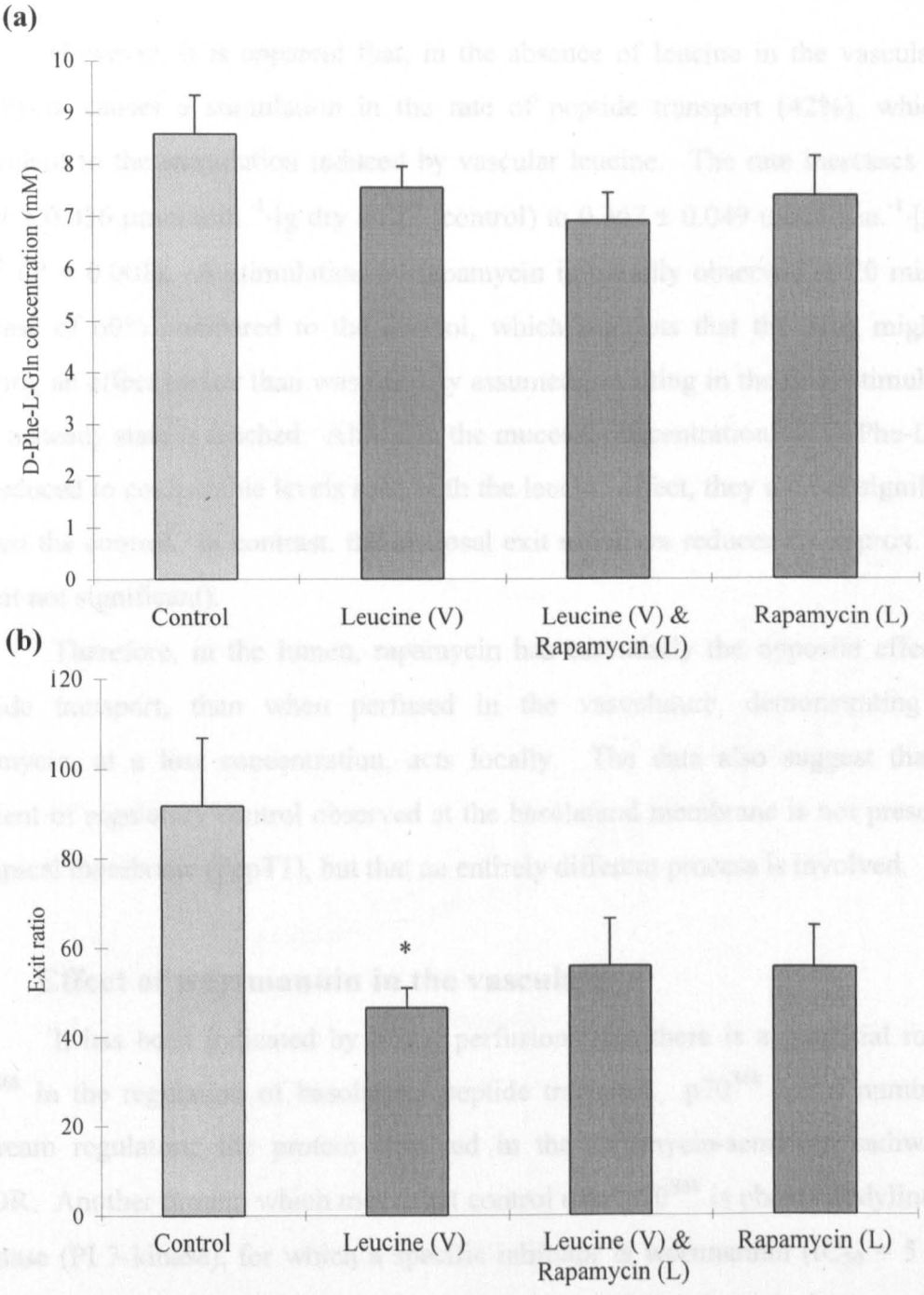

Figure 6.3(II)

Regulation of peptide transport by vascular leucine (10 mM) and luminal rapamycin (25 nM), demonstrated by the effects on the mucosal accumulation (a) and exit ratios (b) of 1 mM D-Phe-L-Gln. Bars represent the mean ± s.e.m. (control, n = 4; leucine (V), n = 6; leucine (V) & rapamycin (L), n = 6; rapamycin (L), n = 6). * $P < 0.05$ depicts a significant difference against the control.

However, it is apparent that, in the absence of leucine in the vasculature, rapamycin causes a stimulation in the rate of peptide transport (42%), which is equivalent to the stimulation induced by vascular leucine. The rate increases from 0.259 ± 0.036 μmol·min.$^{-1}$·[g dry wt.]$^{-1}$ (control) to 0.367 ± 0.049 μmol·min.$^{-1}$·[g dry wt.]$^{-1}$ ($P < 0.001$). A stimulation by rapamycin is initially observed at 20 min; an increase of 60% compared to the control, which suggests that the drug might be exerting an effect earlier than was initially assumed, resulting in the final stimulation once a steady state is reached. Although the mucosal concentrations of D-Phe-L-Gln are reduced to comparable levels seen with the leucine effect, they are not significant against the control. In contrast, the mucosal exit ratios are reduced by approx. 50% (albeit not significant).

Therefore, in the lumen, rapamycin has essentially the opposite effect on peptide transport, than when perfused in the vasculature, demonstrating that rapamycin, at a low concentration, acts locally. The data also suggest that the element of regulatory control observed at the basolateral membrane is not present in the apical membrane (PepT1), but that an entirely different process is involved.

6.6 Effect of wortmannin in the vasculature

It has been indicated by initial perfusions that there is a potential role of $p70^{S6k}$ in the regulation of basolateral peptide transport. $p70^{S6k}$ has a number of upstream regulators; the protein involved in the rapamycin-sensitive pathway is mTOR. Another protein which may exert control over $p70^{S6k}$ is phosphatidylinositol 3-kinase (PI 3-kinase), for which a specific inhibitor is wortmannin (IC_{50} = 5 nM). Thus, perfusions were performed with wortmannin infused through the vasculature (200 nM), with and without leucine, to determine the role of PI 3-kinase in peptide transport regulation. Again the transmural transport, and tissue concentration, of 1 mM D-Phe-L-Gln was measured. The results of these studies are shown in figure 6.4 (I & II).

Wortmannin appeared to have no effect on the leucine-stimulation of transport rate (0.333 ± 0.038 v. 0.356 ± 0.016 μmol·min.$^{-1}$·[g dry wt.]$^{-1}$, $P > 0.1$). Transport percentages at 20 min were decreased slightly (but not significantly) by 13% by wortmannin, however, the final (50 min) percentage was reduced by only 7%, indicating no effect on leucine-stimulated transport by wortmannin. The

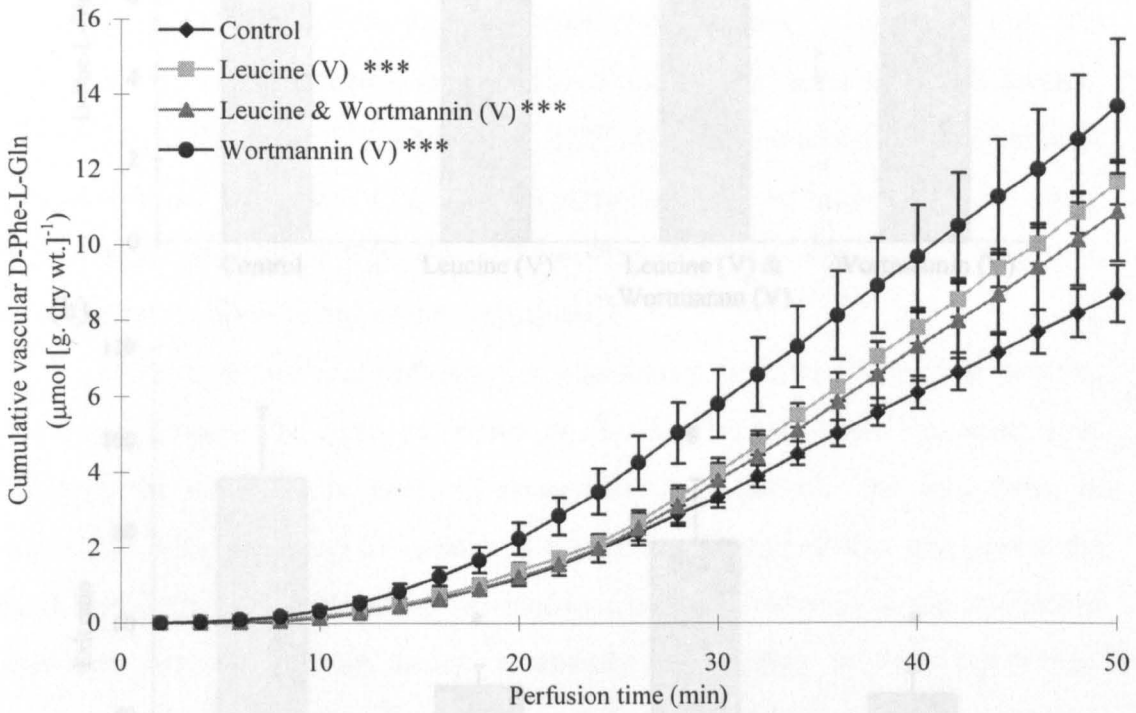

Figure 6.4(I)

Effect of vascular wortmannin (at 200 nM concentration) on the leucine stimulation of 1 mM D-Phe-L-Gln transport at the basolateral membrane, and on control rates of transport. Data points represent the mean ± s.e.m. (control, n = 4; leucine (V), n = 6; leucine & wortmannin (V), n = 6; wortmannin (V), n = 6). *** $P < 0.001$ depicts a significant difference against the control.

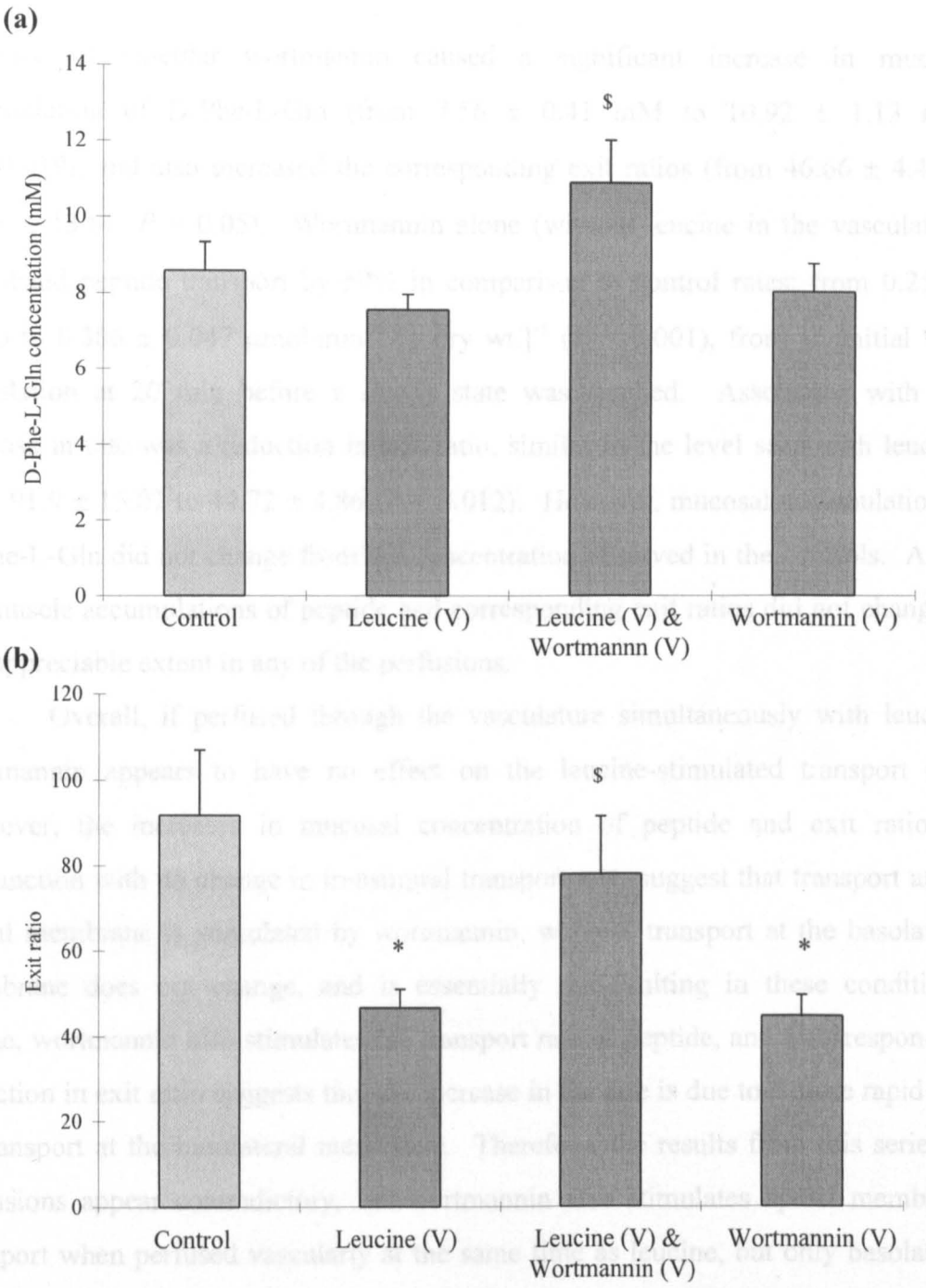

Figure 6.4(II)

Regulation of peptide transport by leucine and vascular wortmannin, demonstrated by the effects on the mucosal accumulation (a) and exit ratios (b) of 1 mM D-Phe-L-Gln. Leucine is present in the vasculature of the jejunum at 10 mM, wortmannin is also in the vasculature at 200 nM, with or without leucine. Bars represent the mean ± s.e.m. (control, n = 4; leucine (V), n = 6; leucine & wortmannin (V), n = 6; wortmannin (V), n = 6). * $P < 0.05$ depicts a significant difference against the control, $^{\$}$ $P < 0.05$ depicts a significant difference against 10 mM leucine (V).

presence of vascular wortmannin caused a significant increase in mucosal accumulation of D-Phe-L-Gln (from 7.56 ± 0.41 mM to 10.92 ± 1.13 mM, $P = 0.019$), and also increased the corresponding exit ratios (from 46.66 ± 4.41 to 78.08 ± 13.61, $P = 0.05$). Wortmannin alone (without leucine in the vasculature) stimulated peptide transport by 50% in comparison to control rates; from 0.259 ± 0.036 to 0.386 ± 0.047 $\mu mol \cdot min.^{-1} \cdot [g\ dry\ wt.]^{-1}$ ($P < 0.001$), from an initial 91% stimulation at 20 min before a steady state was reached. Associated with this increase in rate was a reduction in exit ratio, similar to the level seen with leucine; from 91.9 ± 15.07 to 44.72 ± 4.86 ($P = 0.012$). However, mucosal accumulation of D-Phe-L-Gln did not change from the concentration observed in the controls. Again the muscle accumulations of peptide and corresponding exit ratios did not change to any appreciable extent in any of the perfusions.

Overall, if perfused through the vasculature simultaneously with leucine, wortmannin appears to have no effect on the leucine-stimulated transport rate. However, the increases in mucosal concentration of peptide and exit ratio, in conjunction with no change in transmural transport rate, suggest that transport at the apical membrane is stimulated by wortmannin, whereas transport at the basolateral membrane does not change, and is essentially rate-limiting in these conditions. Alone, wortmannin also stimulates the transport rate of peptide, and a corresponding reduction in exit ratio suggests that the increase in the rate is due to a more rapid rate of transport at the basolateral membrane. Therefore, the results from this series of perfusions appear contradictory, i.e. wortmannin also stimulates apical membrane transport when perfused vascularly at the same time as leucine, but only basolateral membrane transport is stimulated when wortmannin is perfused alone.

6.7 Effect of wortmannin in the lumen

The previous experiments do not reveal conclusive information regarding the role of PI 3-kinase in the regulation of peptide transport at either the apical or basolateral membranes. However, in order to obtain a complete overview of regulation involving PI 3-kinase, as with rapamycin and mTOR, experiments were performed with wortmannin in the lumen (with and without vascular leucine). The results are shown in figure 6.5 (I & II).

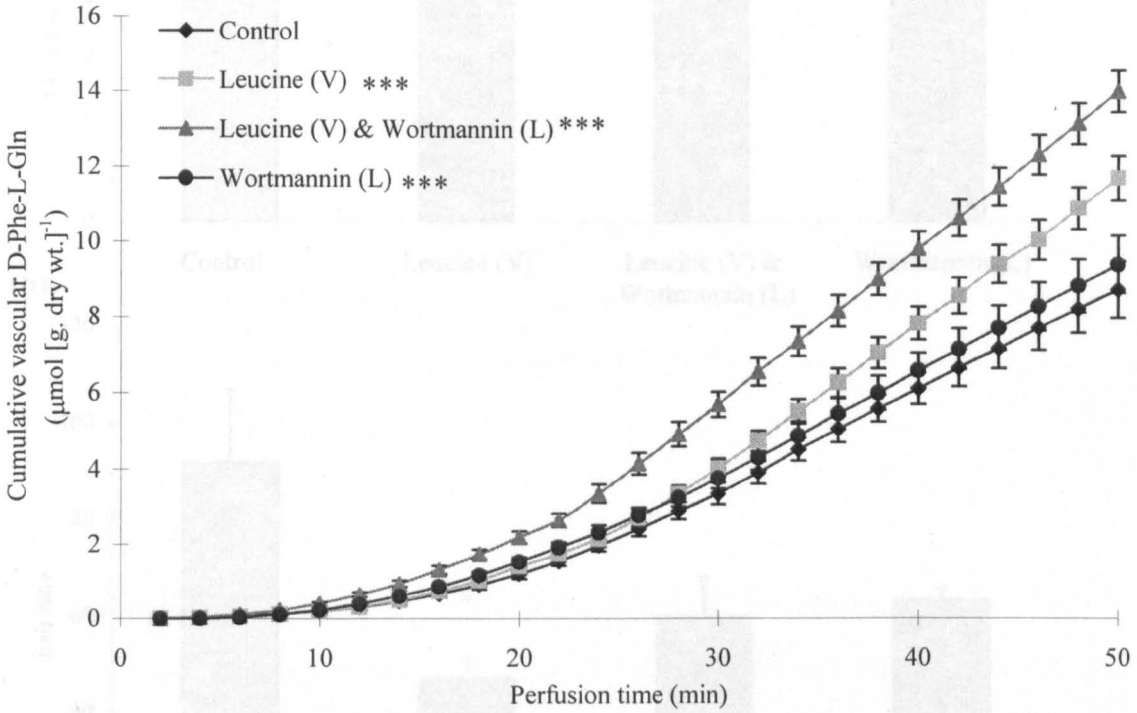

Figure 6.5(I)

Effect of luminal wortmannin (at 200 nM concentration) on the leucine stimulation, and on control rates, of 1 mM D-Phe-L-Gln transport. Data points represent the mean ± s.e.m. (control, n = 4; leucine (V), n = 6; leucine (V) & wortmannin (L), n = 3; wortmannin (L), n = 3). *** $P < 0.001$ depicts a significant difference against the control.

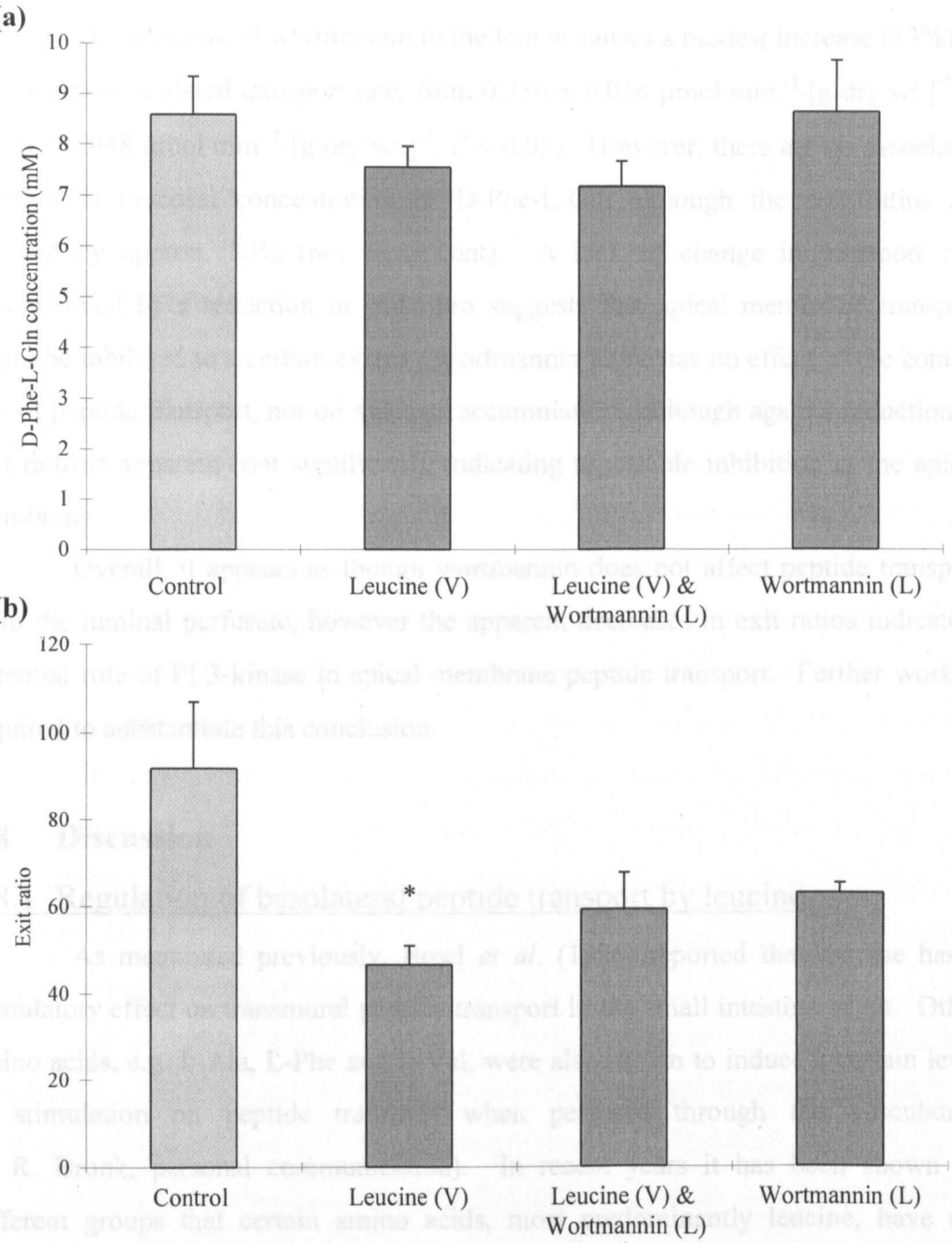

Figure 6.5(II)

Regulation of peptide transport by vascular leucine (10 mM) and luminal wortmannin (200 nM), demonstrated by the effects on the mucosal accumulation (a) and exit ratios (b) of 1 mM D-Phe-L-Gln. Bars represent the mean ± s.e.m. (control, n = 4; leucine (V), n = 6; leucine (V) & wortmannin (L), n = 3; wortmannin (L), n = 3). * $P < 0.05$ depicts a significant difference against the control.

The presence of wortmannin in the lumen causes a modest increase (13%) in the leucine-stimulated transport rate, from 0.356 ± 0.016 μmol·min.$^{-1}$·[g dry wt.]$^{-1}$ to 0.403 ± 0.048 μmol·min.$^{-1}$·[g dry wt.]$^{-1}$, $P < 0.05$). However, there are no associated changes in mucosal concentration of D-Phe-L-Gln although the exit ratios are reduced by approx. 30% (not significant). A lack of change in transport rate accompanied by a reduction in exit ratio suggests that apical membrane transport might be inhibited to a certain extent. Wortmannin alone has no effect of the control rate of peptide transport, nor on mucosal accumulations although again a reduction in exit ratio is apparent (not significant), indicating a possible inhibition at the apical membrane.

Overall, it appears as though wortmannin does not affect peptide transport from the luminal perfusate, however the apparent decreases in exit ratios indicate a potential role of PI 3-kinase in apical membrane peptide transport. Further work is required to substantiate this conclusion.

6.8 Discussion

6.8.1 Regulation of basolateral peptide transport by leucine

As mentioned previously, Boyd *et al.* (1996) reported that leucine has a stimulatory effect on transmural peptide transport in the small intestine of rat. Other amino acids, e.g. L-Ala, L-Phe and L-Val, were also shown to induce a certain level of stimulation on peptide transport when perfused through the vasculature (J. R. Bronk, personal communication). In recent years it has been shown by different groups that certain amino acids, most predominantly leucine, have the ability to specifically activate a cytosolic enzyme; p70^{S6k} (Hara *et al.*, 1998; Patti *et al.*, 1998; Wang *et al.*, 1998; Shigemitsu *et al.*, 1999). This led to using leucine to investigate short-term regulation of transport and the role of a p70^{S6k}-dependent pathway in its control mechanism.

The rate of D-Phe-L-Gln transport was increased significantly when leucine was present in the lumen or the vasculature of the small intestine. It is apparent from tissue data that transport at the basolateral membrane was stimulated to a greater degree than apical membrane transport. Transport by PepT1 might also have been stimulated, albeit to a lesser extent than the basolateral transporter, and as such,

cannot be detected due to the predominance of basolateral membrane transport stimulation.

It is evident that the same regulatory control by leucine is found irrespective of its location of infusion to the small intestine. Therefore, it doesn't matter from which side of the cell that leucine enters, the overwhelming effect is predominant stimulation of the basolateral peptide transporter.

$p70^{S6k}$ is a cytosolic enzyme involved in many varied cellular responses, in particular it is directly involved in translation; its major known substrate being the 40S ribosomal subunit protein S6, which is essential for the translation of mRNAs whose 5'-untranslated region contains a short oligopyrimidine sequence (Hara *et al.*, 1998). Phosphorylation of $p70^{S6k}$ has also been shown to be controlled by the level of nutrients to which the cell is exposed, reflected by the responses to fasting and re-feeding *in vivo*; starvation causes a reduction in $p70^{S6k}$ phosphorylation and, therefore, activation, whereas re-feeding restores the phosphorylation and activity (Hara *et al.*, 1998). This process probably functions to provide additional substrate for the increased level of protein synthesis that is induced. However, these are long-term control aspects which require a time period of days to occur, the effects of leucine on peptide transport seen in these perfusion experiments occur in a time scale of minutes and, as such, are short-term responses.

The activity of $p70^{S6k}$ depends on multi-site phosphorylation of the p70 polypeptide. There are at least three different regions of phosphorylation that have been identified, each of which is independently regulated (Hara *et al.*, 1998);

(1) a series of Ser/Thr-Pro motifs clustered in a pseudosubstrate autoinhibitory domain in the non-catalytic C-terminal tail (Ser_{434}, Ser_{441}, Ser_{447}, Thr_{444} in p70α1)

(2) Thr_{412} situated in a unique hydrophobic region

(3) Thr_{252} situated in the catalytic loop

However, only phosphorylation of Thr_{412} and Thr_{252} are absolutely essential for activity, although insulin causes phosphorylation at all three sites. Depletion of amino acids results in a decrease of phosphorylation of all residues in region (1), while activation of $p70^{S6k}$ by amino acids is associated with increased phosphorylation at these residues in region (1). As such, the stimulation of $p70^{S6k}$

activity, due to increased extracellular amino acid concentrations, is probably due to increased p70 phosphorylation (Hara *et al.*, 1998).

The data from these investigations with leucine implicate $p70^{S6k}$ as a regulator of peptide transport at the basolateral membrane of rat small intestine. The fact that this effect is localised at the basolateral membrane, and is not observed at the apical membrane, suggests that PepT1 is not under the control of $p70^{S6k}$. These data emphasise the distinction between the peptide transporters at the apical and basolateral membranes of the small intestine, i.e. they appear to be different proteins. It corroborates previous work presented in this thesis (chapter 5), and work published by other people (section 1.5), in that the unidentified basolateral peptide transporter is not PepT1.

The work by Shigemitsu and co-workers (1999) investigated the structural requirements of leucine to induce the stimulation in $p70^{S6k}$ activity. It was found that stereoselectivity is crucial, i.e. D-leucine did not activate $p70^{S6k}$. In addition, the primary amine group is also essential for activation, but a free carboxyl group or α-hydrogen is not required.

It isn't known whether the stimulatory effect of leucine on $p70^{S6k}$ is due to a specific receptor situated on the cell surface, or whether it occurs following transport of leucine into the cell (Patti *et al.*, 1998). If an acceptor molecule for leucine does exist (at this time it has only been postulated), it appears that recognition of leucine by the acceptor must be quite specific, due to the predominance of its effects on enzyme activity. Shigemitsu *et al.* (1999) proposed that the amino acid transporter for leucine, i.e. the system L transporter, would probably not be a candidate for the acceptor molecule, because it doesn't possess very strict structural requirements; it also transports Ile, Val, Met, Phe and His residues. Patti and co-workers demonstrated that a mixture of these amino acids, i.e. substrates for the L-transporter, did not induce $p70^{S6k}$ activity to an appreciable extent; leucine alone was shown to be dominant. In addition to the lack of knowledge about the acceptor molecule, the nature of the intracellular signal generated in response to leucine stimulation, that initiates the changes in regulatory protein phosphorylation(s), is also unknown. Despite this, the effect of leucine has been demonstrated to result in phosphorylation of certain sites on $p70^{S6k}$, which is likely to be mediated by Ser/Thr kinases that lie upstream of $p70^{S6k}$ (Patti *et al.*, 1998).

The effect of leucine on $p70^{S6k}$ activation appears to be specific; other kinases, e.g. insulin receptor kinase, protein kinase B (PKB), mitogen-activated protein kinases (MAPK), are not stimulated (Hara *et al.*, 1998; Patti *et al.*, 1998; Wang *et al.*, 1998). Therefore, leucine does not elicit a stress response.

$p70^{S6k}$ activity can be controlled by a number of proteins lying upstream, in various pathways, all of which have not been identified. Two major proteins shown to regulate $p70^{S6k}$ activity are mTOR and PI 3-kinase. To examine whether these two proteins are involved in the leucine-stimulation of basolateral peptide transport, perfusions were performed in the presence of specific inhibitors of the enzymes; rapamycin, which inhibits mTOR, and wortmannin, which inhibits PI 3-kinase.

6.8.2 Role of mTOR in leucine/$p70^{S6k}$-stimulated basolateral peptide transport

mTOR is known to lie upstream of $p70^{S6k}$, and exerts control over its phosphorylation state, and therefore its activation. The cascade pathway is designated 'the FRAP/mTOR pathway (FRAP; FK506-binding protein rapamycin-associated protein) (Shigemitsu *et al.*, 1999). However, the physiologic regulators of the mTOR (FRAP/RAFT-1/RAPT-1) kinase are not known (Hara *et al.*, 1998). Full understanding of the biochemical mechanisms that underlie regulation of $p70^{S6k}$ are also not known, but rapamycin (the substrate for mTOR) is known to cause the dephosphorylation of $p70^{S6k}$ *in vivo* (Shigemitsu *et al.*, 1999). Rapamycin binds to FKBP12, and the rapamycin-FKBP12 complex binds to mTOR, resulting in inhibition of mTOR protein kinase activity. This results in a decrease in $p70^{S6k}$ phosphorylation and activity (Shigemitsu *et al.*, 1999).

The previously mentioned reports (Hara *et al.*, 1998; Patti *et al.*, 1998; Wang *et al.*, 1998; Shigemitsu *et al.*, 1999), which demonstrated that leucine stimulated $p70^{S6k}$ activity, also showed that rapamycin blocked the effects of the amino acid. Therefore, to elucidate whether this mTOR/$p70^{S6k}$ pathway was involved in regulation of basolateral peptide transport, perfusions were performed with rapamycin.

The presence of rapamycin in the vasculature of the small intestine resulted in inhibition of the leucine-stimulated proportion of basolateral peptide transport. However, rapamycin did not affect the normal (control) rates of transport. These data

implicate $p70^{S6k}$ in leucine stimulated basolateral peptide transport, and a role for mTOR in the regulation pathway.

With reference to the $p70^{S6k}$/mTOR pathway proposed to regulate basolateral peptide transport, it is thought that rapamycin does not induce dephosphorylation of $p70^{S6k}$ primarily by inhibiting $p70^{S6k}$ kinases, but by stimulating $p70^{S6k}$ phosphatase activity (Hara *et al.*, 1998). The pathway they suggested is as follows (showing modifications to include effects on basolateral peptide transport);

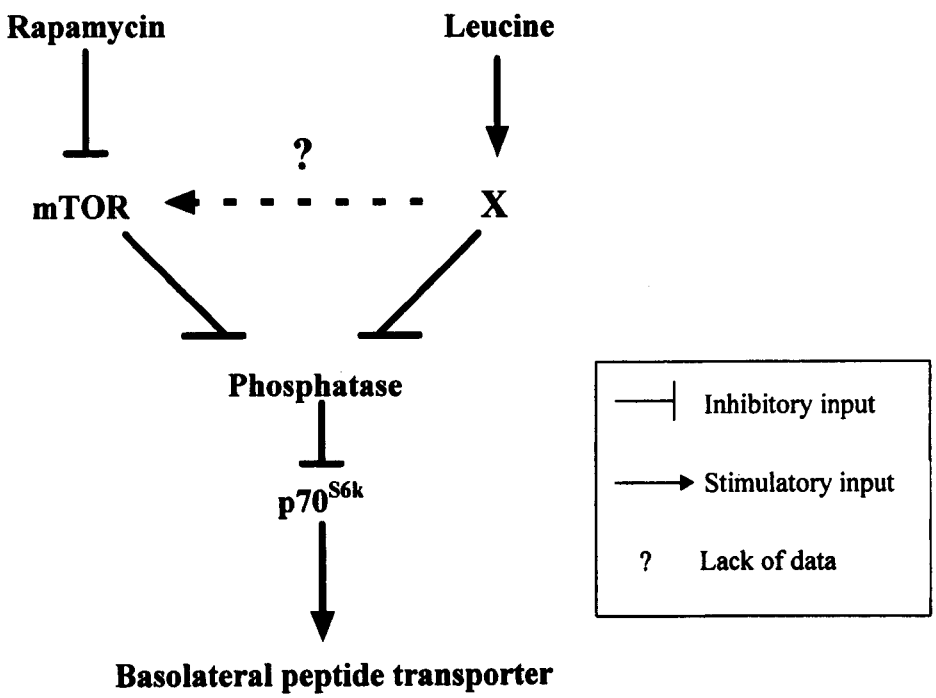

Figure 6.6

Proposed pathway for short-term regulation of peptide transport at the basolateral membrane by $p70^{S6k}$ (Hara *et al.*, 1998).

Hara *et al.* (1998) proposed that leucine could control $p70^{S6k}$ via a common phosphatase, i.e. independent pathways that converge through regulation of this phosphatase. However, the existence of this phosphatase is just speculative; an enzyme, which fulfils the criteria of expected regulatory behaviour, has not been

identified. Control of $p70^{S6k}$ by leucine might otherwise be to regulate mTOR kinase (shown by question mark in diagram), and therefore mTOR would function as a checkpoint control. These two situations are equivalent to the postulated mechanisms thought to be involved in basolateral peptide transport, however, the exact mechanism cannot be deduced from this data alone, further studies are required.

6.8.3 Role of mTOR in the regulation of apical membrane peptide transport

In contrast to the basolateral membrane, peptide transport at the apical membrane was not stimulated by leucine. In addition, the presence of rapamycin at the apical membrane (in the lumen, *in situ*) has a completely different effect than when in the vasculature. It appears not to have any effect on the leucine stimulation at the basolateral membrane, which initially suggests that the drug acts locally, i.e. it doesn't traverse the cell. However, without vascular leucine, rapamycin appears to stimulate peptide transport, to a rate comparable to the leucine-stimulation at the basolateral membrane. A stimulation by rapamycin is initially observed at 20 min, which suggests that the drug might be exerting an effect earlier than was initially assumed, resulting in the final stimulation once a steady state is reached. However, although the exit ratios do not significantly differ from the control perfusions, there appears to be a 50% reduction. The leucine-stimulatory effect at the basolateral membrane and the rapamycin-stimulatory effect are not additive, because the rate remains the same when both are present at their respective membranes, as when either is present alone. Therefore, they might act through a common effector, leading to the same response, or that one pathway might inhibit the second pathway. The precise mechanism cannot be concluded from these data alone.

The data presented here does not reveal the regulatory pathway which controls peptide transport by PepT1, but there is obviously a mechanism of control present, demonstrated by the action of rapamycin. PKC has been implicated in the regulation of apical peptide transport (Brandsch *et al.*, 1994), i.e. PKC inhibits PepT1 activity due to a decrease in V_{max}, but no change in K_m; PKC inhibitors restored peptide transport by blocking the inhibitory effect of PKC. It was postulated that regulation of this kind may involve post-translational modifications due to phosphorylation/dephosphorylation of the transporter protein. This could be either a

direct effect by PKC itself, or indirect via the action of additional protein kinases or phosphatases. Muller *et al.* (1996) also reported a potential role of PKA in regulating PepT1 transport in a cAMP-dependent manner. The effect of rapamycin on apical peptide transport might involve one of these processes.

A potential role of PKC is suggested from the results of these experiments. PKC activation depends upon phosphorylation at three distinct sites: (1) at an activation loop site, (2) a hydrophobic C-terminal site, and (3) a site subject to autophosphorylation (Parekh *et al.*, 2000). The unphosphorylated translation product has little or no intrinsic activity. The process of ligand binding at the membrane results in PKC becoming a substrate for kinases acting on the activation loop site and C-terminal sites. Phosphorylation of these two sites occurs due to two distinct pathways; phosphorylation at both is required for optimum activity (Parekh *et al.*, 1999). This is followed by autophosphorylation of the third site. Phosphorylation of the activation loop is essential for activity of PKC, whereas the two remaining sites play a more subtle role by maintaining a closed conformer that is resistant to phosphatase activity, thereby retaining activation of PKC for a considerable length of time (minutes to hours) (Parekh *et al.*, 2000). Dissociation of the ligand from the membrane surface allows the kinase to diffuse away, although phosphorylation of all three sites maintains the latent activity. The phosphorylated PKC enzyme can then be recruited back to the membrane and re-activated by DAG (diacylglycerol) alone.

PDK1, or a close relative, is responsible for PKC activation loop phosphorylation; constituting one of the distinguishable pathways. mTOR phosphorylates the C-terminal site of PKC in the V5 domain; this is the second pathway. Activation of this latter site is inhibited by rapamycin (Parekh *et al.*, 1999), resulting in a 10-fold decrease in PKC activity. The elements operating between mTOR and PKC are not yet known, but the simplest model would be that mTOR controls a phosphatase that acts upon this PKC site (Parekh *et al.*, 2000).

As mentioned previously, rapamycin in the lumen of the small intestine causes a stimulation in peptide transport, potentially by inhibiting the mTOR-dependent phosphorylation of the C-terminal site of PKC, thereby relieving the inhibition on PepT1 by active PKC. However, further work is required to elucidate fully the nature of the kinase pathway involved in regulation of peptide transport by PepT1.

Overall, the data obtained with vascular leucine and rapamycin (luminal or vascular) indicates that the basolateral transporter is likely to be distinct from PepT1, indicated by the differential regulatory pathways at the two membranes. The results presented in this section corroborate data presented previously in this chapter and in chapter 5. The distinct mechanisms of peptide transport regulation also demonstrate that rapamycin has a localised effect, probably due to the relatively low concentration employed (25 nM).

6.8.4 Role of PI 3-kinase in leucine/p70^{S6k}-stimulated basolateral peptide transport

PI 3-kinase is also known to lie upstream of p70^{S6k}, and its activation results in the production of phosphatidylinositol-3,4,5-triphosphate (PtdIns-3,4,5-P_3) and other inositol lipids phosphorylated in the D-3 position of the inositol moiety (Petritsch *et al.*, 1995). These lipids are thought to act as second messengers that propagate the extracellular signal inside the cell, possibly by activating an intermediate kinase, which is part of a cascade, eventually resulting in p70^{S6k} activation. Some studies have demonstrated a complete inhibitory effect of wortmannin (a PI 3-kinase inhibitor) on the amino acid-stimulation of p70^{S6k} activity (Wang *et al.*, 1998; Patti *et al.*, 1998), whereas others have reported a moderate reduction in activity (Shigemitsu *et al.*, 1999), or no effect at all (Hara *et al.*, 1998). Therefore, because of a possible role of PI 3-kinase in the regulation of basolateral peptide transport through p70^{S6k}, perfusions were performed in the presence of wortmannin.

However, the data arising from these perfusions were confusing. In conjunction with vascular leucine, vascular wortmannin appeared to moderately enhance the leucine-stimulation of transport at the basolateral membranes and also stimulated a little at the apical membrane, whereas alone wortmannin appeared to solely stimulate basolateral membrane transport. Although these data are not clear, it implies that there is a PI 3-kinase-dependent element of control at the basolateral membrane. If PI 3-kinase inhibits peptide transport under control conditions, the inhibition of PI 3-kinase by wortmannin will relieve its inhibitory effect on transport, thereby producing a stimulation of rate. This is a very similar situation as found with rapamycin at the apical membrane, i.e. a stimulatory effect is observed with the drugs

alone, but the anticipated inhibition of the leucine effect due to the action of the drugs on their respective targets was not observed. Therefore it seems as though there might be a wortmannin-sensitive pathway, in addition to a leucine-sensitive pathway, possibly leading to a common effector.

PI 3-kinase acts through PKB to exert its downstream effects on $p70^{S6k}$. However, amino acids do not stimulate PKB activity (Patti *et al.*, 1998; Wang *et al.*, 1998). Therefore, if PI 3-kinase was implicated in the regulation of peptide transport via $p70^{S6k}$, it must be independent of PKB activation, and so another alternative upstream pathway may be involved.

Despite this speculative assumption, the data from these experiments are not clear, and the effects observed with wortmannin in conjunction with leucine are contradictory to the effects seen with wortmannin alone. These data do not, therefore, point to an obvious mechanism and require further work for clarification.

6.8.5 Role of PI 3-kinase in the regulation of apical membrane peptide transport

In contrast to vascular wortmannin, luminal wortmannin has no effect on leucine-stimulated transport, or on control rates. Therefore, this indicates that PI 3-kinase is not involved in regulation of PepT1 transport at the apical membrane. However, because mucosal exit ratios were reduced by the presence of wortmannin in the lumen, PI 3-kinase may be involved in apical peptide transport; further work is required for elucidation of its exact involvement in transport.

As stated previously, PDK1 is involved in phosphorylation and activation of PKC (Parekh *et al.*, 2000). (Parekh *et al.*, 2000). PI 3-kinase is located upstream of PDK1, therefore it might be expected that wortmannin would have a stimulatory effect on apical membrane peptide transport, in the same way that rapamycin does at this membrane. However, this response is not evident, suggesting that if PKC did have a role in the regulation of PepT1 transport, it must be via a pathway which is independent of PI 3-kinase.

Again the data demonstrate that wortmannin acts locally at the membrane to which it was infused. Also apparent is the distinction between PepT1 and the basolateral peptide transporter; rapamycin and wortmannin appear to have reciprocal effects at each membrane:-

Apical membrane

- PI 3-kinase is not involved in regulation of peptide transport
- mTOR regulates transport in an undefined stimulatory capacity, possibly via PKC

Basolateral membrane

- a $p70^{S6k}$/mTOR pathway regulates transport
- an independent PI 3-kinase pathway might also be involved

6.9 Future work

It is clear that although some initial aspects of regulation can be determined using the vascular perfusion technique described (for example, rapamycin-sensitive pathways), other pathways are extremely complicated (for example, wortmannin-sensitive pathways). Other (*in vitro*) methods can be used in conjunction with the perfusion technique to clarify the results obtained, for example, purified membrane vesicles, which completely separate the distinct regulatory situations at the different membranes. However, studies using intact tissue are invaluable for the elucidation of the physiological situation which occurs *in vivo*, which sometimes cannot be deduced from isolated membranes.

6.10 Conclusions

(1) The peptide transporters at the apical (PepT1) and basolateral membranes appear to be distinct proteins, demonstrated by different regulatory processes.

(2) The drugs used in this study (rapamycin & wortmannin) have a localised action, i.e. at the membrane to which they were infused, at the low concentrations employed.

(3) Peptide transport at the apical membrane is regulated by an mTOR-sensitive pathway, which is independent of PI 3-kinase, and might involve PKC (Brandsch *et al.*, 1994; Parekh *et al.*, 1999, 2000).

(4) Peptide transport at the basolateral membrane is regulated by a $p70^{S6k}$/mTOR pathway, which is stimulated by leucine. In addition, a possible role of PI 3-kinase is postulated, which is independent of the $p70^{S6k}$/mTOR pathway.

Overall, certain aspects of short-term regulation of peptide transport in the small intestine have been demonstrated, but further work is required to clarify other ambiguous data. Short-term regulation of intestinal peptide transport has been overlooked thus far, but such knowledge is essential if we are to fully understand the physiological processes behind peptide transport as a whole. These investigations provide an insight into the complexity of the control of transport, and indicate that considerably more studies are needed.

CHAPTER 7: DISCUSSION

All results have been previously discussed in detail at the end of each individual chapter, as such this discussion section will collectively review the important points of this thesis. For a more detailed explanation of the specific results and conclusions, please refer to the relevant chapter.

7.1 Interaction of a potential photoaffinity label with intestinal peptide transporters

The overall aim of this thesis was to investigate the peptide transporters at both the brush-border and basolateral membrane of rat intestinal mucosa, with particular attention to the, as yet unidentified, basolateral transport protein. An approach was taken to specifically label the transporters by using a radioactive photoaffinity labile compound which, when applied to (brush-border or basolateral) membrane vesicles, would covalently attach to the substrate binding site of the transporter in the presence of light and permit detection of the specific protein(s). The potential label is a derivative of a dipeptide known to be accepted as a substrate by the intestinal transporters (Lister *et al.*, 1995). [4-azido-D-Phe]-L-Ala was synthesised by Prof. P. D. Bailey and Dr. I. Collier in the Chemistry department, Heriot Watt University, Edinburgh. Prior to the undertaking of this labelling study, a direct interaction of the potential label with the peptide transporters had to be unequivocally proven. A series of perfusions (luminally and vascularly perfused rat jejunum, *in situ*) demonstrated an efficient dipeptide label-active site interaction (Chapter 3).

[4-azido-D-Phe]-L-Ala was shown to be a substrate for the intestinal peptide transporters (PepT1 and the basolateral transporter) by its extremely rapid, intact transmural transfer from the lumen to the serosa of the jejunum. A significantly lower mucosal concentration of the label, in comparison to D-Phe-L-Gln under the same conditions, suggested that the label is more efficient substrate for the basolateral transporter than PepT1, i.e. exit from the cell occurs at a faster rate than entry.

A direct interaction with the active site of the transporter(s) was demonstrated by the ability of [4-azido-D-Phe]-L-Ala to inhibit the transport of a second dipeptide (D-Phe-L-Gln). This inhibition occurred only when [4-azido-D-Phe]-L-Ala was presented to the cytosolic face of the basolateral transporter (i.e. included in the luminal perfusate), where it prevented exit of D-Phe-L-Gln from the mucosal cells. The presence of [4-azido-D-Phe]-L-Ala on the extracellular side of the basolateral transporter (i.e. included in the vascular perfusate) did not affect D-Phe-L-Gln efflux from the enterocytes. The results from these perfusions collectively indicate an asymmetry of interaction of [4-azido-D-Phe]-L-Ala with the basolateral transporter. The substrate affinity and transport capacity for uptake across the membrane into the cell by the basolateral transporter is considerably lower than when functioning in an efflux direction (Inui *et al.*, 1992; Saito *et al.*, 1993) although some groups dispute this (Thwaites *et al.*, 1993b) stating the reverse is true. Its physiological role is predominantly in the efflux direction, performing an absorptive role within the intestine, i.e. the transfer of peptides from the cell into the bloodstream. Therefore, the label may be able to bind to the exofacial site of the basolateral transporter, but, due to a lower extracellular affinity for substrates, a higher concentration may be required to observe inhibition at the serosal face of the membrane. In summary, the data concerning the basolateral transporter corresponds to the unidirectionality of the absorptive process *in vivo*, which has been indicated for the transporter by a large number of research groups.

Inhibition of substrate transport at the apical membrane (i.e. via PepT1) by [4-azido-D-Phe]-L-Ala is not apparent, however, it may be occurring, albeit to a lower extent than that seen at the endofacial side of the basolateral transporter, and as such cannot be ruled out completely. Previous experiments, by our collaborators in the Department of Human Anatomy, University of Oxford, with PepT1-expressing *Xenopus* oocytes (Boyd *et al.*, personal communication) demonstrated a significant inhibition of D-Phe-L-Gln transport by [4-azido-D-Phe]-L-Ala, therefore proving a direct interaction of the label with PepT1 active site. PepT1 is thought to have a greater capacity for transport than the basolateral transporter (Inui *et al.*, 1992; Saito *et al.*, 1993; Matsumoto *et al.*, 1994; Terada *et al.*, 1999), which may, at least partially, explain the lack of inhibition at the apical membrane. Again, a higher concentration of [4-azido-D-Phe]-L-Ala may be required for inhibition to be detected

at PepT1. Although transport inhibition is not clearly observed at the apical membrane, the rapid transfer rate of the potential label from the lumen to the vasculature demonstrates that it is accepted as a substrate and transported by PepT1 (corroborating the Oxford data). [4-azido-D-Phe]-L-Ala is not traversing the intestinal wall via a paracellular flow mechanism, because this has been previously demonstrated to be negligible (Lister *et al.*, 1995).

Overall, the data demonstrate that [4-azido-D-Phe]-L-Ala can interact with both of the intestinal peptide transporters, and so the structure was further developed to be used as a photoaffinity label to identify the membrane proteins.

7.2 Modifications to the D-Phe-L-Ala structure confers an enhanced affinity for the peptide transporters

An additional, and very interesting, fact emerged from these perfusion studies; the addition of the azide (N_3^+) group to D-Phe-L-Ala, performed for label production, conferred an enhanced interactive ability of the dipeptide substrate with the transporters. The presence of a net positive charge on the structure results in a more rapid rate of transmural transfer, in particular exit across the basolateral membrane is considerably enhanced. This is probably not due to a change in intrinsic activity of the transporters, but to the pH of the perfusate medium. Cationic peptides have been shown previously to be more efficient substrates for PepT1 at a pH of approx. 6.5, whereas anionic and neutral substrates are most efficient at a more acidic pH (5.5) (Temple *et al.*, 1995; Wenzel *et al.*, 1996; Steel *et al.*, 1997; Amasheh *et al.*, 1997). The luminal and vascular perfusate solutions were both at pH 6.8, therefore transport of the cationic label would be maximised, whereas the neutral dipeptides (D-Phe-L-Gln & D-Phe-L-Ala) would be relatively less efficient substrates. These distinct pH dependencies for transport emerge from different H^+ flux coupling ratios of differently charged substrates (section 3.7.4), i.e. anionic substrates are co-transported with $2H^+$, zwitterionic substrates with $1H^+$, and cationic substrates with $1H^+$, but can be transported in the absence of H^+. It is not clear whether the same mechanism is present at the basolateral membrane, due to a lack of knowledge in that area. However, some studies have indicated a proton-dependence in basolateral transport (Dyer *et al.*, 1990; Thwaites *et al.*, 1993a, b; Saito *et al.*, 1993;

Terada *et al.*, 1999), and so equivalent flux coupling ratios for this transporter cannot be disregarded.

7.3 Identification of PepT1 in the apical membrane

A tritiated form of the photoaffinity label ([4-azido-3,5-^{3}H-D-Phe]-L-Ala) was used in an attempt to identify PepT1 from brush-border membrane vesicles (Chapter 4). However, the results were disappointing; a large number of membrane proteins incorporated the dipeptide label. Despite this, the amount of label incorporation, even by the protein that was predominantly labelled, was only 0.003% at maximum and is therefore highly specific with very little random, non-specific covalent binding. However, substrate protection by a dipeptide was not isolated to a single protein species, therefore PepT1 could not be individually detected. It is thought that the high molecular weight proteins, which bound the dipeptide label in a substrate-specific manner, are peptide hydrolases known to be present in great abundance in the apical membrane. These proteins are also specific for peptide substrates, which is the reason why they incorporated the photoaffinity label.

Previous studies by Kramer and co-workers (1987, 1988, 1990a,b), using photolabile derivatives of known PepT1 substrates, identified a 127 kDa microheterogenous protein which they implied could be a component of the peptide transport system. A protein of 130 kDa molecular weight was predominantly labelled in the study presented in this thesis, which is thought to correspond to the 127 kDa protein of Kramer's. Their studies suggested that the protein was not a peptide hydrolase and was present throughout the length of the small intestine (Kramer *et al.*, 1998). Reconstitution of the protein into proteoliposomes resulted in a specific transport activity similar to PepT1, which retained its stereoselectivity for substrates (Kramer *et al.*, 1992). However, investigations by Daniel & Adibi (1993) into the substrate-specific requirements of PepT1 revealed that because the photoreactive azide analogues, i.e. benzylpenicillin, cephalexin, Gly-Pro, that Kramer *et al.* used to label the 127 kDa protein did not contain a free α-amino group, it is unlikely that the labelled protein represents the H^{+}/peptide cotransporter.

There is a major difference in the molecular weight of the protein that was chiefly labelled in this study compared with previously published molecular weight(s) of PepT1. The reported molecular weights of the PepT1 from small

intestine in small mammals are; 71 kDa in rabbit (Fei *et al.*, 1994; Daniel *et al.*, 1996), and 75 kDa in rat (Saito *et al.*, 1995; Ogihara *et al.*, 1996). These values are considerably lower than 130 kDa observed in this study and so this predominantly labelled protein is thought not to be PepT1; the protein may be a protease, or possibly a regulator of peptide transport as previously described by Kramer *et al.* (1987, 1988, 1990a,b). Labelling of PepT1 alone cannot be observed due to the overall high level of incorporation by other proteins, therefore although it is probably present at a molecular weight of approx. 75 kDa, it cannot be individually detected.

Efforts were made to block incorporation of the label by the peptide hydrolases, using bestatin and papain digestion, to leave PepT1 free to be singly identified. Although bestatin is also a substrate for PepT1, a notably higher concentration is needed for interaction with the peptide transporter; three orders of magnitude greater than the concentration which inhibits peptidase activity. For example, peptidase inhibition is observed with a concentration in the range of 5-10 μM (Takano *et al.*, 1994; Kramer *et al.*, 1990b), whereas an IC_{50} of 10 mM was reported for cephalexin uptake into BBMV (Kramer *et al.*, 1990b). However, the results were not as anticipated; 20 μM bestatin failed to prevent hydrolase labelling which, in hindsight, is possibly due to the incubation time employed. It has been proposed that binding of bestatin to peptidases involves a mechanism, which includes a slow conformational change, that takes up to 2 h to achieve (Wilkes & Prescott, 1985). This observation indicates that increasing the incubation time of bestatin with BBMV to 2 h will block labelling of peptidases and allow PepT1 identification.

Although treatment of vesicles with papain has been previously demonstrated to cause an enrichment in peptide transport activity (Ganapathy *et al.*, 1981; Inui *et al.*, 1984) due to cleavage of the peptidases from the surface of the lipid bilayer, in this study photoaffinity label binding by all membrane proteins was abolished. The reason for this is not clear, but may involve an incubation time that was too prolonged.

In summary, PepT1 could not be individually identified from BBMV by the photoaffinity labelling technique due to a high extent of label incorporation by additional membrane proteins other than the peptide transporter. It is a possibility that the relatively low level of label binding by PepT1 may be due to the pH of the equilibration buffer (pH 5.5). Experiments in Chapter 3, corroborated by results

from previous studies (Temple *et al.*, 1995; Wenzel *et al.*, 1996; Steel *et al.*, 1997; Amasheh *et al.*, 1997), indicate that label incorporation might be enhanced at a slightly higher pH (6.5-6.8), due to its net positive charge. Future work of this type should take the distinct pH dependencies of differently charged substrates into account.

7.4 Identification of a candidate basolateral peptide transporter

In contrast to the lack of achievement in identifying PepT1 from BBMV, a 112 kDa protein thought to be a candidate to be the basolateral transporter was successfully identified and isolated from BLMV (Chapter 5). Whereas many proteins in the brush-border membrane incorporated the label, a single discrete peak of radioactivity, representing label-binding by a protein, was detected in basolateral membranes. Ratios of unprotected labelling v. dipeptide-protected labelling was considerably higher with this protein than the others with a lower extent of label incorporation, indicating the predominance of labelling. This pattern of labelling was highly reproducible. Labelling of the 112 kDa protein was abolished by preincubation with a dipeptide, whereas free amino acids had very little effect. D-Phe-L-Gln actually provided a higher degree of protection to the putative basolateral transporter from labelling, when compared to PepT1. This may be due to a combination of the high concentration of D-Phe-L-Gln (16.7 mM), a lower affinity of the basolateral transporter for substrates and a relatively lower capacity for transport, in comparison to PepT1. Therefore, whilst the basolateral transporter would probably be saturated by D-Phe-L-Gln and would therefore not interact with the substantially lower concentration of label (4.2 μM), the higher transport capacity of PepT1 might mean that binding of the label and D-Phe-L-Gln could occur simultaneously.

Also in contrast to brush-border membrane labelling experiments, a considerably higher proportion of the initial label formed a covalent attachment to the 112 kDa protein (6-fold higher than to the predominantly labelled 130 kDa protein in BBMV). This increased level of binding may reflect the situation that was determined in the perfusion experiments (Chapter 3), whereby the label appeared to be a more efficient substrate for the basolateral transporter than for PepT1. However,

potential differences in the abundance of the peptide transporters in their respective membranes, relative to other proteins, must also be acknowledged.

In summary, a candidate for the basolateral peptide transporter was identified by a photoaffinity labelling method. However, the method of detection of a labelled protein did not clarify whether the radioactive peak contained a single protein species. As such, the labelled protein sample was subjected to a second method of separation; IEF. In addition to ensuring that the labelled sample contains an individual protein, this technique allows further information about the protein to be determined, i.e. its isoelectric point. The pI of the protein was shown to be approx. 6.5, whereas the pI of free [4-azido-3,5-^{3}H-D-Phe]-L-Ala was 6.0, therefore the radioactive peak detected in the gels was not due to unbound label.

7.5 Sequence analysis of the candidate basolateral peptide transporter

The technique of photoaffinity labelling, combined with rod gel separation, permitted the isolation of the 112 kDa protein in sufficient quantities to progress towards performing initial sequence analysis. A concentrated radioactively labelled sample of the 112 kDa protein, isolated from rod gels, was subjected to 2-DE using an immobilised pH gradient in the first dimension and standard SDS-PAGE slab gels in the second dimension.

However, the results were not as expected; although a single spot of 112 kDa was present, it was not predominant. In addition, two very dense spots at approx. 40 kDa each could be detected. There were very few other spots that could be detected in the 2-DE gel, which could be attributed to the initial isolation procedure of the 112 kDa protein from other membrane proteins. The abundance of the two 40 kDa spots, coupled with a low density 112 kDa spot, and very little else within the gel, implied that the 112 kDa protein might have been proteolysed, thus resulting in the two spots. However, scintillation counting of the protein spots revealed that none were radioactively labelled. Therefore, during proteolytic degradation of the 112 kDa protein, cleavage of the portion that bound [4-azido-3,5-^{3}H-D-Phe]-L-Ala was thought to have occurred, and the resulting polypeptide eluted from the bottom of the SDS-PAGE gel. Despite the proteolytic breakdown of the labelled 112 kDa protein, work on the candidate basolateral peptide

transporter was progressed. Due to their predominance in the gel, it is assumed that these polypeptides were constituents of the 112 kDa protein, and so analysis continued with these two spots.

To investigate whether proteolysis was responsible for the relatively minor 112 kDa spot, an anti-protease inhibitor cocktail was included in all solutions during isolation and 2-DE of the labelled protein (work performed by Mrs. Julie Affleck). As anticipated, a very dense spot at 112 kDa (pI 6.5) could be detected, associated with the removal of the two 40 kDa spots thought to be proteolytic products. These results corroborated the initial conclusions, and therefore the sequence data that was eventually obtained from the two 40 kDa spots could be attributed to the 112 kDa protein.

A lack of radioactivity following 2-DE of the labelled protein was investigated further. It was thought that the fixing stage of the staining procedure resulted in the prevention of protein elution from the gel prior to scintillation counting. As such, a stain was utilised which did not require fixing; a negative (zinc) stain. However, although radioactivity could be detected to a certain level, it was not abundant enough and so this stain also seemed to be quenching radioactivity to some extent. Therefore, a radioactive spot could not be unequivocally detected following 2-DE. An alternative approach was taken; an IPG strip was focused with the labelled 112 kDa protein, which was then sliced into sections, and these sections were subjected to scintillation counting. Using this method, a peak of radioactivity could be detected, which corresponded to the precise position in the pH gradient in the second dimension gel where the 112 kDa protein focused and was detected by the presence of a spot. Therefore, the protein could then be identified with certainty in the final 2-DE gel.

The two 40 kDa spots, representing the candidate basolateral protein, was analysed by two mass spectrometry techniques; MALDI-TOF (matrix-assisted laser desorption/ionisation time of flight) and Q-TOF (quadrupole time of flight). MALDI-TOF was principally used to obtain a peptide fingerprint, following digestion of the protein with trypsin. The peptide fingerprint of a protein depends entirely on its primary amino acid sequence because trypsin cleaves the polypeptide backbone at the carboxylic sides of lysine and arginine residues, except when adjacent to a proline residue. As such the fingerprint is specific for that individual protein. Proteins can be unequivocally identified from databases from their peptide

fingerprint; the process of searching databases to identify proteins in this way is termed 'peptide fingerprint profiling'.

MALDI-TOF analysis of the peptides produced from the two 40 kDa protein spots revealed 83 peptides in spot A and 53 peptides in spot B. It was very interesting to discover that 24-29 of the peptides detected in spots A and B had identical masses, indicating that they did indeed originate from one single protein (the candidate basolateral transporter). Due to the fact that more peptides were detected from spot A than spot B, it is thought that the original 112 kDa protein was broken down to initially form spot A, and then further proteolysis resulted in another distinct spot (B).

Peptide fingerprint profiling of data from spots A & B, utilised in a combination of different ways, did not match to any protein from any of the databases searched.

Additional sequence information of the candidate basolateral transporter was obtained from Q-TOF analysis. This produced a partial sequence of one of the peptide fragments resulting from the tryptic digest; the sequence was from a peptide detected in spot A. A sequence tag was constructed as follows;

NH_2- / -Thr-Ser-Asn-Phe-Val-Thr-(Ala-Thr-Ser)- / -COOH

The sequence consists of nine amino acid residues; six of which are definite and the remaining three are highly probable (> 99%) (shown in brackets). The sequence tag was used to search databases in an attempt to identify the protein contained within spot A on the 2-DE gel. The six definite residues, or the complete nine residue sequence, were used to search both full length sequence databases and expressed-sequence tag (EST) databases. Although some protein matches were found for the majority of the nine amino acid sequence, a total match to all residues was not evident. In addition, despite the fact that the proteins matched to most of the sequence, their peptide fingerprints did not correlate with the fingerprint of the 112 kDa protein, and therefore could not be identified as a positive match.

Overall, the protein in spots A and B could not be identified by either MALDI-TOF or Q-TOF analysis alone, combined with database searches, nor from a combination of both mass spectrometric analysis methods. If the basolateral

membrane protein were contained within the databases, a positive match would have been found using the data presented here. It is generally accepted that if a protein has been previously isolated, and its sequence is contained within the databases, a peptide fingerprint or a partial sequence will unequivocally find the match (James *et al.*, 1993). It is therefore clear that the 112 kDa protein, which has been specifically photoaffinity labelled with a dipeptide analogue, and which is postulated to be a candidate to be the basolateral peptide transporter, has not been previously identified, and as such appears to be a novel protein.

In the past it has been postulated that PepT1 is responsible for the exit of peptides from the cell across the basolateral membrane, i.e. it was thought that there wasn't a distinct transport protein. During the cloning and expression of rabbit PepT1 by Hediger's group (Fei *et al.*, 1994), hybrid depletion studies performed to block PepT1 expression resulted in a loss of induced Gly-Sar transport activity in *Xenopus laevis* oocytes. As such, they suggested that peptide transport activity in the basolateral membrane is entirely due to PepT1 expression. However, at present there is overwhelming evidence proving the existence of a distinct transporter protein in the basolateral membrane. In particular, PepT1 expression has been immunolocalised exclusively to the apical membrane (Ogihara *et al.*, 1996; Walker *et al.*, 1998), in addition to distinct transport characteristics demonstrated by a number of kinetic studies (section 1.5).

As mentioned, the sequence data presented here does not positively match to any known protein sequence and, as such, reinforces the distinction between PepT1 and the basolateral transporter. Only a few (maximum of 5) of the peptide fragments generated from the candidate basolateral peptide transporter correspond to tryptic peptides of rat PepT1. Interestingly, these five peptides are located in just two loops connecting adjacent transmembrane domains; the majority are located in the notably large extracellular loop connecting TM 9 and 10, and the remainder in the intracellular loop adjoining TM 6 and 7. Sequence analysis comparisons of the peptide transporters cloned thus far have revealed that the conserved sequences are predominantly located in the TM domains, with a lower degree of homology in the interconnecting loops. The fact that only a very small percentage of the tryptic peptides of the candidate basolateral protein match to peptides of PepT1, and that these are found in these loops, implies that they are not the same protein. In addition, the partial sequence of nine (or six) amino acids is not contained within the primary

sequence of rat PepT1, nor any other peptide transporter which has presently been cloned and sequenced.

Subsequent experiments, which studied the short-term regulation of intestinal peptide transport, also provide evidence that the two transporters are not one protein, demonstrated by distinct regulatory processes at the apical and basolateral membranes.

7.6 Short-term regulation of intestinal peptide transport

Although investigations were devised to understand the nature of short-term regulation of peptide transport in the small intestine (Chapter 6), an additional aspect of possible regulation was also observed indirectly, as a result of a separate study (Chapter 3). Therefore, both areas of regulation will be discussed in this section.

7.6.1 Substrate regulation of its own transport

Suprising and unexpected results were obtained when investigating the effects of D-Phe-L-Gln transport under the influence of D-Phe-L-Ala (Chapter 3). It was anticipated that the presence of D-Phe-L-Ala would inhibit transport of the substrate (D-Phe-L-Gln) due to competition for the same active site(s), in the same manner as the photoaffinity label. However, it was observed that D-Phe-L-Ala actually acted to stimulate substrate transport, both from the vascular side and the luminal side of the jejunum, although the stimulation appears to be greater on the basolateral transporter (implied by smaller exit ratios).

Previous investigations (Thamotharan *et al.*, 1998; Walker *et al.*, 1998; Shiraga *et al.*, 1999) have demonstrated that pre-treatment of Caco-2 cells with one dipeptide causes a stimulation in the transport of a second dipeptide; this stimulation occurs at a transcriptional level to provide a more abundant population of transporters at the cell membrane. However, this follows 24-72 h preincubation and so the differences in exposure time to peptide mean that this cannot be the mechanism by which D-Phe-L-Ala is acting in this study.

The results with peptide transport presented here correlate with the conclusions by Sharp *et al.* (1996) on the regulation of sugar transport, whereby an additional rapid response of SGLT1 to jejunal glucose, that preceded the onset of increased protein expression, occurred within 30 min exposure.

The exact mechanism by which the transport stimulation occurs could not be elucidated from these experiments alone. However, due to the rapid time course of stimulation by D-Phe-L-Ala, it seems likely that there may be an aspect of allosteric control involved, indicated by the presence of a sigmoidal curve when D-Phe-L-Gln concentration is plotted against transporter activity.

Whichever the process (Sharp's mechanism / allosteric control), it seems that either D-Phe-L-Ala interacts with the basolateral transporter with greater efficiency than with PepT1, or that it exerts more control at this membrane, or that the basolateral transporter is more sensitive to regulation in this way than PepT1. These results have just touched the surface of peptide transport regulation in this manner and more extensive studies are required to further the understanding the precise mechanism.

7.6.2 Protein kinase cascades involved in regulation of intestinal peptide transport

Previous studies in our laboratory (Boyd *et al.*, 1996) demonstrated that leucine stimulates transmural peptide (D-Phe-L-Gln) transport in rat small intestine. Other amino acids, e.g. L-Ala, L-Phe and L-Val, have also been shown to have a similar effect, albeit to differing extents (J. R. Bronk, personal communication). The time course of the perfusion technique used in these experiments (50 min) indicated an element of short-term regulation of peptide transport.

Subsequent to these results other groups have shown that certain amino acids, most predominantly leucine, have the ability to specifically activate an enzyme located in the cytosol of various cell types; $p70^{S6k}$ (Hara *et al.*, 1998; Patti *et al.*, 1998; Wang *et al.*, 1998; Shigemitsu *et al.*, 1999). The time course of this activation was also in the order of minutes, therefore indicating that this process was also a short-term event. As such, it was postulated that the leucine stimulation of peptide transport demonstrated by Boyd *et* al. (1996) might involve a $p70^{S6k}$-dependent mechanism, therefore leucine was used to investigate short-term regulation of transport and the role of a $p70^{S6k}$-dependent pathway was studied using specific inhibitors of the enzyme.

In order to determine whether leucine had similar or distinct effects on peptide transport at the apical and basolateral membranes, it was perfused through

either the lumen or the vasculature of the small intestine. However, the overall effect was a stimulation in transport rate of D-Phe-L-Gln, predominantly at the basolateral membrane, irrespective of the location of infusion of leucine, indicated by tissue concentration and exit ratio data.

The data from these investigations implicate $p70^{S6k}$ as a regulator of peptide transport at the basolateral membrane of rat small intestine and also emphasise that distinct transporters exist at the apical and basolateral membranes. It corroborates other work presented in this thesis (Chapter 5), and work published by other people (section 1.5), in that the unidentified basolateral peptide transporter is not PepT1.

The activity of $p70^{S6k}$ is controlled by a number of upstream proteins in different pathways, some of which have not yet been identified, although two known proteins are mTOR and PI 3-kinase. The previously mentioned reports (Hara *et al.*, 1998; Patti *et al.*, 1998; Wang *et al.*, 1998; Shigemitsu *et al.*, 1999), which demonstrated that leucine stimulated $p70^{S6k}$ activity, also showed that rapamycin blocked the effects of the amino acid. Perfusions were performed in the presence of specific inhibitors of these enzymes; rapamycin, which inhibits mTOR, and wortmannin, which inhibits PI 3-kinase, to examine whether either of these two proteins are involved in the leucine-stimulation of basolateral peptide transport.

Rapamycin, perfused through the vasculature of the small intestine, resulted in inhibition of the leucine-stimulated proportion of basolateral peptide transport, but did not affect the normal (control) rates. These data implicate $p70^{S6k}$ in leucine stimulated basolateral peptide transport, and a role for mTOR in the regulation pathway. It is thought that rapamycin does not induce dephosphorylation of $p70^{S6k}$ primarily by inhibiting $p70^{S6k}$ kinases, but by stimulating $p70^{S6k}$ phosphatase activity (Hara *et al.*, 1998). The pathway they suggested is shown in figure 6.6 (section 6.8.2).

As reported, leucine did not predominantly stimulate peptide transport at the apical membrane. The presence of rapamycin at the apical membrane (in the lumen) had an opposing effect than when infused to the basolateral membrane in the vascular perfusate. Firstly, it did not function to inhibit the leucine stimulation at the basolateral membrane, suggesting that the low concentration of the drug used induced a local response. Secondly, without vascular leucine, rapamycin stimulated peptide transport from the lumen. This stimulation appeared to initiate before the

20 min time point when leucine was added, therefore rapamycin might be inducing an effect earlier than was initially assumed, resulting in the final stimulation once a steady state has been reached. The stimulation by leucine at the basolateral membrane and the stimulation by rapamycin at the apical membrane are not additive, because the rate remained constant when either or both were present in their respective perfusates. Therefore, they might either exert their effects through a common mediator or one pathway might inhibit a second pathway, resulting in the same response. The precise mechanism cannot be concluded from these data.

The data presented here do not permit elucidation of the regulatory pathway which controls peptide transport by PepT1, but there is obviously a mechanism of control present, as demonstrated by the action of rapamycin. PKC has been implicated in the regulation of apical peptide transport (Brandsch *et al.*, 1994) and mTOR has been shown to phosphorylate the C-terminal site of PKC in the V5 domain; activation of which is inhibited by rapamycin (Parekh *et al.*, 1999). The precise mediators functioning in the pathway between mTOR and PKC are not yet known, but the simplest model would be that mTOR controls a phosphatase that acts upon this PKC site (Parekh *et al.*, 2000). In these perfusions, rapamycin in the lumen stimulated peptide transport, potentially by inhibiting the mTOR-dependent phosphorylation of the C-terminal site of PKC, thereby relieving the inhibition on PepT1 by active PKC.

PI 3-kinase is also known to lie upstream of $p70^{S6k}$; some studies have demonstrated an inhibitory effect of wortmannin (a PI 3-kinase inhibitor) on the amino acid-stimulation of $p70^{S6k}$ activity (Wang *et al.*, 1998; Patti *et al.*, 1998), a moderate reduction in activity (Shigemitsu *et al.*, 1999), or no effect at all (Hara *et al.*, 1998). As such , perfusions were performed in the presence of wortmannin due to a possible role of PI 3-kinase in the regulation of basolateral peptide transport through $p70^{S6k}$. The data arising from these perfusions were confusing, although a PI 3-kinase-dependent element of control at the basolateral membrane was indicated. If PI 3-kinase inhibits peptide transport under control conditions, the inhibition of PI 3-kinase by wortmannin will relieve this inhibitory effect on transport, thereby producing the stimulation in rate which was observed when wortmannin was infused to the intestine in the vascular perfusate. PI 3-kinase can act via PKB, but amino acids have been shown not to stimulate PKB activity, therefore the effect of

wortmannin must be independent of this enzyme, via another pathway. In summary, at the basolateral membrane, there appears to be a wortmannin-sensitive pathway, in addition to a leucine-sensitive pathway, possibly leading to a common effector. Despite this speculative assumption, the data from experiments with vascular wortmannin do not provide a complete picture and do not, therefore, point to an obvious mechanism and, as such, require further work for clarification.

In contrast to vascular wortmannin, luminal wortmannin has no effect on leucine-stimulated transport, or on control rates. Therefore, this indicates that PI 3-kinase is not involved in regulation of PepT1 transport at the apical membrane. However, because mucosal exit ratios were reduced by the presence of wortmannin in the lumen, PI 3-kinase may be involved in apical peptide transport; further work is required for elucidation of its exact involvement in transport. PDK1 is located upstream of, and is involved in phosphorylation and activation of, PKC (Parekh *et al.*, 2000). (Parekh *et al.*, 2000). PI 3-kinase is located upstream of PDK1, therefore it might be expected that wortmannin would have a stimulatory effect on apical membrane peptide transport, in the same way that rapamycin does at this membrane. However, inconclusive effects by luminal wortmannin suggests that if PKC did have a role in the regulation of PepT1 transport, it might be via a pathway which is independent of PI 3-kinase.

In conclusion, the main points gained from these investigations are: (1) the peptide transporters at the apical and basolateral membranes are distinct proteins, (2) at the apical membrane PI 3-kinase may not involved in regulation of PepT1, and mTOR has an undefined stimulatory capacity, possibly via PKC, and (3) at the basolateral membrane a $p70^{S6k}$/mTOR pathway regulates transport and an independent PI 3-kinase pathway might also be involved. The precise mechanisms of regulation require investigation in detail, however, these studies provide initial information and reveal the complexity of short-term regulation of peptide transport in the small intestine, in addition as to how very little we actually know at present.

Overall, the data presented in this thesis provide important information about peptide transport in the small intestine, in particular concerning the basolateral transporter protein which has not, to date, been identified. Only when intestinal peptide transport as a whole has been elucidated, and the mechanisms controlling regulation at both the apical and basolateral membranes been deduced, can efficient

delivery of peptidomimetic drugs be achieved. The crucial element of the future will be the cloning and sequencing of the basolateral peptide transport protein, providing us with a complete picture of intestinal absorption.

(a)

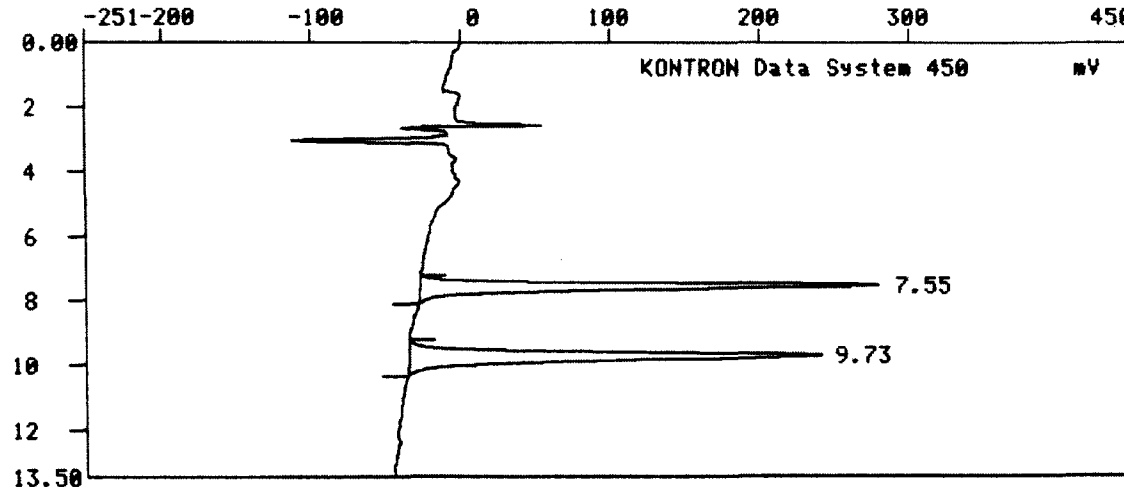

(b)

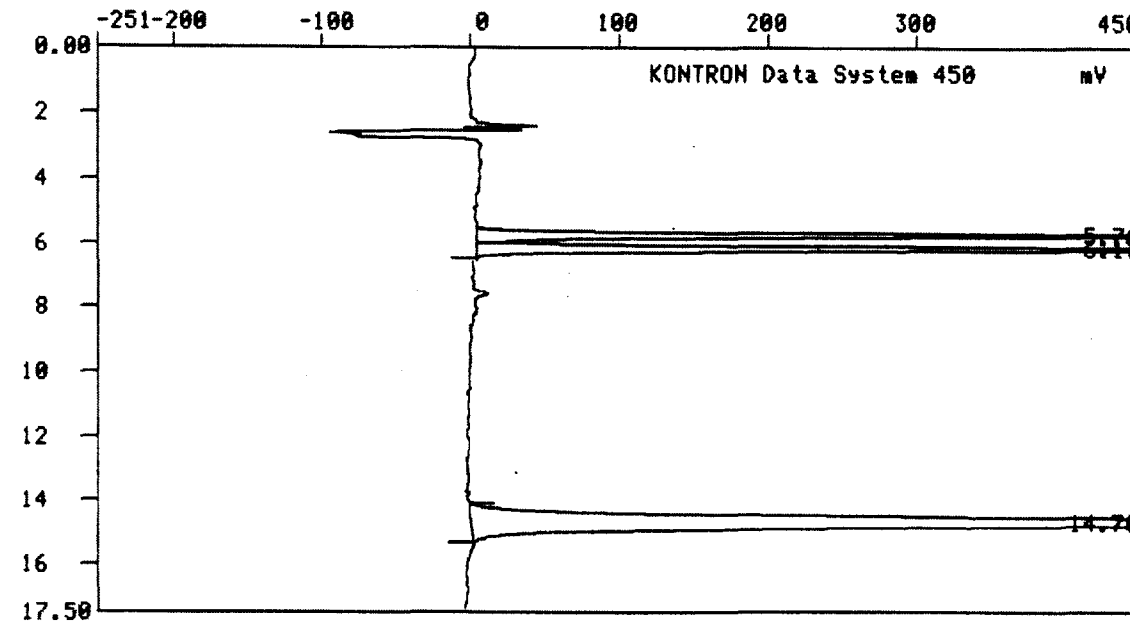

Appendix I

HPLC elution profiles of D-Phe, D-Phe-L-Gln and [4-azido-D-Phe]-L-Ala. Standard samples are run at a concentration of 0.01 mM; the area of the peak is used to calculate the concentration of D-Phe-L-Gln or [4-azido-D-Phe]-L-Ala in vascular samples, following perfusion, by comparison to sample peak areas. (a) The mobile phase is 10% methanol / 90% 21 mM KH_2PO_4; D-Phe elutes at 7.55 min, whereas D-Phe-L-Gln elutes at 9.73 min. (b) The mobile phase is 15% methanol / 85% 21 mM KH_2PO_4; D-Phe elutes at 5.76 min, D-Phe-L-Gln elutes at 6.17 min and [4-azido-D-Phe]-L-Ala elutes at 14.7 min.

Web sites for peptide fingerprint profiling

PeptIdent:	http://www.expasy.ch/tools/peptident
ProFound:	http://www.prowl.rockefeller.edu/cgi-bin/profound
MS-Fit:	http://www.prospector.ucsf.edu/ucsfhtml3.2/msfit.htm
MASCOT:	http://www.matrixscience.com/
MS-Digest:	http://www.prospector.ucsf.edu/ucsfhtml3.2/msdigest.htm

Web sites for peptide sequence tag database searching

TagIdent:	http://www.expasy.ch/tools/tagident
ProteinInfo:	http://www.prowl1.rockefeller.edu/prowl-cgi/proteininfo
MOWSE:	http://srs.hgmp.mrc.ac.uk/cgi-bin/mowse
BLAST:	http://www.ncbi.nlm.nih.gov.blast/

Appendix II

Web sites for the proteomics search tools utilised in the identification of proteins from peptide fingerprints or peptide sequence tags.

Amino acid	Three (one) letter code	Monoisotopic mass	Average mass
Glycine	Gly (G)	57.021	57.052
Alanine	Ala (A)	71.037	71.079
Serine	Ser (S)	87.032	87.078
Proline	Pro (P)	97.053	97.117
Valine	Val (V)	99.068	99.133
Threonine	Thr (T)	101.48	101.105
Cysteine	Cys (C)	103.009	103.145
Isoleucine	Ile (I)	113.084	113.160
Leucine	Leu (L)	113.084	113.160
Asparagine	Asn (N)	114.043	114.104
Aspartate	Asp (D)	115.027	115.089
Glutamine	Gln (Q)	128.059	128.131
Lysine	Lys (K)	128.095 (147)	128.174
Glutamate	Glu (E)	129.043	129.116
Methionine	Met (M)	131.040	131.199
Histidine	His (H)	137.059	137.142
Phenylalanine	Phe (F)	147.068	147.177
Arginine	Arg (R)	156.101 (175)	156.188
Tyrosine	Tyr (Y)	163.063	163.176
Tryptophan	Trp (W)	186.079	186.213

Appendix III

The monoisotopic and average masses (Da) of the twenty common amino acid residues, which are used for mass spectrometric determination of a peptide sequence. Note that leucine and isoleucine, and lysine and glutamine, cannot be differentiated in the sequence due to identical, or very similar, masses. Arginine and lysine residues have a greater mass (+ 19 Da) when cleaved into a y-type ion (from a tryptic peptide) due to their location at the carboxylic end, i.e. plus OH.

Addison, J. M., Burston, D. & Matthews, D. M. (1972). *Clin. Sci.* **43** 907-911. Evidence for active transport of the dipeptide glycylsarcosine by hamster jejunum *in vitro*.

Adibi, S. A. (1997). *Gastroenterology* **113** 332-340. The oligopeptide transporter (PepT1) in human intestine: Biology and function.

Amasheh, S., Wenzel, U., Boll, D., Weber, W. M., Clauss, W. & Daniel, H. (1997). *J. Membrane Biol.* **155** 247-256. Transport of charged dipeptides by the intestinal H^+/peptide symporter PepT1 expressed in *Xenopus laevis* ocytes.

Bai, J. P. F., Subramanian, P., Mosberg, H. I. & Amidon, G. L. (1991). *Pharm. Res.* **8** 593-599. Structural requirements for the intestinal mucosal-cell peptide transporter: The need for N-terminal α-amino group.

Bai, J. P. F. & Amidon, G. L. (1992b). *Pharm. Res.* **9** 969-978. Structural specificity of mucosal-cell transport and metabolism of peptide drugs: Implication for oral peptide drug delivery.

Bailey, P. D. 1990. An introduction to peptide chemistry. *J. Wiley & Sons.*

Bailey, P. D., Boyd, C. A. R., Bronk, J. R., Collier, I. D., Meredith, D., Morgan, K. M. & Temple, C. S. (2000). *Ange. Chem. Int. Ed.* **39** 505-508. How to make drugs orally active: A substrate template for peptide transporter PepT1.

Berteloot, A., Bennetts, R. W. & Ramaswamy, K. (1980). *Biochim. Biophys. Acta* **601** 592-604. Transport characteristics of papain-treated brush-border membrane vesicles. Non-involvement of γ-glutamyltransferase in leucine transport.

Boll, M., Markovich, D., Weber, W. M., Korte, H., Daniel, H. & Murer, H. (1994). *Eur. J. Physiol.* **429** 146-149. Expression cloning of a cDNA from rabbit small intestine related to proton-coupled transport of peptides, β-lactam antibiotics and ACE-inhibitors.

Boll, M., Herget, M., Wagener, M., Weber, W. M., Markovich, D., Biber, J., Clauss, W., Murer, H. & Daniel, H. (1996). *Proc. Natl. Acad. Sci.* **93** 284-289. Expression cloning and functional characterisation of the kidney cortex high-affinity proton-coupled peptide transporter.

Boyd, C. A. R., Cheeseman, C. I. & Parsons, D. S. (1975). *J. Physiol.* **250** 409-429. Amino acid movements across the wall of anuran small intestine perfused through the vascular bed.

Boyd, C. A. R. & Parsons, D. S. (1978). *J. Physiol.* **274** 17-36. Effects of vascular perfusion on the accumulation, distribution and transfer of 3-o-methyl-D-glucose within and across small intestine.

Boyd, C. A. R. & Ward, M. R. (1982). *J. Physiol.* **324** 411-428. A micro-electrode study of oligopeptide absorption by the small intestinal epithelium of *Necturus maculosus.*

Boyd, C. A. R., Bronk, J. R., Lister, N. & Bailey, P. D. (1996). *J. Physiol.* **493** 104P. Stimulatory effect of glutamine on dipeptide transport by the rat small intestine, *in vitro* and *in situ.*

Brandsch, M., Miyamoto, Y., Ganapathy, V. & Leibach, F. H. (1994). *Biochem. J.* **299** 253-260. Expression and protein kinase C-dependent regulation of peptide/H^+ co-transport system in the Caco-2 human colon carcinoma cell line.

Brandsch, M., Ganapathy, V. & Leibach, F. H. (1995). *Am. J. Physiol.* **268** F391-F397. H^+-peptide cotransport in Madin-Darby canine kidney cells: Expression and calmodulin-dependent regulation.

Brandsch, M., Brandsch, C., Ganapathy, M. E., Chew, C. S., Ganapathy, V. & Leibach, F. H. (1997). *Biochim. Biophys. Acta* **1324** 251-262. Influence of proton and essential histidyl residues on the transport kinetics of the H^+/peptide cotransport systems in intestine (PEPT1) and kidney (PEPT2).

Brandsch, M., Thunecke, F., Kullertz, G., Schutkowski, M., Fischer, G. & Neubert, K. (1998). *J. Biol. Chem.* **273** 3861-3864. Evidence for the absolute conformational specificity of the intestinal H^+/peptide symporter, PEPT1.

Bronk, J. R. & Ingham, P. A. (1979) *J. Physiol.* **289** 99-113. Sugar transfer from the lumen of the rat small intestine to the vascular bed.

Bronk, J. R., Lister, N., Bailey, P. D. & Boyd, C. A. R. (1995). *J. Physiol.* **489.P** 105P. Effects on dipeptide transport of reducing the pH in the lumen of rat small intestine, *in vitro.*

Burston, D., Addison, J. M. & Matthews, D. M. (1972). *Clin. Sci.* **43** 823-837. Uptake of dipeptides containing basic and acidic amino acids by rat small intestine *in vitro.*

Celis, J. E. & Bravo, R. (1984). Two-dimensional electrophoresis of proteins. Methods and applications. *Academic Press,* London.

Cheeseman, C. I. & Parsons, D. S. (1974). *Biochim. Biophys. Acta* **373** 523-526. Intestinal absorption of peptides: peptide uptake by small intestine of *Rana pipiens*.

Cheeseman, C. I. & Devlin, D. (1985). *Biochim. Biophys. Acta* **812** 767-773. The effect of amino acids and dipeptides on sodium-ion transport in rat enterocytes.

Cheeseman, C. I. (1986). *Am. J. Physiol.***251** G636-G641. Expression of amino acid and peptide transport systems in rat small intestine.

Cooke, H. J. (1987). Physiology of the gastrointestinal tract. Ed by Johnson, L. R. *Raven Press*, New York.

Corpe, C. P. (1993). *D. Phil Thesis.* Short and long term regulation of sugar absorption, transport and metabolism by rat small intestine.

Corpe, C. P., Basaleh, M. M., Affleck, J. A., Gould, G., Jess, T. J. & Kellett, G. L. (1996). *Pflug. Archives* **432** 192-201. The regulation of Glut5 and Glut2 activity in the adaptation of intestinal brush-border fructose transport in diabetes.

Courchesne, P. L., Luethy, R. & Patterson, S. D. (1997). *Electrophoresis* **18** 369-381. Comparison of in-gel and on-membrane digestion methods at low to sub-pmol level for subsequent peptide and fragment-ion mass analysis using matrix-assisted laser-desorption/ionisation mass spectrometry.

Covitz, K. Y., Amidon, G. L. & Sadee, W. (1998). *Biochemistry* **37** 15214-15221. Membrane topology of the human dipeptide transporter, hPepT1, determined by epitope insertions.

Daniel, H., Morse, E. L. & Adibi, S. A. (1991). *J. Biol. Chem.* **266** 19917-19924. The high and low affinity transport systems for dipeptides in kidney brush border membrane respond differently to alterations in pH gradient and membrane potential.

Daniel, H. & Adibi, S. A. (1993). *J. Clin. Invest.* **92** 2215-2223. Transport of β-lactam antibiotics in kidney brush-border membrane. Determinants of their affinity for the oligopeptide/H^+ symporter.

Daniel, H. (1996). *J. Membrane Biol.* **154** 197-203. Function and molecular structure of brush border membrane peptide/H^+ symporters.

Dantzig, A. H., Hoskins, J., Tabas, L. B., Bright, S., Shepard, R. L., Jenkins, I. L., Duckworth, D. C., Sportsman, J. R., Mackensen, D., Rosteck Jr., P. R. & Skatrud, P. L. (1994). *Science* **264** 430-433. Association of intestinal peptide transport with a protein related to the cadherin superfamily.

Das, M. & Radhakrishnan, A. N. (1975). *Biochem. J.* **146** 133-139. Studies on a wide spectrum intestinal dipeptide uptake system in the monkey and in humans.

Desnuelle, P. (1979). *Eur. J. Biochem.* **101** 1-11. Intestinal and renal aminopeptidase: a model of a transmembrane protein.

Doring, F., Dorn, D., Bachfischer, U., Amasheh, S., Herget, M. & Daniel, H. (1996). *J. Physiol.* **497** 773-779. Functional analysis of a chimeric mammalian peptide transporter derived from the intestinal and renal isoforms.

Doring, F., Will, J., Amasheh, S., Clauss, W., Ahlbrech, H. & Daniel, H. (1998). *J. Biol. Chem.* **273** 23211-23218. Minimal molecular determinants of substrates for recognition by the intestinal peptide transporter.

Dyer, J., Beechey, R. B., Gorvel, J. P., Smith, R. T., Wootton, R. & Shirazi-Beechey, S. P. (1990). *Biochem. J.* **269** 565-571. Glycyl-L-proline transport in rabbit enterocyte basolateral-membrane vesicles.

Edman, P & Begg, G. (1967). *Eur. J. Biochem.* **1** 80-91. A protein sequenator.

Erickson, R. H., Gum Jr, J. R., Lindstrom, M. M., McKean, D. & Kim, Y. S. (1995). *Biochem. Biophys. Res. Commun.* **216** 249-257. Regional expression and dietary regulation of rat small intestinal peptide and amino acid transporter mRNAs.

Fei, Y., Kanai, Y., Nussberger, S., Ganapathy, V., Leibach, F. H., Romero, M. F., Singh, S. K., Boron, M. F. & Hediger, M. A. (1994). *Nature* **368** 563-566. Expression cloning of a mammalian proton-coupled oligopeptide transporter.

Fei, Y., Liu, W., Prasad, P. D., Kekuda, R., Oblak, T. G., Ganapathy, V. & Leibach, F. H. (1997). *Biochemistry* **36** 452-460. Identification of the histidyl residue obligatory for the catalytic activity of the human H^+/peptide cotransporters PEPT1 and PEPT2.

Fei, Y., Fujita, T., Lapp, D. F., Ganapathy, V. & Leibach, F. H. (1998a). *Biochem. J.* **332** 565-572. Two oligopeptide transporters from *Caenorhabditis elegans*: Molecular cloning and functional expression.

Fei, Y., Romero, M. F., Krause, M., Liu, J., Huang, W., Ganapathy, V. & Leibach, F. H. (2000). *J. Biol. Chem.* **275** 9563-9571. A novel H^+-coupled oligopeptide transporter (OPT3) from *Caenorhabditis elegans* with a predominant function as a H^+ channel and an exclusive expression in neurons.

Fei, Y., Liu, J., Fujita, T., Liang, R., Ganapathy, V. & Leibach, F. H. (1998b). *Biochem. Biophys. Res. Commun.* **246** 39-44. Identification of a potential substrate binding domain in the mammalian peptide transporters PepT1 and PepT2 using PepT1-PepT2 and PepT2-PepT1 chimeras.

Ferraris, R. P., Diamond, J. & Kwan, W. W. (1988). *Am. J. Physiol.* **255** G143-G150. Dietary regulation of intestinal transport of the dipeptide carnosine.

Fiske, C. H. & Subbarow, Y. (1925). *J. Biol. Chem.* **66** 375-400. The colourimetric determination of phosphorus.

Freeman, T. C., Bentsen, B. S., Thwaites, D. T. & Simmons, N. L. (1995). *Eur. J. Physiol.* **430** 394-400. H^+/di-tripeptide transporter (PepT1) expression in the rabbit intestine.

Fujita, M., Matsui, H., Nagano, K. & Nakao, M. (1971). *Biochim. Biophys. Acta* **233** 404-408. Asymmetric distribution of ouabain-sensitive ATPase activity in rat intestinal mucosa.

Fujita, T., Majikawa, Y., Umehisa, S., Okada, N., Yamamoto, A., Ganapathy, V. & Leibach, F. H. (1999). *Biochem. Biophys. Res. Commun.* **261** 242-246. σ receptor ligand-induced up-regulation of the H^+/peptide transporter PepT1 in the human intestinal cell line Caco-2.

Ganapathy, M. E., Brandsch, M., Prasad, P. D., Ganapathy, V. & Leibach, F. H. (1995). *J. Biol. Chem.* **270** 25672-25677. Differential recognition of β-lactam antibiotics by intestinal and renal peptide transporters, PepT1 and PepT2.

Ganapathy, V., Mendicino, J. F. & Leibach, F. H. (1981). *Life Sci.* **29** 2451-2457. Effect of papain treatment on dipeptide transport into rabbit intestinal brush border vesicles.

Ganapathy, V. & Leibach, F. H. (1983). *J. Biol. Chem.* **258** 14189-14192. Role of pH gradient and membrane potential in dipeptide transport in intestinal and renal brush-border membrane vesicles from the rabbit.

Ganapathy, V., Pashley, D. H., Fonteles, M. C. & Leibach, F. H. (1984). *Contr Nephrol* **42** 10-18. Peptidases and peptide transport in mammalian kidney.

Ganapathy, V. & Leibach, F. H. (1985). *Am. J. Physiol.* **249** G153-G160. Is intestinal peptide transport energized by a proton gradient?

Ganapathy, V., Miyamoto, Y. & Leibach, F. H. (1987). *Contr. Infusion Ther. Clin. Nutr* **17** 54-68. Driving force for peptide transport in mammalian intestine and kidney.

Ganapathy, V., Miyamoto, Y., Tiruppathi, C. & Leibach, F. H. (1991). *Indian J. Biochem. Biophys.* **28** 317-323. Peptide transport across the animal cell plasma membrane: Recent developments.

Gardner, M. L. G. (1978). *Quart. J. Exp. Physiol.* **63** 93-95. The absorptive viability of isolated intestinal preparation from dead animals.

Graul, R. C. & Sadée, W. (1997). *Pharm. Res.* **14** 388-400. Sequence alignments of the H^+-dependent oligopeptide transporter family PTR: Inferences on structure and function of the intestinal PET1 transporter.

Hamilton, J. D. & McMichael, H. B. (1968). *Lancet* **2** 154-157. Role of the microvillus in the absorption of disaccharides.

Hanson, P. J. & Parsons, D. S. (1976). *J. Physiol.* **255** 775-795. The utlisation of glucose and production of lactate by *in vitro* preparations of rat small intestine: effects of vascular perfusion.

Hara, K., Yonezawa, K., Weng, Q., Kozlowski, M. T., Belham, C. & Avruch, J. (1998). *J. Biol. Chem.* **273** 14484-14494. Amino acid sufficiency and mTOR regulate p70 S6 kinase and eIF-4E BP1 through a common effector mechanism.

Harms, V. & Wright, E. M. (1980). *J. Membrane Biol.* **53** 119-128. Some characteristics of Na/K-ATPase from rat intestinal basal lateral membranes.

Hediger. M. A. & Rhoads, D. B. (1994). *Physiol. Rev.* **74** 993-1026. Molecular physiology of sodium-glucose cotransporters.

Hediger. M. A., Kanai, Y., You, G. & Nussberger, S. (1995). *J. Physiol.* **482** 7s-17s. Mammalian ion-coupled solute transporters.

Hediger, M. A., Coady, M. J., Ikeda, T. S. & Wright, E. M. (1987). *Nature* **330** 379-381. Expression cloning and cDNA sequence of the Na^+/glucose cotransporter.

Hidalgo, I. J., Bhatnagar, P., Lee, C., Miller, J., Cucullino, G. & Smith, P. L. (1995). *Pharm. Res.* **12** 317-319. Structural requirements for interaction with the oligopeptide transporter in Caco-2 cells.

Hillenkamp, F., Karas, M., Beavis, R. C. & Chait, B. T. (1991). *Anal. Chem.* **63** A1193-A1202. Matrix-assisted laser desorption ionization mass-spectrometry of biopolymers.

Hori, R., Okano, T., Kato, M., Maegawa, H & Inui, K. (1988). *J Pharm Pharmacol* **40** 646-647. Intestinal absorption of cephalosporin antibiotics. Correlation between intestinal absorption and brush-border membrane transport.

Hu, M., Subramanian, P., Mosberg, H. I. & Amidon, G. L. (1989). *Pharm. Res.* **6** 66-70. Use of the peptide carrier system to improve the intestinal absorption of L-α-methyldopa: Carrier kinetics, intestinal permeabilities, and *in vitro* hydrolysis of dipeptidyl derivatives of L-α-methyldopa.

Ihara, T., Tsujikawa, T., Fujiyama, Y. & Bamba, T. (2000). *Digestion* **61** 59-67. Regulation of PepT1 peptide transporter expression in the rat small intestine under malnourished conditions.

Inui, K., Okano, T., Takano, M., Saito, H & Hori, R. (1984). *Biochim. Biophys. Acta* **769** 449-454. Carrier-mediated transport of cephalexin via the dipeptide transport system in rat renal brush-border membrane vesicles.

Inui, K., Okano, T., Maegawa, H., Kato, M., Takano, M & Hori, R. (1988). *J. Pharm. Exp. Ther.* **247** 235-241. H^+-coupled transport of p.o. cephalosporins via dipeptide carriers in rabbit intestinal brush-border membranes: Difference of transport characteristics between cefixime and cephradine.

Inui, K., Yamamoto, M. & Saito, H. (1992). *J. Pharm. Exp. Ther.* **261** 195-201. Transepithelial transport of oral cephalosporins by monolayers of intestinal epithelial cell line Caco-2: specific transport systems in apical and basolateral membranes.

James, P., Quadroni, M., Carafoli, E. & Gonnet, G. (1993). *Biochem. Biophys. Res. Commun.* **195** 58-64. Protein identification by mass profile fingerprinting.

Jungblut, P. & Thiede, B. (1997). *Mass Spec. Rev.* **16** 145-162. Protein identification from 2-D gels by MALDI mass spectrometry.

Karas, M. & Hillenkamp, F. (1988). *Anal. Chem.* **60** 2301-2303. Laser desorption ionization of proteins with molecular masses exceeding 10000 Daltons.

Kato, M., Maegawa, H., Okano, T., Inui, K. & Hori, R. (1989). *J. Pharm. Exp. Ther.* **251** 745-749. Effect of various chemical modifiers on H^+ coupled transport of cephradine *via* dipeptide carriers in rabbit intestinal brush-border membranes: Role of histidine residues.

Kellett, G. L. & Barker, E. D. (1989). *Biochim. Biophys. Acta* **992** 128-130. The stimulation of glucose absorption and metabolism in rat jejunum by bradykinin: dependence on the composition of commercial diets.

Kelly, D. E. (1966). *J. Cell Biol.* **28** 51-72. Fine structure of desmosomes, hemidesmosomes and an epidermal globular layer in developing newt epidermis.

Kenny & Maroux. (1982). *Physiol. Rev.* **62** 91-128. Topology of microvillar membrane hydrolases of kidney and intestine.

Kramer, W. (1987). *Biochim. Biophys. Acta* **905** 65-74. Identification of identical binding polypeptides for cephalosporins and dipeptides in intestinal brush-border membrane vesicles by photoaffinity labelling.

Kramer, W., Girbig, F., Leipe, I. & Petzoldt, E. (1988). *Biochem. Pharmacol.* **37** 2427-2435. Direct photoaffinity labelling of binding proteins for β-lactam antibiotics in rat intestinal brush-border membranes with [^{3}H]Benzylpenicillin.

Kramer, W., Dürckheimer, W., Girbig, F., Gutjahr, U., Leipe, I. & Oekonomopulos, R. (1990a). *Biochim. Biophys. Acta* **1028** 174-181. Influence of amino acid side chain modification on the uptake system for β-lactam antibiotics and dipeptides from rabbit small intestine.

Kramer, W., Dechent, C., Girbig, F., Gutjahr, U. & Neubauer, H. (1990b). *Biochim. Biophys. Acta* **1030** 41-49. Intestinal uptake of dipeptides and β-lactam antibiotics. I. The intestinal uptake system for dipeptides and β-lactam antibiotics is not part of a brush border membrane peptidase.

Kramer, W., Gutjahr, U., Girbig, F. & Leipe, I. (1990c). *Biochim. Biophys. Acta* **1030** 50-59. Intestinal absorption of dipeptides and β-lactam antibiotics. II. Purification of the binding protein for dipeptides and β-lactam antibiotics from rabbit small intestinal brush border membranes.

Kramer, W., Girbig, F., Gutjahr, U. & Leipe, I. (1990d). *J. Chrom.* **52** 199-210. Application of high performance liquid chromatography to the purification of the putative intestinal peptide transporter.

Kramer, W., Girbig, F., Gutjahr, U., Kowalewski, S., Adam, F. & Schiebler, W. (1992). *Eur. J. Biochem.* **204** 923-930. Intestinal absorption of β-lactam antibiotics and oligopeptides.

Kramer, W., Gutjahr, U., Kowalewski, S & Girbig, F. (1993). *Biochem. Pharmacol.* **46** 542-546. Interaction of the orally active dianionic cephalosporin cefixime with the uptake system for oligopeptides and α-amino-β-lactam antibiotics in rabbit small intestine.

Kramer, W., Girbig, F., Bewersdorf, U., Kohlrautz, S & Weyland, C. (1998). *Biochim. Biophys. Acta* **1373** 179-194. Structural studies of the H^+/oligopeptide transport system from rabbit small intestine.

Läuger, P & Jauch, P. (1986). *J. Membr. Biol.* **91** 275-84. Microscopic description of voltage effects on ion-driven cotransport systems.

Leibach, F. H. & Ganapathy, V. (1996). *Ann. Rev. Nutr.* **16** 99-119. Peptide transporters in the intestine and the kidney.

Li, J. & Hidalgo, I. J. (1996). *J. Drug Target.* **4** 9-17. Molecular modeling study of structural requirements for the oligopeptide transporter.

Li, J., Tamura, K., Lee, C., Smith, P. L., Borchardt, R. T. & Hidalgo, I. J. 1998). *J. Drug Target.* **5** 317-327. Structure-affinity relationships of Val-Val and Val-Val-Val stereoisomers with the apical oligopeptide transporter in human intestinal Caco-2 cells.

Liang, R., Fei, Y., Prasad, P. D., Ramamoorthy, S., Han, H., Yang-Feng, T. L., Hediger, M. A., Ganapathy, V. & Leibach, F. H. (1995). *J. Biol. Chem.* **270** 6456-6463. Human intestinal H^+/peptide cotransporter.

Lister, N., Sykes, A. P., Bailey, P. D., Boyd, C. A. R. & Bronk, J. R. (1995). *J. Physiol.* **484** 173-182. Dipeptide transport and hydrolysis in isolated loops of rat small intestine: effects of stereospecificity.

Liu, W., Liang, R., Ramamoorthy, S., Fei, Y., Ganapathy, M. E., Hediger, M. A., Ganapathy, V. & Leibach, F. H. (1995). *Biochim. Biophys. Acta* **1235** 461-466. Molecular cloning of PepT2, a new member of the H^+/peptide cotransporter family, from human kidney.

Louvard, D., Maroux, S., Vannier, Ch. & Desnuelle, P. (1975). *Biochim. Biophys. Acta* **375** 236-248. Topological studies on the hydrolases bound to the intestinal brush border membrane. 1. Solubilisation by papain and triton X-100.

Lucas, M. L., Schneider, W., Haberich, F. J. & Blair, J. A. (1975). *Proc. Royal Soc. Lond. B* **192** 39-48. Direct measurement by pH-microelectrode of the pH microclimate in rat proximal jejunum.

Mackenzie, B., Fei, Y., Ganapathy, V. & Leibach, F. H. (1996). *Biochim. Biophys. Acta* **1284** 125-128. The human intestinal H^+/oligopeptide cotransporter hPEPT1 transports differently-charged dipeptides with identical electrogenic properties.

Maenz, D. D. & Cheeseman, C. I. (1986). *Biochim. Biophys. Acta* **860** 277-285. Effect of hyperglycaemia on D-glucose transport across the brush-border and basolateral membrane of rat small intestine.

Matsumoto, S., Saito. H. & Inui, K. (1994). *J. Pharm. Exp. Ther.* **270** 498-504. Transcellular transport of oral cephalosporins in human intestinal epithelial cells, Caco-2: interaction with dipeptide transport systems in apical and basolateral membranes.

Matthews, D. M. (1975). *Physiol. Rev.* **55** 537-608. Intestinal absorption of peptides.

Matthews, D. M., Adibi, S. A. (1976). *Gastroenterology* **71** 151-161. Peptide absorption.

Matthews, D. M. (1991). Protein absorption: development and present state of the subject. *Wiley-Liss,* New York.

McEwan, G. T. A., Daniel, H., Fett, C., Burgess, M. N. & Lucas, M. L. (1988). *Proc. Royal Soc. Lond. B* **234** 219-237. The effect of Escherichia coli STa enterotoxin and other secretagogues on mucosal surface pH of rat small intestine in vivo.

McManus, J. P. A. & Isselbacher, K. J. (1970). *Gastroenterology* **59** 214-221. Effect of fasting versus feeding on the rat small intestine.

Meredith, D & Boyd, C.A.R. (1995). *J. Membrane Biol.* **145** 1-12. Oligopeptide transport by epithelial cells.

Meredith, D & Laynes, R. W. (1996). *Placenta* **17** 173-179. Dipeptide transport in brush-border membrane vesicles (BBMV) prepared from human full-term placentae.

Meredith, D., Temple, C. S., Guha, N., Sword, C. J., Boyd, C. A. R., Collier, I. D., Morgan, K. M. & Bailey, P. D. (2000). *Eur. J. Biochem.* **267** 3723-3728. Modified amino acids and peptides as substrates for the intestinal peptide transporter PepT1.

Merril, C. R. (1981). *Science* **211** 1437-1438. Ultrasensitive stain for proteins in polyacrylamide gels shows regional variation in cerebrospinal fluid proteins.

Miyamoto, Y., Ganapathy, G. & Leibach, F. H. (1986). *J. Biol. Chem.* **261** 16133-16140. Identification of histidyl and thiol groups at the active site of rabbit renal dipeptide transporter.

Miyamoto, Y., Coone, J. L., Ganapathy, V. & Leibach, F. H. (1988). *Biochem. J.* **249** 247-253. Distribution and properties of the glysylsarcosine-transport system in rabbit renal proximal tubule. Studies with isolated brush-border membrane vesicles.

Miyamoto, Y., Thompson, Y. G., Howard, E. F., Ganapathy, V. & Leibach, F. H. (1991). *J. Biol. Chem.* **266** 4742-4745. Functional expression of the intestinal peptide-proton co-transporter in *Xenopus laevis* oocytes.

Miyamoto, Y., Shiraga, T., Morita, K., Yamamoto, H., Haga, H., Taketani, Y., Tamai, I., Sai, Y., Tsuji, A. & Takeda, E. (1996a). *Biochim. Biophys. Acta* **1305** 34-38. Sequence, tissue distribution and developmental changes in rat intestinal oligopeptide transporter.

Mizuma, T., Masubuchi, S. & Awazu, S. (1998). *J. Pharm. Pharmacol* **50** 167-172. Intestinal absorption of stable cyclic dipeptides by the oligopeptide transporter in rat.

Moog, F. (1981). *Sci. Am.* **Nov** 116-125. The lining of the small intestine.

Mørtz, E., Vorm, O., Mann, M. & Roepstorff, P. (1994). *Biol. Mass Spec.* **23** 249-261. Identification of proteins in polyacrylamide gels by mass spectrometric peptide mapping combined with database search.

Muller, U., Brandsch, M., Prasad, P. D., Fei, Y., Ganapathy, V. & Leibach, F. H. (1996). *Biochem. Biophys. Res. Commun.* **218** 461-465. Inhibition of the H^+/peptide cotransporter in the human intestinal cell line Caco-2 by cyclic AMP.

Murer, H & Kinne, R (1980). *J. Membrane Biol.* **55** 81-95. The use of isolated membrane vesicles to study epithelial transport processes.

Nakanishi, T., Tamai, I., Sai, Y., Sasaki, T. & Tsuji, A. (1997). *Cancer Res.* **57** 4118-4122. Carrier-mediated transport of oligopeptides in the human fibrosarcoma cell line HT1080.

Newey, H. & Smyth, D. H. (1960). *J. Physiol.* **152** 367-380. Intracellular hydrolysis of dipeptides during intestinal absorption.

Nicholls, T. J., Leese, H. J. & Bronk, J. R. (1983) *Biochem. J.* **212** 183-187. Transport and metabolism of glucose by rat small intestine.

Nussberger, S., Steel, A., Trotti, D., Romero, M. F., Boron, W. F. & Hediger, M. A. (1997). *J. Biol. Chem.* **272** 7777-7785. Symmetry of H^+ binding to the intra- and extracellular side of the H^+-coupled oligopeptide cotransporter PepT1.

Ogihara, H., Saito, H., Shin, B., Terada, T., Takenoshita, S., Nagamachi, Y., Inui, K. & Takata, K. (1996). *Biochem. Biophys. Res. Commun.* **220** 848-852. Immuno-localisation of H^+/peptide cotransporter in rat digestive tract.

Ogihara, H., Suzuki, T., Nagamachi, Y., Inui, K. & Takata, K. (1999). *Hist. J.* **31** 169-174. Peptide transporter in the rat small intestine: Ultrastructural localisation and the effect of starvation and administration of amino acids.

Oh, D., Sinko, P. J. & Amidon, G. L. (1993). *J. Pharm. Sci.* **82** 897-900. Characterisation of the oral absorption of some β-lactams: Effect of the α-amino side chain group.

Paulson, I. T. & Skurray, R. A. (1994). *Trends in Biochem. Sci.* **19** 404. The POT family of transport proteins.

Pappenheimer, J. R. & Reiss, K. Z. (1987). *J. Membrane Biol.* **100** 123-136. Contribution of solvent drag through intercellular junctions to absorption of nutrients by the small intestine of the rat.

Parekh, D. B., Ziegler, W., Yonezawa, K., Hara, K & Parker, P. J. (1999). *J. Biol. Chem.* **274** 34758-34764. Mammalian TOR controls one of two kinase pathways acting upon nPKCδ and nPKCε.

Parekh, D. B., Ziegler, W. & Parker, P. J. (2000). *EMBO J.* **19** 496-503. Multiple pathways control protein kinase C phosphorylation.

Patti, M. E., Brambilla, E., Luzi, L., Landaker, E. J. & Kahn, C. R. (1998). *J. Clin. Invest.* **101** 1519-1529. Bidirectional modulation of insulin action by amino acids.

Pennington, A. M. (1992). *D. Phil Thesis.* Short-term regulation of glucose absorption, transport and utilisation by rat small intestine.

Petritsch, C., Woscholski, R., Edelmann, H. M. L., Parker, P. J. & Ballou, L. M. (1995). *Eur. J. Biochem.* **230** 431-438. Selective inhibition of p70 S6 kinase activation by phosphatidylinositol 3-kinase inhibitors.

Plumb, J. A., Burston, D., Baker, T. G. & Gardner, M. L. G. (1987). *Clin. Sci.* **73** 53-59. A comparison of the structural integrity of several commonly used preparations of rat small intestine *in vitro*.

Pritchard, P. J. (1969). *Nature* **221** 369-371. Role of intestinal microvilli and glycocalyx in the absorption of disaccharides.

Raeissi, S. D., Li, J. & Hidalgo, I. J. (1999). *J. Pharm. Pharmacol* **51** 35-40. The role of an α-amino group on H^+-dependent transepithelial transport of cephalosporins in Caco-2 cells.

Saito, H & Inui, K. (1993). *Am. J. Physiol.* **265** G289-G294. Dipeptide transporters in apical and basolateral membranes of the human intestinal cell line Caco-2.

Saito, H., Okuda, M., Terada, T., Sasaki, S. & Inui, K. (1995). *J. Pharm. Exp. Ther.* **275** 1631-1637. Cloning and characterisation of a rat H^+/peptide cotransporter mediating absorption of β-lactam antibiotics in the intestine and kidney.

Saito, H., Terada, T., Okuda, M., Sasaki, S. & Inui, K. (1996). *Biochim. Biophys. Acta* **1280** 173-177. Molecular cloning and tissue distribution of rat peptide transporter PepT2.

Saito, H., Motohashi, H., Mukai, M. & Inui, K. (1997). *Biochem. Biophys. Res. Commun.* **237** 577-582. Cloning and characterisation of a pH-sensing regulatory factor that modulated transport activity of the human H^+/peptide cotransporter, PepT1.

Sawada, K., Terada, T., Saito, H., Hashimoto, Y. & Inui, K. (1999). *J. Pharm. Exp. Ther.* **291** 705-709. Recognition of L-amino acid ester compounds by rat peptide transporters PepT1 and PepT2.

Sharp, P. A., Debnam, E. S. & Srai, S. K. (1996). *Gut* **39** 545-550. Rapid enhancement of brush-border glucose uptake after exposure of rat jejunal mucosa to glucose.

Shevchenko, A., Wilm, M. & Mann, M. (1996a). *Anal. Chem.* **68** 850-858. Mass spectrometric sequencing of proteins from silver-stained polyacrylamide gels.

Shevchenko, A., Jensen, O. N., Podtelejnikov, A. V., Sagliocco, F., Wilm, M., Vorm, O., Mortensen, P., Shevchenko, A., Boucherie, H. & Mann, M. (1996b). *Proc. Natl. Acad. Sci.* **93** 14440-14445. Linking genome and proteome by mass spectrometry: Large scale identification of yeast proteins from two dimensional gels.

Shevchenko, An., Wilm, M., Vorm, O., Jensen, O. N., Podtelejnikov, A. V., Neubauer, G., Shevchenko, Al., Mortensen, P. & Mann, M. (1996c). *Biochem. Soc. Trans.* **24** 893-900. A strategy for identifying gel-separated proteins in sequence databases by MS alone.

Shigemitsu, K., Tsujishita, Y., Miyake, H., Hidayat, S., Tanaka, N., Hara, K. & Yonezawa, K. (1999). *FEBS Lett.* **447** 303-306. Structural requirement of leucine for activation of p70 S6 kinase.

Shiraga, T., Miyamoto, K., Tanaka, H., Yamamoto, H., Taketani, Y., Morita, K., Tamai, I., Tsuji, A. & Takeda, E. (1999). *Gastroenterology* **116** 354-362. Cellular and molecular mechanisms of dietary regulation on rat intestinal H^+/peptide transporter PepT1.

Sigrist-Nelson, K. (1975). *Biochim. Biophys. Acta* **394** 220-226. Dipeptide transport in isolated intestinal brush border membrane.

Steel, A., Nussberger, S., Romero, M. F., Boron, W. F., Boyd, C. A. R. & Hediger, M. A. (1997). *J. Physiol.* **498** 563-569. Stoichiometry and pH dependence of the rabbit proton-dependent oligopeptide transporter PepT1.

Takahashi, K., Nakamura, N., Terada, T., Okano, T., Futami, T., Saito, H. & Inui, K. (1998). *J. Pharm. Exp. Ther.* **286** 1037-1042. Interaction of β-lactam antibiotics with H^+/peptide cotransporters in rat renal brush-border membranes.

Takano, M., Tomita, Y., Katsura, T., Yasuhara, M., Inui, K & Hori, R. (1994). *Biochem. Pharmacol.* **47** 1089-1090. Bestatin transport in rabbit intestinal brush-border membrane vesicles.

Takuwa, N., Shimada, T., Matsumoto, H. & Hoshi, T. (1985). *Biochim. Biophys. Acta* **814** 186-190. Proton-coupled transport of glycylglycine in rabbit renal brush-border membrane vesicles.

Tanaka, H., Miyamoto, K. I., Morita, K., (1998). *Gastroenterology* **114** 714-723. Regulation of the PepT1 peptide transporter in the rat small intestine in response to 5-fluorouracil-induced injury.

Temple, C. S., Bronk, J. R., Bailey, P. D. & Boyd, C. A. R. (1995). *Eur. J. Physiol.* **430** 825-829. Substrate-charge dependence of stoichiometry shows membrane potential is the driving force for proton-peptide cotransport in rat renal cortex.

Temple, C. S., Bailey, P. D., Bronk, J. R. & Boyd, C. A. R. (1996). *J. Physiol.* **494** 795-808. A model for the kinetics of neutral and anionic dipeptide-proton cotransport by the apical membrane of rat kidney cortex.

Temple, C. S., Stewart, A. K., Meredith, D., Lister, N. A., Morgan, K. M., Collier, I. D., Vaughan-Jones, R. D., Boyd, C. A. R., Bailey, P. D. & Bronk, J. R. (1998). *J. Biol. Chem.* **273** 20-22. Peptide mimics as substrates for the intestinal peptide transporter.

Terada, T., Saito, H., Mukai, M. & Inui, K. (1996). *FEBS Lett.* **394** 196-200. Identification of the histidine residues involved in substrate recognition by a rat H^+/peptide cotransporter, PepT1.

Terada, T., Saito, H., Mukai, M. & Inui, K. (1997a). *J. Pharm. Exp. Ther.* **281** 1415-1421. Characterisation of stably transfected kidney epithelial cell line expressing rat H^+/peptide cotransporter, PepT1: localisation of PepT1 and transport of β-lactam antibiotics.

Terada, T., Saito, H., Mukai, M. & Inui, K. (1997b). *Am. J. Physiol.* **273** F706-711. Recognition of β-lactam antibiotics by rat peptide transporters, PepT1 and PepT2, in LLC-PK_1 cells.

Terada, T., Saito, H. & Inui, K. (1998). *J. Biol. Chem.* **273** 5582-5585. Interaction of β-lactam antibiotics with histidine residues of rat H^+/peptide cotransporters, PepT1 and PepT2.

Terada, T., Sawada, K., Saito, H., Hashimoto, Y. & Inui, K. (1999). *Am. J. Physiol.* **276** G1435-G1441. Functional characteristics of basolateral peptide transporter in the human intestinal cell line Caco-2.

Terada, T., Saito, H., Sawada, K., Hashimoto, Y. & Inui, K. (2000). *Pharm. Res.* **17** 15-20. N-terminal halves of rat H^+/peptide transporters are responsible for their substrate recognition.

Thamotharan, M., Zonno, V., Storelli, C. & Ahearn, G. A. (1996). *Am. J. Physiol.* **270** R948-R954. Basolateral dipeptide transport by the intestine of the teleost *Oreochromis mossambicus*.

Thamotharan, M., Bawani, S. Z., Zhou, X. & Adibi, S. A. (1998). *Proc. Assoc. Am. Phys.* **110** 361-368. Mechanism of dipeptide stimulation of its own transport in a human intestinal cell line.

Thamotharan, M., Bawani, S. Z., Zhou, X. & Adibi, S. A. (1999a). *Metabolism* **48** 681-684. Functional and molecular expression of intestinal oligopeptide transporter (PepT1) after a brief fast.

Thamotharan, M., Bawani, S. Z., Zhou, X. & Adibi, S. A. (1999b). *Am. J. Physiol.* **276** C821-C826. Hormonal regulation of oligopeptide transporter PepT1 in a human intestinal cell line.

Thompson, A. B. R. & Dietschy, J. M. (1977). *J. Theoretical Biol.* **64** 277-294. Derivation of the equations that describe the effects of unstirred water layers on the kinetic parameters of active transport processes in the intestine.

Thwaites, D. T., Brown, C. D. A., Hirst, B. H. & Simmons, N. L. (1993a). *J. Biol. Chem.* **268** 7640-7642. Transepithelial glycylsarcosine transport in intestinal Caco-2 cells mediated by expression of H^+-coupled carriers at both apical and basal membranes.

Thwaites, D. T., Brown, C. D. A., Hirst, B. H. & Simmons, N. L. (1993b). *Biochim. Biophys. Acta* **1151** 237-245. H^+-coupled dipeptide (glysylsarcosine) transport across apical and basal borders of human intestinal Caco-2 cell monolayers display distinctive characteristics.

Thwaites, D. T., Hirst, B. H. & Simmons, N. L. (1993c). *Biochem. Biophys. Res. Commun.* **194** 432-438. Direct assessment of dipeptide/H+ symport in intact human intestinal (Caco-2) epithelium: a novel method utilising continuous intracellular pH measurement.

Thwaites, D. T., Cavet, M., Hirst, B. H. & Simmons, N. L. (1995). *Br. J. Pharmacol.* **114** 981-986. Angiotensin-converting enzyme (ACE) inhibitor transport in human intestinal epithelial (Caco-2) cells.

Tse, C. M., Brant, S. R., Walker, M. S., Pouyssegur, J. & Donowitz, M. (1992). *J. Biol. Chem.* **267** 9340-9347. Cloning and sequencing of a rabbit cDNA encoding an intestinal and kidney-specific Na^+/H^+ exchanger isoform (NHE-3).

Tsuji, A., Tamai, I., Nakanishi, M., Terasaki, T. & Hamano, S. (1990). *Pharm. Res.* **7** 308-309. Mechanism of the absorption of the dipeptide α-methyldopa-Phe in intestinal brush-border membrane vesicles.

Walker, D., Thwaites, D. T., Simmons, N. L., Gilbert, H. J. & Hirst, B. H. (1998). *J. Physiol.* **507** 697-706. Substrate upregulation of the human small intestinal peptide transporter, hPepT1.

Wang, X., Campbell, L. E., Miller, C. M. & Proud, C. G. (1998). *Biochem. J.* **334** 261-267. Amino acid availability regulates p70 S6 kinase and multiple translation factors.

Wenzel, U., Gebert, I., Weintraut, H., Weber, W., Clauβ, W. & Daniel, H. (1996). *J. Pharm. Exp. Ther.* **277** 831-839. Transport characteristics of differently charged cephalosporin antibiotics in oocytes expressing the cloned intestinal peptide transporter PepT1 and in human intestinal Caco-2 cells.

Wilkes, S. H. & Prescott, J. M. (1985). *J. Biol. Chem.* **260** 13154-13162. The slow, tight binding of bestatin and amastatin to aminopeptidases.

Yamashita, T., Shimada, S., Guo, W., Sato, K., Kohmura, E., Hayakawa, T., Takagi, T. & Tohyama, M. (1997). *J. Biol. Chem.* **272** 10205-10211. Cloning and functional expression of a brain peptide/histidine transporter.

Yeung, A. K., Basu, S. K., Wu, S. K., Chu, C., Okamoto, C. T., Hamm-Alvarez, S. F., von Grafenstein, H., Shen, W., Kim, K., Bolger, M. B., Haworth, I. S., Ann, D. K. & Lee, V. H. L. (1998). *Biochem. Biophys. Res. Commun.* **250** 103-107. Molecular identification of a role for tyrosine 167 in the function of the human intestinal proton-coupled dipeptide transporter (hPepT1).

Yuasa, H., Amidon, G. L. & Fleisher, D. (1993). *Pharm. Res.* **10** 400-404. Peptide carrier-mediated transport in intestinal brush-border membrane vesicles of rats and rabbits: Cephradine uptake and inhibition.